Elucidation of the Functional Role of Rat Lysozyme-Like Proteins in the Male Reproductive Tract

Doctor of Philosophy

By

G. Narmadha

08LAPH08

DEPARTMENT OF ANIMAL BIOLOGY

SCHOOL OF LIFE SCIENCES

UNIVERSITY OF HYDERABAD

HYDERABAD- 500 046

September 2014

Elucidation of the Functional Role of Rat Lysozyme-Like Proteins in the Male Reproductive Tract

A thesis submitted to University of Hyderabad for the award of Ph. D. degree in the Department of Animal Biology

By

G. Narmadha

(08LAPH08)

Department of Animal Biology

School of Life Sciences

University of Hyderabad

Hyderabad- 500 046

September 2014

University of Hyderabad

(A central University established in 1974 by an Act of Parliament)

Department of Animal Biology
School of Life Sciences
University of Hyderabad
Hyderabad-500 046

DECLARATION

I, G. Narmadha, hereby declare that this thesis entitled **"Elucidation of the functional role of rat lysozyme-like proteins in the male reproductive tract"** submitted by me under the guidance and supervision of Dr. Suresh Yenugu is an original and independent research work. I also declare that it has not been submitted previously in part or in full to this University or any other University or Institution for the award of any degree or diploma.

Name : G. Narmadha

Reg. No : 08LAPH08

Signature :

Date :

University of Hyderabad

(A central University established in 1974 by an Act of Parliament)

Department of Animal Biology
School of Life Sciences
University of Hyderabad
Hyderabad-500 046

CERTIFICATE

This is to certify that the thesis entitled **"Elucidation of the functional role of rat lysozyme-like proteins in the male reproductive tract"** is a record of bonafide work done by Miss. G. Narmadha, for the Ph.D. programme in the Department of Animal Biology, University of Hyderabad, under my guidance and supervision. The thesis has not been submitted previously in part or full to this or any other University or Institution for the award of any degree or diploma.

Dr. Suresh Yenugu
(Supervisor)

Head of the Department

Dean of the School

Acknowledgements

With deep sense of gratitude, I express my heartfelt appreciation to Dr. Suresh Yenugu my supervisor, whom I am aware of as a friendly teacher from my M.Sc. days. It's his motivation during my master's that has led me to pursue my doctorate. I thank him very much for giving me an opportunity to work with him. I also thank him for his valuable guidance, insightful comments, encouragement and the free hands with which I could work in his laboratory. I am very grateful to members of the doctoral committee, Prof. P. Appa Rao and Dr. M.Brahmanandam for their critical comments and timely suggestions. My thanks to the Head, Department of Animal Sciences, Prof. B. Senthilkumaran, and former Heads Prof. Manjula Sritharan and Prof. S. Dayananda for providing us with good equipment and facilities to carry out the work. I thank the Dean Prof A. S. Raghavendra and former Dean, Prof. R. P. Sharma, Prof. G. Aparna Dutta and Prof. M. Ramanadham for allowing me to use the school facilities. I would like to express my sincere thanks to Prof. Aparna Dutta, Dr. Niyaz Ahmed , Dr. Arun Kumar and their lab members for tending me their helping hands in all possible forms. Completing this work would have been very difficult without the support and friendship of members of the school of life sciences.

A special thanks to my wonderful colleagues Dr. Barnali, Rajesh and Madhu for their help cooperation and enjoyable working hours. I would like to extend my thanks to all the present and former project students of the lab. I would like to thank Dr. Suraj for his invaluable assistance in experiments with rabbits and rats. A very special thanks to Mr. Durgesh, Dr.Archana and Dr. Umapathy, CCMB for their help in CASA analysis.

To my friends (Saravanan Prabhu, Jayaphrabha, Jubendradass, Kiruthiga, Jamuna, Vijiyalakshmi, Shehnaz Begum, Chaitanya, Jyothi, Venkat, Bimo, Debu and Prasu) thank you for your continued friendship and support. I am blessed to have such wonderful souls around me. This is a great opportunity to express my gratitude to my best buddy Kishore, thank you for all the support and encouragement you give me. Mr. Narsimha is gratefully appreciated for maintaining laboratory. I thank Mr. Ankinedu, Mr. Jagan & Ms. Jyothi from department office who helped me in different endeavors during my work here. I would like to extend my thanks to members of CIL for their assistance. I thank my school principal Sr. Fathima Mary and my Physics teacher Mrs. Metilda Mary for motivating me.

Many thanks to the kids Aadithiyan, Subiksha and Yashaswi for always being there to make me smile and for the playful time that recharges me. From the bottom of my heart I would like to express my gratitude to my beloved sister Abiramy, for her everlasting support and love. I thank almighty for being born in such a sweet family and am deeply indebted to my parents for everything I could achieve. I dedicate this thesis to my loving amma-Amudhavalli and appa – Ganapathy.

TABLE OF CONTENTS

ABBREVIATIONS

Absorbance at 600nm	A_{600}
Alanine	Ala
Alpha	α
Arginine	Arg
Aspartate	Asp
Base pair	bp
Beta	β
Complementary deoxyribonucleic acid	cDNA
Deoxyribonucleic acid	DNA
Diethylpyrocarbonate	DEPC
Glutamate	Glu
Glutamine	Gln
Horseradish peroxidase	HRP
hour	h
Isoleucine	Ile
Isopropyl-β-D-1-thiogalactopyranoside	IPTG
Kilobases	kb
Kilodalton	kd
Litre	L
Lysine	Lys
Micrograms	µg
Microliter	µl
Milligrams	mg
Millilitre	ml
millimolar	mM
minute	min
Molar	M
Molecular weight	MW
Nanograms	ng
O.D	Optical density
Polyacrylamide gel electrophoresis	PAGE

Radio-immunoprecipitation Assay	RIPA
Reverse transcription- Polymerase chain reaction	RT-PCR
Revolutions per minute	rpm
Ribonucleic acid	RNA
Root mean square deviation	RMSD
seconds	sec
Serine	Ser
Sodium dodecyl sulphate	SDS
Threonine	Thr
Tris buffered saline	TBS
Tris buffered saline-triton	TBS-T
Tyrosine	Tyr
Units	U
Volts	V

ABSTRACT

ABSTRACT

Lysozymes are hydrolases that are divided into 6 different families, based on their distribution and function. They are c-type, g-type, i-type, plant, phage and bacterial. C-type lysozymes are predominantly expressed among a wide variety of species. Most recently, lysozyme like (LYZL) proteins that belong to the c-type lysozyme family were identified, which include the six members namely LYZL1, SLLP1/LYZL3, LYZL4, LYZL5, LYZL6 and LYZL7. Recently, the importance of mouse *SLLP1* as a receptor for glycoprotein interaction during fertilization was reported. However, the exact role of LYZL proteins in general physiology and in male reproductive function in particular has not been studied. Hence, we attempted to characterize the rat LYZL proteins with specific reference to male reproductive tract function.

Our results indicate that the rat LYZL proteins are encoded by separate genes and are not isoforms. Phylogenetic analysis showed that they are highly conserved and are distributed in various organisms. *In silico* analysis of the primary, secondary and tertiary structures of LYZL proteins revealed that they are homologous to chicken lysozyme, suggesting that *Lyzl* genes would have arose from a common ancestor. Among the LYZL proteins characterized, only LYZL1 and LYZL6 have conserved the lysozyme active site residues. *Lyzl* mRNA transcripts seem to be expressed predominantly in male reproductive tract. Their expression was not developmentally regulated and androgen independent. Immunostaining revealed the presence of these proteins in male reproductive tract tissues and on spermatozoa. LYZL1 and 6 display peptidoglycan binding property and they possess muramidase, isopeptidase and antibacterial activities, whereas the remaining proteins did not. The role of LYZL proteins in sperm function was evaluated by incubating spermatozoa with LYZL6 antibodies. *In vitro* LYZL6 neutralization seems to inhibit calcium influx and acrosome reaction suggesting that

they have important role in sperm function. *In vivo* studies using rats immunized with LYZL6 displayed spermatozoa with reduced hypermotility and decreased fertility. Taken together, these results suggests that LYZL6 may have a role in sperm function.

RATIONALE

RATIONALE

The male reproductive tract is a specialized organ system that plays a key role in the continuation of the species by producing germ cells. Production of germ cells is dependent on a variety of factors such as endogenous steroid production and the secretion of a number of factors by the epithelial cells of the male reproductive tract. Spermatozoa that are produced by the testes are immature and pass through the epididymis to interact with a wide variety of proteins, resulting in gaining mobility and fertilizing ability. The role of testicular and epididymal proteins in sperm function and their potential to be used as male contraceptives has been reported. However, emphasis on the identification of the role of reproductive tract proteins continue to be an active area of research to identify potential male contraceptives. Hence, in this study we attempted to characterize and decipher the functional role of rat lysozyme-like proteins. Though these proteins are known to be expressed in the male reproductive tract, their precise role in male reproductive function is not known. With this rationale we formed the following objectives.

Objectives of the study

1. Molecular characterization of rat lysozyme-like proteins *in silico.*
2. Expression profiling and biochemical characterization of rat lysozyme-like proteins.
3. Evaluate the functional importance of rat lysozyme-like proteins in male reproduction.

INTRODUCTION

INTRODUCTION

Male reproductive system

The male reproductive system is a combination of organs and glands that is present in the lower abdominal part of the body. The organs of the male reproductive system include testes, epididymides, vas deferens, seminal vesicle, prostate gland and Cowper's gland (Figure 1). The main function of the reproductive system is to produce, nourish and transport spermatozoa into the female reproductive tract for fertilization of the oocyte. In addition, it also secretes hormones that are responsible for primary and secondary sexual characters. Although it is disposable for living of the organism, it is indispensable for propagation of the organism.

Development of reproductive organs

During embryonic stage, reproductive system develops from the intermediate mesoderm along with the urinary tract. Embryos retain the ability to develop into a male or female until 7 weeks. Subsequently, due to exposure to male determining factors of the Y chromosome, epididymal duct starts arising from the Wolffian ducts (Brennan et al., 1998; Schmahl, Eicher, Washburn, & Capel, 2000; Svingen & Koopman, 2013). Following an increase in testosterone, seminal vesicles and prostate glands of the male reproductive tract are formed. Simultaneously the default female reproductive organs formation is suppressed by the male determining factors (Nef 2000). Germinal cells of the testis are arrested at mature phase in the first trimester. Testes formed in the abdominal cavity lie next to the internal inguinal ring until seventh fetal month which then descends to the scrotum at the later stage of pregnancy. Male neonates possess testes that are descended completely out of the abdominal cavity (Malas, Sulak, & Oztürk, 1999; Barsoum & Yao, 2006; Wilhelm, Yang, & Thomas, 2013).

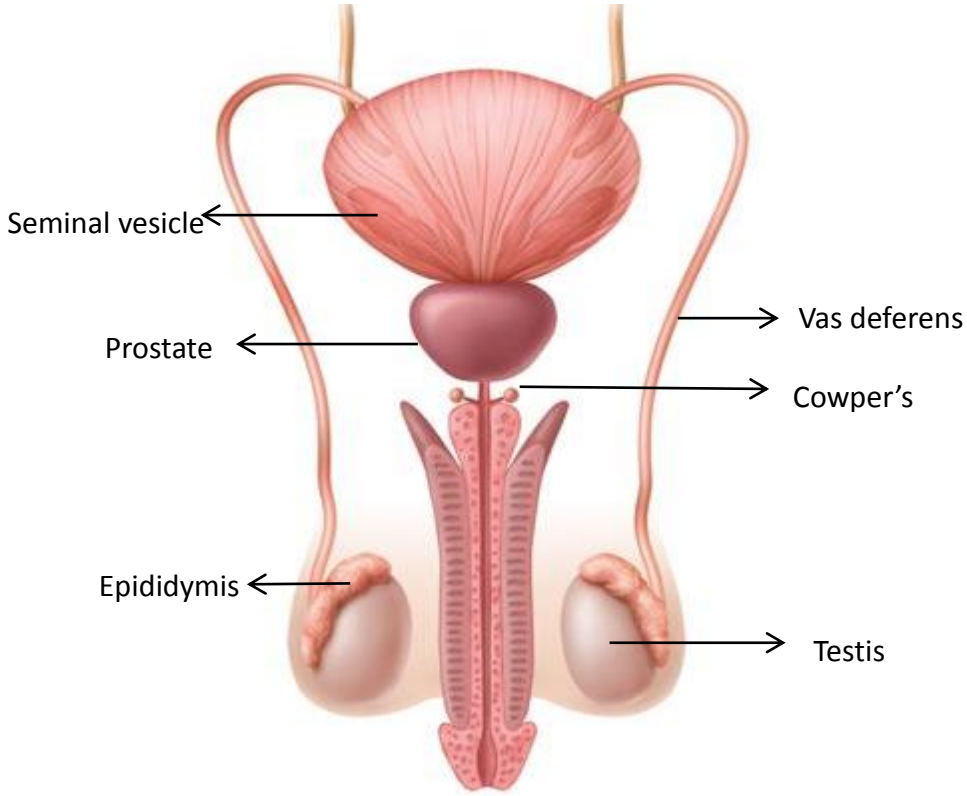

Figure 1: *Male reproductive system (Image adopted from http://marshscience7.blogspot.in).*

Testis

A pair of testes covered individually by a pouch of soft smooth muscle tissue is located in the scrotum situated behind the penis. Testis is ovoid in shape and is a part of external genital tract. It is connected to abdominal cavity by spermatic cord. In humans each testis is about 1.5 inches long by 1 inch wide. Testes are involved in androgen production, mainly the testosterone which stimulates the production of germ cells (spermatogenesis) and also secondary sex characteristics (Hansson et al. 1976; Franchimont 1983). At puberty due to rise in testosterone, the spermatogonial stem cells differentiate to spermatogonia resulting in spermatogenesis and this process is continued throughout the life time of the individual, though the efficiency of the spermatogenesis varies with age according to testosterone levels (Sizonenko 1989) .

Spermatogenesis

Spermatogenesis takes place in the seminiferous tubule of the testis (Figure 2). The spermatogonial stem cells (spermatogonium A -diploid) at puberty start to proliferate and differentiate into spermatogonium B (diploid). They are then differentiated into a diploid primary spermatocyte cells, followed by differentiation into secondary spermatocyte, spermatid and spermatozoa (haploid) (Oatley & Brinster 2012). The spermatozoa thus formed enter into the lumen of the seminiferous epithelium and are protected from host immune system by blood testis barrier formed between adjacent Sertoli cells (Dym & Fawcett, 1970; Jiang et al., 2014). Testosterone that is required for initiation and maintenance of this process is secreted by the Leydig cells. In humans it takes atleast 64 days to complete one cycle of spermatogenesis (Heller & Clermont, 1963; Amann, 2008).

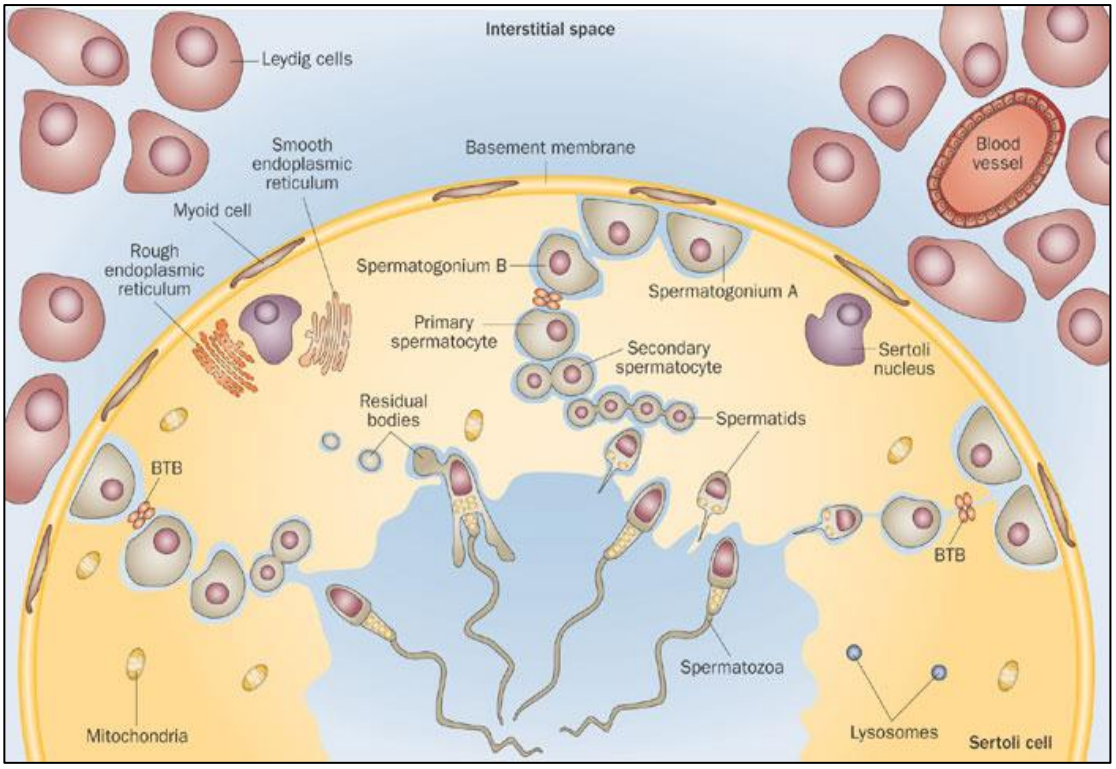

Figure 2: *Overview Spermatogenesis (adopted and modified from Rato et al., 2012). BTB-blood testis barrier.*

Epididymis

The epididymis is highly convoluted tubule where spermatozoa undergo maturation. It connects the vasa efferentia of the testes with the vas deferens (Figure 3). The head of the epididymis attaches to the same end of the testes where the blood vessels and nerves enter. The epididymis is differentiated into three regions namely caput, corpus and cauda (Robaire & Hinton 2006).

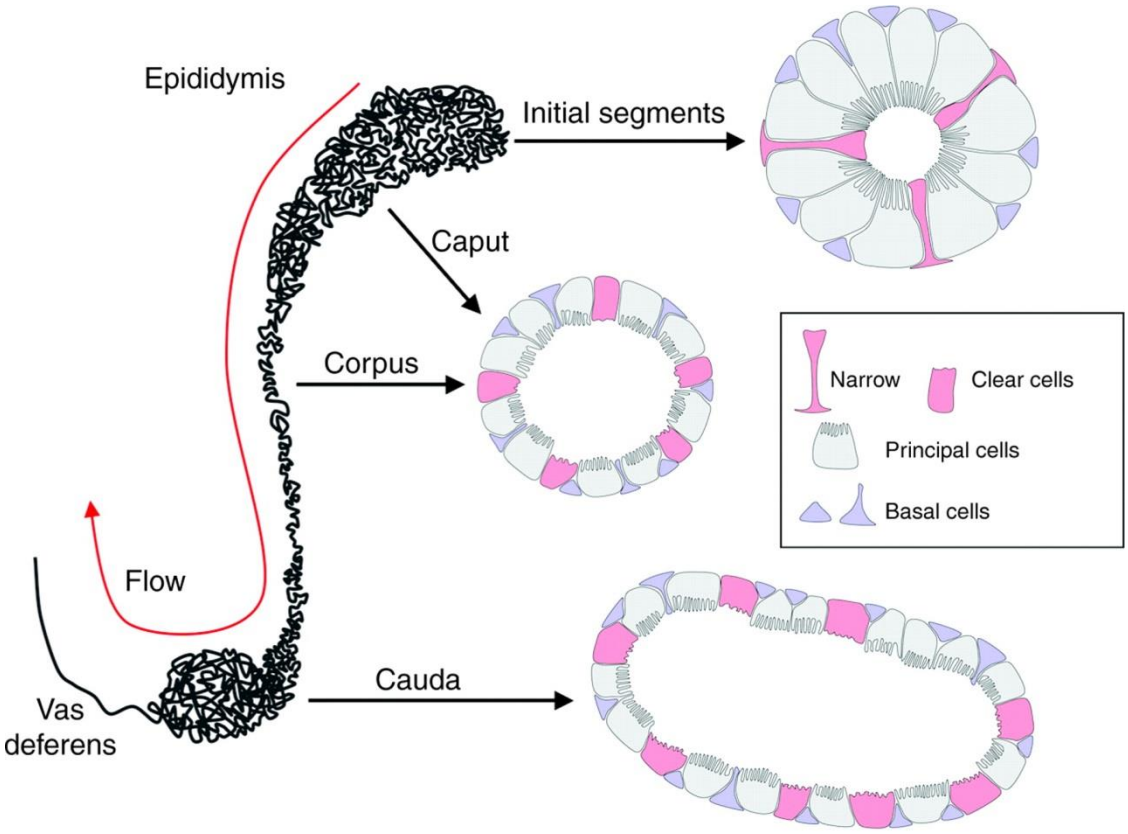

Figure 3: *Epididymis and its cross section (adopted from Shum, et. al.2009).*

The caput is the broad flat end of proximal or spermatic cord. The corpus is an intermediate narrow part and the cauda is distal enlarged end, with mature spermatozoa. The epididymis is mainly composed of 3 cell types namely principal, basal and clear cells. The basal cells are considered as the progenitor for principal cells. The principal cells possess cilia like structures and are non-motile. The clear cells that are predominant in tail region contain more

of lysosomes that help is absorption and degradation of luminal fluid (Shum et al. 2009). By orchestrating the absorption and secretion process, epididymis offer the microenvironment required for the maturation of spermatozoa. The epididymis is androgen dependent and testosterone is required for the maintenance of epididymal functions (Majumder & Turkington 1976). The number of spermatozoa stored in the epididymis has been related to the rate of sperm production by the testes. Spermatozoa undergo functional maturation depending on the epididymal secretions, which are under the endocrine regulation of testes (Cornwall 2009). The plasma membrane of testicular spermatozoa undergoes extensive remodelling in the epididymis by different mechanisms like rearrangement and modification of existing components, addition or coupling of new glycoproteins, and removal of lipid and protein constituents (Huszar G et al. 1997). These processes appear to be regulated by the epididymal proteins in the lumen (Olson & Hamilton, 1978; Nikolopoulou, Soucek, & Vary, 1985) .The epididymis has been shown to play important role in reabsorption and digestion of cytoplasmic fragments, which are eliminated during spermatogenesis (Temple-Smith 1984). The cauda epididymis contains the matured spermatozoa, that have the ability to swim and fertilize the ovum, whereas the spermatozoa from the upper regions of the epididymis do not possess both the abilities (Mahony et al. 1993).

Seminal Vesicle

Seminal vesicles are sac like tubulated structures located posterior to the urinary bladder and their main function is to secrete semen. 50% of the seminal plasma content is contributed by the seminal vesicles and the secretions contain fructose, proteins, phosphates, potassium and prostaglandins (Aumüller & Riva 1992). The secretions of both the seminal vesicles are drained to ampulla of the ejaculatory duct. The fructose from seminal vesicle is considered as energy source for sperm. Prostaglandins help in fertilization of ovum by helping in the peristaltic movement of fallopian tubes (Oliw, Sprecher, & Hamberg, 1986; Clavert, Cranz,

& Bollack, 1990). The proteins secreted by the seminal vesicles are hormonally regulated and are stimulators of sperm motility (Gonzales 2001).

Prostate gland

It is the largest male accessory gland located near the posterior end of the urinary bladder. After birth, the prostate gland undergoes regression followed by quiescence until puberty and then into maturation phase (Kumar & Majumder 1995). The main function of the prostate gland is to secrete semen which contains array of molecules that are required for the sperm function. The prostate gland secretions are slightly alkaline in nature that render protection to spermatozoa from the acidic environment of the female reproductive tract and it also secretes zinc which has antibacterial activity (Fair & Parrish 1981). The prostatic acid phosphatase enzyme secreted by the gland is a marker for prostate cancer (Seamonds et al. 1986).

Cowper's gland

The bulbourethral gland is otherwise called as Cowper's gland. It is a pea nut shaped exocrine gland with a diameter of 1 cm. It is located inferior to the prostate and at the beginning of the penis. It secretes a clear and viscous fluid which helps in increasing the volume and density of the semen (Beil & Hart 1973). During sexual arousal it secretes a pre-ejaculate that lubricates the passage of the sperm. The pre-ejaculate also neutralizes the acidity of the residual urine in urethra thereby making it hospitable for the spermatozoa (Chughtai et al. 2005).

Spermatozoa

Spermatozoa are highly specialized cells and are organized into three regions namely head, mid piece and tail. The head region is mostly occupied by the nucleus and acrosome but also contains a small amount of cytoplasm (Fawcett 1958). The midpiece has been described as

the power plant of the sperm, since the mitochondria are concentrated in this area. They line up end-to-end in the strands that spiral to form a twisted helix (Szollosi 1965). The sperm tail resembles a flagellum; two centrioles from the mid piece extend into the tail. There are two fibrils surrounded by a ring of nine peripheral pairs of fibrils. These fibrils are contractile and produce movement of the sperm tail (Pease 1963). The plasma membrane of cauda spermatozoa has a different composition and different properties than the caput spermatozoa. These changes are responsible for the ability of cauda spermatozoa to fertilize oocytes.

Scrotum

Scrotum is a thin sac like structure that is located behind the penis and in front of the anus. It has two compartments that contain one testis each. The function of the scrotum is to protect testes and to maintain testes at slightly lower temperature than the body. The temperature is controlled by contracting or relaxing the muscles thereby moving the testes close or far from the abdomen (Mickelsen et al. 1981). Spermatogenesis is affected if the testes is maintained at higher temperature than the usual. It is also observed that right testes is located slightly lower than the left testes in the scrotum due to difference in left and right side organ descent during development (Malas et al. 1999).

Penis

It is the main copulatory organ that delivers the semen into the female reproductive tract. It is located outside the abdominal cavity and acts as a passage for urine and also for semen.

Semen

It is a slight yellowish liquid which contains mixture of organic and inorganic compounds and mature spermatozoa. Semen is produced mainly from seminal vesicle although the components of semen are contributed by other organs. It acts as medium through which

spermatozoa are delivered to the female reproductive tract. It also contains various enzymes and proteins that maintain and protect the spermatozoa (Juyena & Stelletta, 2012; Owen & Katz, 2005).

Fertilization

It is the process of male gamete fusing with the female oocyte to form zygote. After ejaculation, the male gametes rest in the uterus of the female reproductive tract for certain period to attain capacitation and undergo hyperactivation (Ikuma et al. 1989). Contents of the semen in combination with female reproductive tract help the sperm in attaining capacitation (Kanwar et al. 1979). The hyperactivated spermatozoa then swim up into the fallopian tube to fertilize the oocyte (Töpfer-Petersen et al. 2000). When the secondary oocyte is encountered by the spermatozoa, an array of changes takes place in both the spermatozoa and the oocyte to form the zygote. For example spermatozoa releases hyaluronidase to degrade the cumulus layer of the oocyte (Kimura et al., 2009; Martin-Deleon, 2011). During fertilization spermatozoa is believed to first interact with zona pellucida proteins (ZP) that act as ligand on the oocyte. The ZP3 protein of the zona interacts with receptor in the spermatozoa and send signals for acrosome reaction (Crozet 1994).

The spermatozoa undergo an exocytotic reaction called as acrosome reaction to release active enzymes that help in its penetration into the oocyte (Harper et al. 2008). Once the sperm membrane fuses with the oocyte membrane, cascade of events takes place resulting in cortical reaction (Saling 1991). The cortical reaction causes increase in perivitelline space, while the sperm nucleus is engulfed by the oocyte cytoplasm, which triggers a calcium wave in the oocyte (Whitaker 2006). This results in signalling events that avoid penetration of multiple spermatozoa thus polyspermy, by hardening the oocyte membrane (Gadella & Evans 2011).

During fertilization only the nucleus of the sperm enters the oocyte resulting in zygote formation (Ramalho-Santos et al. 2002).

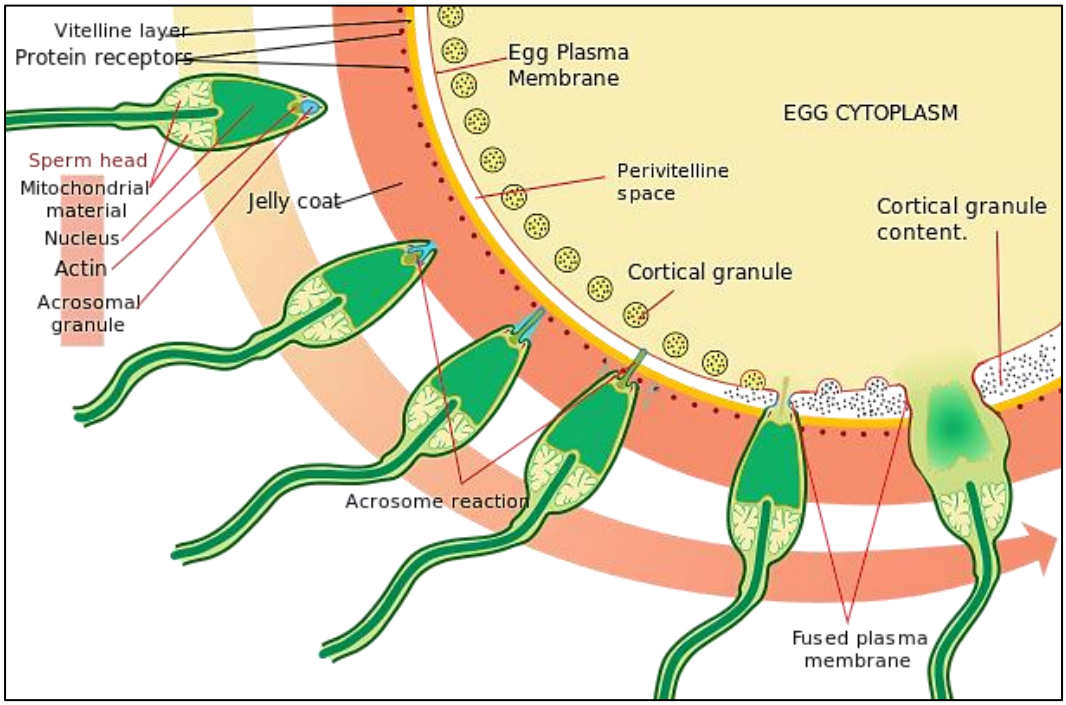

Figure 4: *Events of fertilization (adopted from http://commons.wikimedia.org/wiki/ File: Acrosome_reaction_diagram_en.svg).*

Mucosal surface of the male reproductive tract

Mucosal surface is the thin layer that covers the epithelium of many organs. The thin fluid secreted by the mucosal layer plays an important role as lubricant and as barrier against harsh biological conditions. The mucosal layer also plays a crucial role in innate immunity by hosting immune cells and related molecules. For example, lymphocytes and toll-like receptors (TLRs) in the mucosal layer are important for recognition and evasion of foreign particles (Forchielli and Walker 2005; Lavelle et al. 2010). Nevertheless, the mucosal surface is a dwelling place for many microbes which is evident from the presence of commensals in respiratory (Beck et al. 2012), digestive (Walker 2013) and urinary tracts of the humans (Rampersaud et al. 2012). Although microbes are present in the above said systems the male reproductive tract is specialized in a way that it can be compartmentalized.

Microbes are present only in the penile region of the male reproductive tract, whereas the remaining parts stay sterile (Montagnini Spaine et al. 2000). It may be due to the fact that the male reproductive tract is continuous and infection to it may cause serious threat to propagation of species. For example prostatitis is caused when the commensals of the penile region ascend to the prostate (Roberts et al. 1997) and is related to male infertility (Alshahrani et al. 2013). This implies the importance of maintaining microbe free environment of upper male genital tract organs and strong mechanisms that should operate to keep the system sterile. Unlike other mucosal systems, the distribution and properties of immunocompetent cells of the male genital tract are dependent on the hormones (Nguyen et al. 2014). On the other hand, the male reproductive tract is immunologically privileged (especially the adaptive immunity) by the presence of blood testes barrier in order to protect the haploid spermatozoa (Fijak & Meinhardt 2006). This suggests the dynamic nature of the male reproductive tract. Therefore the mucosal immunity of the male reproductive tract is managed by innate immune machinery along with the secretions of the male reproductive tract.

Secretions of the male reproductive tract

It is well established that the epithelial surfaces of the male reproductive tract secrete an array of proteins into the lumen. These secretions include host defense effector molecules (Hall et al. 2007), antimicrobial peptides (Wang et al. 2012), enzymes and protease inhibitors (Rand et al. 2011). Further they also secrete proteins that are thought to have roles in sperm production, protection and maturation (Dacheux et al. 2003).

Testicular secretions

Along with the spermatozoa, the testes also secretes some proteins and ions such as potassium, chloride and bicarbonate into the lumen of the seminiferous tubule. In general, the secretions of the testes are rich in ions. One of the prominent proteins present in the testicular secretion is androgen binding protein (ABP) (French & Ritzén 1973). It is secreted by the Sertoli cells and the androgens are made available to the cells through ABP. Some of the other proteins present in the testicular secretions include cysteine rich secretory protein (CRISP2) (Ernesto et al. 2012), testes specific protein 1 (TPX1) (Du et al. 2006) (Sivashanmugam et al. 1999) and sperm acrosomal membrane associated protein (SAMP32) (Hao et al. 2002). The secretions of the testes are collected at the rete testes and passed to the epididymis.

Epididymal secretions

The initial segment of the epididymis absorbs some of the fluids secreted from the testes, whereas the remaining part including immature spermatozoa pass through the tubular structures of epididymis. **S**permatozoa and testicular secretions combine with epididymal secretions in the epididymal lumen, that allow the mammalian spermatozoa to undergo a series of complex and sequential events thereby allowing them to acquire the capacity for vitellus fusion, penetration and fertilization. It is reported that epididymis secretes proteins such as HongrES1 (Zhou et al. 2008) and HE4 (Kirchhoff 1998) that are added on to the sperm surface and play role in fertilization. The epididymis also secretes cystatin 11 (CST11) (Jiborn et al. 2004), lactoferrin (Jin et al. 1997), human cathelicidin antimicrobial peptide (hCAP18) (Malm et al. 2000), ESP13.2 (Yudin et al. 2003), members of the SPAG11 family (Yenugu et al. 2006) and defensins (Hall et al. 2007) which have been shown to have antibacterial activity. Some of the members of defensin and SPAG11 family are shown to

have role in fertilization, suggesting bifunctional role for these proteins in epididymal innate immunity and reproductive functions (Yudin et al. 2003). During transit from the epididymis until fertilization, the spermatozoa undergo several biochemical and physiological changes. At this stage, the spermatozoa are unable to undergo transcription and translation (Hamatani 2012), hence it depends on the peripheral proteins and post-translational modifications to perform its function. This notion supports the importance of the secretory proteins in the male reproductive tract.

Results of the recent efforts made to analyse the secretome of the male reproductive tract through proteomics approach were encouraging. Mapping of the testicular proteins and their relation with epididymal proteins are given in figure 4. By comparing the proteomes of testes, epididymis and spermatozoa it reported that 47% of the proteins in the sperm are intrinsic and are acquired from testes (Li et al. 2011). 23% of the proteins are extrinsic that are acquired from the environment, clearly suggesting that secretory proteins in the lumen are added on to the sperm surface.

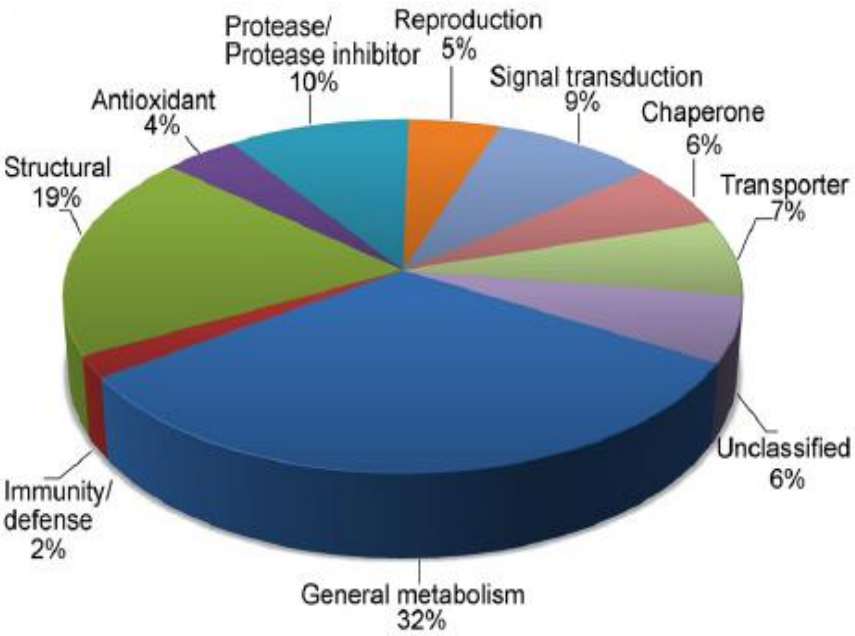

Figure 4: *Testicular proteins categorized by function.*

It is also reported that acrosomal protein content of caput and caudal sperm are different, suggesting that sperm undergoes changes during the transit. Moreover, the presence of amyloidogenic proteins in the acrosomal matrix of the spermatozoa was observed (Guyonnet et al. 2012). Amyloid formation is one of the mechanism to sort proteins of secretory pathway (Stettler et al. 2009) and to attain stable structure to execute a biological function. For example cystatin-related epididymal spermatogenic (CRES) protein is present in the germ cells and also in the acrosome region of the sperm (Syntin & Cornwall 1999). It is antimicrobial (Wang et al. 2012) and is reported to form amyloids *in vitro* and *in vivo* (Whelly et al. 2012).

Along with cystatin-c, cystatin 8 and premelanosome protein, presence of lysozyme-like 1, 3, 4 and 5 (LYZL1, LYZL3, LYZL4 and LYZL5) proteins in the acrosomal matrix of the mouse spermatozoa was reported (Guyonnet et al. 2012). The LYZL proteins that are similar to lysozyme also possess the amyloidogenic domains suggesting that they may play important role like CRES proteins. Given the importance of amyloidogenic secretory proteins for the fertility of the individual and perpetuation of the species, it is essential to understand the genes involved in the production, protection and maturation of spermatozoa. Though some of the LYZL proteins are reported, the role of LYZL proteins in the male reproductive function are not yet studied.

Lysozyme

Lysozyme is an antimicrobial enzyme that was discovered by Alexander Fleming in 1930s. It belongs to the group of enzymes called glycoside hydrolases and catalyses the hydrolysis of the glycosidic linkage to release smaller sugars. In nature, the glycosidases are involved in degradation of biomass such as cellulose and hemicellulose, anti-bacterial defense strategies, pathogenesis mechanisms and normal cellular functions such as trimming mannosidase

involved in N-linked glycoprotein biosynthesis. Together with glycosyltransferases, glycosidases form the major catalytic machinery for the synthesis and breakage of glycosidic bonds. Lysozymes hydrolyse the β-glycosidic linkages between N-acetyl muramic acid and N-acetyl glucosamine in the peptidoglycan of bacterial cell walls (Chipman et al. 1967). They also can bind polymers of N-acetyl glucosamine. The antimicrobial activity of lysozyme is potent against certain Gram-positive bacteria and to a much lesser degree against Gram-negative bacteria. Further, a chemical similarity between peptidoglycan and chitin allows some lysozymes to hydrolyse chitin (Skujiņś et al. 1973), but less efficiently than their natural substrate (Boller et al. 1983; Jekel, Hartmann, and Beintema 1991). The known physiological functions of lysozymes include inactivation of viruses, immune regulatory activity, ant-inflammatory and antitumor activity. Lysozyme has been shown to interact with DNA with similar affinity as that of histone associated DNA (Lin et al. 2009). This binding mechanism is considered as one of the reason for the anti-HIV activity of lysozyme. Very recently Kajla et al. have showed a surprising role for lysozyme c1(LYSC1). They have reported that LYSC1 can interact with *Plasmodium* oocysts and can protect them in *Anopheles* midgut (Kajla et al. 2011). In humans, a positive relationship between seminal plasma lysozyme levels and sperm motility has been reported (Mendeluk et al. 1997). Basing on their physical and functional properties, the lysozymes are classified into six families (figure 5) (Lien CalleWaert et al. 2010).

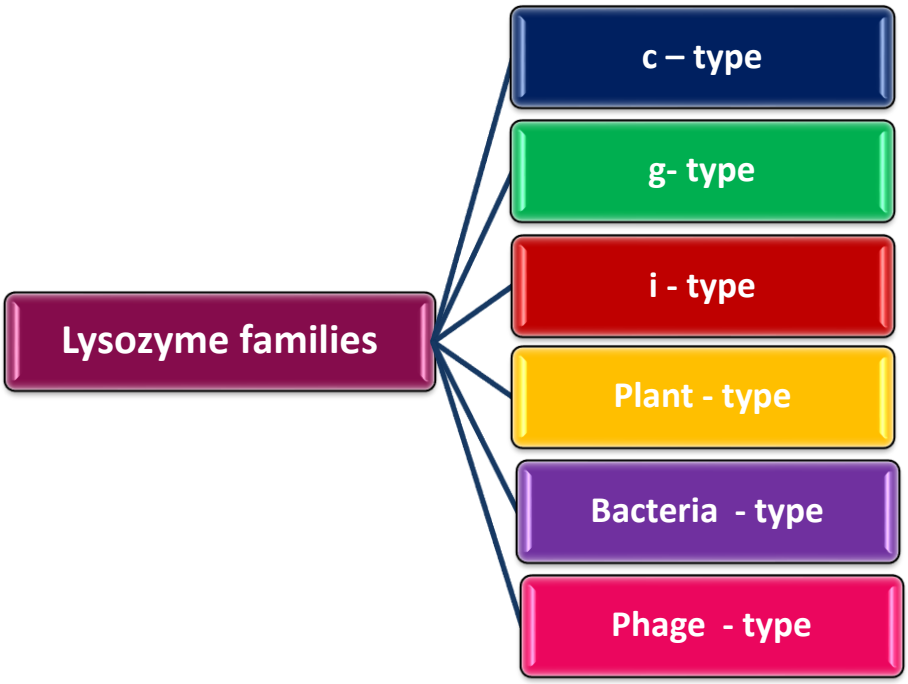

Figure 5: *Classification of lysozyme family.*

C-type

The c-type stands for chicken type or the conventional type lysozyme. Among the different lysozyme types, the c-type are widely distributed across the species. They participate in antibacterial defenses to form components of the innate immune system. Their distribution among white blood cells (Tyshko & Gavrilenko 1991) , macrophages and in a number of secretions such as tears (Sen & Sarin 1986), saliva (Jenzano et al. 1986), mucosal secretions and human milk (Jolles & Jolles 1961) strengthen their role in innate immune defense (You et al. 2010).

G-type

G type is otherwise called as goose-type. They were initially identified in goose and found to be distributed among most of the avian species and also among other organisms (Larsen et al. 2009). The g-type lysozymes are present in mammals but their functions are not clear. In

general they were reported to have antibacterial activity. The g-type lysozymes possess slightly higher molecular weight range than the c-type lysozymes. Some of the g-type lysozymes are not secretory (Irwin & Gong 2003).

I-type

The i-type stands for invertebrate-type and are found only among invertebrates. They play an important role in invertebrate immune system. Their presence in mollusks is well established (Marcela et al. 2009). The i-type lysozymes possess isopeptidase activity (Baskova et al. 2001), though it is not universal for all the i-type lysozymes. Since most of the invertebrates dwell in water or on decomposed material they tend to ingest more bacteria. It is believed that the i- type lysozyme present in the gut area play a role in digestion by breaking down the bacteria ingested by these organisms (Xue et al. 2007).

Plant-type

P- type lysozymes exists in many of the plant species especially in the latex (Beintema & Terwisscha van Scheltinga 1996). Most of the lysozymes in plant species are bifunctional and they seem to have chitinase activity in addition to lysozyme activity and that the former is more pronounced. Notable feature of the plant type lysozymes is that they are basic in nature and the chitinase activity contributes to their antifungal activity (Wang et al. 2005) .

Bacteria-type

B-type lysozymes are conserved in bacteria that contain peptidoglycan. It is believed that they play a vital role during bacterial cell enlargement and division (Höltje 1996). The soluble lytic transglycosylase (SLT) present in the *E. coli* is reported to act on succulus which is one of the major step during bacterial cell division and these SLTs belong to lysozyme superfamily (Thunnissen, Isaacs, & Dijkstra, 1995) .

Phage type

The phage lysozymes encoded by the bacteriophage genome play a vital role during the lytic cycle. It helps in lysing the cell wall of the bacteria releasing the phages. The phage lysozymes are also useful in infecting the bacteria where the membrane damage is essential (Fastrez 1996).

Lysozyme-like proteins

Besides the classical lysozymes, a group of lysozyme-like (*Lyzl*) genes were identified and are found to be conserved and distributed among various species. LYZL proteins are found to be present in the cystoviridae family of phages. Although their sequences are fairly diverged from lysozyme they have been shown to possess similar fold patterns and active sites as that of lysozyme (Pei & Grishin 2005). Sequence analysis of vertebrate *Lyzl* genes suggest that the LYZL proteins have features that are characteristic to lysozyme. LYZL proteins identified till date are LYZL1, LYZL2, SLLP1/LYZL3, LYZL4, LYZL5, LYZL6 and LYZL7 and are predominantly expressed in the male reproductive tract of humans (Zhang et al. 2005).

Alpha lactalbumin is otherwise called as LYZL7, it belongs to glycoside hydrolase family and is a homologous protein of lysozyme. The primary sequence and the three dimensional structure are identical to lysozyme. However, the expression pattern and functions of the lactalbumin are different from lysozyme. Lactalbumin is expressed mainly in mammary glands and is present in milk of almost all the mammals. It is involved in lactose production, calcium binding and non-bacteriolytic unlike lysozyme. Recently, a modified form of lactalbumin HAMLET (human lactalbumin made lethal to tumors) was reported to have apoptotic activity against tumor cells (Hallgren et al. 2008).

Among the *Lyzl* genes, *Lyzl3/Sllp1* was found to be expressed specifically in the male reproductive tract (Mandal et al. 2003). Spermatozoa incubated with antibodies to human SLLP1 failed to fertilize eggs, thereby demonstrating a role in male reproductive function. Microscopic studies revealed that LYZL3 is located in the acrosomal region before capacitation and moves towards the equatorial segment after capacitation, suggesting that LYZL3 may be an intra-acrosomal protein that is tightly bound to the sperm membrane. Further, interaction studies performed using LYZL3 and oocyte lysate revealed that it may interact with SAS1B an oolemma protein (Sachdev et al. 2012) and the same was confirmed by surface plasmon resonance. Similarly, incubation of spermatozoa with the mouse LYZL4 antibodies resulted in loss of fertilizing ability (Sun et al. 2011). In the mouse, LYZL6 was reported to be present in testes, epididymis and spermatozoa and is antimicrobial in nature (Wei et al. 2013).

REFERENCES

Alshahrani, S., McGill, J. & Agarwal, A., 2013. Prostatitis and male infertility. *Journal of reproductive immunology*, 100(1), pp.30–6.

Amann, R.P., 2008. The cycle of the seminiferous epithelium in humans: a need to revisit? *Journal of andrology*, 29(5), pp.469–87.

Aumüller, G. & Riva, A., 1992. Morphology and functions of the human seminal vesicle. *Andrologia*, 24(4), pp.183–96.

Barsoum, I. & Yao, H.H.-C., 2006. The road to maleness: from testis to Wolffian duct. *Trends in endocrinology and metabolism: TEM*, 17(6), pp.223–8.

Baskova, I.P. et al., 2001. Separation of monomerizing and lysozyme activities of destabilase from medicinal leech salivary gland secretion. *Biochemistry. Biokhimiia*, 66(12), pp.1368–73.

Beck, J.M., Young, V.B. & Huffnagle, G.B., 2012. The microbiome of the lung. *Translational research : the journal of laboratory and clinical medicine*, 160(4), pp.258–66.

Beil, R.E. & Hart, R.C., 1973. Cowper's Gland Secretion in Rat Semen Coagulation: II. Identification of the Potentiating Factor Secreted by the Coagulating Glands. *Biol Reprod*, 8(5), pp.613–617.

Beintema, J.J. & Terwisscha van Scheltinga, A.C., 1996. Plant lysozymes. *Experientia*, 75(1), pp.75–86.

Boller, T. et al., 1983. Chitinase in bean leaves: induction by ethylene, purification, properties, and possible function. *Planta*, 157(1), pp.22–31.

Brennan, J. et al., 1998. Sry and the testis: molecular pathways of organogenesis. *The Journal of experimental zoology*, 281(5), pp.494–500.

Chipman, D.M., Grisaro, V. & Sharon, N., 1967. The binding of oligosaccharides containing N-acetylglucosamine and N-acetylmuramic acid to lysozyme. The specificity of binding subsites. *The Journal of biological chemistry*, 242(19), pp.4388–94.

Chughtai, B. et al., 2005. A neglected gland: a review of Cowper's gland. *International journal of andrology*, 28(2), pp.74–7.

Clavert, A., Cranz, C. & Bollack, C., 1990. Functions of the seminal vesicle. *Andrologia*, 22 Suppl 1, pp.185–92.

Cornwall, G. a, 2009. New insights into epididymal biology and function. *Human reproduction update*, 15(2), pp.213–27.

Crozet, N., 1994. [Acrosome reaction and fertilization]. *Contraception, fertilité, sexualité (1992)*, 22(5), pp.328–30.

Dacheux, J.-L., Gatti, J.L. & Dacheux, F., 2003. Contribution of epididymal secretory proteins for spermatozoa maturation. *Microscopy Research and Technique*, 61(1), pp.7–17.

Du, Y. et al., 2006. Human testis specific protein 1 expression in human spermatogenesis and involvement in the pathogenesis of male infertility. *Fertility and sterility*, 85(6), pp.1852–4.

Dym, M. & Fawcett, D.W., 1970. The Blood-Testis Barrier in the Rat and the Physiological Compartmentation of the Seminiferous Epithelium. *Biol Reprod*, 3(3), pp.308–326.

Ernesto, J.I. et al., 2012. Evaluation of Testicular Sperm CRISP2 as a Potential Target for Contraception. *Journal of andrology*, 33(6), pp.1360–1370.

Fair, W.R. & Parrish, R.F., 1981. Antibacterial substances in prostatic fluid. *Progress in clinical and biological research*, 75A, pp.247–64.

Fastrez, J., 1996. Phage lysozymes. *Experientia*, 75, pp.35–64.

Fawcett, D.W., 1958. The Structure of the Mammalian Spermatozoon. *International Review of Cytology*, 7, pp.195–234.

Fijak, M. & Meinhardt, A., 2006. The testis in immune privilege. *Immunological reviews*, 213, pp.66–81.

Forchielli, M.L. & Walker, W.A., 2005. The role of gut-associated lymphoid tissues and mucosal defence. *The British journal of nutrition*, 93 Suppl 1, pp.S41–8.

Franchimont, P., 1983. Regulation of gonadal androgen secretion. *Hormone research*, 18(1-3), pp.7–17.

French, F.S. & Ritzén, E.M., 1973. Androgen-binding protein in efferent duct fluid of rat testis. *Journal of reproduction and fertility*, 32(3), pp.479–83.

Gadella, B.M. & Evans, J.P., 2011. Membrane fusions during mammalian fertilization. *Advances in experimental medicine and biology*, 713, pp.65–80.

Gonzales, G.F., 2001. Function of seminal vesicles and their role on male fertility. *Asian journal of andrology*, 3(4), pp.251–8.

Guyonnet, B. et al., 2012. Isolation and proteomic characterization of the mouse sperm acrosomal amtrix. , pp.1–48.

Hall, S.H. et al., 2007. Characterization and functions of beta defensins in the epididymis. *Asian journal of andrology*, 9(4), pp.453–62.

Hallgren, O. et al., 2008. Apoptosis and tumor cell death in response to HAMLET (human alpha-lactalbumin made lethal to tumor cells). *Advances in experimental medicine and biology*, 606(1), pp.217–40.

Hamatani, T., 2012. Human spermatozoal RNAs. *Fertility and sterility*, 97(2), pp.275–81.

Hansson, V. et al., 1976. Hormones and hormonal target cells in the testis. *Andrologia*, 8(3), pp.195–202.

Hao, Z. et al., 2002. SAMP32, a testis-specific, isoantigenic sperm acrosomal membrane-associated protein. *Biology of reproduction*, 66(3), pp.735–44.

Harper, C. V et al., 2008. Dynamic resolution of acrosomal exocytosis in human sperm. *Journal of cell science*, 121(Pt 13), pp.2130–5.

Heller, C.G. & Clermont, Y., 1963. Spermatogenesis in Man: An Estimate of Its Duration. *Science*, 140(3563), pp.184–186.

Höltje, J. V, 1996. Bacterial lysozymes. *Experientia*, 75(1), pp.65–74.

Huszar G, Sbracia M, Vigue L, Miller DJ, S.B., 1997. Sperm plasma membrane remodeling during spermiogenetic maturation in men: relationship among plasma membrane beta 1,4-galactosyltransferase, cytoplasmic creatine phosphokinase, and creatine phosphokinase isoform ratios. *Biology of reproduction*, 56(4), pp.1020–1024.

Ikuma, K. et al., 1989. [Role of sperm passage through cervical mucus: fertilizing capacity tested by in vitro fertilization with zona-free hamster eggs]. *Nihon Sanka Fujinka Gakkai zasshi*, 41(2), pp.167–72.

Irwin, D.M. & Gong, Z., 2003. Molecular evolution of vertebrate goose-type lysozyme genes. *Journal of molecular evolution*, 56(2), pp.234–42.

Jekel, P.A., Hartmann, B.H. & Beintema, J.J., 1991. The primary structure of hevamine, an enzyme with lysozyme/chitinase activity from Hevea brasiliensis latex. *European journal of biochemistry / FEBS*, 200(1), pp.123–30.

Jenzano, J.W., Hogan, S.L. & Lundblad, R.L., 1986. Factors influencing measurement of human salivary lysozyme in lysoplate and turbidimetric assays. *Journal of clinical microbiology*, 24(6), pp.963–7.

Jiang, X.-H. et al., 2014. Blood-testis barrier and spermatogenesis: lessons from genetically-modified mice. *Asian journal of andrology*, 16(4), pp.572–80.

Jiborn, T. et al., 2004. Cystatin C is highly expressed in the human male reproductive system. *Journal of andrology*, 25(4), pp.564–72.

Jin, Y.Z. et al., 1997. Direct evidence for the secretion of lactoferrin and its binding to sperm in the porcine epididymis. *Molecular reproduction and development*, 47(4), pp.490–6.

Jolles, P. & Jolles, J., 1961. Lysozyme from Human Milk. *Nature*, 192(4808), pp.1187–1188.

Juyena, N.S. & Stelletta, C., 2012. Seminal plasma: an essential attribute to spermatozoa. *Journal of andrology*, 33(4), pp.536–51.

Kajla, M.K. et al., 2011. A New Role for an Old Antimicrobial : Lysozyme c-1 Can Function to Protect Malaria Parasites in Anopheles Mosquitoes. *PloS one*, 6(5), p.e19649.

Kanwar, K.C., Yanagimachi, R. & Lopata, A., 1979. Effects of human seminal plasma on fertilizing capacity of human spermatozoa. *Fertility and sterility*, 31(3), pp.321–7.

Kimura, M. et al., 2009. Functional roles of mouse sperm hyaluronidases, HYAL5 and SPAM1, in fertilization. *Biology of reproduction*, 81(5), pp.939–47.

Kirchhoff, C., 1998. Molecular characterization of epididymal proteins. *Reviews of reproduction*, 3(2), pp.86–95.

Kumar, V.L. & Majumder, P.K., 1995. Prostate gland: Structure, functions and regulation. *International Urology and Nephrology*, 27(3), pp.231–243.

Larsen, A.N. et al., 2009. Molecular characterisation of a goose-type lysozyme gene in Atlantic cod (Gadus morhua L .). *Fish and Shellfish Immunology*, 26(1), pp.122–132.

Lavelle, E.C. et al., 2010. The role of TLRs, NLRs, and RLRs in mucosal innate immunity and homeostasis. *Mucosal immunology*, 3(1), pp.17–28.

Li, J. et al., 2011. Mapping of the Human Testicular Proteome and its Relationship With That of the Epididymis and Spermatozoa. *molecular and cellular proteomics*, 3(3), pp.1–11.

Lien CalleWaert, C.M., Callewaert, L. & Michiels, C.W., 2010. Lysozymes in the animal kingdom. *J Biosci*, 35(March), pp.127–160.

Lin, K.-C. et al., 2009. Characterization of the interactions of lysozyme with DNA by surface plasmon resonance and circular dichroism spectroscopy. *Applied biochemistry and biotechnology*, 158(3), pp.631–41.

Mahony, M.C. et al., 1993. Functional and morphological features of spermatozoa microaspirated from the epididymal regions of cynomolgus monkeys (Macaca fascicularis). *Biology of reproduction*, 48(3), pp.613–20.

Majumder, G.C. & Turkington, R.W., 1976. Regulation by testosterone and serum protein of DNA synthesis in the developing epididymis of the rat. *The Journal of endocrinology*, 70(1), pp.105–15.

Malas, M.A., Sulak, O. & Oztürk, A., 1999. The growth of the testes during the fetal period. *British Journal of urology international*, 84(6), pp.689–92.

Malm, J. et al., 2000. The human cationic antimicrobial protein (hCAP-18) is expressed in the epithelium of human epididymis, is present in seminal plasma at high concentrations, and is attached to spermatozoa. *Infection and immunity*, 68(7), pp.4297–302.

Mandal, A. et al., 2003. SLLP1, a unique, intra-acrosomal, non-bacteriolytic, c lysozyme-like protein of human spermatozoa. *Biology of reproduction*, 68(5), pp.1525–37.

Marcela, S., Procha, P. & Bilej, M., 2009. Identification and cloning of an invertebrate-type lysozyme from Eisenia andrei ˇ ilerova. *developmental and comparative immunology*, 33(1), pp.932–938.

Martin-Deleon, P.A., 2011. Germ-cell hyaluronidases: their roles in sperm function. *International journal of andrology*, 34(5 Pt 2), pp.e306–18.

Mendeluk, G.R., Blanco, A.M. & Bregni, C., 1997. Viscosity of human seminal fluid: role of lysozyme. *Archives of andrology*, 38(1), pp.7–11.

Mickelsen, W.D., Paisley, L.G. & Dahmen, J.J., 1981. The effect of season on the scrotal circumference and sperm motility and morphology in rams. *Theriogenology*, 16(1), pp.45–51.

Montagnini Spaine, D. et al., 2000. Microbiologic aerobic studies on normal male urethra. *Urology*, 56(2), pp.207–10.

Nef, S., 2000. Hormones in male sexual development. *Genes & Development*, 14(24), pp.3075–3086.

Nguyen, P. V et al., 2014. Innate and adaptive immune responses in male and female reproductive tracts in homeostasis and following HIV infection. *Cellular & molecular immunology*.

Nikolopoulou, M., Soucek, D.A. & Vary, J.C., 1985. Changes in the lipid content of boar sperm plasma membranes during epididymal maturation. *Biochimica et biophysica acta*, 815(3), pp.486–98.

Oatley, J.M. & Brinster, R.L., 2012. The germline stem cell niche unit in mammalian testes. *Physiological reviews*, 92(2), pp.577–95.

Oliw, E.H., Sprecher, H. & Hamberg, M., 1986. Isolation of two novel E prostaglandins in human seminal fluid. *The Journal of biological chemistry*, 261(6), pp.2675–83.

Olson, G.E. & Hamilton, D.W., 1978. Characterization of the surface glycoproteins of rat spermatozoa. *Biology of reproduction*, 19(1), pp.26–35.

Owen, D.H. & Katz, D.F., 2005. A review of the physical and chemical properties of human semen and the formulation of a semen simulant. *Journal of andrology*, 26(4), pp.459–69.

Pease, D.C., 1963. The ultrastructure of flagellar fibrils. *The Journal of Cell Biology*, 18(2), pp.313–326.

Pei, J. & Grishin, N. V, 2005. COG3926 and COG5526: a tale of two new lysozyme-like protein families. *Protein science*, 14(10), pp.2574–81.

Ramalho-Santos, J., Schatten, G. & Moreno, R.D., 2002. Control of membrane fusion during spermiogenesis and the acrosome reaction. *Biology of reproduction*, 67(4), pp.1043–51.

Rampersaud, R., Randis, T.M. & Ratner, A.J., 2012. Microbiota of the upper and lower genital tract. *Seminars in fetal & neonatal medicine*, 17(1), pp.51–7.

Rand, M.G.O. et al., 2011. Functional studies of eppin. *Biochemical Society transactions*, 39(1), pp.1447–1449.

Rato, L. et al., 2012. Metabolic regulation is important for spermatogenesis. *Nature reviews. Urology*, 9(6), pp.330–8.

Robaire, B. & Hinton, B.T., 2006. The Epididymis. *Knobil and Neill's Physiology*, Third edit, pp.1071–1148.

Roberts, R.O. et al., 1997. A review of clinical and pathological prostatitis syndromes. *Urology*, 49(6), pp.809–821.

Sachdev, M. et al., 2012. Oocyte speci fi c oolemmal SAS1B involved in sperm binding through intra-acrosomal SLLP1 during fertilization. *Developmental Biology*, 363(1), pp.40–51.

Saling, P.M., 1991. How the egg regulates sperm function during gamete interaction: facts and fantasies. *Biology of reproduction*, 44(2), pp.246–51.

Schmahl, J. et al., 2000. Sry induces cell proliferation in the mouse gonad. *Development (Cambridge, England)*, 127(1), pp.65–73.

Seamonds, B. et al., 1986. Evaluation of prostate-specific antigen and prostatic acid phosphatase as prostate cancer markers. *Urology*, 28(6), pp.472–9.

Sen, D.K. & Sarin, G.S., 1986. Biological variations of lysozyme concentration in the tear fluids of healthy persons. *The British journal of ophthalmology*, 70(4), pp.246–8.

Shum, W.W.C. et al., 2009. Regulation of luminal acidification in the male reproductive tract via cell-cell crosstalk. *The Journal of experimental biology*, 212(11), pp.1753–61.

Sivashanmugam, P. et al., 1999. Cloning and characterization of an androgen-dependent acidic epididymal glycoprotein/CRISP1-like protein from the monkey. *Journal of andrology*, 20(3), pp.384–93.

Sizonenko, P.C., 1989. Physiology of puberty. *Journal of endocrinological investigation*, 12(8 Suppl 3), pp.59–63.

Skujiņś, J., Puķite, A. & McLaren, A.D., 1973. Adsorption and reactions of chitinase and lysozyme on chitin. *Molecular and cellular biochemistry*, 2(2), pp.221–8.

Stettler, H. et al., 2009. Determinants for chromogranin A sorting into the regulated secretory pathway are also sufficient to generate granule-like structures in non-endocrine cells. *The Biochemical journal*, 418(1), pp.81–91.

Sun, R. et al., 2011. Lyzl4 , a novel mouse sperm-related protein , is involved in fertilization. *Acta biochimica et biophysica sinica*, 3(1), pp.1–8.

Svingen, T. & Koopman, P., 2013. Building the mammalian testis: origins, differentiation, and assembly of the component cell populations. *Genes & development*, 27(22), pp.2409–26.

Syntin, P. & Cornwall, G.A., 1999. Immunolocalization of CRES (Cystatin-related epididymal spermatogenic) protein in the acrosomes of mouse spermatozoa. *Biology of reproduction*, 60(6), pp.1542–52.

Szollosi, D., 1965. The fate of sperm middle-piece mitochondria in the rat egg. *Journal of Experimental Zoology*, 159(3), pp.367–377.

Temple-Smith, P.D., 1984. Phagocytosis of sperm cytoplasmic droplets by a specialized region in the epididymis of the brushtailed possum, Trichosurus vulpecula. *Biology of reproduction*, 30(3), pp.707–20.

Thunnissen, A.M., Isaacs, N.W. & Dijkstra, B.W., 1995. The catalytic domain of a bacterial lytic transglycosylase defines a novel class of lysozymes. *Proteins*, 22(3), pp.245–58.

Töpfer-Petersen, E., Petrounkina, A.M. & Ekhlasi-Hundrieser, M., 2000. Oocyte-sperm interactions. *Animal reproduction science*, 60-61, pp.653–62.

Tyshko, N.A. & Gavrilenko, T.I., 1991. [The lysozyme content of phagocytosing peripheral blood cells in sarcoidosis patients]. *Vrachebnoe delo*, (7), pp.71–3.

Walker, W.A., 2013. Initial intestinal colonization in the human infant and immune homeostasis. *Annals of nutrition & metabolism*, 63 Suppl 2, pp.8–15.

Wang, L. et al., 2012. Antimicrobial activity and molecular mechanism of the CRES protein. *PloS one*, 7(11), p.e48368.

Wang, S. et al., 2005. First report of a novel plant lysozyme with both antifungal and antibacterial activities. *Biochemical and biophysical research communications*, 327(3), pp.820–7.

Wei, J. et al., 2013. Characterisation of Lyzls in mice and antibacterial properties of human LYZL6. *Asian Journal of Andrology*, 14(6), pp.834–830.

Whelly, S. et al., 2012. Nonpathological extracellular amyloid is present during normal epididymal sperm maturation. *PloS one*, 7(5), p.e36394.

Whitaker, M., 2006. Calcium at fertilization and in early development. *Physiological reviews*, 86(1), pp.25–88.

Wilhelm, D., Yang, J.X. & Thomas, P., 2013. Mammalian sex determination and gonad development. *Current topics in developmental biology*, 106, pp.89–121.

Xue, Q.-G. et al., 2007. A new lysozyme from the eastern oyster (Crassostrea virginica) indicates adaptive evolution of i-type lysozymes. *Cellular and molecular life sciences*, 64(1), pp.82–95.

Yenugu, S. et al., 2006. Identification, cloning and functional characterization of novel sperm associated antigen 11 (SPAG11) isoforms in the rat. *Reproductive biology and endocrinology*, 4, p.23.

You, S.-J. et al., 2010. Multifunctional peptides from egg white lysozyme. *Food Research International*, 43(3), pp.848–855.

Yudin, A.I. et al., 2003. ESP13.2, a member of the beta-defensin family, is a macaque sperm surface-coating protein involved in the capacitation process. *Biology of reproduction*, 69(4), pp.1118–28.

Zhang, K. et al., 2005. Molecular Cloning and Characterization of Three Novel Lysozyme-Like Genes , Predominantly Expressed in the Male Reproductive System of Humans , Belonging to the C-Type Lysozyme / Alpha-Lactalbumin Family 1. *Biology of reproduction*, 1071(73), pp.1064–1071.

Zhou, Y. et al., 2008. An epididymis-specific secretory protein HongrES1 critically regulates sperm capacitation and male fertility. *PloS one*, 3(12), p.e4106.

CHAPTER 1

- *Molecular characterization of rat lysozyme-like protein in silico.*

INTRODUCTION

Understanding the complex biological process at the cellular level is facilitated by the availability of novel *in silico* techniques to analyse samples on a large scale. The development of high-throughput techniques such as whole genome sequencing, DNA microarray and protein microarray has offered researchers a multitude of opportunities to study various processes at molecular level. This had a direct impact in the field of bioinformatics, which is clearly evident from the availability of a vast number of repositories or databases. Affordable access and availability of these tools to analyse large scale data has made *in silico* studies a hot spot in recent years. *In silico* studies also supported investigations that led to significant biological discoveries in drug discovery, where time consumption is reduced manifold. Therefore researchers use *in silico* approaches as the starting point to characterise the role of genes and proteins. In this study, we characterized the rat lysozyme-like (*Lyzl*) genes and proteins using *in silico* tools to understand their genomic neighbourhood, gene structure, protein domains, evolutionary status, conservation of sequence and tertiary structure.

Lysozyme (E.C. 3.2.1.17) represents an important class of polysaccharide-hydrolysing enzymes (also called muramidase or N-acetylmuramide glycanhydrolase). They hydrolyse peptidoglycans which contain alternating β-1-4 linked residues of N-acetyl glucosamine and N-acetylmuramic acid (Chipman et al. 1967) and are classified into c-type, g-type, i-type, plant type and phage type. They serve in antibacterial defense (Pellegrini et al. 1997) thereby forming a part of the innate immune system, which is also evidenced by their distribution among white blood cells (Hansen & Andersen 1973), tissue macrophages (Allen et al. 1984) and in a number of secretions such as tears (Sen & Sarin 1986), saliva (Jenzano et al. 1986) , nasal mucus (Dajani et al. 2005) and human milk (Jolles & Jolles 1961) as well as in avian egg white (Gordon Alderton & Fevold 1945). The chemical

similarity between peptidoglycan and chitin allows some lysozymes to hydrolyse chitin, but less efficiently than their natural substrate (Boller et al. 1983; Jekel, Hartmann, and Beintema 1991). Lysozyme has the distinction that it is the protein with highest number of crystal structures, thus demonstrating the vast amount of scientific interest it has generated.

Recently, a new class of proteins namely lysozyme-like (LYZL) proteins were reported in many species. LYZL proteins identified till date are LYZL1, LYZL2, SLLP1/LYZL3, LYZL4, LYZL5, LYZL6 and LYZL7 and are predominantly expressed in male reproductive tract (Zhang et al. 2005) . They belong to the c-type lysozyme family of lysozyme. The role of LYZL proteins in reproductive physiology has gained importance. For example, the mouse SLLP1/LYZL3 was found to play a key role in fertilization by acting as possible receptor for the interaction of glycoproteins on the ovum (Sachdev et al. 2012). Although the LYZL proteins are reported they are not well characterized in many species including the rat. Therefore this part of the study focuses on *in silico* analysis of rat LYZL proteins.

MATERIALS AND METHODS

Primary structure analysis

The rat genome (build RGSC v3.4) was searched using the BLAST program available at the NCBI website to identify the rat *Lyzl* genes. Chicken lysozyme gene sequence was used as a query to find out similar sequences present in the rat genome. Sequences of the rat *Lyzl* genes were then analysed using various *in silico* tools to understand its primary, secondary and tertiary structure (Table 1).

Table 1: Tools used for *in silico* analysis

S. No	Analysis	Tool used	Website
1	Sequence retrieval	NCBI nucleotide	http://www.ncbi.nlm.nih.gov/nuccore/
2	Similarity search	NCBI BLAST	http://blast.ncbi.nlm.nih.gov/Blast.cgi
3	Multiple sequence alignment	T-COFFEE	http://tcoffee.crg.cat/
4	Pairwise alignment	CLUSTALW	http://www.genome.jp/tools/clustalw/
5	Conserved Domain prediction	NCBI CDD	http://www.ncbi.nlm.nih.gov/cdd/
6	General properties	EXPASY server	http://expasy.org/proteomics
7	Post translational modification	Sequence manipulation suite	http://www.bioinformatics.org/sms2/

Genomic neighbourhood analysis

Various factors are known to affect the expression of one or several genes simultaneously. These includes cis regulatory elements such as transcription factor binding sites in the upstream of gene (spanning a few bases) or organisation of chromosomes into territories within the nucleus (spanning entire chromosomes) (Rodríguez, Kirby, and Hinton 2001; Chatterjee and Lufkin 2012) . In addition to the above, genomic neighbourhoods (spanning several megabases) contribute to an important level of regulation of gene expression (Zhang et al. 2013; De and Babu 2010). The concept of genomic neighbourhood discussed here is distinct from segments referred to as co-expression domains, which are regions containing clusters of highly expressed genes on the chromosome. Here we discuss genomic neighbourhood in terms of sequence of the genes that are present next to the gene of interest and also the orientation of the gene. Genomic neighbourhood analysis was performed based on the genome assemblies deposited in NCBI and Ensembl. The organization of genes adjacent to the *Lyzl* genes was used to determine whether the genes of interest reside in conserved genomic neighbourhoods.

Phylogenetic analysis

Phylogeny is the means for studying the evolutionary relationship of a gene. Although phylogeny can be studied using both DNA and protein sequences, using the latter is preferred due to the redundancy of nucleotides. LYZL protein sequences were collected from various organisms and multiple sequence alignment was performed. Phylogenetic tree was constructed from the multiple sequence alignment to understand the evolution of LYZL proteins and their conservation among various organisms. Neighbourhood joining method was used for phylogenetic tree construction. Unrooted tree was constructed with

the maximum sequence difference of 0.85. The phylogenetic tree was constructed using phylogenetic tree option in the BLAST program.

Domains / Motif prediction

Proteins having similar functions may not show appreciable homology yet may contain sequences of amino acid residues that are highly conserved among all referred to as motifs. Motif prediction was performed for rat LYZL proteins using Multiple Em for Motif Elicitation program (http://meme.nbcr.net/meme/cgi-bin/meme.cgi) (Ma et al. 2014).

Secondary structure prediction

The Self-Optimized Prediction Method with Alignment (SOPMA) is a tool to predict the secondary structure of a protein. Based on the primary sequence of a protein, SOPMA will predict its secondary structure (Geourjon & Deléage 1995). According to this method, short homologous sequence of amino acids will tend to form similar secondary structure. Therefore LYZL protein sequences were analysed by SOPMA program to predict the possible secondary structures like α-helix, β-turn, extended strand and random coil. The program gives the output in the form of percentage of each secondary structure present in the given protein sequence (Frishman & Argos 1995).

Molecular modeling

SWISS MODEL is a fully automated protein structure homology-modeling server, accessible via the ExPASy web server, or from the program Deep View (Swiss Pdb-Viewer). Full length sequence of the LYZL proteins in FASTA/Raw format or SwissProt / UniProt accession code that are retrieved from NCBI were given as a input for the program. Signal peptide was not included in the input sequence, since they were predicted to be secretory proteins. The output was generated as a 3D model using nearest homolog

as a template with higher sequence identity using BLOSUM 45, 62, 80 at different Pfam value (Arnold et al. 2006).

Model validation

PROCHECK is a tool to determine the stereochemical quality of a protein structure by analysing the atomic contacts, cysteine bridge, torsion angles, planarity, residues, secondary structure, bond angles and Ramachandran plot (Ramachandran et al. 1963). The structure file of modelled proteins was given as input for the program and the result in graphical form was analysed to verify the solidarity of the models. Proteins showing more than 90% in the core region and not more than 5% in the disallowed region are considered as good model. In the cases where the models does not meet the requirements of quality structure, modeling was repeated after loop refinement, energy minimization and the structures were validated by analysing the stereochemical features using PROCHECK (Laskowski et al. 1996). PyMOL, a visualization system on an open source foundation is used for producing high quality 3D images of small molecules and biological macromolecules, was used to visualize the structure of the modelled rat LYZL proteins.

Docking analysis

GOLD (Genetic Optimization for Ligand Docking) program was used to analyse the binding ability of LYZL proteins to N-acetyl glucosamine (NAG) trisaccharide (Jones et al. 1995). It comprises of five steps namely receptor protein preparation, ligand preparation, docking, scoring and evaluation of the interaction results. The flow chart of analysis is given below.

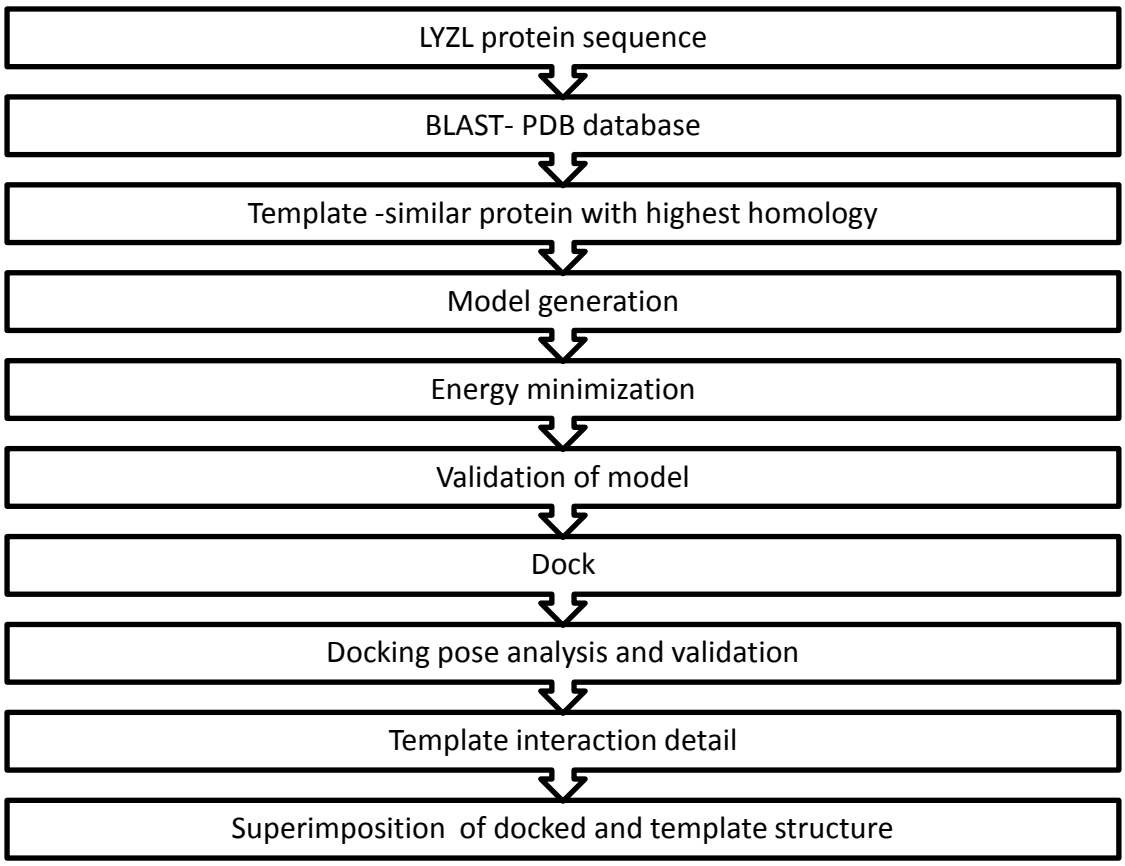

Since the three dimensional structure data was not available for the LYZL proteins, we generated the model and validated them as described previously. Hydrogen molecules were added to the receptor protein using PyMOL. The ligand molecule was retrieved from PubChem and ChemBank as canonical files or sdf files. The tautomers of the ligand were prepared and the ligand molecule in mol2 format was given as input for GOLD. To get the best results, we performed both rigid body docking and flexible docking. The protein molecule and the ligand were imported into GOLD. Docking was run in a particular way such that a particular atom number was given from the identified active site. The GOLD was setup to run at an active site radius of 10.0 Å. The output folder was also specified. All the other fitness function parameters and the genetic algorithm parameters were kept in default mode. The GOLD was run and the output was viewed using Goldmine and Silver. The output was produced as GOLD Fitness scores and different energy functions. The fitness scores were mainly considered for the results and the screening. The docking scores

of 40 and above were only considered positive. The output of these protein-ligand complexes were exported as PDB files using GoldMine. These complexes were then analysed using molecular graphics viewers Discovery studio or PyMOL. The output was analysed for the properties such as hydrogen bonding and Vander Waal's interaction using LigPlot (Wallace et al. 1995).

RESULTS

In silico characterization

in silico analysis of *Lyzl* genes were carried out and the attributes of the proteins were analysed using different computational tools. We identified six rat *Lyzl* genes and are named *Lyzl*1, *3, 4, 5, 6* and *7*. As shown in table 2, *Lyzl* genes are located on different chromosomes and are not clustered despite their higher similarity, suggesting that they are not isoforms coded from a single gene. *Lyzl4* gene sequence was found to be predicted. The mRNA sequence of *Lyzl4* was reported to GenBank and was assigned the accession no. NM_001246183.1. The protein sequences (LYZL 1-7) of the *Lyzl* genes were deduced and their theoretical molecular weight range between 16-18 kDa and their pI values are between 4-8. Further, all the LYZL proteins have signal peptide suggesting that they are secretory in nature. LYZL1 and LYZL6 conserved the chicken lysozyme active site residues namely Glu54 and Asp71. Surprisingly, LYZL4 and 5 conserved only one of the active site residues, i.e. Glu54, whereas LYZL3 and LYZL7 did not possess any of active site amino acids. The four conserved disulphide bridges characteristic to c-lysozyme were found to be present in all the rat LYZL proteins. Except for LYZL7, none of the LYZL proteins have calcium binding site though, they have the calcium binding domain. Glycosylation sites are present only in LYZL5 and LYZL7. Phosphorylation sites were found in all the LYZL proteins. The GRAVY index (which is the measure of hydrophilicity) of all the LYZL proteins are in the negative range suggesting that they are hydrophilic in nature.

Table 2: General features of rat LYZL proteins

Attribute	*Lyzl1*	*Lyzl3*	*Lyzl4*	*Lyzl5*	*Lyzl6*	*Lyzl7*
Chromosome	17	10	8	X	10	7
Gene accession	NC_005116.2	NC_005109	NC_005107.2	NW_047933.1	NC_005109	NC_005106.2
Gene length	13425	7560	4427	3184	5486	2699
Total no. of exons	5	6	4	4	4	4
mRNA accession	NM_001108882.1	NM_001105820	XM_343507.4	NM_001108058.1	NM_001135833	NM_012594.1
Length of mRNA	855	939	580	553	801	480
CDS	143-589	333-824	1-438	1-483	81-527	1-480
Protein accession no.	NP_001102352.1	NP_001099290.1	XP_343508.4	NP_001101528.1	NP_001129305.1	NP_036726.1
No. of amino acids	148	163	145	160	148	160
mol. wt (kda)	16.5	18	16.3	18.1	17	17.8
PI	8.38	6.4	5.79	5.36	5.74	4.74
O-glycosylation*	Nil	Nil	Nil	90,92	Nil	156
GRAVY index	-0.305	-0.299	-0.002	-0.241	0.117	-0.117
Phosphorylation *	19, 55, 135, 138, 59, 102, 53, 57, 72	32, 39	70, 133, 63	S77, 82, 140, 141, 144, 150, 175, T-8, 81, Y-177	88, 81, 86	S-53, 82, T-23, Y-37, 55
Localization	secretory	secretory	secretory	secretory	secretory	Secretory
Signal peptide *	1 to 19	1 to 36	1 to 19	1 to 21	1 to 19	1 to 19
Disulfide bonds*	25-145, 49-133, 83-98, 94-112	41-161, 65-149, 99-114, 110-128	25-143, 49-30, 84-95, 91-109	27-147, 51-135, 85-100, 96-114	25-145, 49-133, 83-98, 94-112	25-139, 47-130, 80-96, 92-110
Active site*	conserved(54, 71)	Not conserved	Partially conserved (54)	Partially conserved (54)	conserved(54, 71)	Not conserved
Calcium binding site*	Nil	Nil	Nil	Nil	Nil	97,108

** -numbers indicate the position(s) of amino acid(s) in the protein.*

Multiple sequence alignment

The multiple sequence alignment was performed using T-COFFEE program for comparing the similarity among the rat LYZL proteins (Figure 1.1). About 70% of the amino acids are displayed in red colour demonstrating high similarity of the amino acid sequence among the LYZL proteins. It is interesting to note that though there is high similarity, the amino acid sequences are not identical. The 8 cysteine residues are highly conserved among all the proteins.

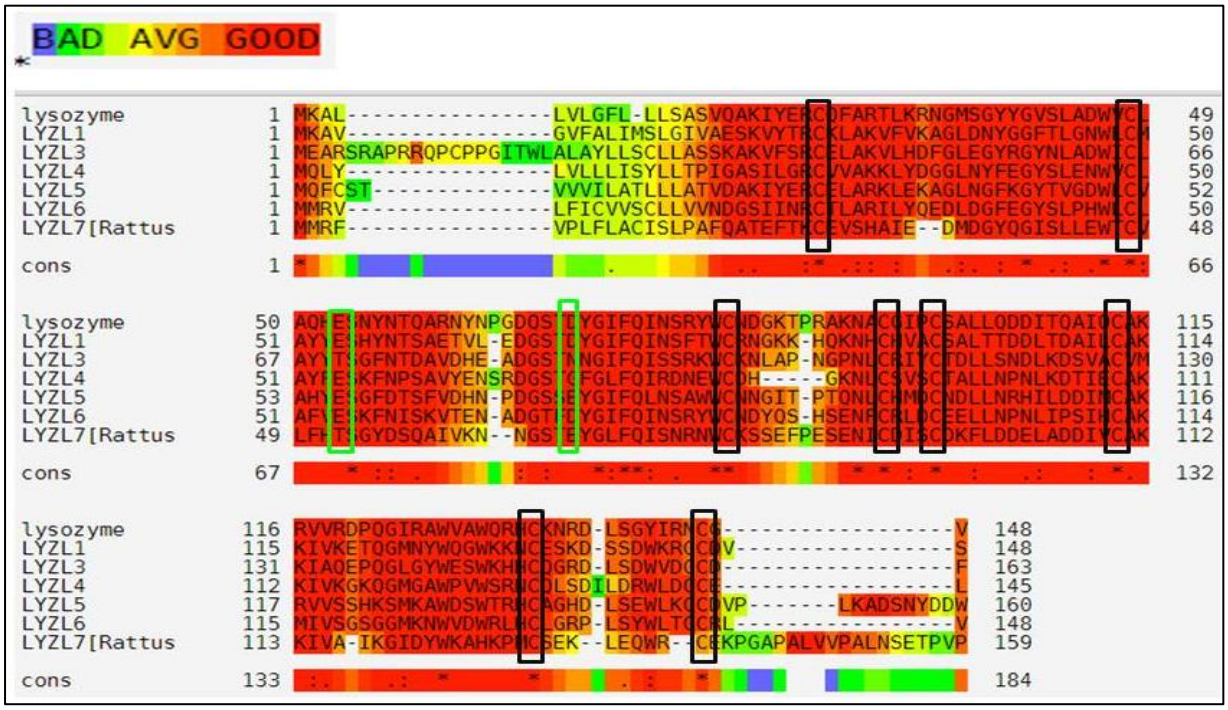

Figure 1.1: *Alignment of rat lysozyme and LYZL proteins. Green colour boxed amino acids represent the active site and black boxed amino acids are the conserved 8 cysteines.*

Pairwise identity and similarity

The pairwise identity among rat, mouse and human LYZL proteins was performed using CLUSTALW2 tool available at EBI website. Similarly, protein BLAST program was used to study the pairwise similarity (Figure 1.2). Rat LYZL proteins seem to be more similar to

their mouse counterparts than with the human counterparts. Highest identity was exhibited by LYZL4 and LYZL6 in all the three species, whereas lowest pairwise identity was observed for LYZL6 and LYZL7. The similarity score among the rat LYZL proteins was found to be in the range of 45-65, whereas the identity lies between the 27-43.

	Rat						Mouse						Human					
LYZ	LYZL1	LYZL3	LYZL4	LYZL5	LYZL6	LYZL7	LYZL1	LYZL3	LYZL4	LYZL5	LYZL6	LYZL7	LYZL1	LYZL3	LYZL4	LYZL5	LYZL6	LYZL7
LYZL1	100	65	59	66	55	55	81	69	61	59	60	58	76	61	58	63	56	60
LYZL3	42	100	60	65	59	59	40	89	64	64	62	62	40	73	59	64	62	60
LYZL4	43	43	100	64	47	49	41	46	91	62	60	53	40	43	73	61	59	46
LYZL5	41	38	41	100	62	58	39	39	39	87	64	60	40	41	36	78	66	58
LYZL6	37	37	47	42	100	55	40	43	47	43	82	54	39	43	43	42	71	56
LYZL7	26	27	30	27	23	100	32	32	34	28	27	70	32	32	30	31	27	67

Figure 1.2: *Pairwise identity and similarity analysis of rat, mouse and human* LYZL *proteins.* -Identity score, -similarity score, -similarity score among the rat proteins.

Conserved domain/ motif analysis

The conserved domains present in the LYZL proteins were studied using CDD tool. Figure 4 shows a typical conserved domain analysis for LYZL1. The lysozyme-like superfamily domain, calcium binding domain and the catalytic cleft were evident in LYZL1. Such a domain structure was observed in all the other LYZL proteins (data not shown). LYZL7 contains the lacatalbumin domain in addition to these domains.

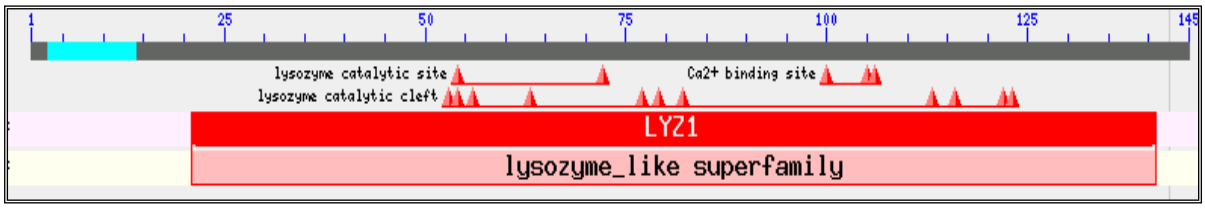

Figure 1.3: *Conserved domain and motif analysis of rat LYZL1 protein. Blue-signal peptide, grey –length of protein. Red triangles-position of important amino acids in corresponding motifs , red box –domain.*

Amphipathicity analysis

The nature of amino acids present along the length of LYZL proteins were analysed by MEME motif prediction program. We observed that the hydrophilic amino acids are distributed towards the amino terminal whereas the hydrophobic amino acids are present towards the carboxy terminal (Figure 1.4). The central part of the proteins contain neutral amino acids. Such a distribution indicates that LYZL proteins are amphipathic in nature. LYZL7 is an exception, since it does not contain the hydrophilic domain in the amino terminal region.

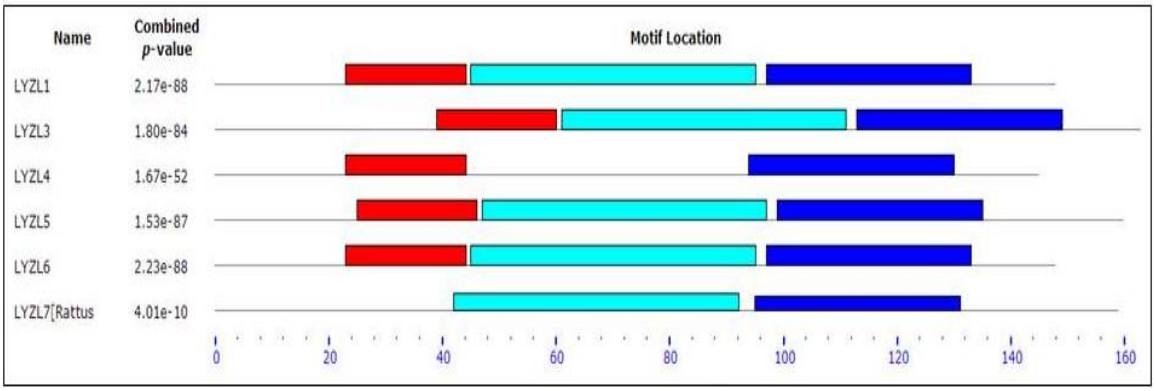

Figure 1.4: *Distribution of hydrophilic, neutral and hydrophobic amino acids along the length of rat LYZL proteins.* ■ *– hydrophilic (K, R),* ■ *- Neutral (Y),* ■ *- Hydrophobic (A, C, F, I, L, V, W and M).*

Genomic neighbourhood of *Lyzl* genes

Genomic neighbourhood analysis reveals that the rat *Lyzl* genes in general are positioned among other genes similar to that of mouse and human except for *Lyzl5* and *Lyzl6*. Neighbourhood genes towards the downstream side of human *Lyzl5* gene seem to be different from mouse and rat. They have undergone a gene duplication event due to which *Spaca5b*/*Lyzl5b* gene is present in case of human, but not in rat and mouse (Figure 1.5). Neighbourhood of *Lyzl6* for rat and mouse seems to be almost similar whereas, in case of

humans it seems to be located entirely in a different neighbourhood, suggesting that a possible recombination has taken place in the recent past after the evolution of mouse.

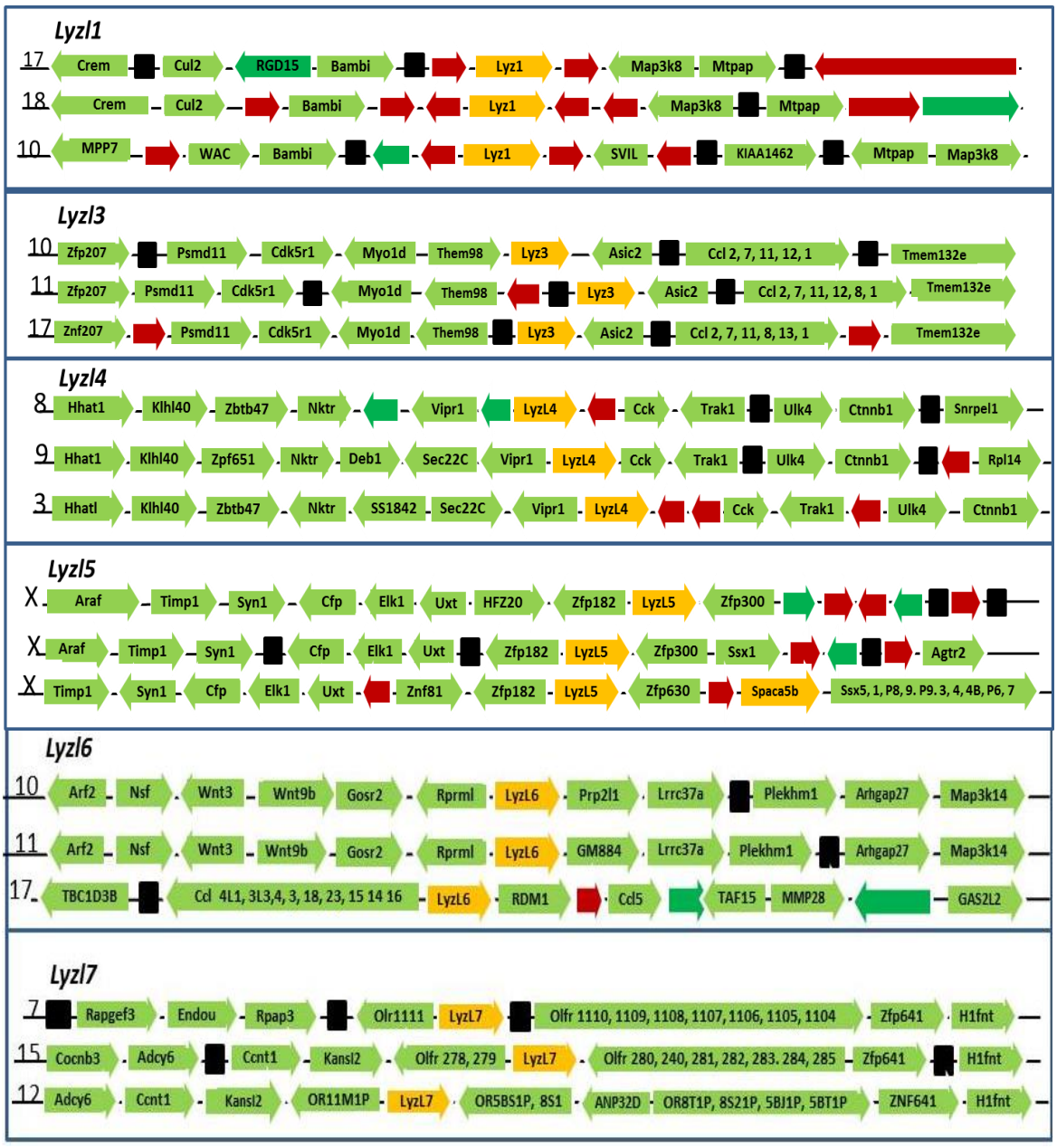

Figure 1.5: *Genomic neighbourhood analysis of rat, mouse and human Lyzl* genes**.** *Green arrows with names represent the genes and directions of the arrow represent the direction of sense strand. Black, red and green arrows indicate noncoding, pseudo and hypothetical genes respectively. Numbers in the beginning of each row indicates the chromosome number and are shown in the order of rat, mouse and human***.**

Phylogenetic analysis of LYZL proteins

The presence of multiple *Lyzl* genes in all mammalian genomes, as well as in the genomes of several other vertebrate species (Figures 1.6 - 1.11), raises the possibility that the *Lyzl* gene family may have amplified early in vertebrate evolution. The phylogenetic analysis reveals that the LYZL proteins are present widely among various organisms especially the vertebrates. The rat LYZL proteins seem to have orthologs in rodents, placentals and primates.

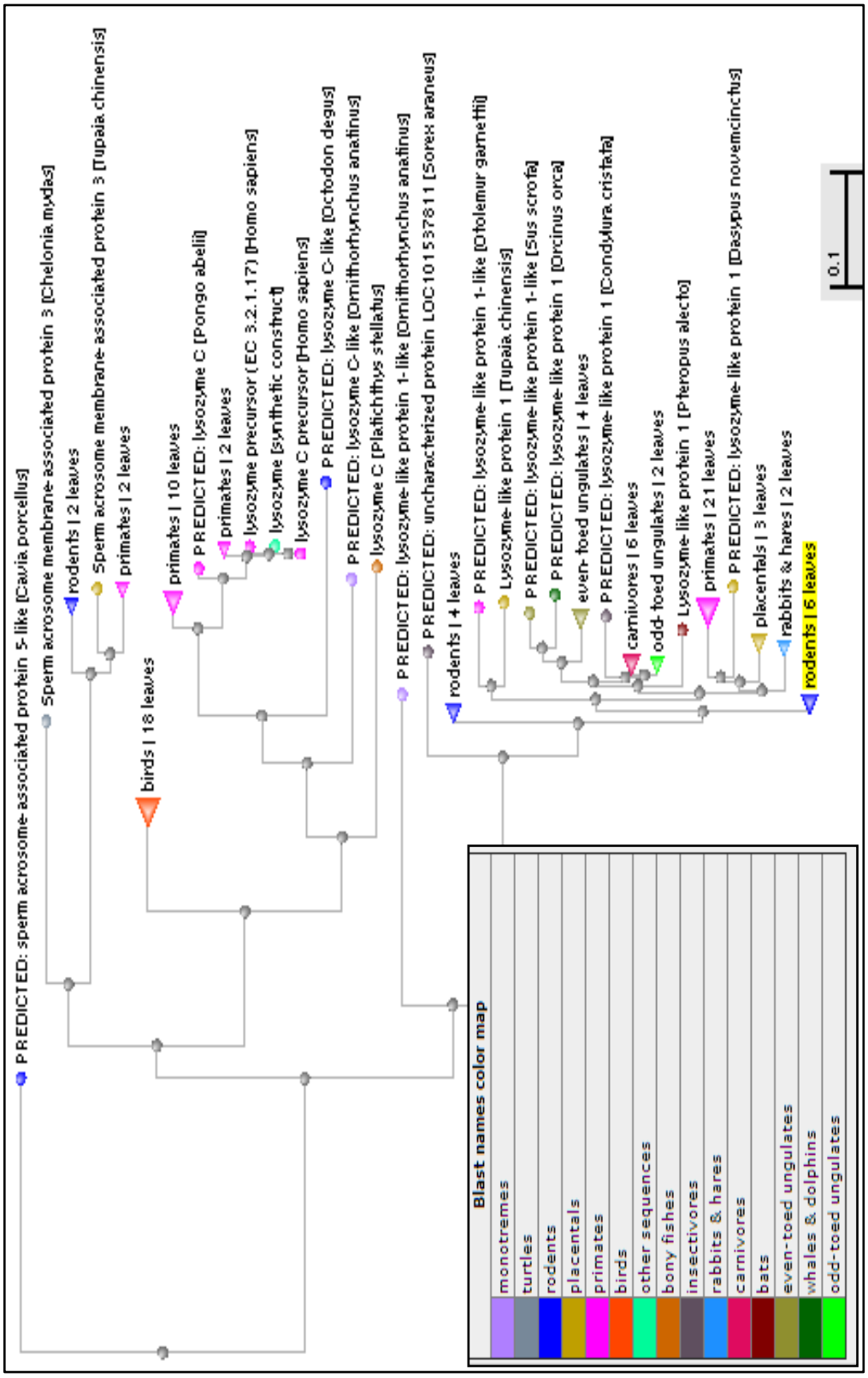

Figure 1.6: *A neighbor joining phylogenetic tree obtained for* LYZL1*, along with colour map, to show its conservation and distribution across the animal kingdom. It clearly depicts its conservation among the vertebrates and especially in mammals, grouping all* LYZL1 *in to a single clade.*

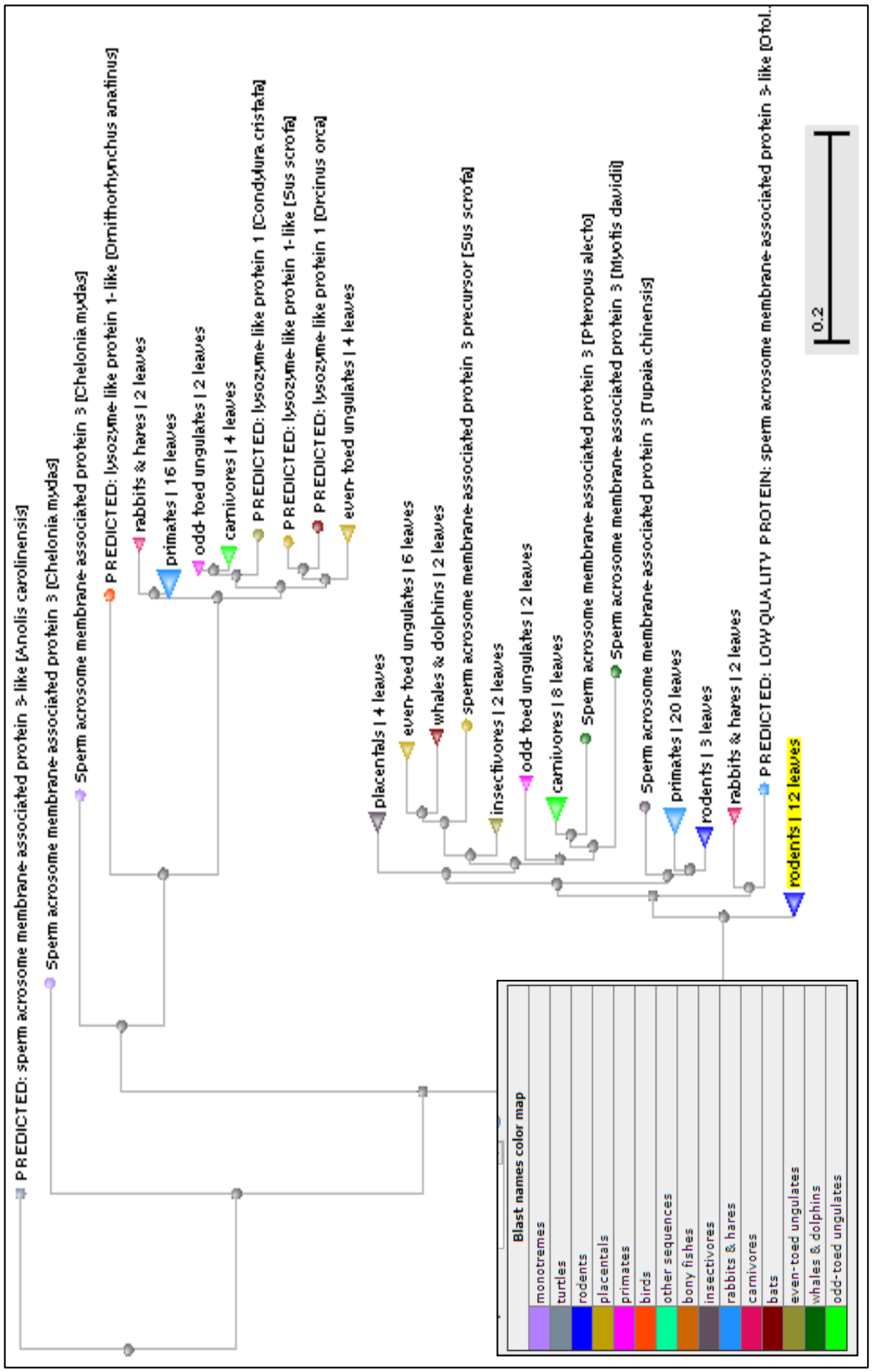

Figure 1.7: *A neighbor joining phylogenetic tree obtained for* LYZL3*, along with colour map, to show its conservation and distribution across the animal kingdom. It clearly depicts its conservation among the mammals, grouping all* LYZL3 *in to a single clade.*

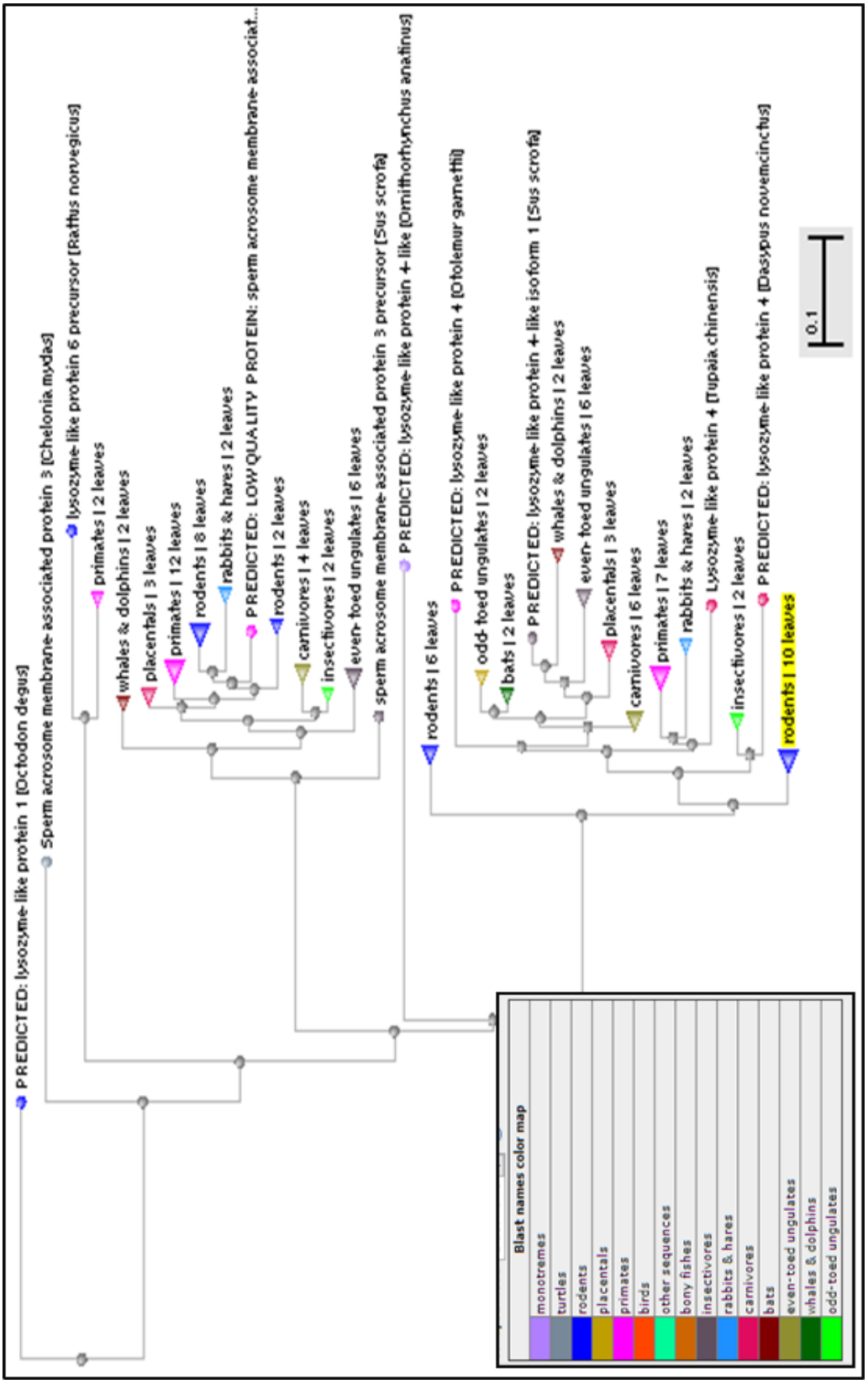

Figure 1.8: *A neighbor joining Phylogenetic tree obtained for* LYZL4*, along with colour map, to show its conservation and distribution across the animal kingdom. It clearly depicts its conservation among the vertebrates and especially in mammals, grouping all* LYZL4 *in to a single clade.*

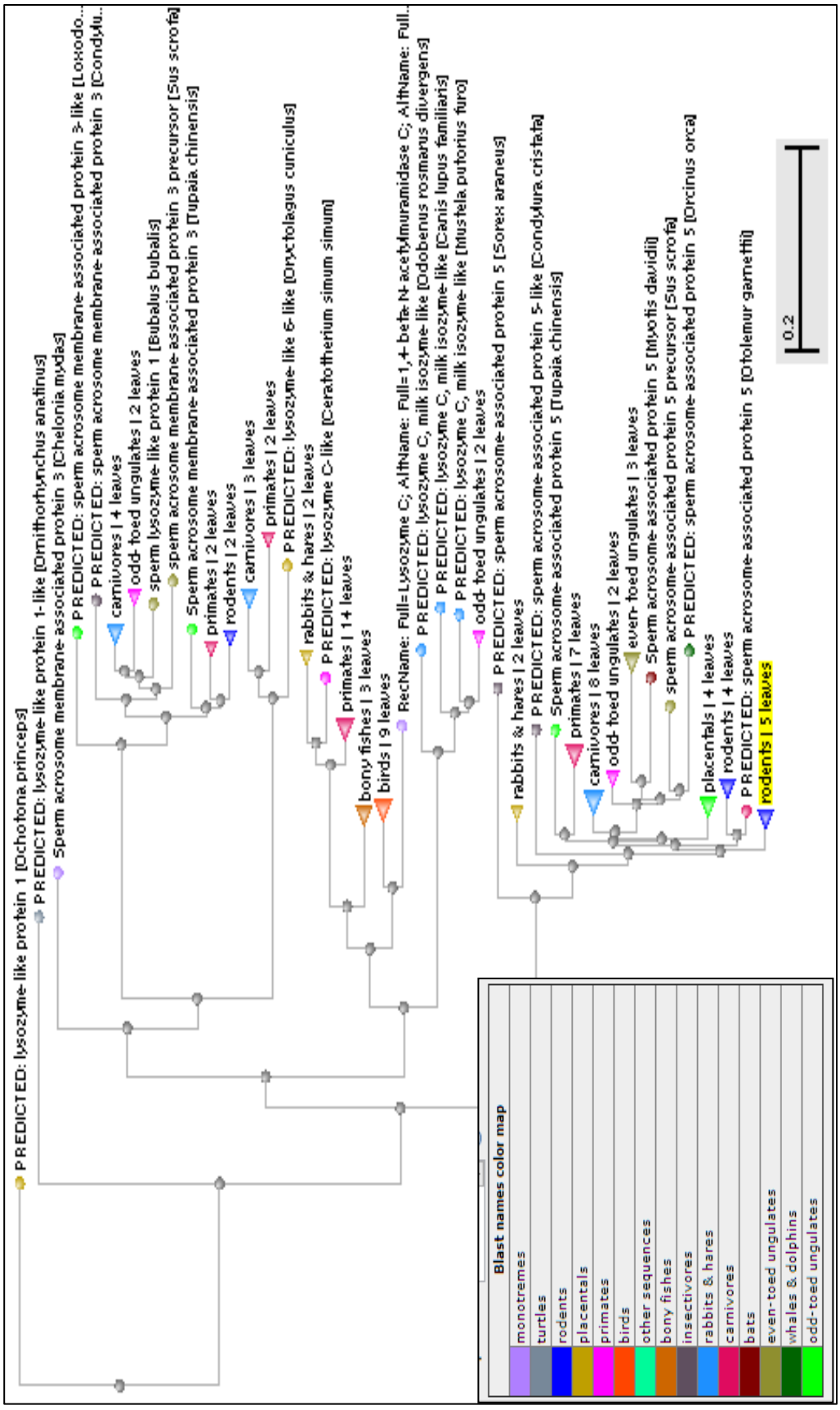

Figure 1.9: *A neighbor joining phylogenetic tree obtained for* LYZL5*, along with colour map, to show its conservation and distribution across the animal kingdom. It clearly depicts its conservation among the vertebrates and especially in mammals, grouping all* LYZL5 *in to a single clade with mammals.*

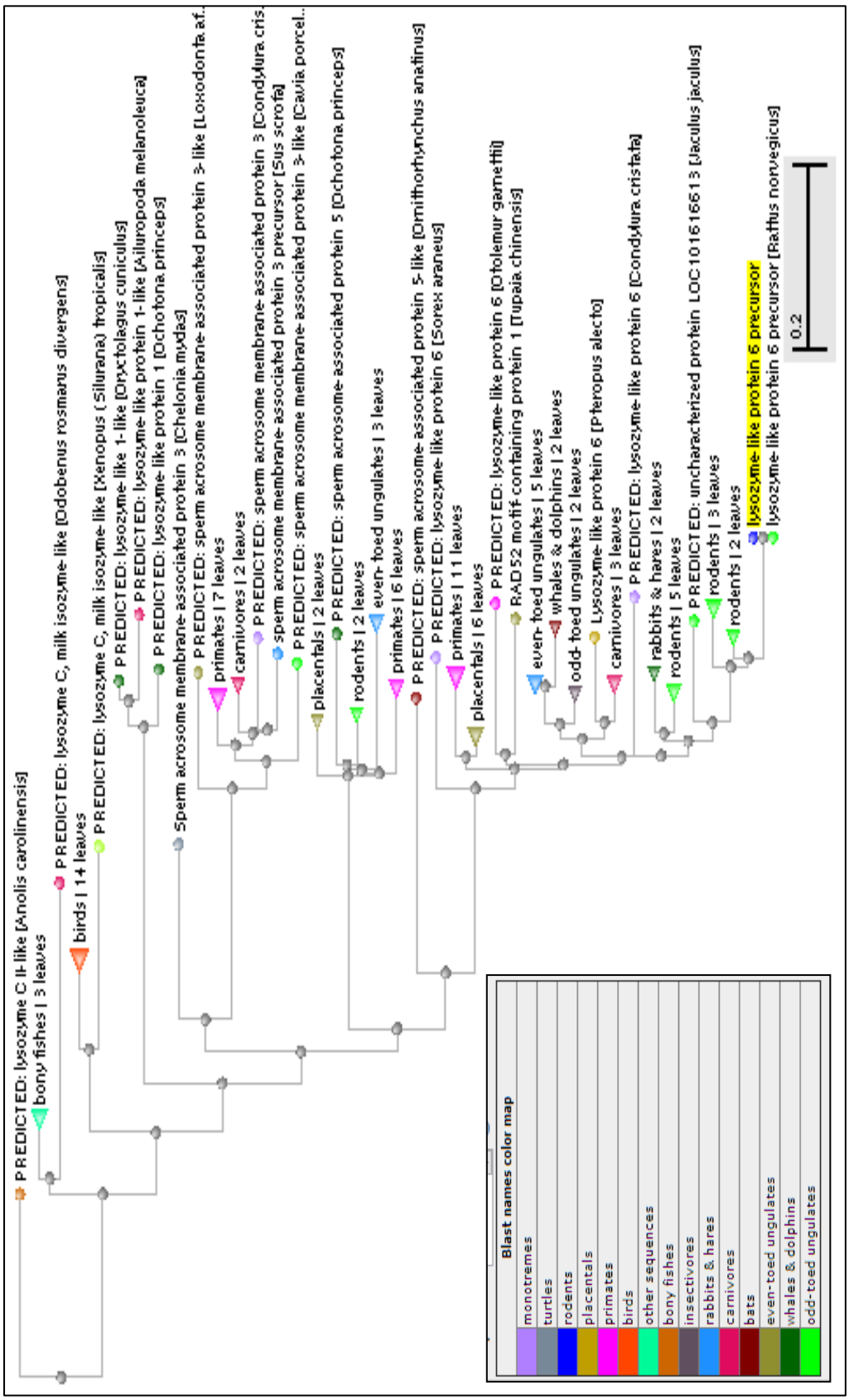

Figure 1.10: *A neighbor joining phylogenetic tree obtained for* LYZL6*, along with colour map, to show its conservation and distribution across the animal kingdom. It clearly depicts its conservation among the vertebrates and especially in mammals, grouping all* LYZL6 *in to a single clade.*

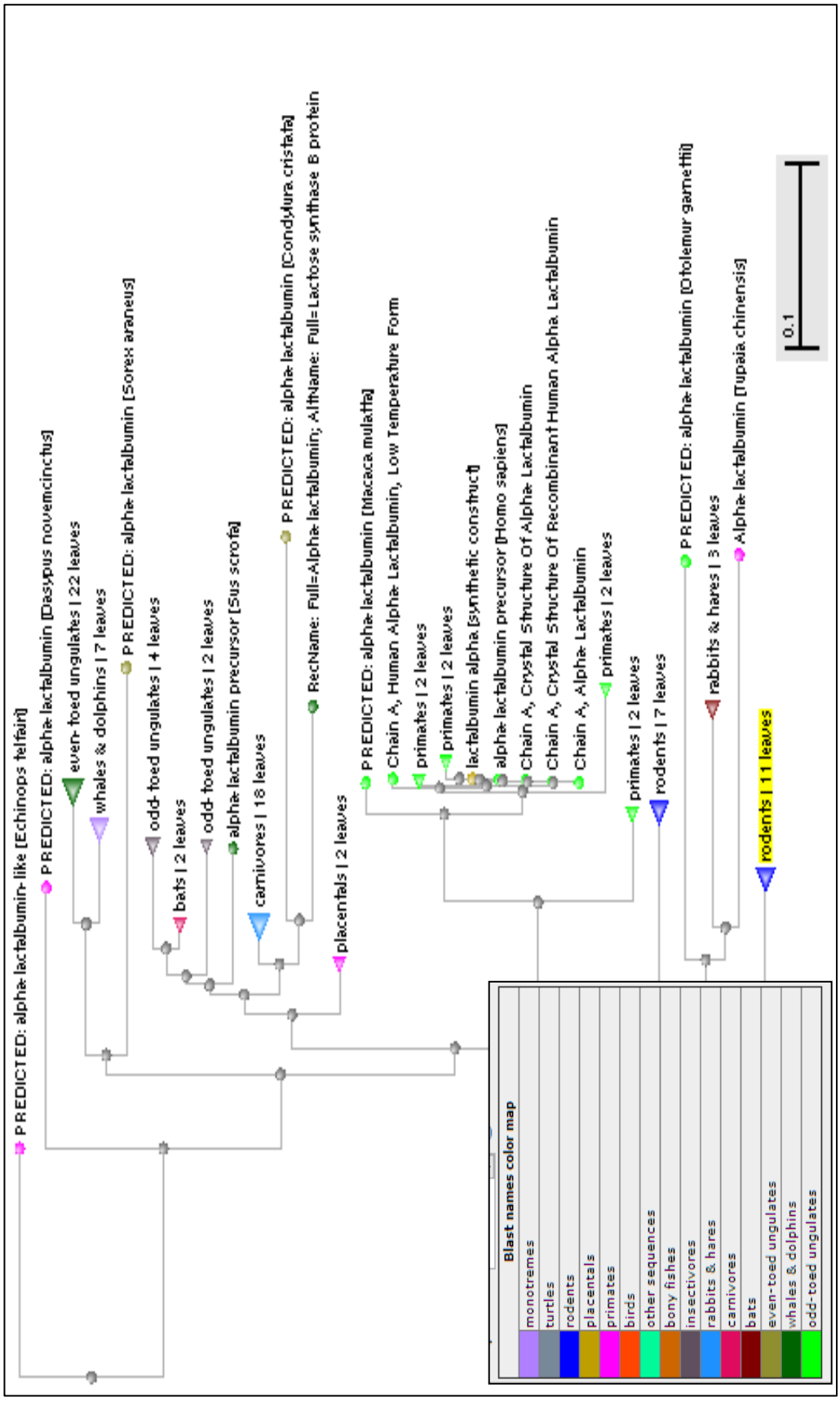

***Figure 1.11**: A neighbor joining phylogenetic tree obtained for* LYZL7*, along with colour map, to show its conservation and distribution across the animal kingdom. It clearly depicts its less conservation among mammals, grouping all* LYZL7 *in to a single clade.*

Secondary structure prediction

The secondary structure prediction for rat LYZL proteins using SOPMA showed that LYZL 1, 5, 6 and 7 contains 42, 44, 44 and 44 percent of α-helix respectively, suggesting that they have predominantly α-helical pattern. LYZL3 and 4 contains 39 and 55 percent of random coil and at the same time α-helix content is also comparably higher.

Table 3: Secondary structure prediction for LYZL proteins

Protein	α-helix	Extended strand	β-turn	Random coil
LYZL1	42	16	7	35
LYZL3	37	15	9	39
LYZL4	38	21	14	55
LYZL5	44	17	8	31
LYZL6	44	18	9	28
LYZL7	44	15	6	36

Values are given in percent.

Molecular modeling

LYZL1

The three dimensional structure (Figure 1.12A) of LYZL1 was predicted by SWISS MODEL using hen egg white lysozyme fused with fibrinogen as a template. LYZL1 showed 58% similarity with the template. The modelled structure was validated using PROCHECK. Ramachandran plot (Figure 1.12B) analyses showed that 71.6% of residues are in most favoured region, 26.7% in additionally allowed regions, 1.7% in generously allowed regions and none in the disallowed region (Figure 1.12C). The reliability and correlation of the predicted model was measured in terms of G- factor and root mean square deviation (RMSD) between the template and the modelled protein. The model designed for rat LYZL1 had a G- factor of 0.11 and RMSD of 0.261.

A

B

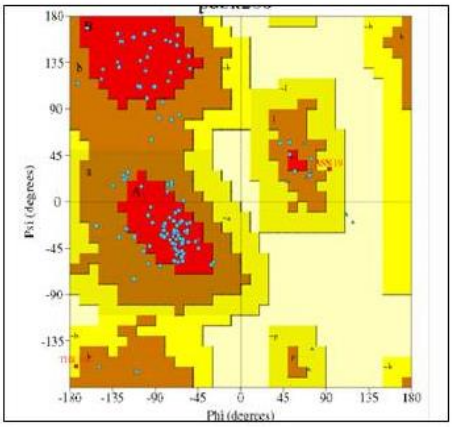

C

		No. of residues	%-tage
Most favoured regions	[A,B,L]	83	71.6%**
Additional allowed regions	[a,b,l,p]	31	26.7%
Generously allowed regions	[~a,~b,~l,~p]	2	1.7%
Disallowed regions	[XX]	0	0.0%
Non-glycine and non-proline residues		116	100.0%
End-residues (excl. Gly and Pro)		2	
Glycine residues		10	
Proline residues		0	
Total number of residues		128	

Figure 1.12: *A-Modelled structure of* LYZL1*, showing β- sheets in yellow, helices in red, loop regions in green and disulphide bonds in spheres. B- Ramachandran plot for the modelled protein. C- Amino acid distribution in Ramachandran plot.*

LYZL3

For LYZL3, mouse sperm lysozyme like protein1 (SLLP1) protein was used as template because of a homology of 86.61%. The model generated (Figure 1.13A) was verified by Ramachandran plot, G- factor and superimposition analyses. Ramachandran plot (Figre1.13B) analysis indicates that 89.3% of the amino acids are in most favourable core region, whereas 11.7% are in additionally allowed region (Figure 1.13C). None of the residues were in disallowed region. G-factor value was 0.03 which is within the agreeable limit showing that the model does not possess any unusual bonds. Further, the superimposition value was shown to be 0.09 which is in agreement with the Ramachandran plot and G-factor results.

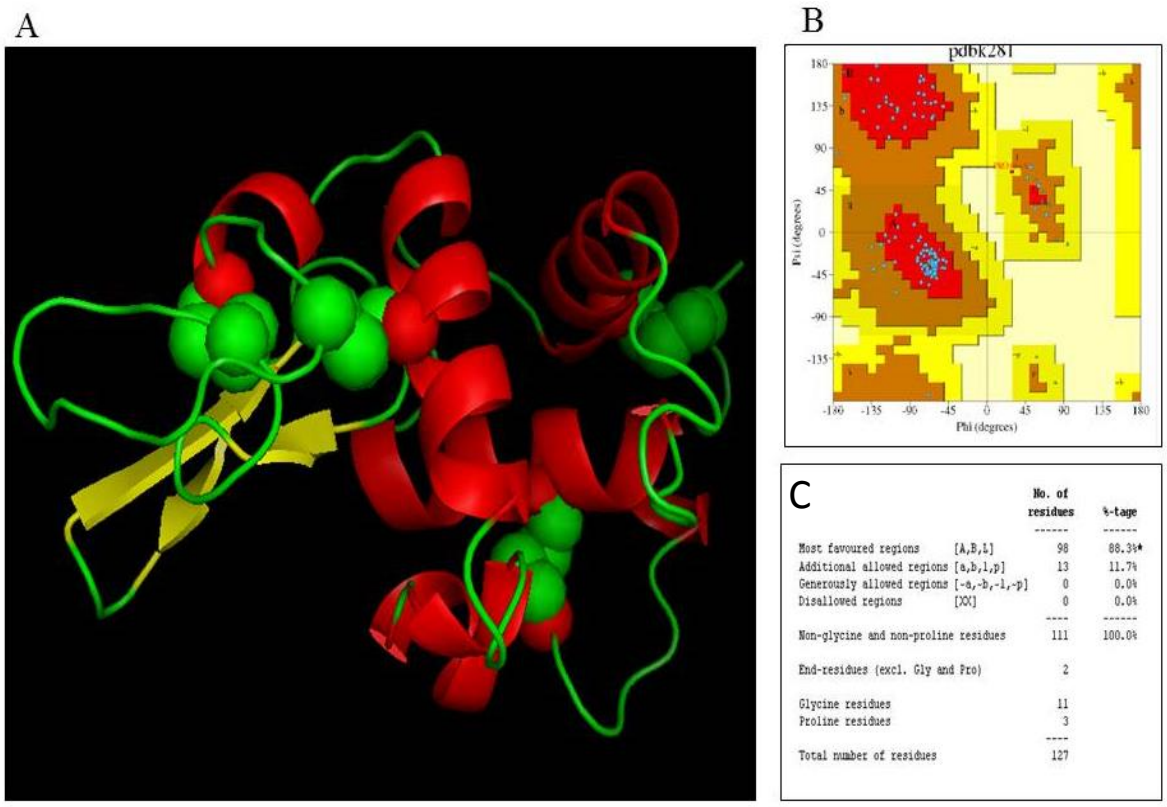

Figure 1.13: *A-Modelled structure of* LYZL3, *showing β- sheets in yellow, helices in red, loop regions in green and disulphide bonds in spheres. B- Ramachandran plot for the modelled protein. C- Amino acid distribution in Ramachandran plot.*

LYZL4

Mouse SLLP1 was found to be the best template for LYZL4 since the identity was 45%. The model generated (Figure 1.14A) according to Ramachandran plot (Figure 1.14B) had 90.8% of the residues in the most favoured regions, 9.2% in the additionally allowed regions and none of the amino acids in the disallowed regions (Figure 1.14C). Altogether the generated model seems to be reliable by Ramachandran plot with a G-factor value of -0.12. The RMSD value was 0.405 which was within the agreeable limit. A helix present in mouse SLLP1 was not observed in rat LYZL4.

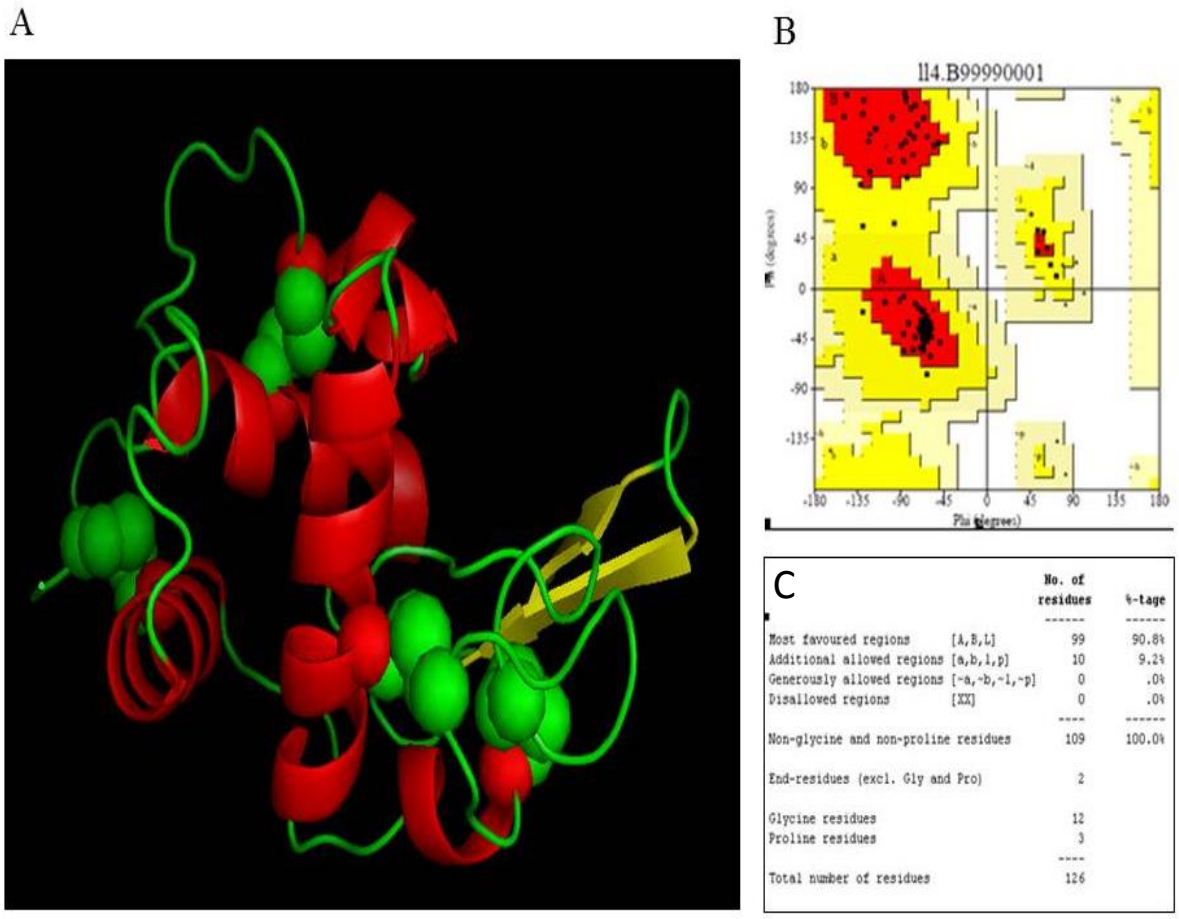

Figure 1.14: *A-Modelled structure of* LYZL4 *showing β- sheets in yellow, helices in red, loop regions in green and disulphide bonds in spheres. B- Ramachandran plot for the modelled protein. C- Amino acid distribution in Ramachandran plot.*

LYZL5

Canine lysozyme, which showed an identity of 48% with rat LYZL5, was used as the template. The modelled protein (Figure 1.15A) according to Ramachandran plot (Figure 1.15B) contained 84.2% of the residues in most favoured region, 14.9% in additionally allowed region and 0.9% in generously allowed region (Figure 1.15C). It has a G-factor value of 0.12 and the RMSD value of 0.306, validating the model generated.

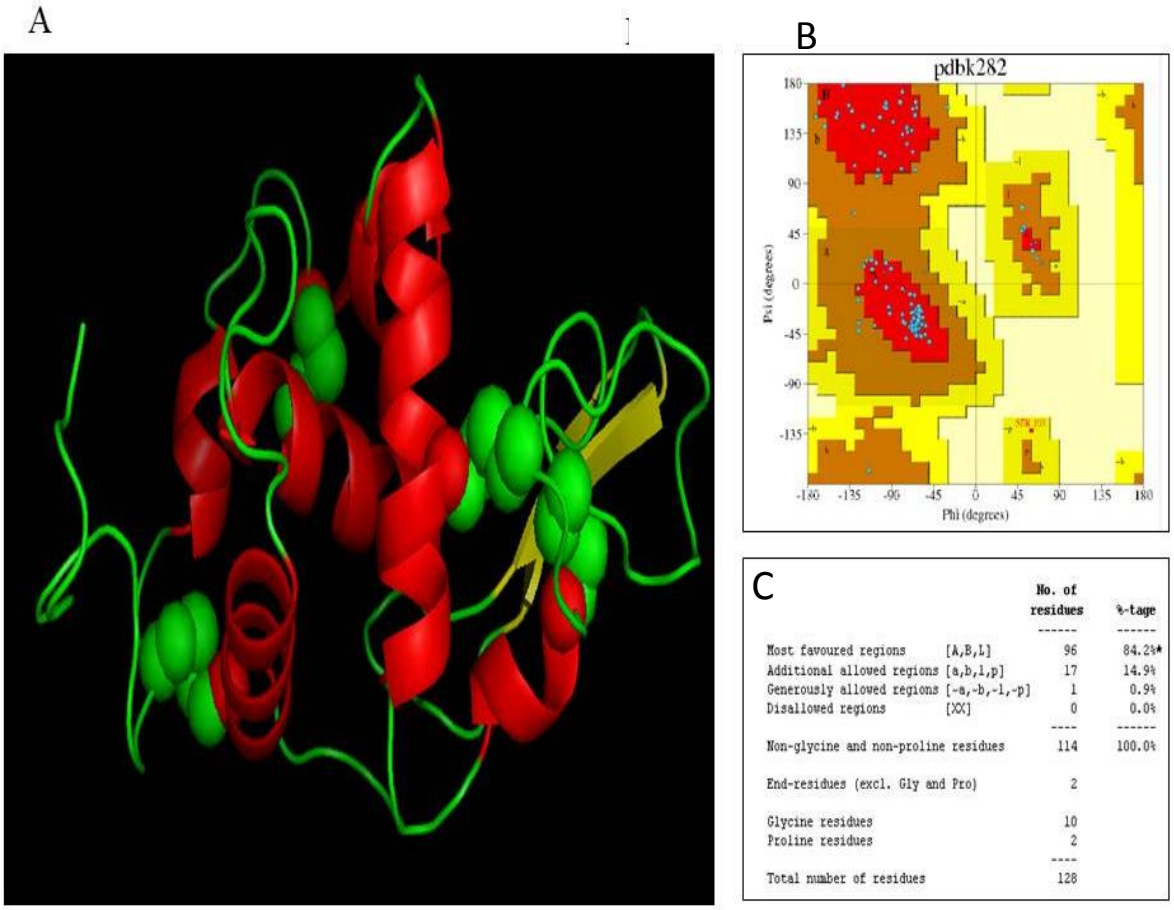

Figure 1.15: *A-Modelled structure of* LYZL5 *showing β- sheets in yellow, helices in red, loop regions in green and disulphide bonds in spheres. B- Ramachandran plot for the modelled protein. C- Amino acid distribution in Ramachandran plot.*

LYZL6

LYZL6 was modelled (Figure 1.16A) using mouse SLLP1 as template which showed 45.67% identity. Ramachandran plot (Figure 1.16B) indicates that 86.6% of the amino acids are in most favoured region and 13.4% in generously allowed region (Figure 1.16C). Moreover, detailed analysis of the modelled protein shows that the helices are little bigger than the template but similar in structure to SLLP1. G-factor was found to be 0.04 and the RMSD value was found to be 0.11, which are in agreeable limits.

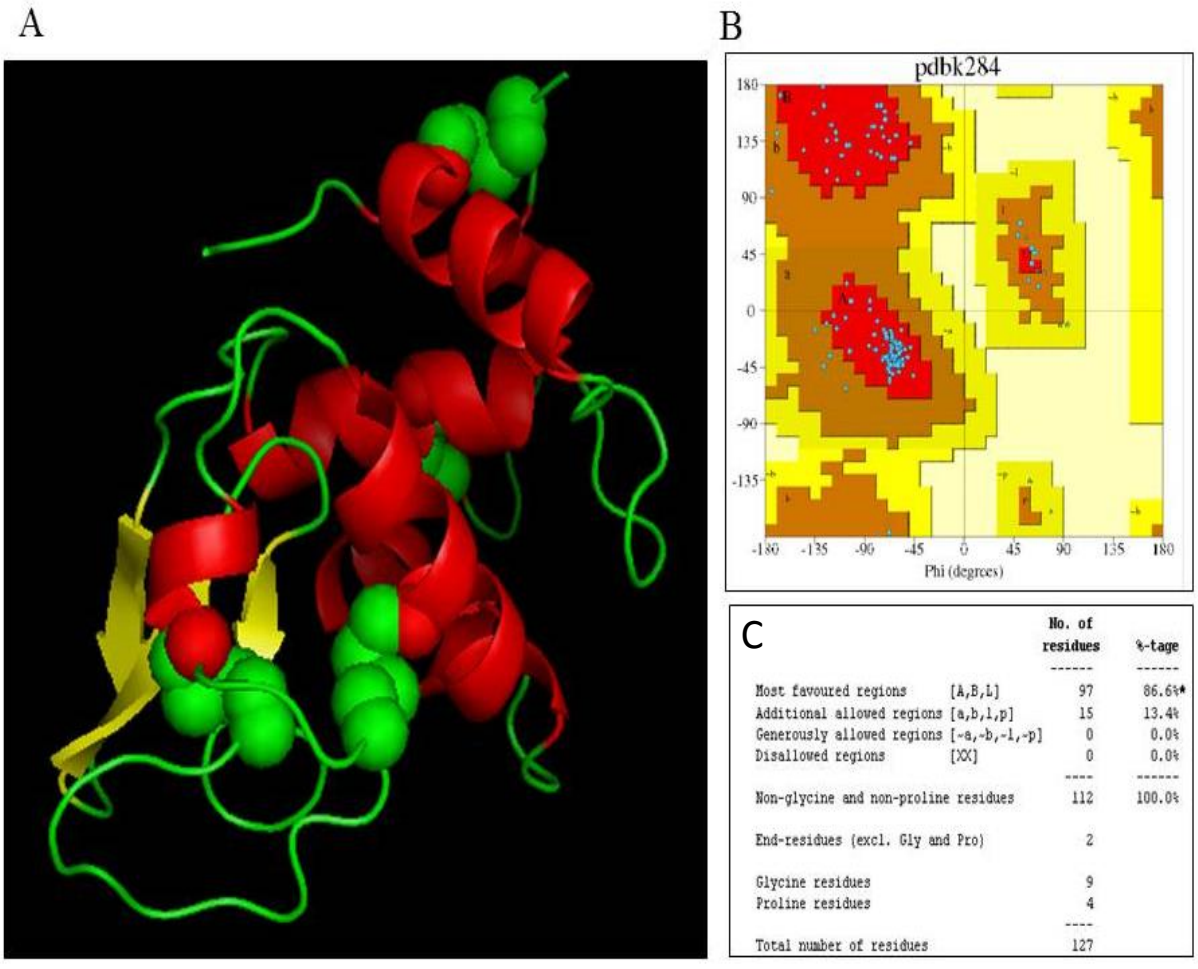

Figure 1.16: *A-Modelled structure of* LYZL6 *showing β- sheets in yellow, helices in red, loop regions in green and disulphide bonds in spheres. B- Ramachandran plot for the modelled protein. C- Amino acid distribution in Ramachandran plot.*

LYZL7

LYZL7 was modelled (Figure 1.17A) using α-lacatalbumin as template, since they had an identity of 86.7%. Ramachandran plot (Figure 1.17B) showed 83.2% of the residues to be in most favoured regions while 15.9% of the residues in additionally allowed regions and 0.9% of the residues to be in generously allowed region (Figure 1.17C). The G-factor value was 0.13 and the RMSD value was also 0.13 which are within suggested limits for a reliable model.

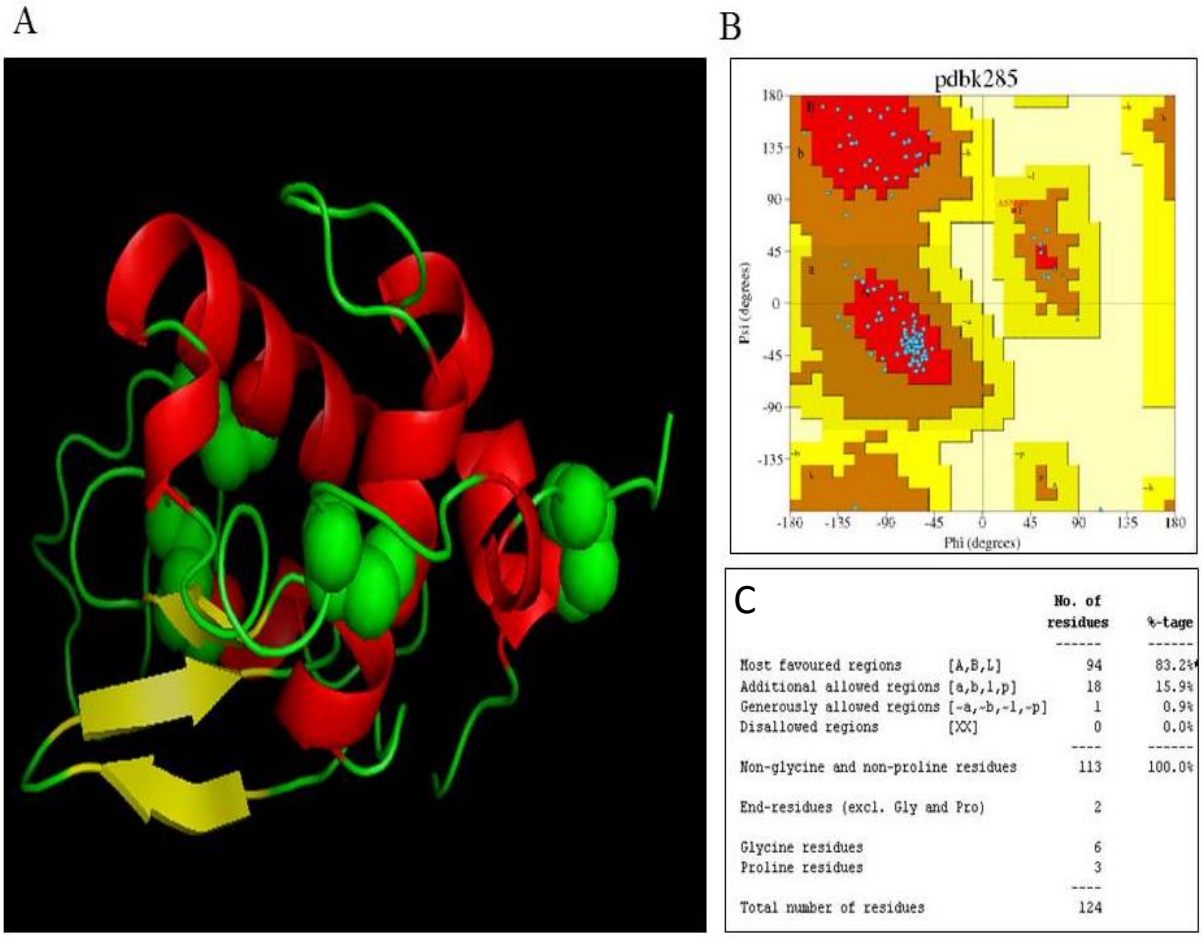

Figure 1.17: *A-Modelled structure of* LYZL7 *showing β- sheets in yellow, helices in red, loop regions in green and disulphide bonds in spheres. B- Ramachandran plot for the modelled protein. C- Amino acid distribution in Ramachandran plot.*

Molecular docking studies

Docking studies gives important information regarding the structural interactions between the two proteins or between the protein and its ligand. There are different types of docking such as blind docking, flexible docking and rigid body docking. To gain further insights into the functional aspects of the LYZL proteins, docking of the LYZL proteins with N-acetyl-D-glucosamine (NAG), one of the component of peptidoglycan was carried out. In the template search by pBLAST against PDB, hen egg lysozyme bound to NAG trisaccharide was chosen as the best template for all the LYZL proteins. Predicted structure was validated by Ramachandran plot and superimposed with the template. RMSD values were also checked to confirm the reliability of the model. Thus, the modelled protein structure was used for docking studies. Docking was done using GOLD software and structures were analysed using PyMOL.

As a first step, the template (chicken egg lysozyme) was analysed to find out the amino acids that are interacting with or in close proximity to the ligand (NAG), so that the docking can be done using the same pose against similar regions for LYZL proteins. The amino acids of chicken egg lysozyme that interacted with the ligand and the type of interaction are shown in table 4. It is evident that there are side chain and main chain interactions between the ligand and the chicken egg lysozyme. Moreover, it is clear that the NAG interacts with the active site (Gln57 and Asp59) cleft.

The LYZL proteins that were modelled using the chicken lysozyme as a template were compared for similarity in the ligand interacting regions. Docking was carried out against amino acids in those regions using GOLD. Docking was performed initially by flexible docking. Since the ligand is quite bigger with more of rotatable bonds, flexible docking did

not show appreciable interaction. Therefore, rigid body docking was adopted, for which the ligand molecule (NAG trisacharide) was considered to be rigid.

Table 4: Amino acids of chicken lysozyme that interact with NAG

Amino acid residue	Interacting part	Interaction type
Asp52	Side chain	Hydrogen bond
Trp62	Side chain	Hydrogen bond
Trp63	Side chain	Hydrogen bond
Asp101	Side chain	Hydrogen bond
Asn 103	Side chain	Hydrogen bond
Ala107	Side chain	Hydrogen bond
Gln57	Main chain	Hydrogen bond
Asp59	Main chain	Hydrogen bond
Trp108	Side chain	Hydrophobic
Ile58	Side chain	Hydrophobic
Leu75	Side chain	Hydrophobic

Analysis of the ligand interacting region shows that chicken lysozyme has 11 amino acids in the interacting region in the close proximity of ligand that are possibly brought together by three dimensional folding. On comparison with chicken lysozyme, LYZL 1 has 5 amino acid residues that can interact with the ligand whereas the remaining 6 residues are replaced by similar amino acids but are not identical (Table 4). Similar pattern was

observed for other LYZL proteins (Table 4). These results show that the amino acids in the binding region among the LYZL proteins are not identical but similar (Table 5).

Table 5: Amino acids of chicken and rat LYZL proteins that interact with NAG

LYZ	D52	W62	W63	D101	N103	A107	Q57	D59	I58	L75	W108
LYZL1	D	T	W	E	Q	Y	Q	N	I	H	W
LYZL3	D	Y	W	G	G	N	Q	N	I	F	W
LYZL4	G	E	W	G	Q	A	Q	R	I	L	W
LYZL5	E	W	W	S	K	A	Q	N	L	L	W
LYZL6	N	K	W	E	Q	Y	Q	S	I	L	W
LYZL7	E	N	W	-	K	Y	Q	S	I	I	W

Underline indicates the substrate interacting amino acid that is similar to chicken lysozyme.

Further analyses were carried out to obtain docking score by GOLD. The GOLD fitness represents the reliability of the docking and grading of the affinity between protein and the ligand (higher is the fitness score higher the reliability and binding affinity).

According to GOLD fitness score shown in table 6, LYZL1 and LYZL6 had a score of 50.81 and 45.89 respectively. Such a high score indicates their ability to strongly interact with NAG. The other proteins had lower scores and this could be due to absence of the active site amino acids.

Table 6: Docking of LYZL proteins with NAG

Proteins	Gold fitness score	Binding
LYZL1	50.81	Maybe
LYZL3	26.58	May not
LYZL4	39.40	May not
LYZL5	18.91	May not
LYZL6	45.89	Maybe
LYZL7	22.90	May not

LYZL1 and LYZL6 may bind to NAG in the same fashion as that of chicken egg lysozyme, as reflected by the docking scores (Table 6). Rat LYZL proteins docked with NAG were superimposed with the chicken lysozyme bound to NAG trisaccharide. As shown in figure 1.18, LYZL1 and LYZL6 displayed a complete superimposition with chicken lysozyme without any distortion of either the protein or ligand at any location. The remaining rat LYZL proteins did not show a complete overlap in the ligand region although there is complete overlap in the protein part indicating that these proteins may not interact with the substrate.

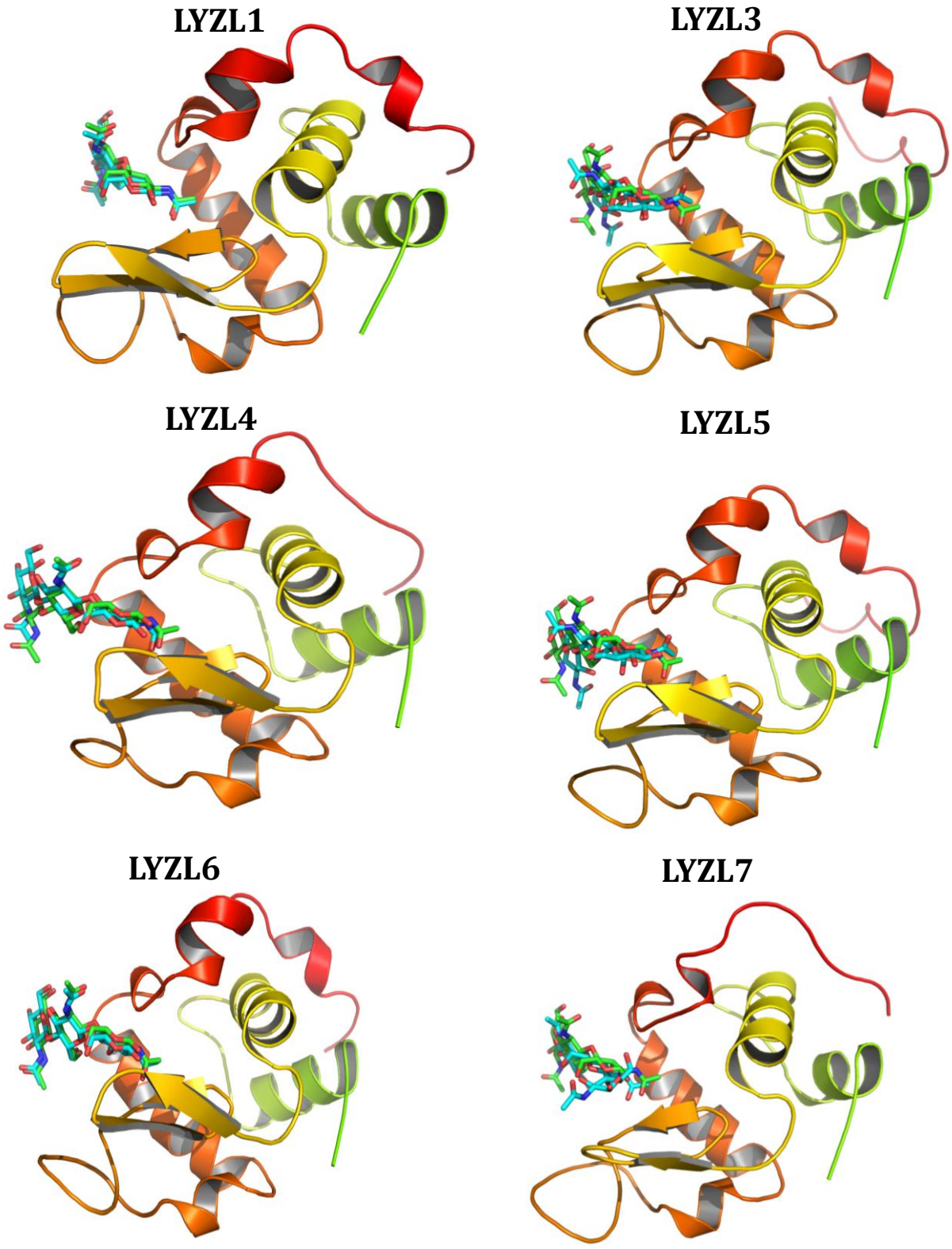

Figure 1.18: *Molecular modeling showing the superimposition of rat* LYZL *and NAG complex with chicken lysozyme-NAG complex. NAG is represented in the form of stick model and the protein in cartoon model.*

In depth docking analysis of rat LYZL1 showed that the NAG binds and fits completely into the active site (Figure 1.19). Further, LigPlot analysis (Figure 1.20) shows that LYZL1 has hydrogen bond interactions with the ligand. Trp63, Asn59 are interacting with ligand by forming hydrogen bonds of length 3.03 and 2.65 respectively. In addition to this, Thr62, Tyr106 and Ile58 are some of the residues that display hydrophobic interactions with the ligand.

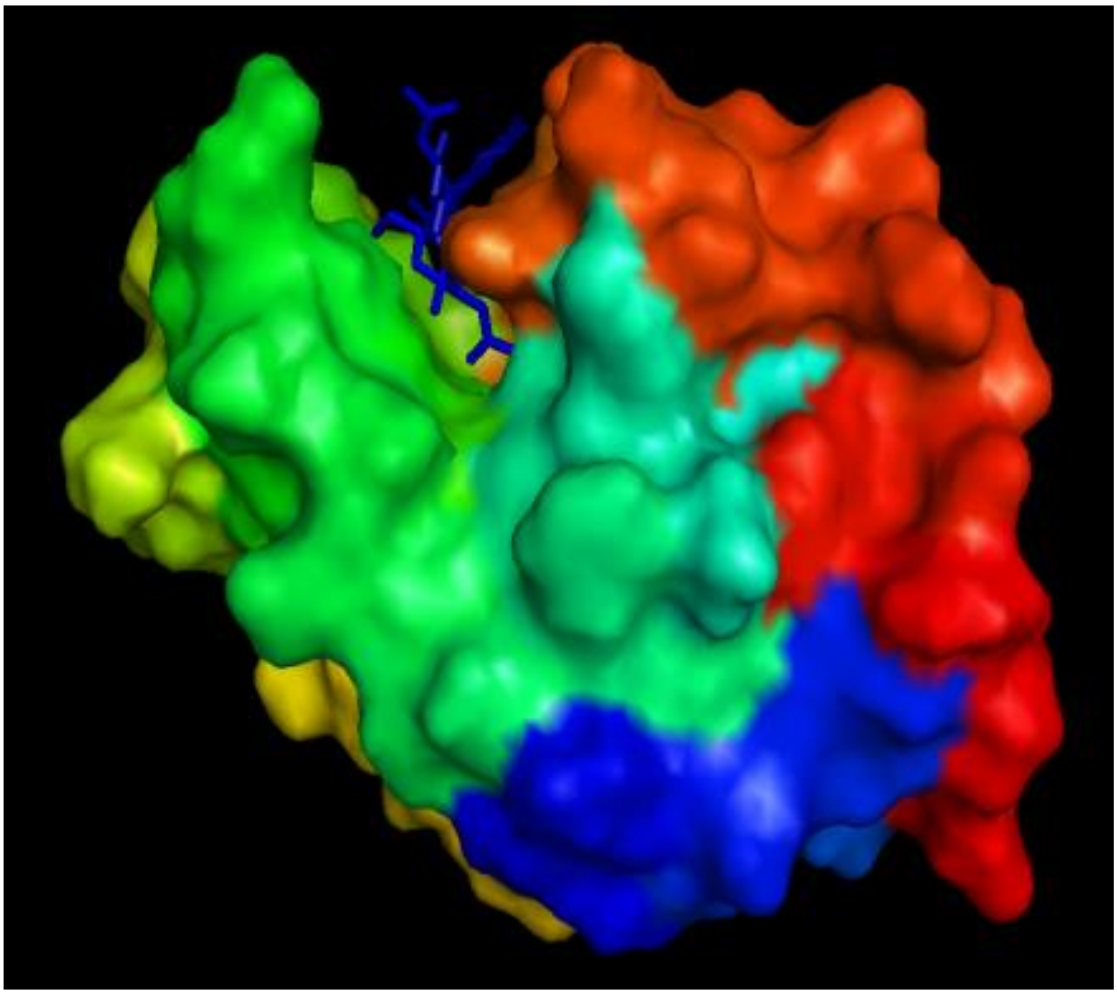

Figure 1.19: *Rat* LYZL1 *shown as surface model and the binding of NAG to the protein. NAG is shown in stick model.*

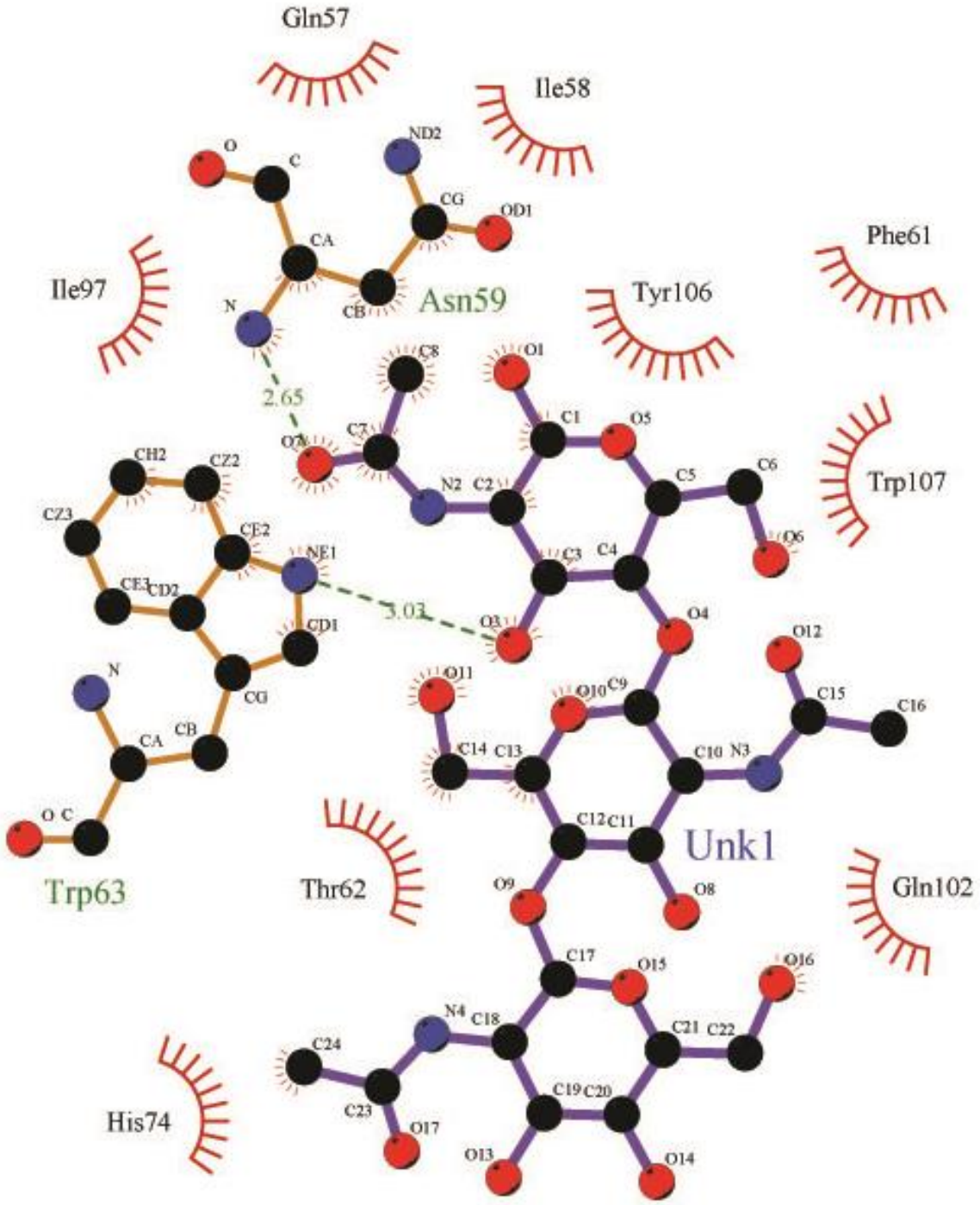

Figure 1.20: *LigPlot analysis for the interaction of* LYZL1 *with NAG.*

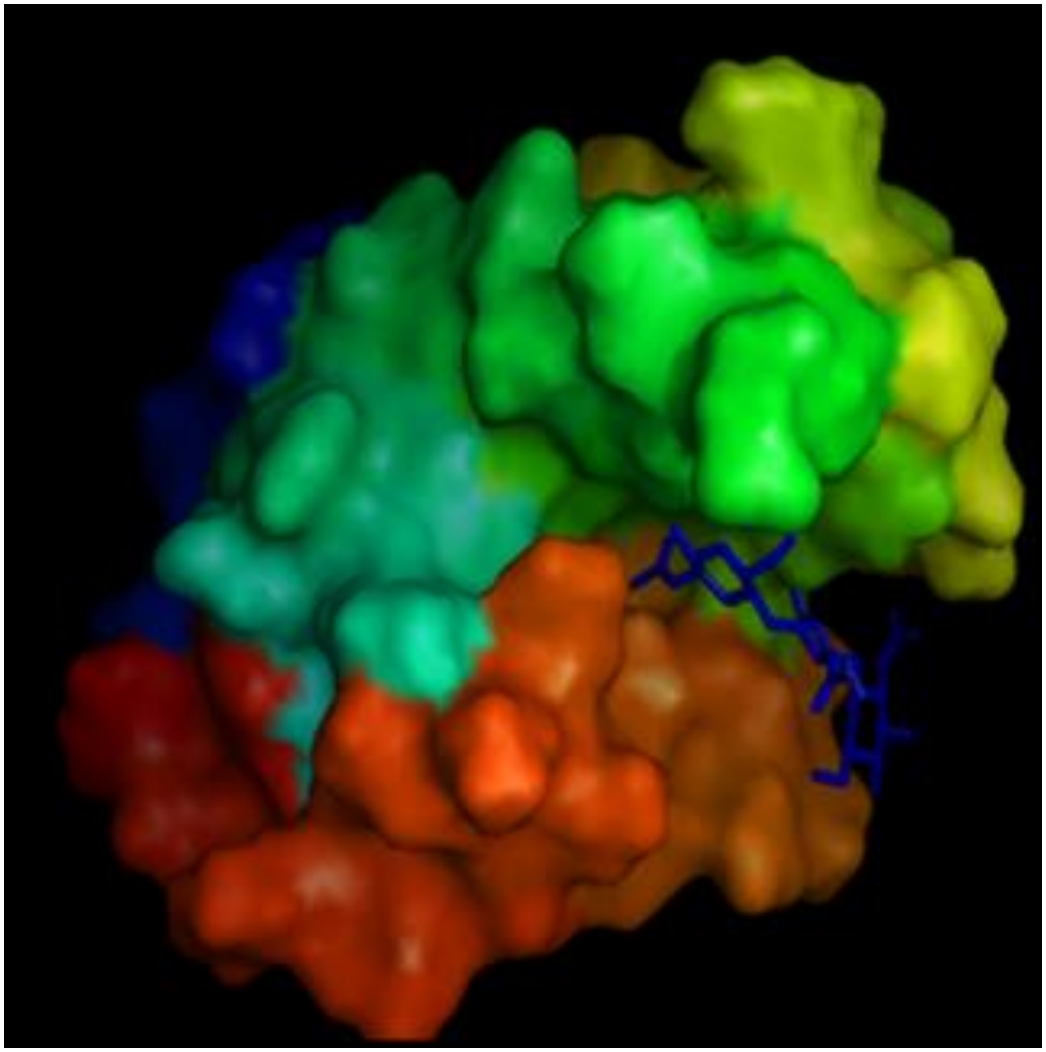

Figure 1.21: *Rat* LYZL6 *shown as surface model and the binding of NAG to the protein. NAG is shown in stick model.*

Detailed docking analysis of LYZL6 revealed that NAG binds and fits into the cleft of the active site (Figure 1.21). LigPlot analyses (Figure 1.22) indicates that Tyr106 forms two hydrogen bonds of length 3.07 and 3.11 with ligand, Trp63 forms a hydrogen bond of length 3.03. In addition to this, Lys62 forms a hydrogen bond of length 3.26 with the ligand. Other than these residues Trp107, Ile97, Ile58 and Gln102 are the other residues that show hydrophobic interaction with the ligand.

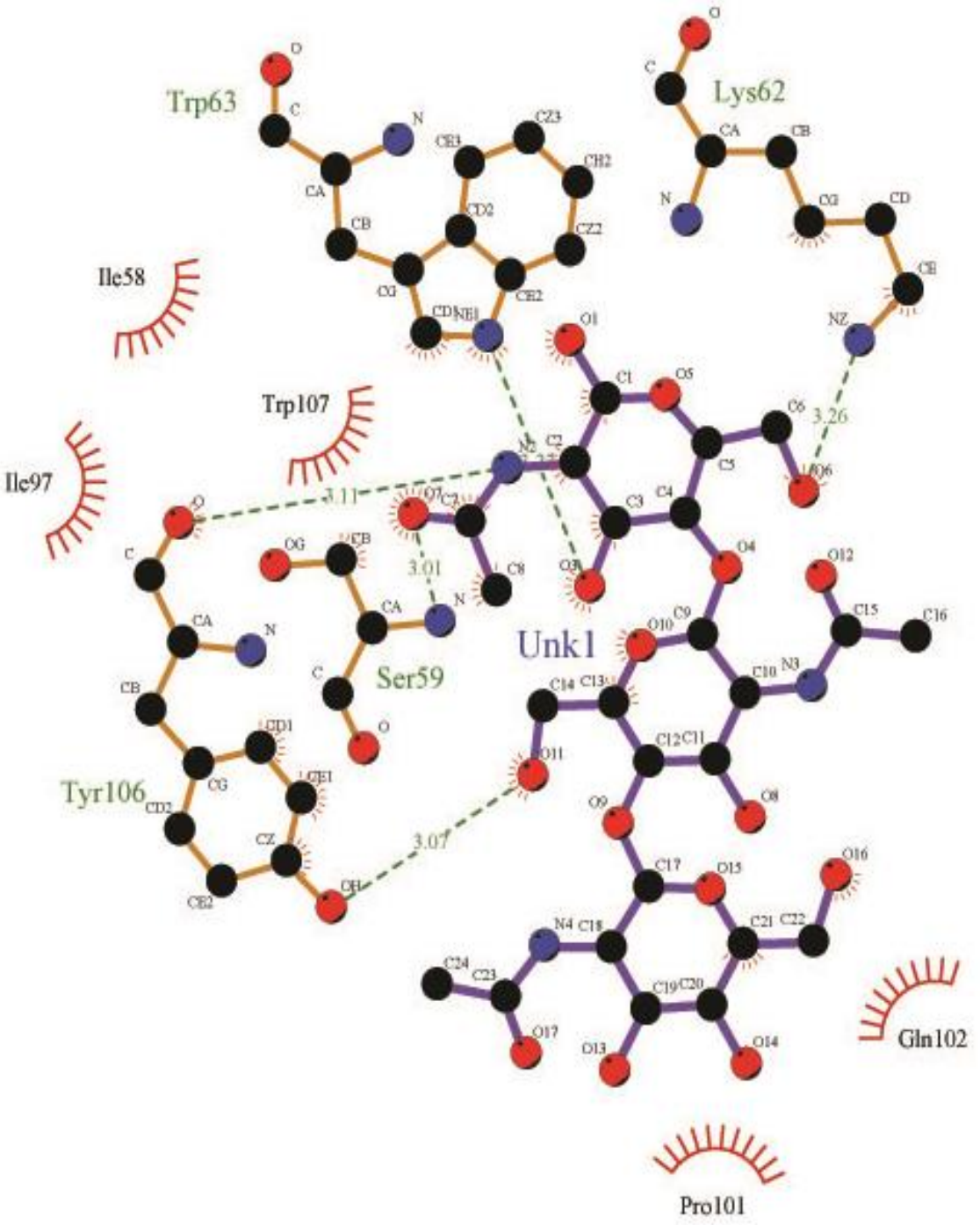

Figure 1.22: *LigPlot analysis for the interaction of* LYZL6 *with NAG.*

Discussion

In this part of the study we report the molecular characterization of rat LYZL proteins using *in silico* methods. The rat *Lyzl* genes were found to be located on different chromosomes suggesting that they are independent genes and are not isoforms coded by a single gene. Analysis of general characters of rat LYZL proteins shows that these proteins have similar physical properties. The LYZL proteins are composed of 140-160 amino acids and their molecular weight range between 16-18kDa. The pI for the LYZL proteins are in the acidic range (below pH 7) except for LYZL1 (pI 8.38). The LYZL proteins also seems to have glycosylation and phosphorylation sites suggesting their possible role in cellular signalling (Ghosh et al. 2013). Post translational modifications are crucial for some protein in the male reproductive tract function (Wiwanitkit 2010; Ashrafzadeh, Karsani, and Nathan 2013). It is possible that the predicted post-translational modifications of LYZL proteins may contribute to reproductive function.

Similarity search for all the LYZL proteins using BLAST shows that these proteins are very similar to c-type lysozyme (McKenzie 1996). Multiple sequence alignment of LYZL proteins reveal that these proteins are very similar to each other although less identical. Other notable feature observed is the conservation of the 8 cysteines which are involved in the formation of four disulphide bonds, a characteristic feature of c-type lysozyme. The catalytic mechanism of c-type lysozymes involves the interaction of Glu35 and Asp52 of the active site with beta-1,4 glycosidic bond of the substrate (Kirby 2001). LYZL1 and LYZL6 possess these active site residues Glu35 and Asp52, and the remaining proteins have conserved them partially (LYZL4 and LYZL5 possess Glu35) or do not (LYZL3 and LYZL7). However, all the LYZL proteins contain the additional substrate binding sites. These findings along with the similarity analysis suggest that these proteins could have arisen from single gene due to divergence at later time points. The pairwise identity and

similarity study performed shows that rat LYZL proteins are closer to mouse counterparts than with humans. Further, these analyses also clearly demonstrate that LYZL7 is slightly different from the remaining LYZL proteins, which is evident by less similarity and identity with lysozyme. LYZL7 is the unique protein among the group which possess calcium binding site whereas, the remaining proteins lack this site and is not a feature of c-type lysozyme but of the lacatalbumin.

The conserved domain analysis shows that all the LYZL proteins uniformly possess lysozyme like superfamily domain which is rich in helix structures and all of them also possess signal peptide suggesting that they are all secretory proteins similar to that of lysozyme. LYZL proteins seems to be amphipathic and this further supports the secretory nature of these proteins, because the presence of hydrophobic and hydrophilic ends (amphipathicity) in the same molecule helps the molecule stay stable in both the environment and also helps the molecule in passing through or partition into the membrane lipid bilayer. This ability to associate with membrane is an important feature for antimicrobial proteins (Mihajlovic & Lazaridis 2012). The amphipathic nature of LYZL proteins predicts antimicrobial property for these proteins.

The secondary structure analysis performed shows that the LYZL proteins exhibit α-helical pattern predominantly, similar to that of lysozyme (Ibrahim et al. 2001). This observation further confirms that the LYZL proteins are not similar only in the primary structure level but also in the second dimension, i.e. in secondary structure level also.

Molecular modeling studies revealed that the LYZL proteins have strikingly similar three dimensional structures. None of the predicted models have residues in the disallowed regions. Further, superimposing studies with the template used, also confirmed that the predicted structures are of good quality, where the G factor analysis also showed agreeable

scores indicating that the models generated can be used for further analysis. The molecular modeling of LYZL proteins further shows the striking similarity in three dimensional structure of these proteins. They resemble lysozyme in possessing a predominant α-helical fold and a β-sheet at the core near the substrate binding region. This feature is one of the landmark property of lysozyme superfamily proteins (Wohlkönig et al. 2010).

Interacting ability of LYZL1 and LYZL6 with N-acetyl glucosamine (docking study) suggests that the presence of active site amino acids in these proteins could be the possible reason. In depth analysis of the interaction study also suggests that the active site region where the substrate binds are surrounded by similar amino acids but not identical amino acids. Altogether it is clear that the primary, secondary and tertiary structures of LYZL proteins are similar to lysozyme. Striking similarity of these proteins in all the three dimensions along with conservation of these genes in the vertebrate organism suggests that the *Lyzl* genes could have arose by gene duplication event from a common ancestor gene in the past before the evolution of vertebrates.

REFERENCES

Allen, P.M., Strydom, D.J. & Unanue, E.R., 1984. Processing of lysozyme by macrophages: identification of the determinant recognized by two T-cell hybridomas. *Proceedings of the National Academy of Sciences of the United States of America*, 81(8), pp.2489–93.

Arnold, K. et al., 2006. The SWISS-MODEL workspace: a web-based environment for protein structure homology modelling. *Bioinformatics (Oxford, England)*, 22(2), pp.195–201.

Ashrafzadeh, A., Karsani, S.A. & Nathan, S., 2013. Mammalian sperm fertility related proteins. *International journal of medical sciences*, 10(12), pp.1649–57.

Boller, T. et al., 1983. Chitinase in bean leaves: induction by ethylene, purification, properties, and possible function. *Planta*, 157(1), pp.22–31.

Chatterjee, S. & Lufkin, T., 2012. Regulatory genomics: Insights from the zebrafish. *Current topics in genetics*, 5, pp.1–10.

Chipman, D.M., Grisaro, V. & Sharon, N., 1967. The binding of oligosaccharides containing N-acetylglucosamine and N-acetylmuramic acid to lysozyme. The specificity of binding subsites. *The Journal of biological chemistry*, 242(19), pp.4388–94.

Dajani, R. et al., 2005. Lysozyme secretion by submucosal glands protects the airway from bacterial infection. *American journal of respiratory cell and molecular biology*, 32(6), pp.548–52.

De, S. & Babu, M.M., 2010. Genomic neighbourhood and the regulation of gene expression. *Curr Opin Cell Biol*, 22(3), pp.326–333.

Frishman, D. & Argos, P., 1995. Knowledge-based protein secondary structure assignment. *Proteins*, 23(4), pp.566–79.

Geourjon, C. & Deléage, G., 1995. SOPMA: significant improvements in protein secondary structure prediction by consensus prediction from multiple alignments. *Computer applications in the biosciences : CABIOS*, 11(6), pp.681–4.

Ghosh, S. et al., 2013. Prolonged glycation of hen egg white lysozyme generates non amyloidal structures. *PloS one*, 8(9), p.e74336.

Gordon Alderton, W.H.W. and H.L. & Fevold, 1945. Isolation of lysoyzme from egg white. *The Journal of biological chemistryjournal of biological che*, 157(1), pp.43–58.

Hansen, N.E. & Andersen, V., 1973. Lysozyme activity in human neutrophilic granulocytes. *British journal of haematology*, 24(5), pp.613–23.

Ibrahim, H.R., Thomas, U. & Pellegrini, A., 2001. A Helix-Loop-Helix Peptide at the Upper Lip of the Active Site Cleft of Lysozyme Confers Potent Antimicrobial Activity with Membrane Permeabilization Action. *The journal of biological chemistry*, 276(47), pp.43767–43774.

Jekel, P.A., Hartmann, B.H. & Beintema, J.J., 1991. The primary structure of hevamine, an enzyme with lysozyme/chitinase activity from Hevea brasiliensis latex. *European journal of biochemistry / FEBS*, 200(1), pp.123–30.

Jenzano, J.W., Hogan, S.L. & Lundblad, R.L., 1986. Factors influencing measurement of human salivary lysozyme in lysoplate and turbidimetric assays. *Journal of clinical microbiology*, 24(6), pp.963–7.

Jolles, P. & Jolles, J., 1961. Lysozyme from Human Milk. *Nature*, 192(4808), pp.1187–1188.

Jones, G., Willett, P. & Glen, R.C., 1995. Molecular recognition of receptor sites using a genetic algorithm with a description of desolvation. *Journal of molecular biology*, 245(1), pp.43–53.

Kirby, A.J., 2001. The lysozyme mechanism sorted -- after 50 years. *Nature structural biology*, 8(9), pp.737–9.

Laskowski, R.A. et al., 1996. AQUA and PROCHECK-NMR: programs for checking the quality of protein structures solved by NMR. *Journal of biomolecular NMR*, 8(4), pp.477–86.

Ma, W., Noble, W.S. & Bailey, T.L., 2014. Motif-based analysis of large nucleotide data sets using MEME-ChIP. *Nature protocols*, 9(6), pp.1428–50.

McKenzie, H.A., 1996. alpha-Lactalbumins and lysozymes. *Experientia*, 75(1), pp.365–409.

Mihajlovic, M. & Lazaridis, T., 2012. Charge distribution and imperfect amphipathicity affect pore formation by antimicrobial peptides. *Biochimica et biophysica acta*, 1818(5), pp.1274–83.

Pellegrini, A. et al., 1997. Identification and isolation of a bactericidal domain in chicken egg white lysozyme. *Journal of applied microbiology*, 82(3), pp.372–8.

Ramachandran, G.N., Ramakrishnan, C. & Sasisekharan, V., 1963. Stereochemistry of polypeptide chain configurations. *Journal of Molecular Biology*, 7(1), pp.95–99.

Rodríguez, C.M., Kirby, J.L. & Hinton, B.T., 2001. Regulation of gene transcription in the epididymis. *Reproduction (Cambridge, England)*, 122(1), pp.41–8.

Sachdev, M. et al., 2012. Oocyte speci fi c oolemmal SAS1B involved in sperm binding through intra-acrosomal SLLP1 during fertilization. *Developmental Biology*, 363(1), pp.40–51.

Sen, D.K. & Sarin, G.S., 1986. Biological variations of lysozyme concentration in the tear fluids of healthy persons. *The British journal of ophthalmology*, 70(4), pp.246–8.

Wallace, A.C., Laskowski, R.A. & Thornton, J.M., 1995. LIGPLOT: a program to generate schematic diagrams of protein-ligand interactions. *Protein engineering*, 8(2), pp.127–34.

Wiwanitkit, V., 2010. Potential protein post-translational modification in ERp57: A phenotype marker for male fertility. *Journal of human reproductive sciences*, 3(3), pp.146–7.

Wohlkönig, A. et al., 2010. Structural Relationships in the Lysozyme Superfamily : Significant Evidence for Glycoside Hydrolase Signature Motifs V. N. Uversky, ed. *PloS one*, 5(11), pp.1–10.

Zhang, K. et al., 2005. Molecular Cloning and Characterization of Three Novel Lysozyme-Like Genes , Predominantly Expressed in the Male Reproductive System of Humans , Belonging to the C-Type Lysozyme / Alpha-Lactalbumin Family 1. *Biology of reproduction*, 1071(73), pp.1064–1071.

Zhang, Y. et al., 2013. Biomolecular event trigger detection using neighborhood hash features. *Journal of theoretical biology*, 318, pp.22–8.

CHAPTER 2

❖ *Expression profiling and biochemical characterization of rat lysozyme-like proteins.*

INTRODUCTION

Proteins secreted by the epithelial surfaces of the male reproductive tract contribute to its physiological function. Examples include CRISP1, 2 and 4 (Ernesto et al. 2012), SAMP32 (Hao et al. 2002), cystatin C (Jiborn et al. 2004), SPAG11 family members (Yenugu et al. 2004) and CRES (Syntin & Cornwall 1999). Further, lysozymes are also one such group of proteins secreted by the male reproductive tract. Lysozymes are present in most of the biological fluids including semen (Mårdh & Colleen 1974). Measuring lysozyme levels in semen was recommended as a marker of infertility (Kuz'min et al. 1991). Origin of lysozyme present in the semen is very interesting. Analysis of the prostate and seminal vesicle fractions indicate that it is secreted equally by these two glands (Tauber et al. 1976).

Lysozymes are divided into six families based on their distribution and functions. They are g-type, i-type, c-type, plant, phage and bacterial. The c-type lysozyme is the predominant type and widely expressed in many species. Some of the species in the animal kingdom possess more than one type of lysozyme. For example mollusks possess both g-type and i-type lysozymes (Lien CalleWaert et al. 2010). The expression pattern of individual lysozymes seems to vary from species to species (Irwin & Gong 2003). Though the primary structure of these proteins are diverse, their three dimensional structure seems to be very similar (Wohlkönig et al. 2010). A common feature of most lysozymes is that they possess antibacterial activity. In spite of their strong binding ability towards lipopolysaccharide, they are more potent against Gram positive bacteria than Gram negative bacteria (Ohno & Morrison 1989). It is interesting to note that the decapeptide of lysozyme despite the absence of muramidase activity site, possess antibacterial activity. Few of the i-type lysozymes are bifunctional with both muramidase and isopeptidase activity. The isopeptidase activity contributes to the breakdown of the isopeptide bond formed between glutamine and lysine during blood clotting thereby a role in regulating blood flow.

Recently a group of lysozyme- like (*Lyzl*) genes that belong to c-type lysozyme family were identified. Zhang et al., have reported the mRNA expression of *Lyzl*2, *Lyzl3*, *Lyzl4* and *Lyzl6* in humans tissues. *Lyzl*2, *Lyzl4* and *Lyzl6* mRNA were found to be expressed only in the testes and *Lyzl*3 was found to be expressed in testes and pancreas (Zhang et al. 2005). Sperm lysozyme-like protein 1 (SLLP1 or LYZL3) was found to be an intra-acrosomal and non-bacteriolytic c-type lysozyme-like protein in human spermatozoa (Mandal et al. 2003). LYZL4 is a sperm bound protein with a role in fertilization (Sun et al. 2011) and is expressed in testes and epididymidis. These studies point to the fact that LYZL proteins are expressed predominantly in male reproductive tract. However in-depth analysis of their expression pattern and biochemical functions in general physiology and in the male reproductive function in particular are lacking. Hence, in this part of the study we attempted to characterize the expression of *Lyzl* genes and their protein products. Biochemical characterization was also undertaken to understand their role in general physiology.

MATERIALS AND METHODS

Total RNA isolation

Wistar rats aged 90 days were obtained from National Centre for Laboratory Animal Sciences, National Institute of Nutrition, Hyderabad. The animals were sacrificed and the following tissues were collected: brain, heart, lungs, liver, kidney, spleen, ovary, uterus, cervix, caput, corpus, cauda, testis, seminal vesicles and prostrate. The tissues were immediately snap frozen and stored at -80°C. Total RNA was extracted using TRIzol reagent (Invitrogen) (Chomczynski & Sacchi 2006). Briefly, 10 mg of tissue was ground with liquid nitrogen to make fine powder and 1 ml of TRIzol was added and vortexed for 10 min. The homogenate was centrifuged at 10,000 rpm for 10 min at 4°C. 200 µl of chloroform was added and mixed well and centrifuged for phase separation. The supernatant was then collected and equal quantity of isopropanol was added and centrifuged. The resulting pellet was then washed twice with 70% ethanol and air dried before dissolving in DEPC treated water. The purified RNA was then quantified using NanoDrop (Thermo Scientific) and the quality of the RNA was confirmed by agarose gel electrophoresis.

cDNA generation

To 2 µg of total RNA, 0.2 µg of oligo dT was added and the final volume was made upto to 10 µl with water. The mixture was incubated at 65°C for 5 min and a cocktail (containing 10 U reverse transcriptase (Promega), 10 U RNase inhibitor (Fermentas), 5X reverse transcriptase buffer, 10 mM dNTPs and water) was added and subjected to thermal cycling in a thermal cycler as per the manufacturer's instruction. The cDNA generated was stored at -20°C.

Polymerase chain reaction

Gene specific primers for rat *Lyzl1*, *Lyzl3 Lyzl4 Lyzl5 Lyzl6 and Lyzl7* were designed, synthesized (Table 7) and used for polymerase chain reaction (PCR) to study *Lyzl* gene

expression in various tissues. The number of cycles to amplify each cDNA in the linear range was determined by preliminary PCR under the following conditions: 94°C for 1 min followed by 30 cycles at 94°C for 30 sec, 58°C for 30 sec and 72°C for 30 sec, and with a final round of extension at 72°C for 10 min. The internal control gene glyceraldehyde 3 phosphate dehydrogenase (*Gapdh*) was amplified with the same conditions. PCR amplified gene products were analysed by electrophoresis on 2% agarose gels.

Table 7: Gene specific primers used in this study

Gene	Primer sequence (5' --->3')	No. of bases	Amplicon size (bp)
Lyzl1 FP	TGTCGGTGTCTTCGCCCTAAT T	22	408
Lyzl1 RP	GAC GAG TCT TTG CTC TCA CAG T	22	
Lyzl3 FP	TCC AGC AAG GCC AAG GTC TTC A	22s	398
Lyzl3 RP	TAG AAG TCA CAG CCA TCC ACC CA	23	
*Lyzl4 FP1**	ATG TGG GCA CTG TTG ACA CCA	21	602
*Lyzl4 RP1**	CTA CAC CAT TGA TCC TGC TCC A	22	
*Lyzl4 FP2**	GTG GTG ATT GAG GAT TCC TTC AG	21	641
*Lyzl4 RP2**	ATG GAG GCA CCA ATC GGA GTC A	22	
*Lyzl4 FP3**	ATG CAG CTG TAC CTG GTG CTT CT	23	603
*Lyzl4 RP3**	GCT GGTTTATTCTGCACCTTGTAC C	25	
Lyzl5-FP	CACGCATGC**A**AAGATTTATGAACGCTGTG	29	420
Lyzl5-RP	CAGGTCGACTCACCAGTCATCATAGT	26	
Lyzl6 FP	TAT CTG TGT GGT GAG CTG CCT TCT	24	322
Lyzl6 RP	TGC ACA GTG GAT GGA TGGAAT GAG	24	
Lyzl7-FP	TATGCATGC**T**ACAGAGTTTACAAAATGTGA	30	441
Lyzl7-RP	AGGTCGACTTAGGGAACAGGTGTTTCTGAAT	31	

*FP- forward primer; RP-reverse primer; *-used for amplifying the full length sequence.*

To study the androgen regulation of *Lyzl* transcripts, epididymides were obtained from sham operated, castrated and testosterone supplemented Wistar rats (n = 5 in each group). Testosterone supplementation was by a 20 mg dihydrotestosterone pellet implanted subcutaneously immediately after castration. The animals were sacrificed 14 days after castration. All procedures involving animals were performed in accordance with the guidelines established by the institute's animal ethical committee (IAEC). For studies on the developmental regulation of *Lyzl* genes, testes and epididymides were obtained from 10- to 60-day old Wistar rats.

Cloning of rat *Lyzl* genes

The full length cDNA of rat *Lyzl 1*, *3*, *4*, *5*, *6* and *7* without the signal peptide were amplified and cloned into pQE80m vector.

Table 8: Cloning details

Gene	*Lyzl1*	*Lyzl3*	*Lyzl4*	*Lyzl5*	*Lyzl6*	*Lyzl7*
Insert size (bp)	687	684	674	717	687	720
Restriction sites used	*Sph1, Sal1*	*Sph1, Sal1*	*BamHI, Hind III*	*Sph1, Sal1*	*Sph1, Sal1*	*Sph1, Sal1*
MW of the recombinant proteins (kDa)	16.2	17.27	15.4	17.7	16.7	17.27
pI of the recombinant proteins	8.59	6.28	7.02	6.17	6.43	5.58

Using gene specific primers, the coding region of *Lyzl* genes without their signal peptide was amplified from testes cDNA. The amplified PCR products were purified and digested using appropriate restricting enzymes (Table 8). The digested PCR products were then purified, quantified and ligated into pQE80m vector. After ligation, each plasmid was transformed into *E.coli DH5α* and ampicillin resistant colonies were checked by colony PCR for presence of the insert. Plasmid was isolated from positive clones that showed right amplicon size. They were then sequenced to confirm the presence of the insert, its orientation and reading frame. Details of restriction sites used, size of the insert and the predicted size of the recombinant protein are given in table 8.

Recombinant protein production

Plasmids containing one of the *Lyzl* coding region were transformed into *E.coli BL21* to express the recombinant protein. The bacterial cells were then plated on Luria Bertani (LB) agar plates containing ampicillin as the selection marker. Single colony was inoculated into LB medium and incubated over night at 37°C for 16 h with shaking. 2% of the overnight culture was inoculated into 2 L of fresh LB medium. The culture was allowed to grow until it reaches an A_{600} = 0.5. Protein expression was induced with 1mM IPTG for 3 hr. After induction, bacterial cells were pelleted and stored at -80°C. The cytosolic and inclusion body fractions of the bacterial cells were checked to identify the localization of the recombinant protein. Since the LYZL proteins were present in the inclusion body fraction, they were purified under denaturation conditions. Briefly, 5 ml of buffer A (6M Guanidine HCl, 0.1M NaH_2PO_4, 0.01M Tris HCl, pH 8) was added to 1 g of bacterial cell pellet and lysed for 30 min, followed by centrifugation at 10,000 rpm for 30 min at 4°C. The supernatant was then incubated with 1 ml of 50% Ni-NTA resin which was prewashed with buffer A. After binding for 30 min, the column was packed and washed sequentially with urea buffers of gradient pH (buffer B (8M Urea, 0.1M NaH_2PO_4, 0.01M Tris HCl, pH 8),

buffer C (buffer B at pH 6.3) and buffer D (buffer B at pH 5.9)). The recombinant protein was then eluted with buffer E (buffer B at pH 4.5) after washing with buffer D1 (20mM Tris, 20mM Imidazole, 5mM BME, 500mM NaCl, 10% glycerol pH 5.8) to remove the non-specific proteins. Purity of the eluted fractions were checked by separating them on SDS-PAGE and visualizing the bands by coomassie brilliant blue staining.

The identity of the purified recombinant protein was confirmed by Western blotting using anti-His tag antibody. Protein fractions separated on 15% SDS-PAGE and electrotransfered to PVDF membrane at 25V for 16h were probed with rabbit anti-His antibody (Santa Cruz Biotechnology) and then incubated with anti-rabbit secondary antibody (Bangalore Genei) tagged with HRP. Protein bands were detected using chemiluminescence kit (GE healthcare). The fractions that contained the protein of interest were dialysed extensively at 4°C against 10 mM sodium phosphate buffer, pH 7.4.

Raising of polyclonal antibodies

New Zealand white rabbits aged four months were obtained from National Institute of Nutrition, Hyderabad and acclimatized to animal house conditions for 1 week. Preimmune serum was collected and checked for cross reactivity with recombinant LYZL proteins and male reproductive tract tissue lysates by Western blotting. After confirmation of non-cross reactivity, rabbits were immunized intradermally with 600 µg of the recombinant protein mixed with equal volume of Freund's complete adjuvant. Booster doses containing 600 µg protein was mixed in Freund's incomplete adjuvant were administered on 3^{rd} and 28^{th} day. Antibody titer was checked on 35^{th} day and final bleeding was done on 42^{nd} day (Xiao et al. 2004). Each antibody was checked for cross reactivity against each and every LYZL protein to ensure there is no cross reactivity within recombinant LYZL proteins.

Immunoblotting

Testes, caput, cauda, seminal vesicles and prostate tissues were collected from 90 day old Wistar rats and 10% homogenates were prepared in RIPA buffer containing protease inhibitors. The homogenate was then centrifuged at 10,000 rpm for 10 min to remove the debris and concentration of the protein in the supernatant was quantified by Lowry's method. For sperm lysate preparation, 5 X 10^6 spermatozoa were suspended in 1 ml of RIPA buffer, sonicated, centrifuged and the protein concentration estimated. 100 µg of the total protein was separated by electrophoresis on 15% SDS PAGE and transferred to nitrocellulose membrane at 25V for 16 h. The membrane was then stained with Ponceau stain to check the integrity of the transfered proteins and then blocked with 5% skim milk for 2h at room temperature. The membrane was then probed with primary antibody (immune serum) for 1h followed by washes with TBS and TBS-T. It was then incubated with anti-rabbit HRP tagged secondary antibody followed by washes with TBS and TBS-T each for 10 min. At the end of washing, the membrane was developed using chemiluminescence kit.

Immunolocalization

Wistar rats aged 90 days were dissected to collect the testes, spermatozoa and epididymides. Testes were fixed by immersing in Bouin's solution for 6 h at 37°C followed by washing in 70% ethanol untill it destained completely before proceeding with embedding in paraffin wax. Epididymides were fixed by immersing in 4% paraformaldehyde for 12 h and then washed in PBS before block preparation and embedding.

Serial sections (five microns) of testes and epididymides were preheated to 60°C for 5 min followed by xylene wash for 10 min. They were then washed in gradient alcohol (70-100%) followed by phosphate buffered saline (PBS) wash each for 10 min. Antigen retrieval was

carried out by heating the slides in 10 mM citrate buffer pH 6.5 for 12 min in an oven. They were then washed with PBS and permeabilized by incubating in PBS containing 1% triton X-100 (PBST) for 15 min. Tissue sections were blocked with 10% goat serum for 45 min at 37°C followed by incubation with immune serum (1:500 dilution) for 1 h 30 min at 37°C or at 4°C overnight. The slides were then washed in PBS thrice and incubated with anti-rabbit antibody tagged with TRITC or FITC for 1 h followed by three washes with PBS for 10 min each. 4', 6-diamidino-2-phenylindole (DAPI) was used to stain the nucleus. The sections were then mounted with antifade and stored at 4°C in dark. Images were taken using confocal microscope(Khobarekar et al. 2007)(Khobarekar et al. 2007). In the case of spermatozoa, smears on glass slides were prepared and air dried. They were then permeabilized with PBST, blocked with 10% goat serum and processed in a similar way as that of tissue sections.

Circular Dichroism

Circular dichroism was performed for recombinant LYZL proteins using Jasco J-810 spectropolarimeter. Quartz cell with a path length of 0.2 cm was loaded with 200 µl of 0.1µg/µl protein and scanned in the far UV region (180-260 nm). Three scans at a scan speed of 50 nm/min were accumulated and the polarimetry data was collected for every 1 nm. The data thus collected was used for calculating mean residue ellipticity (MRE) and the spectrum was plotted (Sreerama & Woody 2004). In addition, the spectra of appropriate blank solution, 10 mM phosphate buffer was subtracted from the spectrum of the protein. Percentage of secondary structure elements were calculated using K2D3 tool of Dichroweb (Louis-Jeune et al. 2011).

Muramidase Assay

The muramidase assay is based on the cleavage of β-glycosidic bond between N-acetyl muramide and N-acetyl glucosamine (Markart et al. 2004). Reduction in O.D at 450 nm is observed as the glycosidic bonds are broken. The muramidase activity of recombinant rat LYZL proteins was determined. Briefly, recombinant rat LYZL protein was incubated with 2 ml of *M. lysodeikticus* cells in 50 mM KH_2PO_4-NaOH buffer, pH 7.0, and the decrease in turbidity was monitored at 450 nm in a spectrophotometer for every 60 min until 6 h. Change in O.D (Δ O.D) was calculated by subtracting the final O.D from initial O.D. Muramidase activity was expressed as Δ O.D. Lysozyme was used as a positive control.

Isopeptidase Assay

The isopeptidase activity assay is based on the cleavage of L-γ-glutamine-p-nitroanilide (L-γ-Glu-pNA) to produce p-nitroanilide (pNA), which exhibits absorbance at 405 nm (Takeshita et al. 2003). Recombinant rat LYZL proteins were added to the reaction mixture containing 1.75 mM L-γ-Glu-pNA in 0.05 M 3-(N-morpholino) propane sulfonic acid (MOPS) buffer, pH 7, containing 0.01M NaCl and the formation of pNA was monitored spectrophotometrically at 405 nm for every 1 h until 6 h. Activity was expressed as Δ O.D. Lysozyme was used as positive control.

Antibacterial Assay

Colony forming units (CFU) assay was employed to test the antibacterial activity (Yenugu et al. 2003). Briefly, overnight cultures of *E. coli* XL-1 blue were grown to mid-log phase (A_{600} = 0.4 – 0.5) and diluted with 10 mM sodium phosphate buffer (pH 7.4). Approximately 2 X 10^6 CFU/ml of bacteria was incubated at 37˚C with 10–100 μg/ml of the recombinant LYZL protein and aliquots of the assay mixture were taken at 30, 60, 90 and

120 min after the start of incubation. The assay mixtures were serially diluted with 10 mM sodium phosphate buffer (pH 7.4) and 100 µl of each was spread on a Luria–Bertani agar plate and incubated at 37˚C overnight to allow full colony development. The resulting colonies were hand counted and plotted as log CFU/ml. Lysozyme was used as a positive control.

Scanning Electron Microscopy

E.coli were treated with recombinant LYZL protein for 120 min and the bacterial cells were fixed in Karnovks's fixative solution (2% paraformaldehyde, 2.5% glutraldehyde in 0.1M phosphate buffer) for overnight at 4°C. They were then serially washed with graded alcohol (30% to 100%) for dehydration and finally suspended in acetone before embedding on carbon tape. The samples were then coated with gold and then observed under scanning electron microscope (Yenugu et al. 2004). Lysozyme was used as a positive control.

Membrane potential measurement

The effect of LYZL protein on the bacterial membrane potential and permeability was determined by using $DiOC_2(3)$ and TO-PRO-3 respectively (Novo et al. 2000). $DiOC_2(3)$ emits green fluorescence as a single molecule, which varies with cell size and is independent of membrane potential. The red fluorescence of $DiOC_2(3)$ is due to dye aggregation and depends on both size and membrane potential. Therefore the ratio of red to green is attained to measure the membrane potential. TO-PRO-3 is a DNA binding dye and is impermeable to live cells. Due to its ability to enter into membrane compromised cells it is used as dead cell indicator. The dead cells are eliminated when measuring the fluorescence of $DiOC_2(3)$. *E. coli* grown to mid log phase were diluted in 10 mM sodium phosphate buffer pH 7.4 to a final concentration of 10^6 to 10^7cells / ml and then treated with 100 µg of recombinant LYZL protein or 15 µM of the bacterial membrane potential

disruptor carbonyl cyanide m-chlorophenyl hydrazine (CCCP) for 2 h at 37 ^{0}C in orbital shaker. The cells were then washed in 10 mM phosphate buffer, pH 7.4 followed by incubation with 30 µM $DiOC_2(3)$ and 100 nM TO-PRO-3 for 5 min at room temperature. At the end of incubation, bacterial cells were washed and analysed in a flow cytometer (BD LSR Fortessa). The far red fluorescence of TO-PRO-3 is measured in the PerCP-Cy5-5A. The green and red fluorescence of dye $DiOC_2(3)$ was measured in FITC and PE-Texas Red-A channel respectively.

Peptidoglycan binding assay

96 well plates coated with 40 µg/ml peptidoglycan (PGN) (50µl) or hyaluronan were incubated at 37˚C and at 60˚C for overnight and 30 min respectively. The plates were then blocked with 1 mg/ml BSA for 2 h and varying concentrations of the recombinant LYZL protein was added to the wells and incubated for 3 h. The wells were then washed 4 times with PBS-T (PBS with 0.1% Tween-20), followed by sequential incubation with primary antibody (1:1000) against the LYZL protein being tested and HRP conjugated secondary antibody (1:10000). After thorough washing, O-Phenylenediamine (OPD) was used to measure the amount of antibody bound to the protein complex and the binding efficiency is measured in terms of ELISA index (EI). ELISA index is calculated by dividing the average O.D of test samples with average O.D of control samples (Wang et al. 2011) . Lysozyme was used as a positive control.

Hyaluronidase activity assay

0.8% hyaluronan in 300 mM phosphate buffer (pH 7.4) was mixed with melted agarose (0.8%). 100 µl of the gel was dispersed into each well of a microtitre plate. After solidification 50 µl phosphate buffer (pH 7.4) containing varying concentrations of recombinant LYZL protein was added to each well and incubated for 17 h. At the end of the

incubation, solutions were removed and the hyaluronan was precipitated by adding 100 µl of 10% cetyl pyridinium chloride and incubating for 30 min at 37˚C. The turbidity developed was read at 595 nm (Handwaskar et al. 2007). Hyaluronidase activity was measured in terms of decrease in turbidity (or O.D). Hyaluronidase was used as a positive control.

Free radical scavenging assay

This assay is based on the ability of 1,1-diphenyl-2-picrylhydrazyl (DPPH) to undergo reduction due to the presence of an odd electron, and thus exhibits a strong absorption maximum at 517 nm (You et al. 2010). As this electron becomes paired off in the presence of a hydrogen donor, a free radical scavenging antioxidant, the absorption capacity decreases, resulting in decolorization. 0.04% of 1, 1 diphenyl-2-picryl hydrazyl (DPPH) was dissolved in methanol. To 100 µl of DPPH solution, varying concentrations of recombinant LYZL protein was added and incubated at room temperature for 30 min. Free radical scavenging capacity was assessed by measuring the discoloration of DPPH at 517 nm. Lysozyme was used as a positive control.

Statistical Analysis

Statistical analysis were performed using ANOVA and Student's t-test available in Sigma Plot software (SPSS Inc., Chicago, IL, USA). Values shown are mean $\pm$ SD.

RESULTS

Lyzl gene expression

Using gene specific primers, *Lyzl1, Lyzl3, Lyzl4, Lyzl5, Lyzl6* and *Lyzl7* expression was analysed in various rat tissues. Since the full length sequence of *Lyzl4* was not reported it was amplified, sequenced and submitted to GenBank, NCBI and was given the accession no. NM_001246183.1. Among the male reproductive tract tissues, *Lyzl* genes were expressed only in the testis (Figure 2.1). However, *Lyzl7* expression was detected in the cauda along with testis. Further, analysis using cDNA obtained from non-reproductive tissues and female reproductive tissues indicated that *Lyzl* 3, 5 and 6 transcripts are confined only to the testis. *Lyzl1, 4* and *7* were found to be expressed in non-reproductive tissues as well (Figure 2.1).

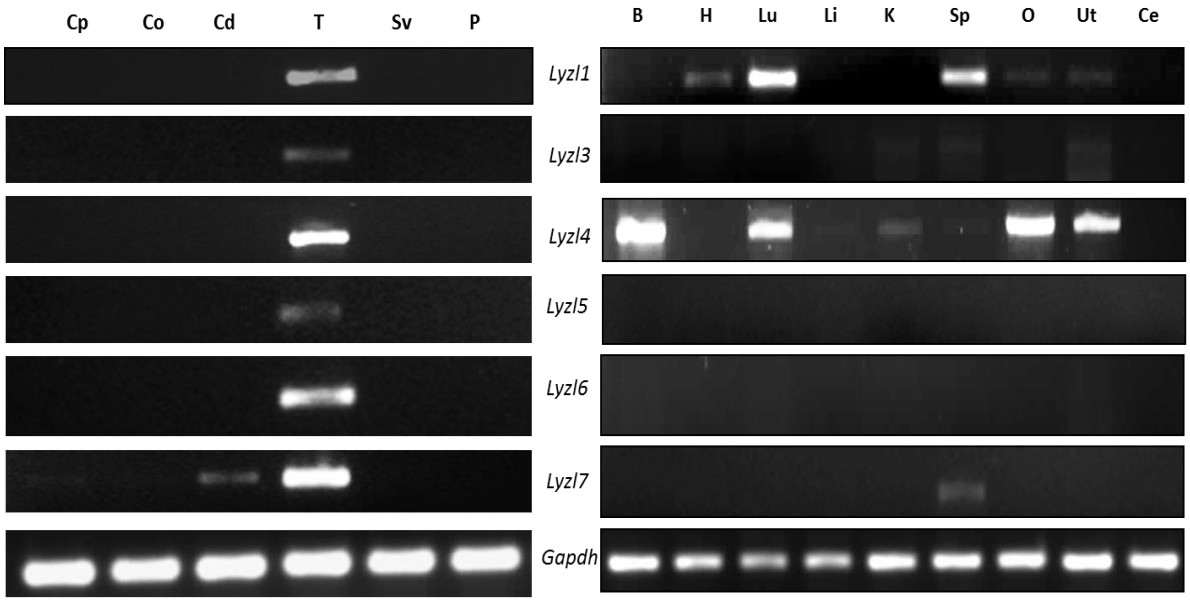

Figure 2.1: *Expression of Lyzl genes in the male reproductive and non- reproductive tissues. RNA isolated from different tissues of rats were reverse transcribed and used for gene specific PCR. Gapdh was used as internal control. Cp-caput, Co-corpus, Cd-cauda, T- testes, Sv-seminal vesicle,, P-prostate, B-Brain, H- Heart, Lu-Lungs, Li-Liver, K-Kidney, Sp-Spleen, O-Ovary, Ut-Uterus, Ce-Cervix, Gapdh-Glyceraldehyde 3 phosphate*

Gene expression in the male reproductive tract is under the influence of androgens. To elucidate the influence of androgen variation, PCR analyses for *Lyzl* genes were carried out using total RNA isolated from the epididymidis and testes of 20–60 day old rats. Though the expression of *Lyzl* transcripts is absent in the epididymis obtained from the adult rats, it is possible that they may be expressed in the younger rats during postnatal development. In the epididymis, none of the *Lyzl* genes analysed in this study was expressed at all the ages during development (Figure 2.2). In the testes, the *Lyzl* transcripts seem to be expressed in all the age groups starting from 30 days (Figure 2.2).

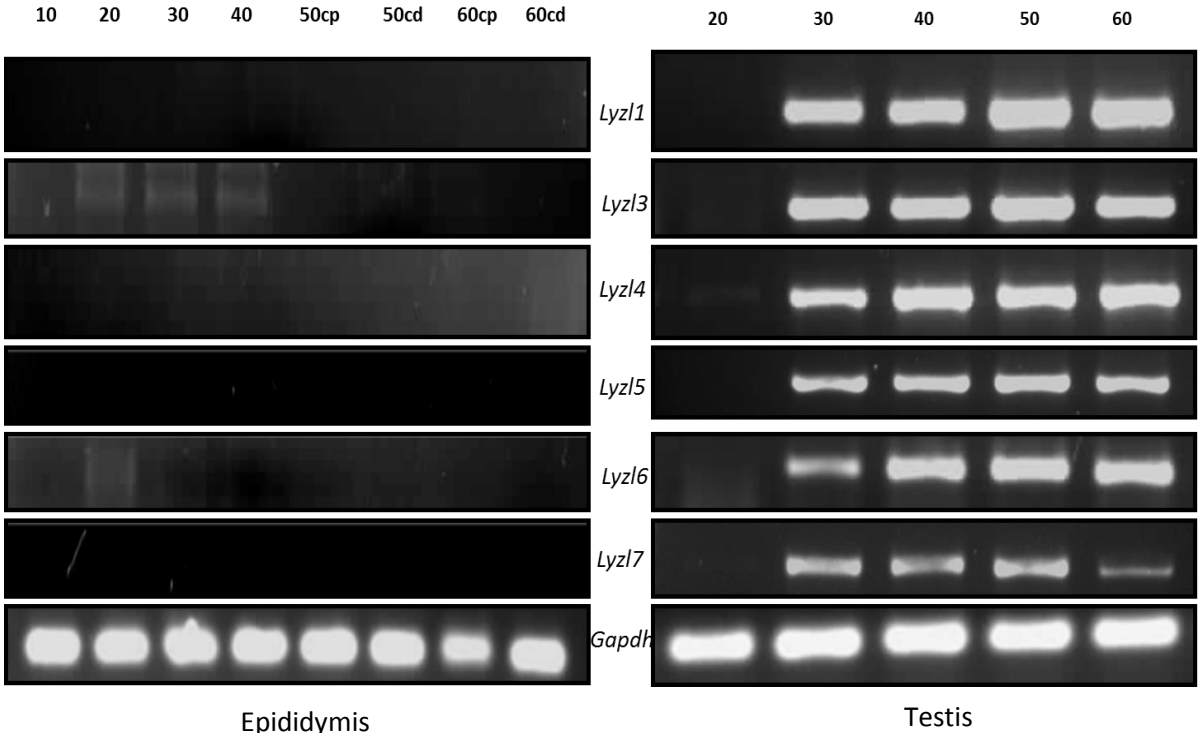

Figure 2.2: *Developmental regulation of Lyzl genes in epididymidis and testes.* *RT PCR for Lyzl genes in epididymis and testes collected from rats of different age groups. 10, 20, 30, 40, 50 and 60 are the age of rats in days. cp- caput, cd-cauda. Gapdh was used as the internal control.*

Cloning and recombinant protein production

Cloning strategy was planned using Vector NTI program. The coding region of the *Lyzl* genes was cloned into pQE80m vector (Figure 2.3). The vector was obtained as kind gift from Dr. Susan Hall, University of North Carolina, U.S.A. The vector contains a T5 promoter followed by ribosomal binding site and a 6X histidine polylinker which codes for N-terminal 6X histidine tag. The coding region is cloned next to the polylinker by making use of the multiple cloning sites (MCS). The vector contains stop codons in all the three frames besides the beta lactamase (*bla*) gene, which confers ampicillin resistance. Details of the restriction sites used, size of the insert and the predicted size of the recombinant proteins are given in table 8. After ligation, plasmids were transformed into *E.coli DH5α* and colonies were checked by colony PCR for presence of the insert using standard vector primers. PCR amplicons corresponding to the size of the respective insert size were observed in majority of the colonies tested (Figure 2.4).

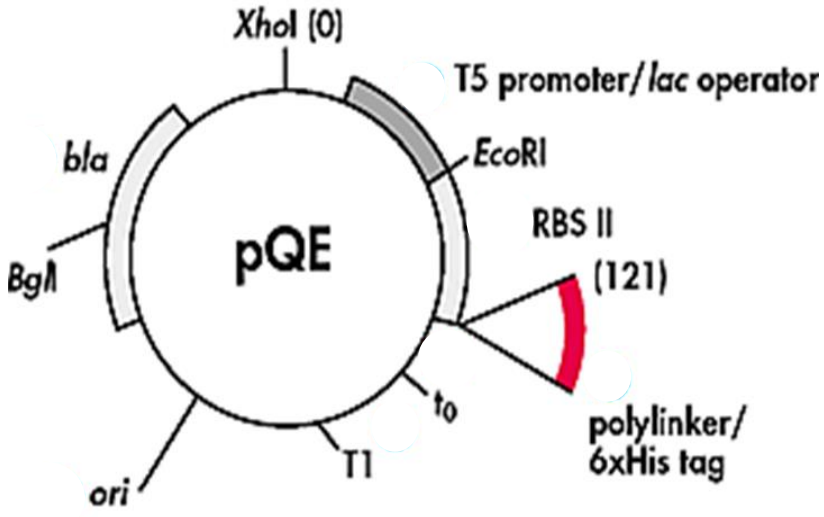

Figure 2.3: *The generalized map of pQE vector (adopted from Qiagen).*

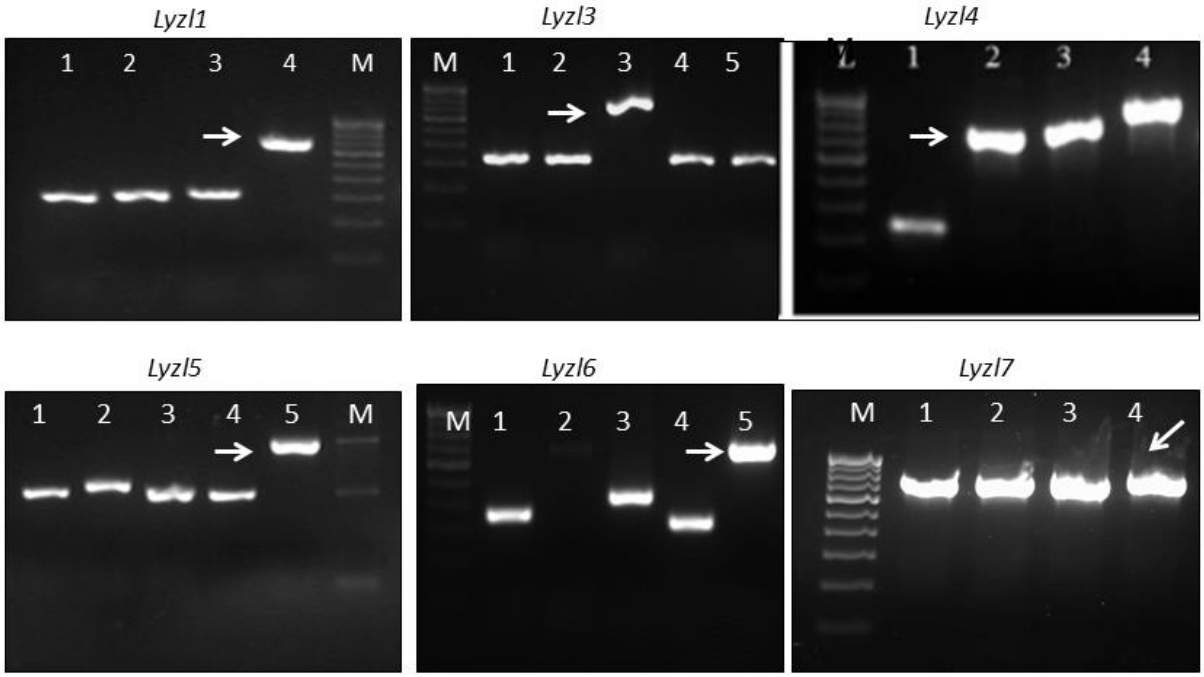

Figure 2.4: *Cloning of Lyzl genes into pQE80m vector**.** Colony PCR using single colonies obtained after transforming E.coli DH5α with plasmids containing Lyzl1-7 inserts. Arrow indicates the expected amplicon size.*

PCR amplicons from the positive clones were amplified and sequencing analyses confirmed the presence of the insert in proper orientation and in frame with the 6X His-tag. Plasmids isolated from positive clones were propagated into *E.coli BL21* to express the recombinant protein by IPTG induction. 6X His-tagged proteins were purified using nickel nitrilotriacetate matrix and were found to have minimum contamination as observed on SDS- PAGE and staining with commaassie brilliant blue (Figure 2.5). Western blotting using anti-His antibody confirmed the identity of the purified proteins basing on the molecular weight (Figure 2.6). In few cases we could observe dimer or trimer formation of the recombinant protein. They were confirmed to be derived from monomers, since they formed monomers upon reduction with tris (2 carboxy) ethyl phosphine (TCEP).

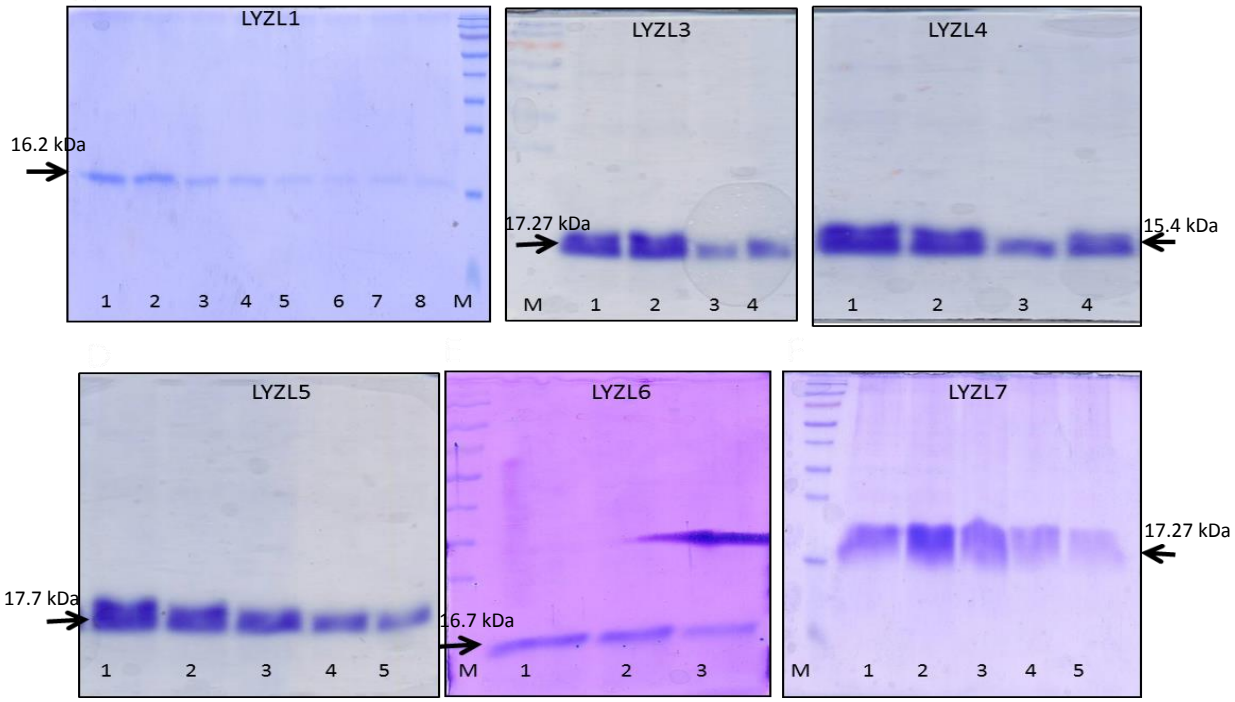

Figure 2.5: *Recombinant protein purification of* LYZL *proteins. Purified recombinant protein fractions were analysed on 15% SDS PAGE. M indicates molecular weight marker. Arrows indicate the purified protein of interest. Numbers indicate the protein fraction number when eluted with buffer E.*

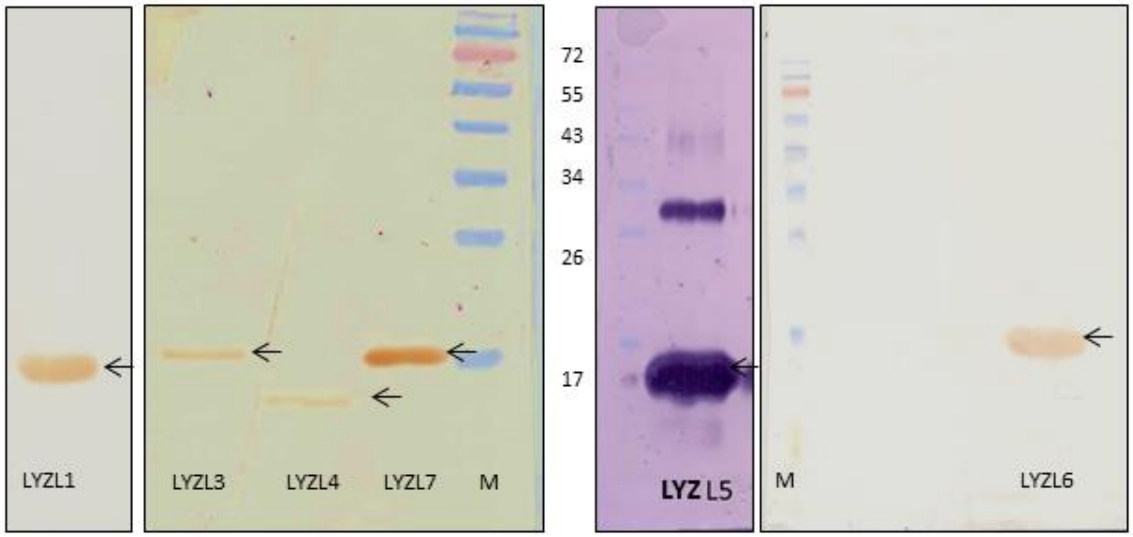

Figure 2.6*: Western blot analysis of the recombinant LYZL proteins. Immunoblot of recombinant* LYZL *proteins using anti-His tag antibody. M indicates molecular weight marker. Arrows indicate protein of interest.*

Antibody Generation

Recombinant protein was injected intradermally by standard methods and the antibody titer was checked by dot blot. Cross reactivity among the antibodies was checked by Western blotting analysis for all the LYZL proteins with each immune sera. No cross reactivity was observed (Figure 2.7) suggesting that the antibodies generated are specific to the individual LYZL proteins.

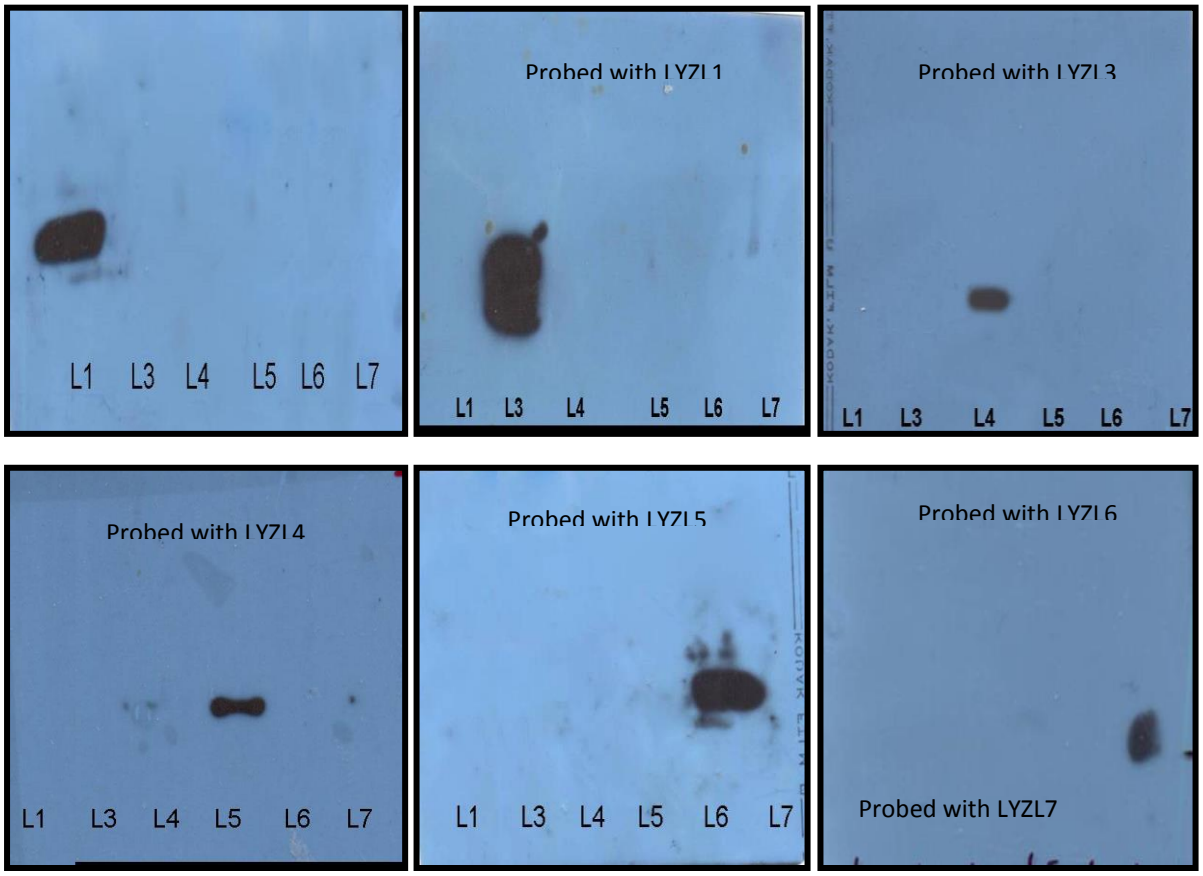

Figure 2.7: *Cross reactivity of antibodies between recombinant* LYZL *proteins. Immunoblots showing the specificity of the antibodies generated. All the* LYZL *proteins were probed with each and every* LYZL *antibody. L1- Lysozyme- like1, L3- Lysozyme-like3, L4- Lysozyme-like 4, L5- Lysozyme-like 5, L6- Lysozyme-like 6 and L7- Lysozyme-like 7.*

Expression of LYZL proteins

Since mRNA expression of the *Lyzl* genes was found in the rat male reproductive tissues, their translation products (proteins) were also analysed by immunoblotting. LYZL1, 3, 4 and 5 are expressed only in testes (Figure 2.8). LYZL6 is observed in both epididymidis and testes. LYZL3, 4 and 6 were detected on sperm, whereas, the other proteins were not. LYZL7 expression was not detected in any of the tissues analysed (Figure 2.8).

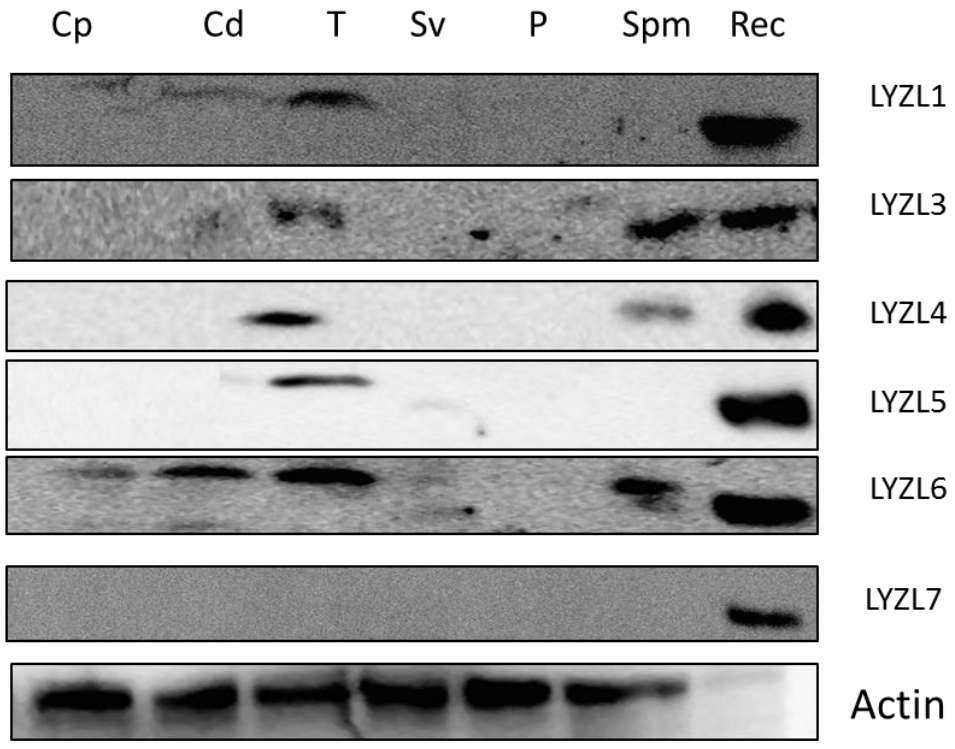

Figure 2.8: LYZL *protein expression in male reproductive tract. Immunoblotting of* LYZL *proteins in male reproductive tract tissues. The blots were probed with immune serum specific to each protein. Cp-caput, Cd-cauda, T-testes, Sv-seminal vesicles, P-prostate, Spm-sperm, Rec-recombinant protein***.**

Immunolocalization of LYZL proteins

LYZL1 protein was localised only in the testes, especially in the germinal epithelium. It was also detected in the head region of spermatozoa obtained from adult rats (Figure 2.9). Similarly, LYZL 3, 4, and 5 (Figure 2.10, 2.11 and 2.12 respectively) were found to be localised in the testes and on the spermatozoa. LYZL3 and 5 are localized to head region of the spermatozoa. LYZL4 expression in the sperm was restricted to tail region (Figure 2.11). LYZL6 expression was detected in both in the epididymidis and testes and also in the head region of the spermatozoa (Figure 2.13). LYZL7 expression was undetectable in all the tissues analysed (Figure 2.14).

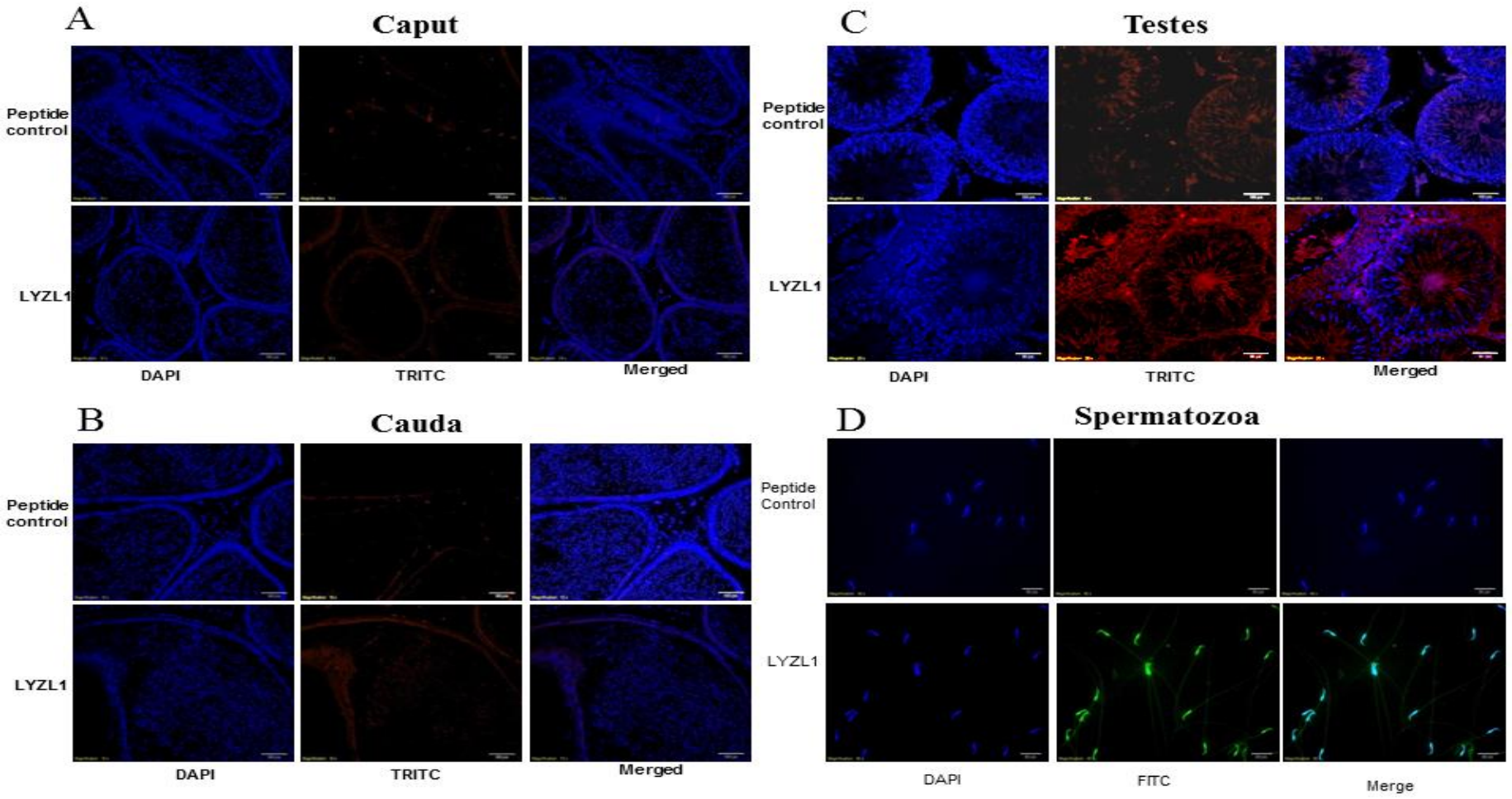

Figure 2.9: *Immunolocalization of* LYZL1. *Serial sections of the rat testes and epididymides were incubated with antigen preadsorbed immune serum (peptide control) or immune serum raised against* LYZL1, *followed by TRITC (Tetramethylrhodamine-5-(and-6)-Isothiocyanate (5(6)) tagged secondary antibody and counter stained with DAPI (4',6-diamidino-2-phenylindole) nuclear stain. Spermatozoa were stained with FITC (fluorescein Isothiocyanate) tagged secondary antibody.*

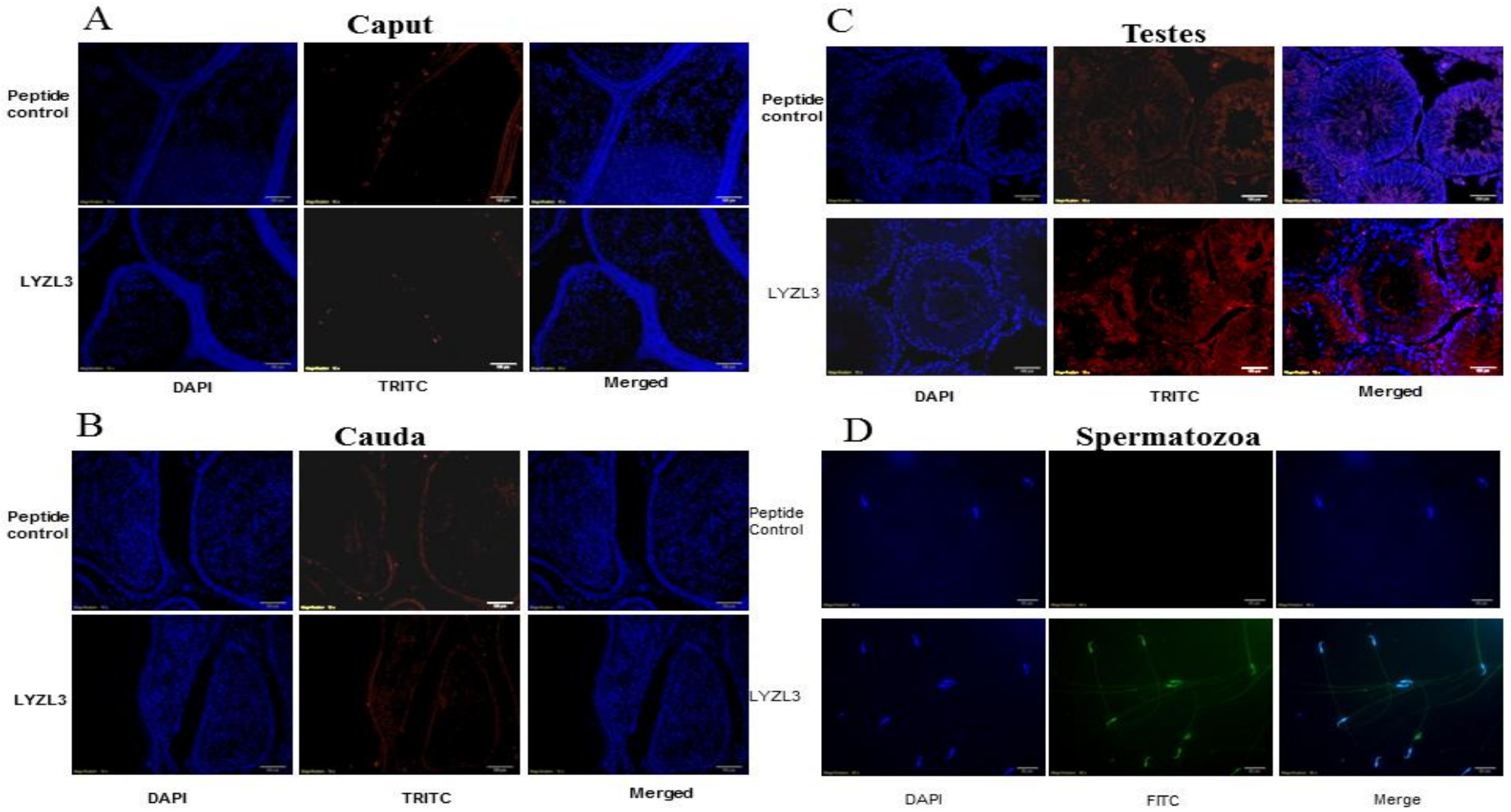

Figure 2.10: *Immunolocalization of* LYZL3*. Serial sections of the rat testes and epididymides were incubated with antigen preadsorbed immune serum (peptide control) or immune serum raised against* LYZL3*, followed by TRITC (Tetramethylrhodamine-5-(and-6)-Isothiocyanate (5(6)) tagged secondary antibody and counter stained with DAPI (4',6-diamidino-2-phenylindole) nuclear stain. Spermatozoa were stained with FITC (fluorescein Isothiocyanate) tagged secondary antibody.*

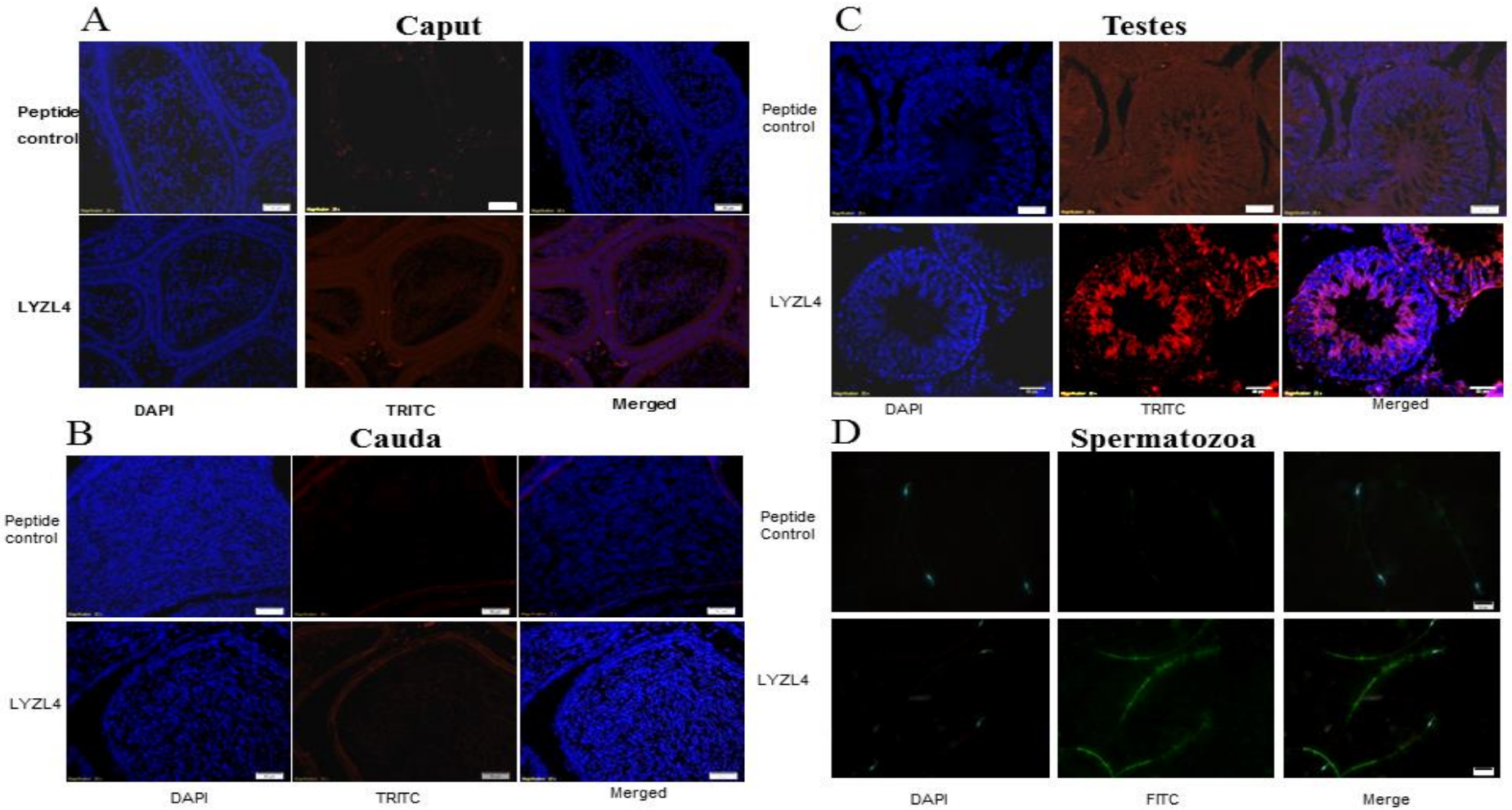

Figure 2.11: *Immunolocalization of* LYZL4. *Serial sections of the rat testes and epididymides were incubated with antigen preadsorbed immune serum (peptide control) or immune serum raised against* LYZL4, *followed by TRITC (Tetramethylrhodamine-5-(and-6)-Isothiocyanate (5(6)) tagged secondary antibody and counter stained with DAPI (4', 6-diamidino-2-phenylindole) nuclear stain. Spermatozoa were stained with FITC (fluorescein Isothiocyanate) tagged secondary antibody.*

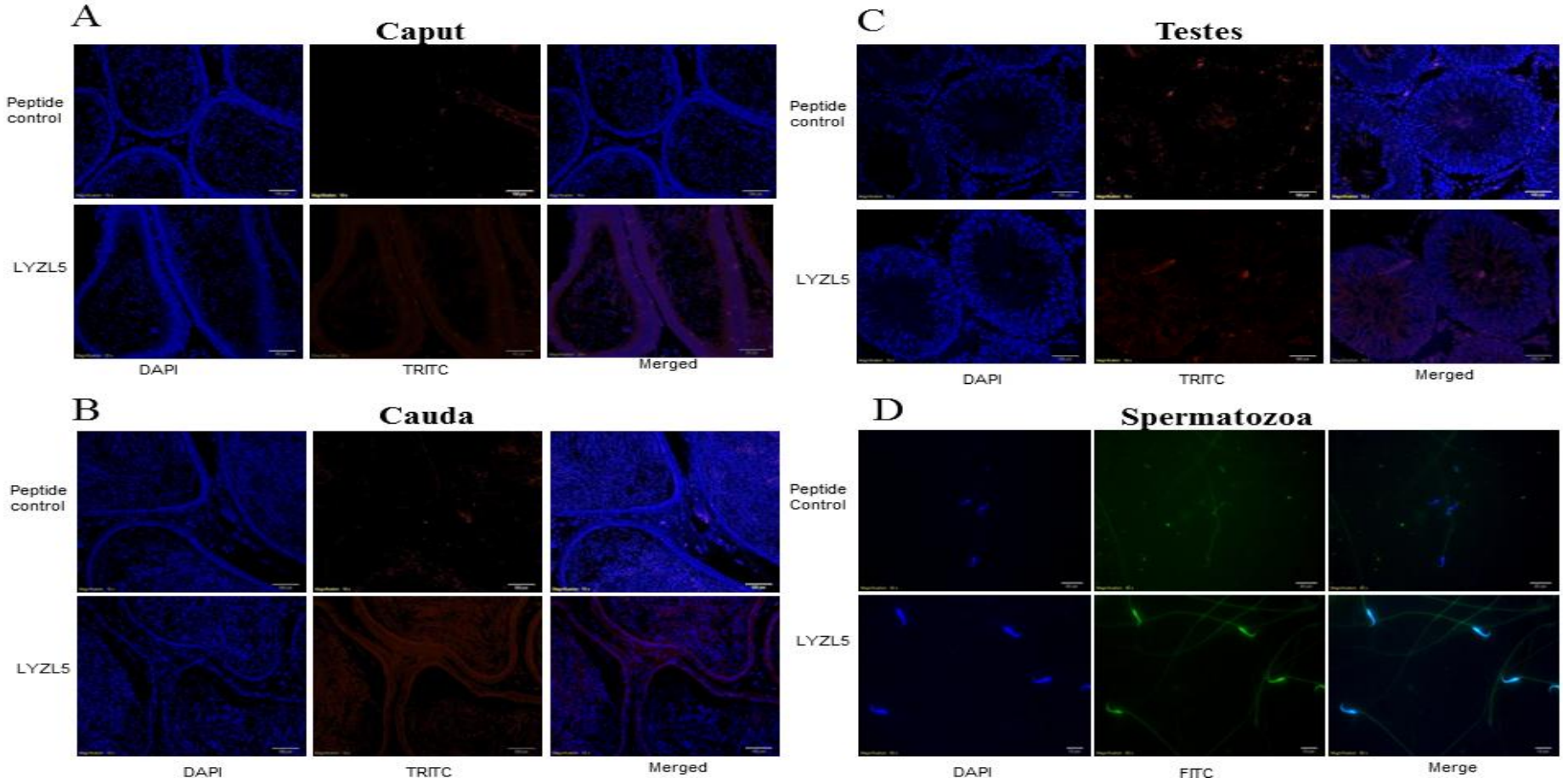

Figure 2.12: *Immunolocalization of* LYZL5. *Serial sections of the rat testes and epididymides were incubated with antigen preadsorbed immune serum (peptide control) or immune serum raised against* LYZL5, *followed by TRITC (Tetramethylrhodamine-5-(and-6)-Isothiocyanate (5(6)) tagged secondary antibody and counter stained with DAPI (4',6-diamidino-2-phenylindole) nuclear stain. Spermatozoa were stained with FITC (fluorescein Isothiocyanate) tagged secondary*

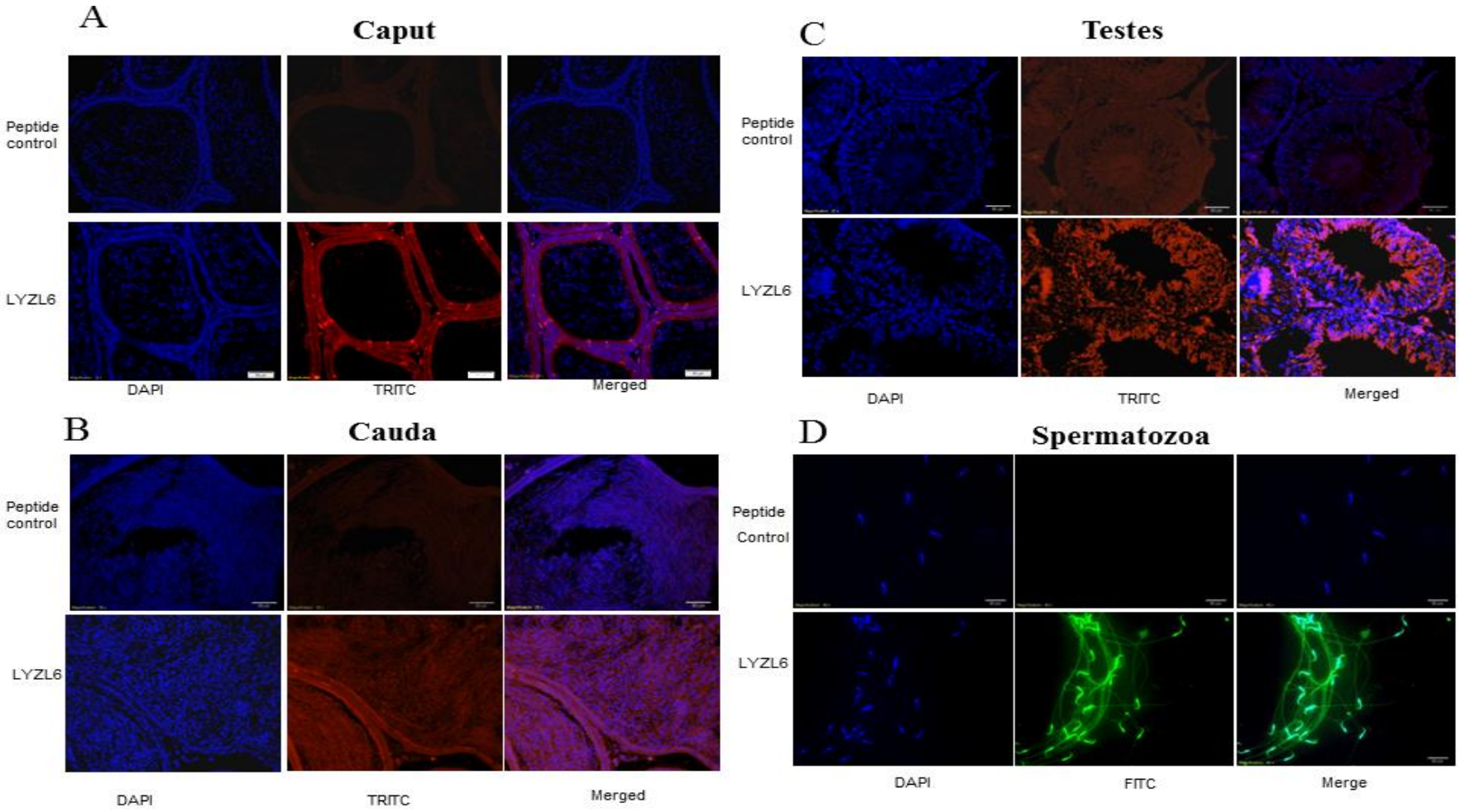

Figure 2.13: *Immunolocalization of* LYZL6. *Serial sections of the rat testes and epididymides were incubated with antigen preadsorbed immune serum (peptide control) or immune serum raised against* LYZL6, *followed by TRITC-Tetramethylrhodamine-5-(and-6)-Isothiocyanate (5(6)) tagged secondary antibody and counter stained with DAPI (4',6-diamidino-2-phenylindole) nuclear stain. Spermatozoa were stained with FITC (fluorescein Isothiocyanate) tagged secondary antibody.*

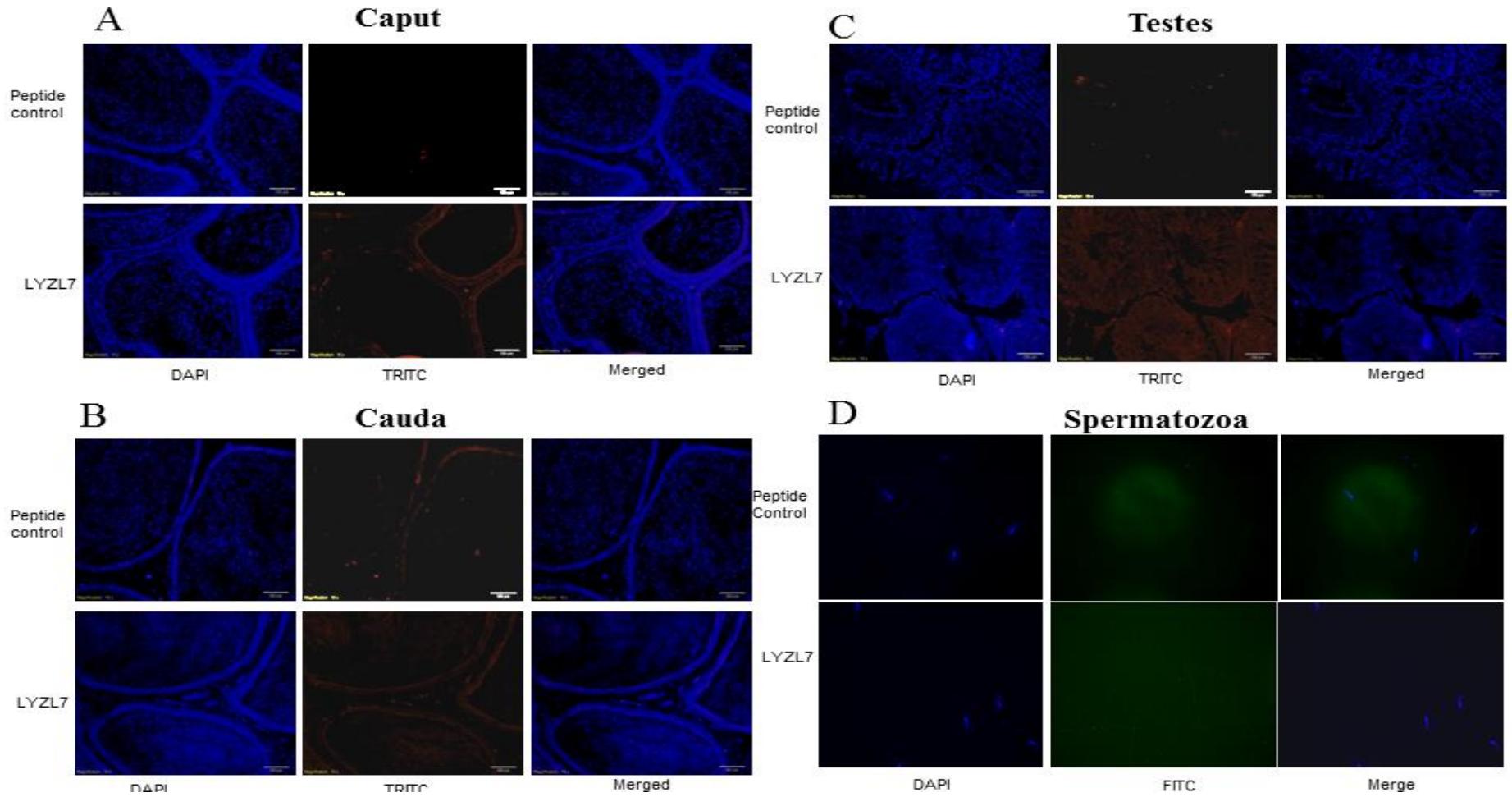

Figure 2.13: *Immunolocalization of* LYZL7. *Serial sections of the rat testes and epididymides were incubated with antigen preadsorbed immune serum (peptide control) or immune serum raised against* LYZL7, *followed by TRITC- Tetramethylrhodamine-5-(and-6)-Isothiocyanate (5(6)) tagged secondary antibody and counter stained with DAPI (4',6-diamidino-2-phenylindole) nuclear stain. Spermatozoa were stained with FITC (fluorescein Isothiocyanate) tagged secondary antibody.*

The tissue specific mRNA and protein expression analysed by RT-PCR, Western blotting and immunofluorescence correlated to a large extent (Table 9). The presence of LYZL6 protein in the epididymidis (though the mRNA was not detected by RT-PCR) could be due to carry over of this protein by the moving spermatozoa. The absence of LYZL7 protein in all the tissues suggests that its mRNA may not be translated though it is detected by RT-PCR in the testes. The discrepancies within Western blotting and IHC results with regard to the expression of LYZL proteins on spermatozoa could be due to difference in the detection range of the two methods. Altogether these results suggest that the LYZL proteins are expressed predominantly in testes and also on spermatozoa.

Table 9: Summary of the mRNA and protein expression pattern

LYZL proteins	mRNA Expression (PCR)			Protein Expression (Western Blotting)				Temporal Localization (IHC)			
	Cp	Cd	T	Cp	Cd	T	Spm	Cp	Cd	T	Spm
LYZL1	-	-	+	-	-	+	-	-	-	+	+
LYZL3	-	-	+	-	-	+	+	-	-	+	+
LYZL4	-	-	+	-	-	+	+	-	-	+	+
LYZL5	-	-	+	-	-	+	-	-	-	+	+
LYZL6	-	-	+	+	+	+	+	+	+	+	+
LYZL7	-	+	+	-	-	-	-	-	-	-	-

Cp-caput,Cd- cauda, T- testes, Spm-sperm. + and – indicates presence and absence respectively.

Secondary structure analysis

Circular dichroism was performed to understand the folding of the recombinant LYZL proteins. Mean residue ellpticity (MRE) was calculated by using θ values (machine reading), molecular weight and concentration of the recombinant protein and were plotted against the wavelength. The CD spectra of recombinant LYZL proteins (Figure 2.15) show a peak at 210 nm which is characteristic of a α-helical protein. Further, MRE values for each recombinant protein when tested using K2D3 (secondary structure analysis program) showed that these proteins contain α-helix pattern (Table 10) in their structure.

Table 10: Secondary structure measurement of LYZL proteins

Protein	α-helix	β-sheet	Random coil
LYZL1	**87.41%**	**0.21 %**	**12.38%**
LYZL3	**43.1%**	**31.9%**	**25.0%**
LYZL4	**54.6%**	**2.63%**	**42.77%**
LYZL5	**60.95%**	**0.19%**	**38.86%**
LYZL6	**65.89%**	**1.05%**	**33.06%**
LYZL7	**23.39%**	**24.55%**	**52.06%**

LYZL proteins exhibit homology with lysozyme and conserve the lactalbumin domain and the 8 cysteine motifs. It is possible that they may exhibit muramidase and isopeptidase activities.

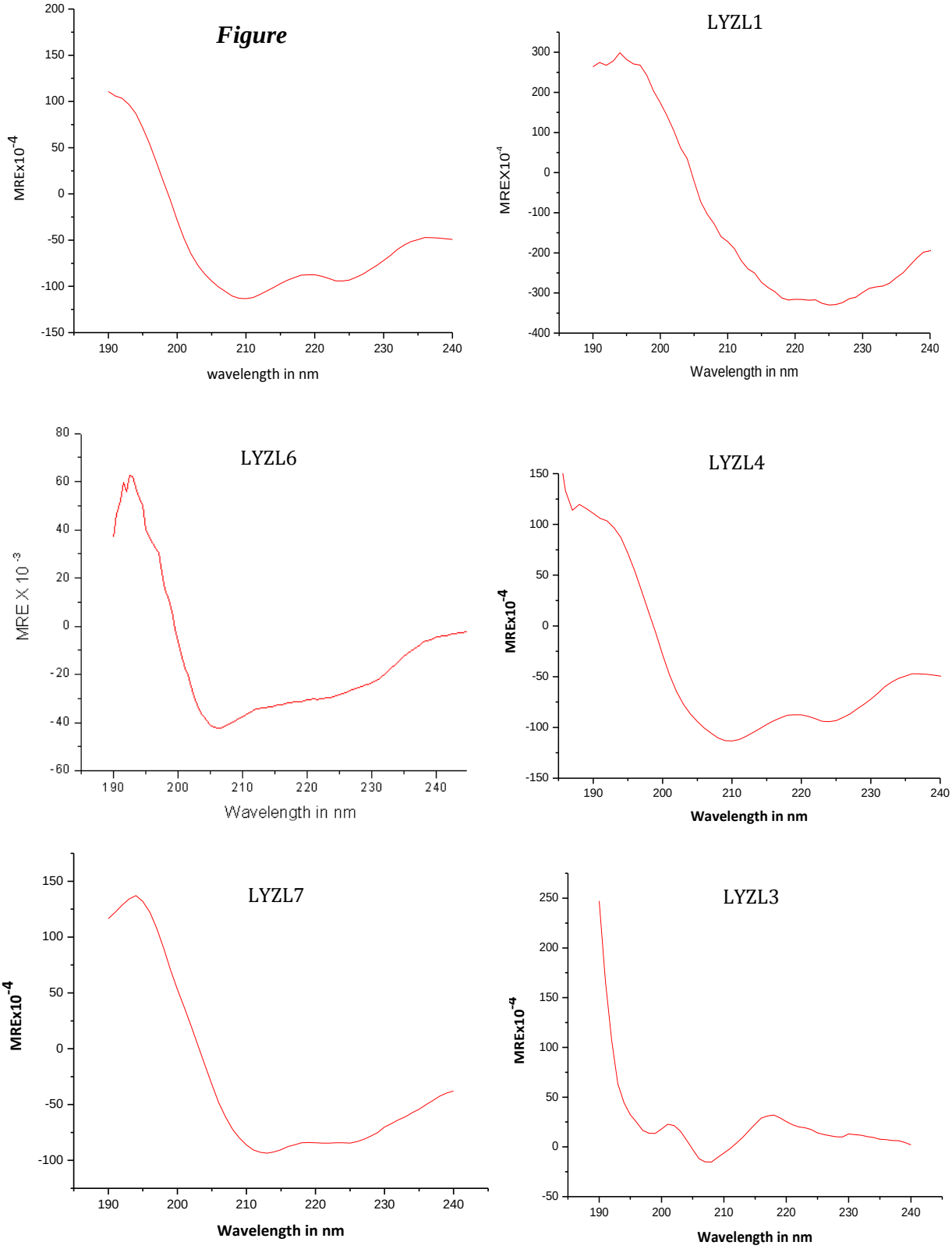

Figure 2.15: *Circular dichroism spectra of recombinant* LYZL *proteins measured in terms of mean residue ellipticity (MRE).*

Muramidase assay

Only LYZL1 and LYZL6 proteins exhibited muramidase activity whereas the remaining LYZL proteins did not show any activity (Figure 2.16). The activity exhibited was concentration dependent and was comparable to the positive control, lysozyme.

Isopeptidase assay

Among the LYZL proteins that were tested, only LYZL1 and LYZL6 displayed isopeptidase activity in a concentration dependent manner, whereas LYZL3, 4, 5 and 7 did not exhibit any isopeptidase activity (Figure 2.17).

Antibacterial assay

Colony forming units (CFU) assay was employed to test the antibacterial activity of LYZL proteins. LYZL1 and LYZL6 exhibited bacterial killing activity, whereas the remaining proteins failed to decrease bacterial count (Figure 2.18). This may be due to absence of the active site in these proteins.

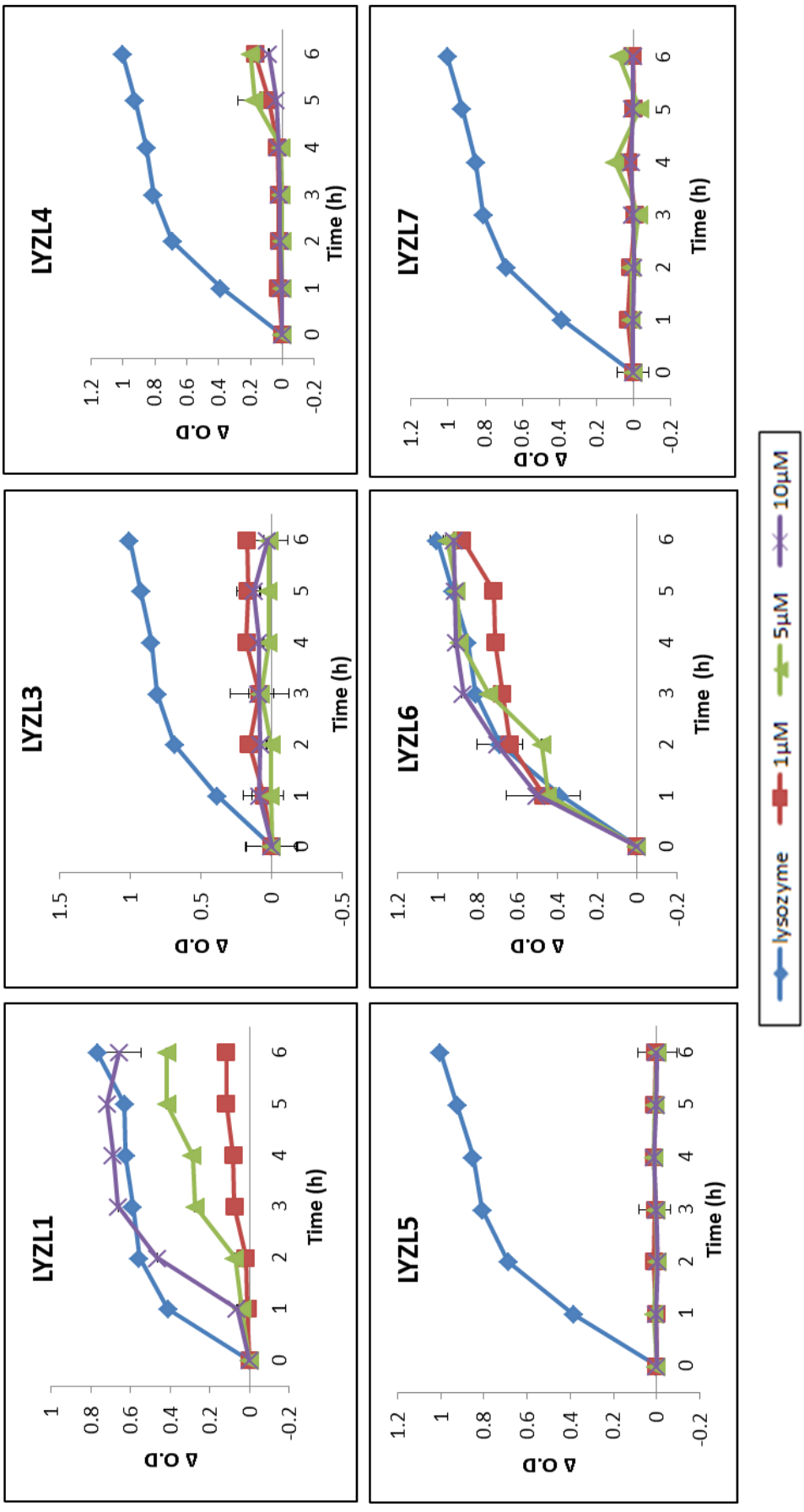

Figure 2.16: *Muramidase activity of* LYZL *proteins. Varying concentrations (1, 5 and 10 μM) of recombinant* LYZL *proteins were incubated with M. lysodeikticus and the O.D monitored at 450nm. Lysozyme was used as a positive control. Values shown are mean +/- SD.*

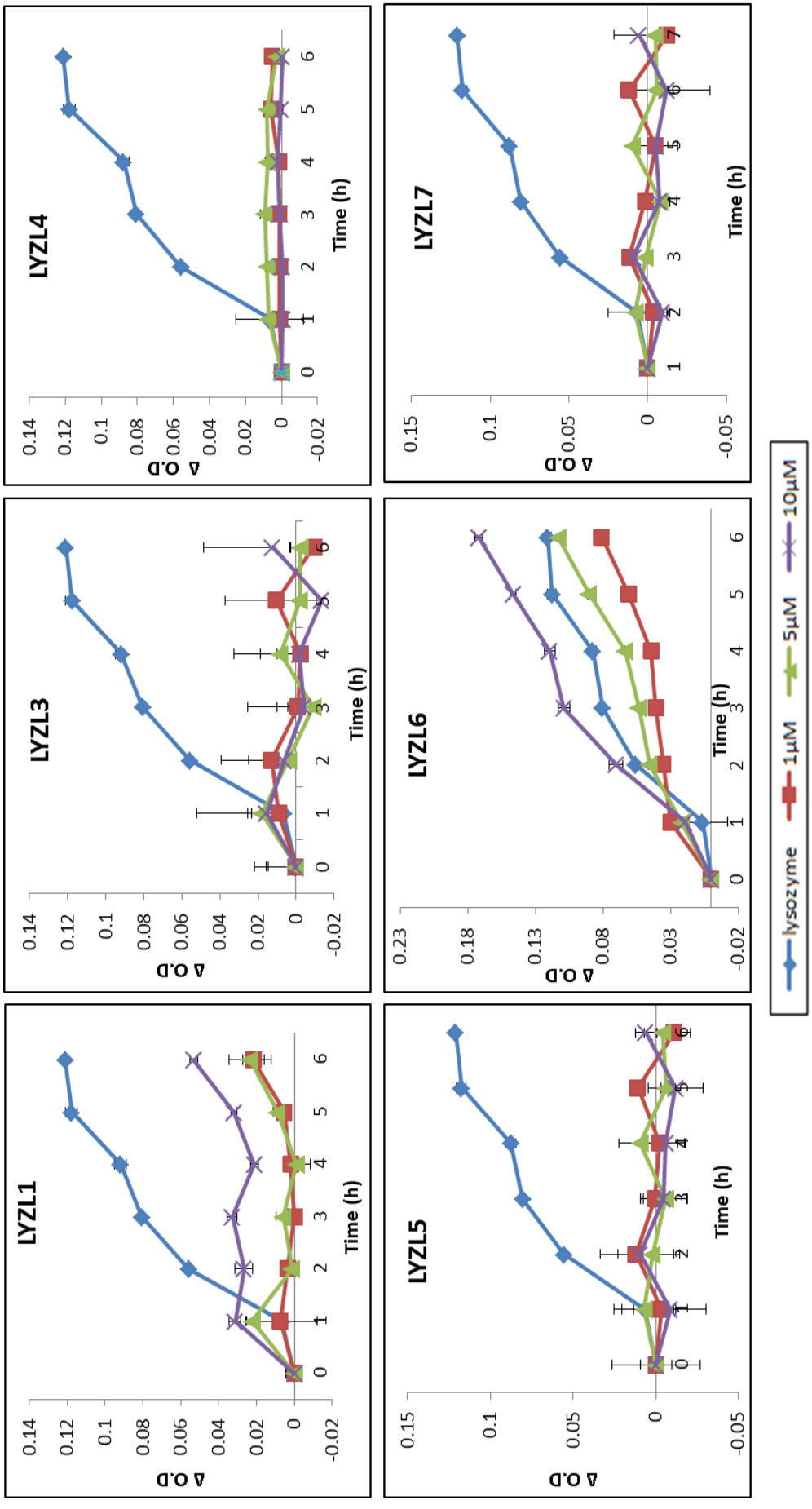

Figure 2.16: *Muramidase activity of* LYZL *proteins. Varying concentrations (1, 5 and 10 µM) of recombinant* LYZL *proteins were incubated with M. lysodeikticus and the O.D monitored at 450nm. Lysozyme (1µM) was used as a positive control. Values shown are mean* $\pm$ *SD.*

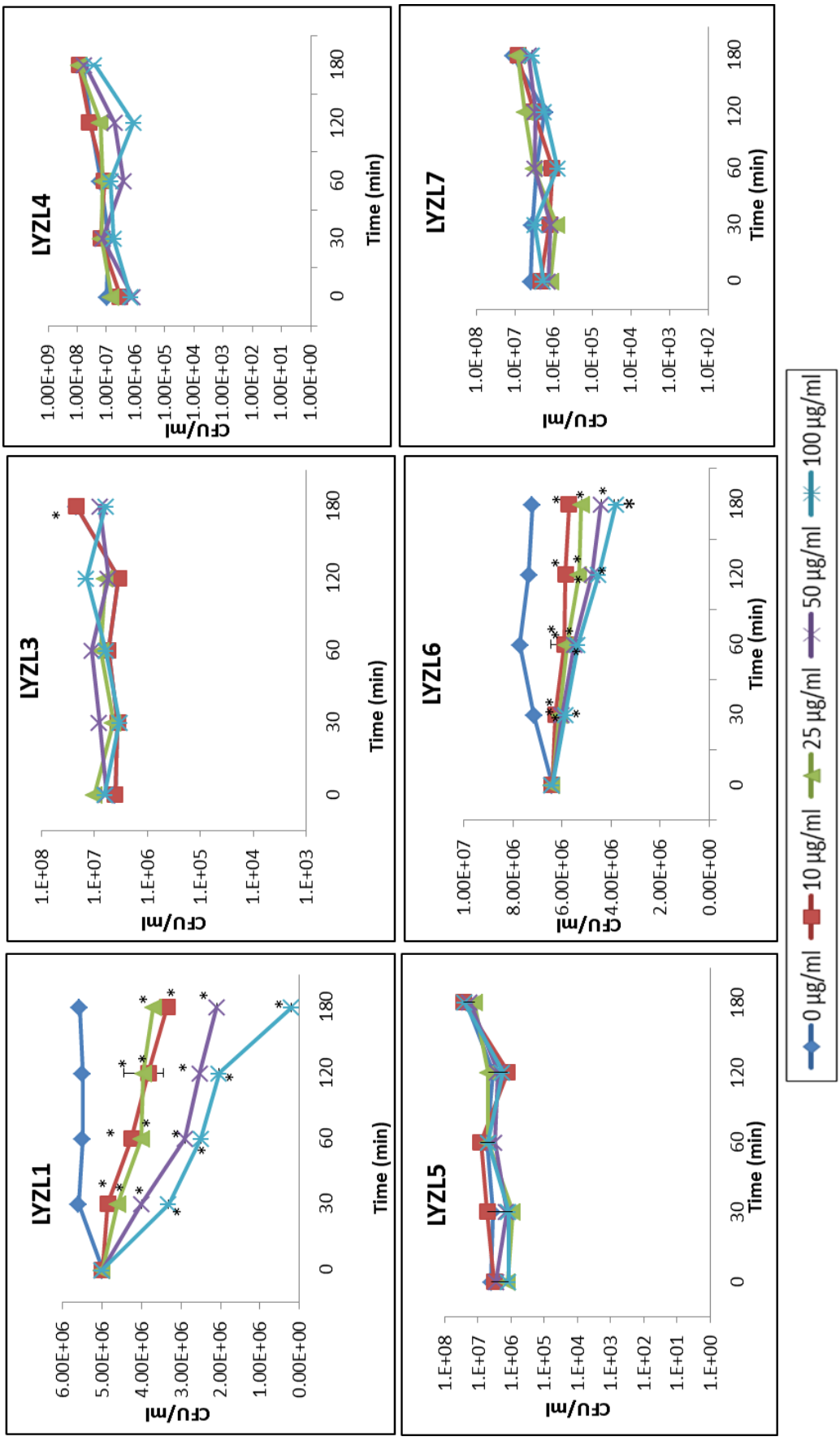

Figure 2.17: *Isopeptidase activity of recombinant* LYZL *proteins. Varying concentrations of (1, 5 and 10 µM) of recombinant* LYZL *proteins were incubated L-γ-Glu-pNA and the O.D monitored at 405nm. Lysozyme (1µM) was used as positive control. Values shown are mean ± SD.*

Scanning Electron Microscopy

E.coli treated with recombinant LYZL1 and LYZL6 were observed under electron microscope to study the morphological changes caused by these proteins. PBS treated *E.coli* cells show normal smooth surface (Figure 2.19) whereas the LYZL1 and LYZL6 treated cells display rough cell surface with membrane blebbing. In addition, release of cytosolic content of the bacterial cells was observed. The actions of these proteins are similar to that exhibited by lysozyme.

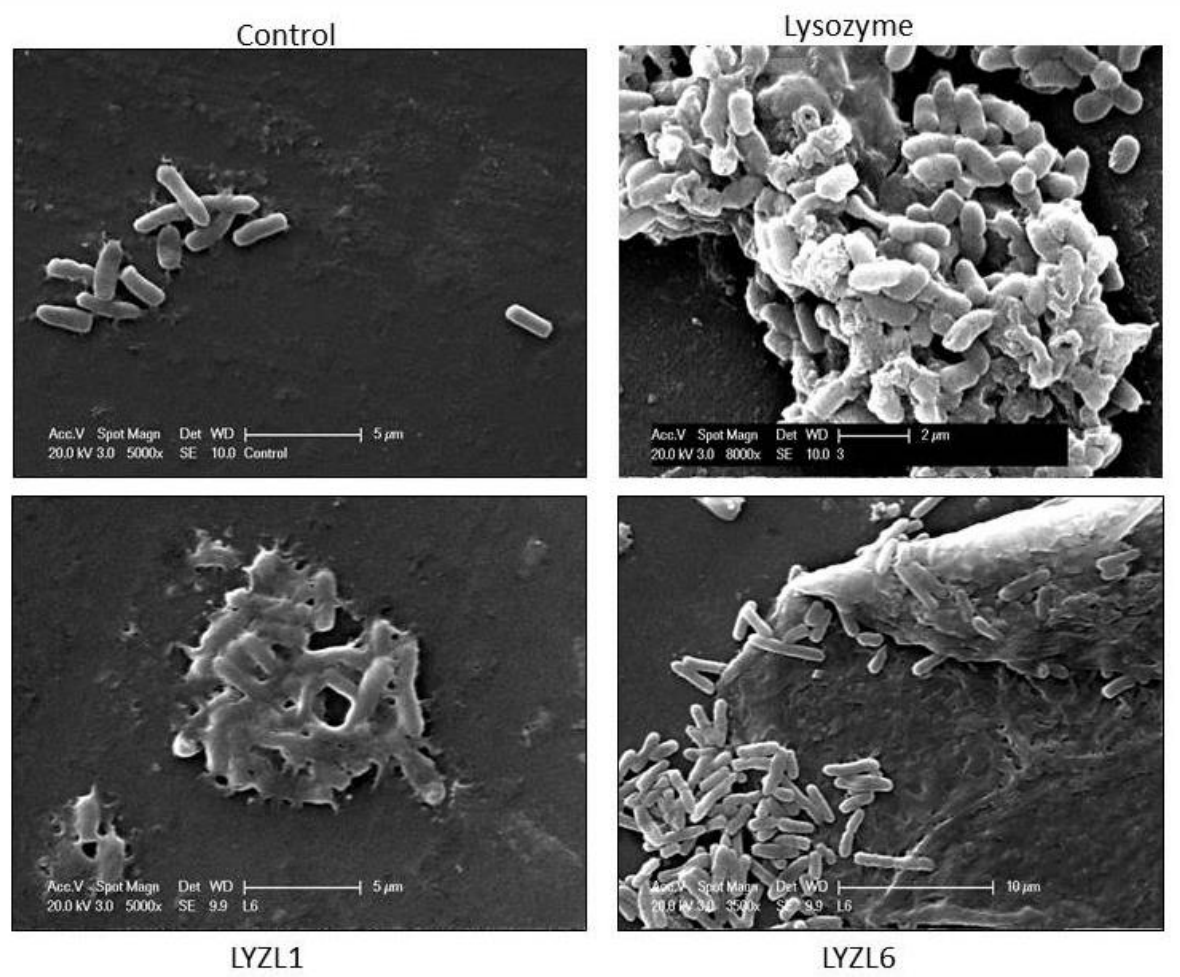

Figure 2.19: *Effect of recombinant* LYZL1 and LYZL6 *on the morphology of E. coli. Scanning electron micrographs of E. coli treated with 100 µg/ml recombinant* LYZL *proteins for 2 h. Lysozyme (10 µg/ml) was used as positive control.*

Measurement of membrane potential and Permeability

The membrane potential and permeability of the bacterial cells treated with recombinant LYZL proteins was measured using $DiOC_2(3)$. Figure 2.20A shows the measurement of $DiOC_2(3)$ fluorescence in FITC-A (green) and PE-Texas Red-A (red) channel. The mean fluorescence intensity on PE Texas Red-A channels denotes the aggregation of the dye due to increased membrane potential. CCCP treatment caused decrease in membrane potential thereby decreased mean fluorescence intensity in PE-Texas Red-A channel. Green fluorescence is the measure of cell size to detect aggregation. CCCP treatment did not cause aggregation of bacterial cells which is indicated by the mean fluorescence intensity in FITC-A channel. Treatment of cells with recombinant LYZL1 and 6 caused increase in green fluorescence showing that they possibly tend to aggregate bacterial cells. Normalized ratio between the red and green fluorescence shows the membrane potential independent of cell size. Addition of recombinant LYZL1 or 6 protein to *E. coli* resulted in decreased ratio of red/green fluorescence in comparison to phosphate buffer treated bacterial cells (Figure 2.20B), suggesting clump formation and also change in membrane potential due to addition of these proteins. The bacterial cells treated with lysozyme also showed a change in the membrane potential similar to CCCP. TOPRO-3fluorescence is measured in PerCP-Cy5-5A channel. Increase in mean fluorescence intensity denotes increase in the membrane permeability.

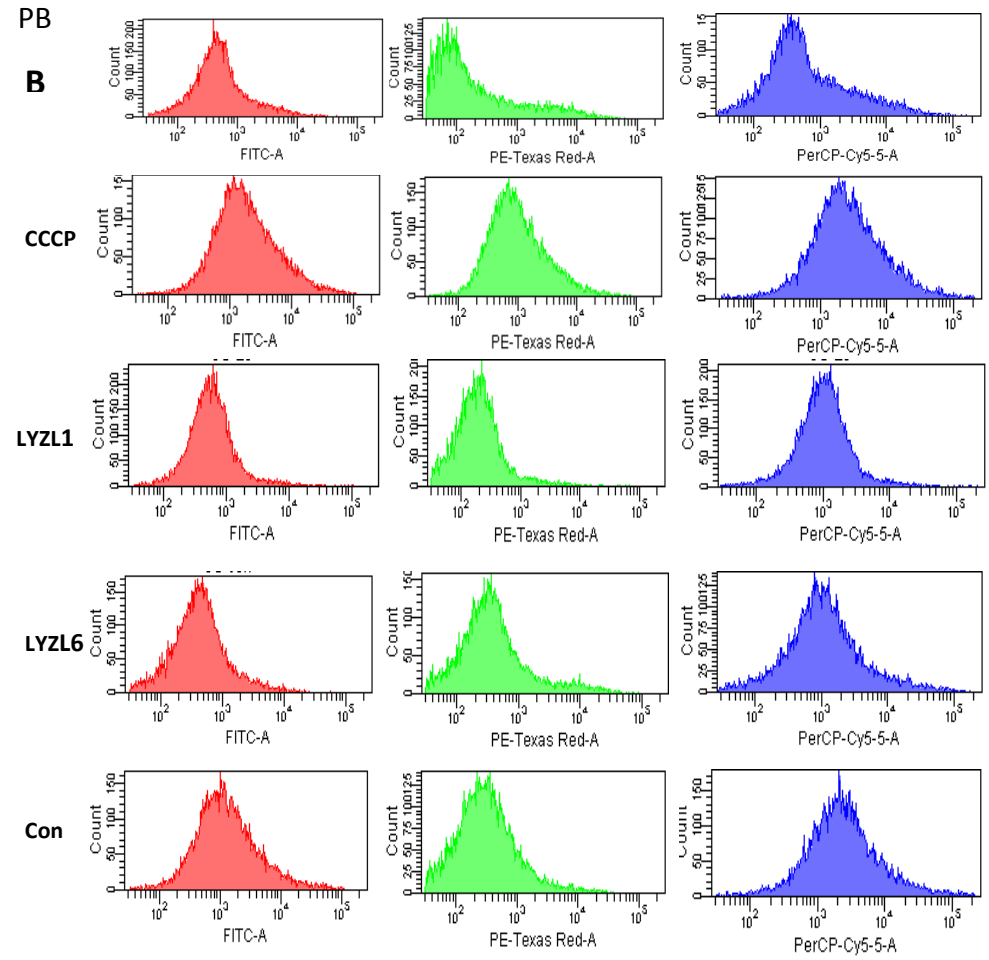

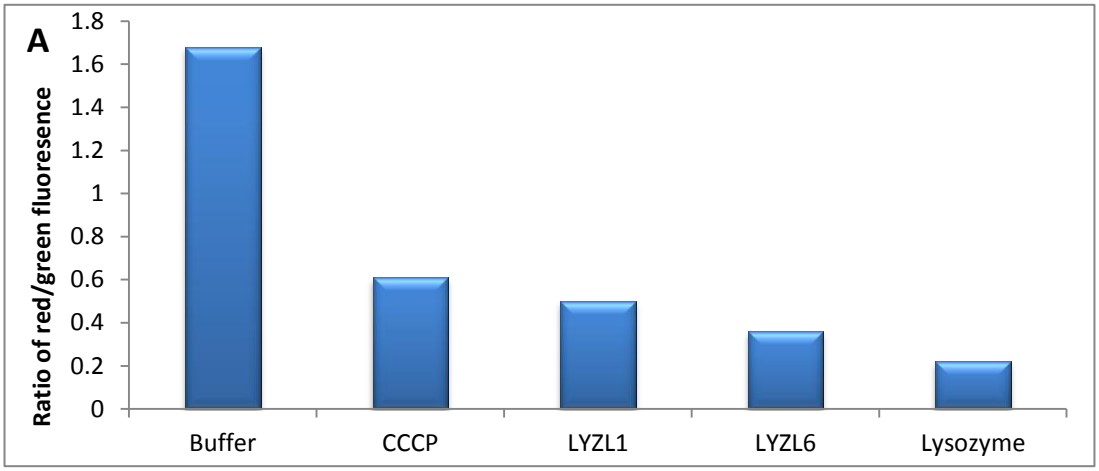

Figure 2.20: *Dye based membrane potential measurement in E. coli treated with recombinant* LYZL *proteins using flow cytometry. A- MFI measurements of the cells in FITC, PE-Texas Red A and PerCP-Cy5-5-A channels. B- Membrane potential measured in terms of ratio of mean fluorescence intensity of red/green.*

Peptidoglycan binding ability

LYZL domain, which has the catalytic cleft and is responsible for binding to cell wall component was found to be present in all the rat LYZL proteins. We observed that though all LYZL proteins possess the domain, only LYZL1 and LYZL6 show antimicrobial activity. Hence, analysing the binding efficiency of the LYZL proteins with the bacterial cell wall components may help in understanding the differential antibacterial ability. As anticipated, lysozyme displayed a concentration dependent peptidoglycan binding ability. LYZL1 and LYZL6 had higher peptidoglycan binding ability than LYZL3, 4, 5 and 7 which may be due to presence of active site in LYZL1 and 6. However, the binding ability of all the LYZL proteins was significantly less than lysozyme at all the concentrations tested.

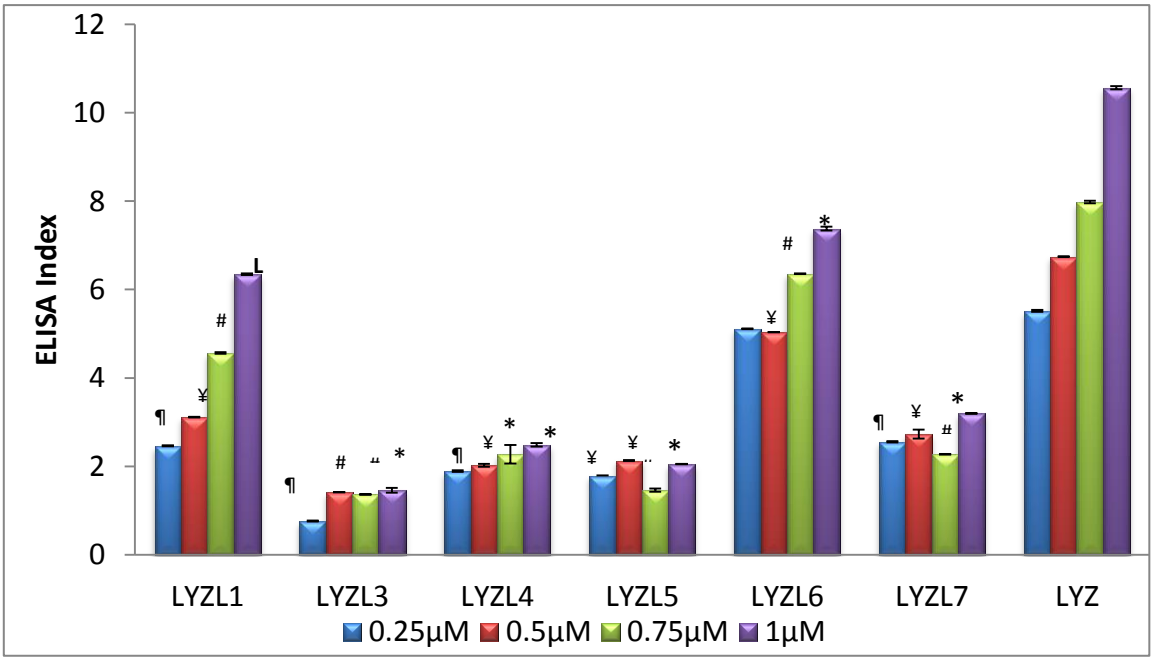

Figure 2.21: *ELISA based peptidoglycan binding assay. 40 µg/ml peptidoglycan coated plate was incubated with 0.25, 0.5, 0.75 and 1µM of the recombinant proteins. Affinity of protein bound to peptidoglycan was measured in terms of colour produced during development after probing with corresponding primary and secondary antibody. Values shown are mean ± SD. *, #, ¥ and ¶ indicates p<0.05 compared to the corresponding concentration of lysozyme.*

Hyaluronan binding ability

Lysozyme exhibited hyaluronan binding in a dose dependent manner which may be due to chemical similarity between hyaluronan and peptidoglycan. Among the LYZL proteins tested, LYZL3 had the highest hyaluronan binding ability followed by LYZL4, LYZL5, LYZL1 and LYZL7. LYZL7 displayed hyaluronan binding similar to that of lysozyme. LYZL6 had the least hyaluronan binding ability.

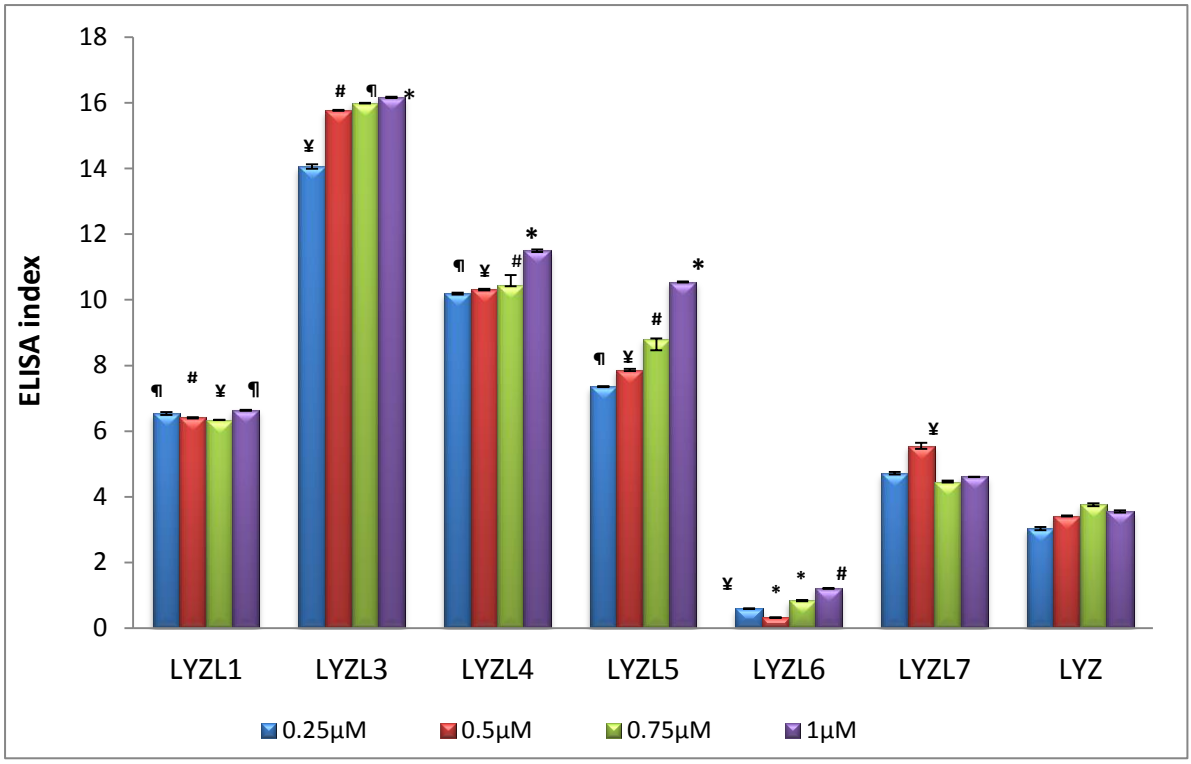

Figure 2.22: *ELISA based hyaluronan binding assay. 40 µg/ml hyaluronan coated into the wells of a microtitre plate was incubated with 0.25, 0.5, 0.75 and 1µM of the recombinant protein. Protein binding to peptidoglycan was measured by ELISA based colour detection. ELISA index was calculated by subtracting the average O.D of negative control and dividing the resultant by the negative control O.D. Values shown are mean ± SD. *, #, ¥ and ¶ indicates p<0.05 compared to the corresponding concentrations of lysozyme.*

Hyaluronidase activity

Hyaluronidase used as a positive control caused the clearance of cetyl pyridinium chloride resulting in decrease of O.D at 595 nm. Surprisingly, though LYZL proteins had hyaluronan binding ability, none of them exhibited hyaluronidase activity at all the concentrations tested (Figure 2.23).

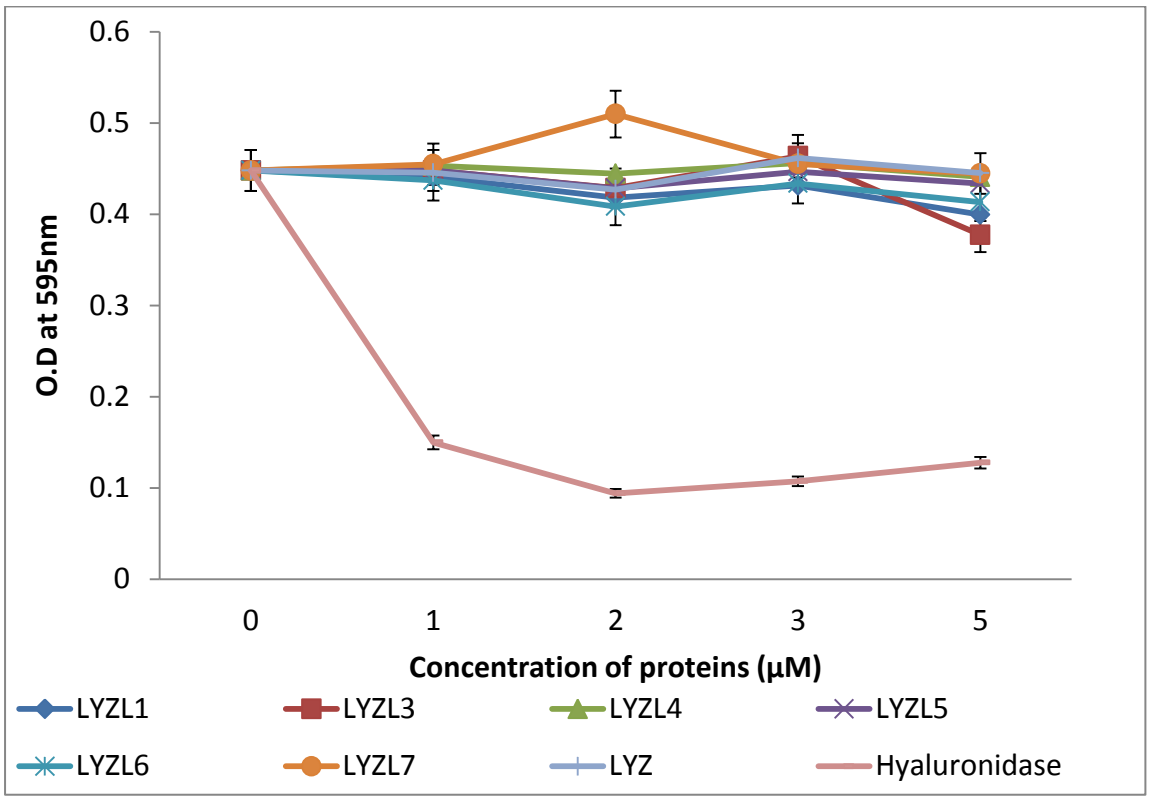

Figure 2.23: *Hyaluronidase activity of* LYZL *proteins. Hyaluronan mixed agarose incubated with different concentrations of recombinant LYZL proteins. The amount of cetyl pyridinium chloride precipitate cleared is a measure of hyaluronidase activity. Hyaluronidase was used as positive control. Values shown are mean ± SD.*

Free radical scavenging activity

Lysozyme exhibited potent free radical scavenging activity, which is evident by the discoloration of DPPH and there by decrease in the O.D at 517 nm. Except for LYZL5 and LYZL6, all other LYZL proteins caused a decrease in the O.D of DPPH at 517 nm in a dose dependent manner. Among them LYZL4 had the highest antioxidant potential.

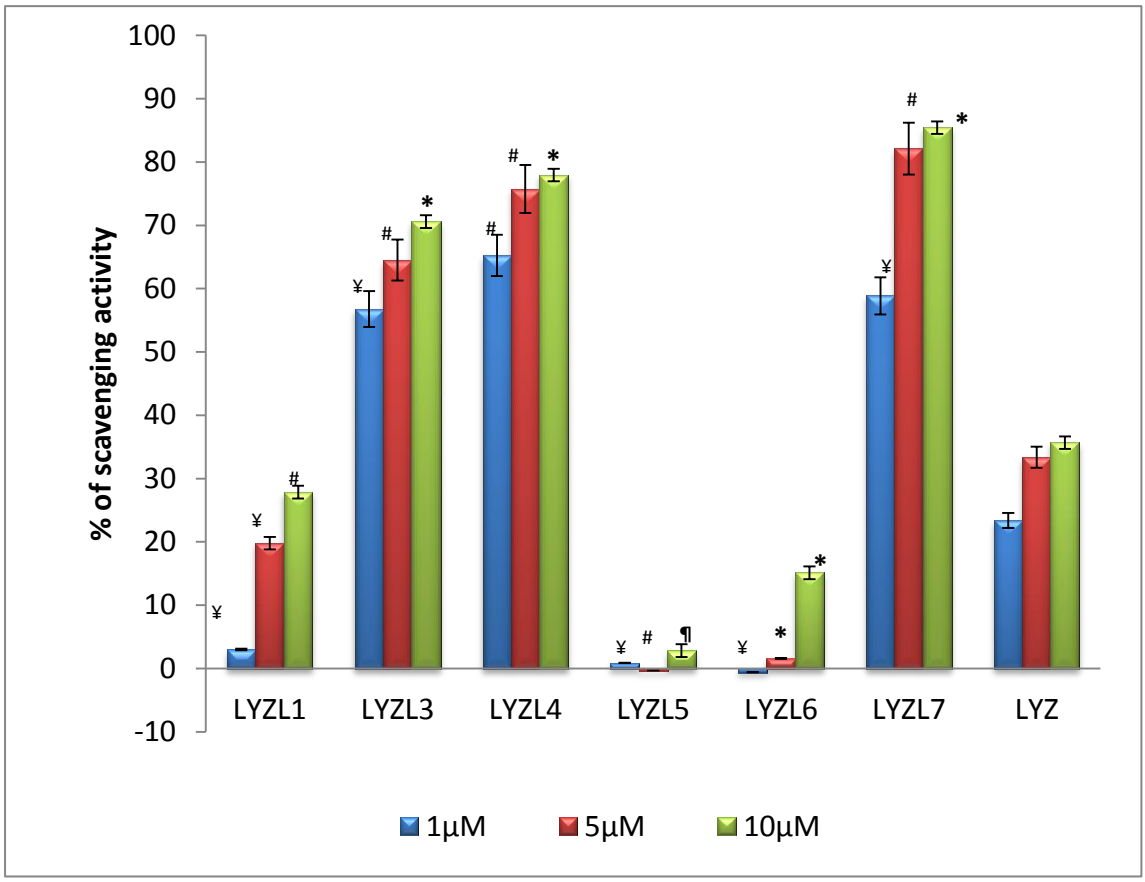

Figure 2.24: *Free radical scavenging assay. DPPH solution was incubated with varying concentrations of recombinant* LYZL *protein and the decrease in O.D was measured at 517 nm. Lysozyme was used a control. Radical scavenging activity was expressed in terms of percentage. Values shown are mean ± SD. *, #, ¥ and ¶ indicates p<0.05 compared to the corresponding concentration of lysozyme.*

DISCUSSION

In the present study we report the expression pattern of rat *Lyzl* transcripts and proteins. This is the first comprehensive study undertaken to analyse the expression of rat *Lyzl* mRNA and protein. Some of the *Lyzl* mRNA transcripts were found to be expressed only in testes in the male reproductive tract. Such an exclusive expression in the testis suggests a role for these proteins in spermatogenesis. In addition to their expression in testis LYZL1, 4 and 7 are expressed in other non-reproductive tissues suggesting that these proteins may have roles beyond reproduction. Human LYZL4 transcripts were detected in the testes and pancreas similar to the expression pattern observed in this study (Zhang et al. 2005). The expression of mouse *Lyzl* genes in testes and epididymidis was also reported (Sun et al. 2011). Further LYZL4 was detected in brain and lungs in addition to testes and epididymidis in mouse (Wei et al. 2013). Our results indicate the expression of *Lyzl*4 in brain, lungs, kidney, ovary and uterus in addition of testes and epididymidis. Our results are more or less similar to that observed in earlier reports. However there are variations in the tissue expression pattern of these genes in different species indicating a possible variation in functional role in different species.

Developmental regulation of a wide variety of genes due to the fluctuations of androgens at various stages in the male reproductive system has been studied extensively (Rodríguez et al. 2001). Androgen levels in the rat epididymis decline from birth until 20 days but remain at a substantial level of approximately 10 ng/g tissue (35 nM) until approximately 40 days when the levels begin to increase to that of the adult, between 15–20 ng/g. Serum testosterone levels in the young rat remain low and do not begin to increase to adult levels until 35–40 days of age (Wei et al. 2013)(Wei et al. 2013). *Lyzl* mRNA transcripts were not detected in the epididymides obtained from 20–60 day old rats. It is possible that their expression pattern is not androgen dependent in this organ system. Testicular androgen

variation during development in the rat was reported to be significantly different from the epididymis. A steady increase in testosterone levels occurs in the rete testis of 30-130 day old rats (Harris & Bartke 1981). In this study, the presence of *Lyzl1, 3, 4, 5, 6* and *7* mRNA transcripts was observed in the testes starting from 30 day post natal development. The expression pattern of *Lyzl* transcripts analysed in this study seem to correlate with the minimal androgen levels from day 20 to day 40 and increased androgen in the adult, suggesting that *Lyzl* gene expression may be androgen dependent during development in the testis. Androgen dependent expression of *Lyzl4* during development was reported in the mouse testis (Wei et al. 2013). Further studies are required to determine the molecular mechanisms that operate in controlling the expression of *Lyzl* transcripts during development.

The general properties of the recombinant proteins (sequence, molecular weight, pI) correlated well with the predicted properties. In previous reports expression of mRNA transcripts of *Lyzl* genes was reported. This is the first study to report the LYZL proteins expression pattern in male reproductive tract by immunolocalization and Western blotting. Localization of LYZL proteins in growing spermatids and in the germinal epithelium indicates that they may have role in spermatogenesis. LYZL4 was found to be localised in tail portion of mouse (Sun et al. 2011). Similar observation was made in case of LYZL6 (Wei et al. 2013). Our results are in consistent with earlier reports. Though some of the proteins are testis specific, they were detected in epididymis also. This could be due to the movement of these proteins along with luminal fluid from testis to epididymis.

Epididymal proteins secreted into the lumen play a key role in sperm maturation (Lassere et al. 2001). For example human PH34 which is secreted by the epididymal epithelium is added to sperm surface and is required for fertilization (Boué et al. 1996). Moreover, certain men with idiopathic infertility show decreased amount of P34H proteins in the seminal

plasma along with fertilization failure, suggesting that this protein can be used as marker for sperm maturation (Boué & Sullivan 1996). Besides this, some of epididymal proteins are known to exhibit potent antimicrobial activity, thereby forming important components of male reproductive tract innate immunity. Human epididymal protein (HE2) is shown to possess potent antimicrobial activity (Yenugu et al. 2004). BIN1b which belongs to the defensin family is secreted in the epididymis and is proven to play important role in sperm maturation and motility, besides antibacterial activity (Guo et al. 2009).

Lysozyme, because of its ability to cleave the glycosidic bond of peptidoglycan, displays potent antimicrobial activity (Ibrahim et al. 2001). Human semen contains lysozyme and is shown to have a positive role on viscosity of the semen (Mendeluk et al. 1997). In this study, we demonstrated that LYZL1 and 6 display potent antibacterial activity against *E. coli*. The antibacterial activity of LYZL proteins was demonstrated in other species. For example, human LYZL6 was found to be a potent antibacterial protein (Wei et al. 2013). LYZL3, 4, 5 and 7 did not display antibacterial activity. This could be due to the lack of essential amino acids in the active site. The human c-type lysozyme SLLP1, was non-bacteriolytic similar to rat LYZL3, 4, 5 and 7 (Mandal et al. 2003). Substrate binding assays also indicate that only LYZL1 and 6 exhibit higher affinity to bind peptidoglycan in comparison with the remaining proteins.

Similar trend was observed in muramidase and isopeptidase assays. These properties can be attributed to the presence of active site residues in LYZL1 and 6. Except LYZL5 and 6, all the LYZL proteins exhibit free radical scavenging activity. The free radical scavenging activity of lysozymes is attributed to the disulphide bonds in these proteins (Memarpoor-yazdi et al. 2011). The hyaluronan binding ability of the recombinant LYZL proteins shows the multiple functions played by these proteins. To conclude this part of the study, we report

that rat LYZL proteins are predominantly expressed in the male reproductive tract and they are biochemically similar to that of lysozyme.

REFERENCES

Boué, F., Blais, J. & Sullivan, R., 1996. Surface localization of P34H an epididymal protein, during maturation, capacitation, and acrosome reaction of human spermatozoa. *Biology of reproduction*, 54(5), pp.1009–17.

Boué, F. & Sullivan, R., 1996. Cases of human infertility are associated with the absence of P34H an epididymal sperm antigen. *Biology of reproduction*, 54(5), pp.1018–24.

Chomczynski, P. & Sacchi, N., 2006. The single-step method of RNA isolation by acid guanidinium thiocyanate-phenol-chloroform extraction: twenty-something years on. *Nature protocols*, 1(2), pp.581–5.

Ernesto, J.I. et al., 2012. Evaluation of Testicular Sperm CRISP2 as a Potential Target for Contraception. *Journal of andrology*, 33(6), pp.1360–1370.

Guo, C. et al., 2009. Recombinant expression and characterization of an epididymis-specific antimicrobial peptide BIN1b/SPAG11E. *Journal of biotechnology*, 139(1), pp.33–7.

Handwaskar, R.U.C. et al., 2007. Hyaluronidase and collagenase inhibitory activities of the herbal formulation Triphala guggulu. , 32(June), pp.755–761.

Hao, Z. et al., 2002. SAMP32, a testis-specific, isoantigenic sperm acrosomal membrane-associated protein. *Biology of reproduction*, 66(3), pp.735–44.

Harris, M.E. & Bartke, A., 1981. Androgen levels in the rete testis fluid during sexual development. *Experientia*, 37(4), pp.426–7.

Ibrahim, H.R., Thomas, U. & Pellegrini, A., 2001. A Helix-Loop-Helix Peptide at the Upper Lip of the Active Site Cleft of Lysozyme Confers Potent Antimicrobial Activity with Membrane Permeabilization Action. *The journal of biological chemistry*, 276(47), pp.43767–43774.

Irwin, D.M. & Gong, Z., 2003. Molecular evolution of vertebrate goose-type lysozyme genes. *Journal of molecular evolution*, 56(2), pp.234–42.

Jiborn, T. et al., 2004. Cystatin C is highly expressed in the human male reproductive system. *Journal of andrology*, 25(4), pp.564–72.

Khobarekar, B.G. et al., 2007. Studies on the expression of 80-kDa human sperm antigen in rat testis and epididymis. *The journal of histochemistry and cytochemistry*, 55(7), pp.753–62.

Kuz'min, M.D. et al., 1991. The diagnosis of male infertility based on the lysozyme level in sperm. *Laboratornoe delo*, 1(7), pp.39–41.

Lassere, A. et al., 2001. Human epididymal proteins and sperm function during fertilization: un update. *Biological Research*, 34(3-4), pp.165–178.

Lien CalleWaert, C.M., Callewaert, L. & Michiels, C.W., 2010. Lysozymes in the animal kingdom. *Journal of biosciences*, 35(March), pp.127–160.

Louis-Jeune, C., Andrade-Navarro, M.A. & Perez-Iratxeta, C., 2011. Prediction of protein secondary structure from circular dichroism using theoretically derived spectra. *Proteins*, 80(12), pp.374–481.

Mandal, A. et al., 2003. SLLP1, a unique, intra-acrosomal, non-bacteriolytic, c lysozyme-like protein of human spermatozoa. *Biology of reproduction*, 68(5), pp.1525–37.

Mårdh, P.A. & Colleen, S., 1974. Lysozyme in Seminal Fluid of Healthy Males and Patients with Prostatitis and in Tissues of the Male Uro-Genital Tract. *scandinavian journal of urology and nephrology*, 8(3), pp.179–183.

Markart, P. et al., 2004. Comparison of the microbicidal and muramidase activities of mouse lysozyme M and P. *biochemical journal*, 380(2), pp.385–392.

Memarpoor-yazdi, M., Asoodeh, A. & Chamani, J., 2011. A novel antioxidant and antimicrobial peptide from hen egg white lysozyme hydrolysates. *Journal of Functional Foods*, 4(1), pp.278–286.

Mendeluk, G.R., Blanco, A.M. & Bregni, C., 1997. Viscosity of human seminal fluid: role of lysozyme. *Archives of andrology*, 38(1), pp.7–11.

Novo, D.J. et al., 2000. Multiparameter Flow Cytometric Analysis of Antibiotic Effects on Membrane Potential , Membrane Permeability , and Bacterial Counts of Staphylococcus aureus and Micrococcus luteus. *Antimicrobial agents and chemotherapy*, 44(4), pp.827–834.

Ohno, N. & Morrison, D., 1989. Lipopolysaccharide interaction with lysozyme. Binding of lipopolysaccharide to lysozyme and inhibition of lysozyme enzymatic activity. *J. Biol. Chem.*, 264(8), pp.4434–4441.

Rodríguez, C.M., Kirby, J.L. & Hinton, B.T., 2001. Regulation of gene transcription in the epididymis. *Reproduction*, 122(1), pp.41–8.

Sreerama, N. & Woody, R.W., 2004. Computation and Analysis of Protein Circular Dichroism Spectra. *methods in enzymology*, 2(2), pp.1–27.

Sun, R. et al., 2011. Lyzl4 , a novel mouse sperm-related protein , is involved in fertilization. *Acta biochimica et biophysica sinica*, 3(1), pp.1–8.

Syntin, P. & Cornwall, G.A., 1999. Immunolocalization of CRES (Cystatin-related epididymal spermatogenic) protein in the acrosomes of mouse spermatozoa. *Biology of reproduction*, 60(6), pp.1542–52.

Takeshita, K. et al., 2003. A small chimerically bifunctional monomeric protein : Tapes japonica lysozyme. *Cellular and molecular life sciences*, 60(1), pp.1944–1951.

Tauber, P.F. et al., 1976. Components of human split ejaculates. II. Enzymes and proteinase inhibitors. *Journal of reproduction and fertility*, 46(1), pp.165–71.

Wang, S. et al., 2011. Phosvitin Plays a Critical Role in the Immunity of Zebrafish Embryos via Acting as a Pattern Recognition Receptor and an. *The journal of biological chemistry*, 286(25), pp.22653–22664.

Wei, J. et al., 2013. Characterisation of Lyzls in mice and antibacterial properties of human LYZL6. *Asian Journal of Andrology*, 14(6), pp.834–830.

Wohlkönig, A. et al., 2010. Structural Relationships in the Lysozyme Superfamily : Significant Evidence for Glycoside Hydrolase Signature Motifs. *PloS one*, 5(11), pp.1–10.

Xiao, L.-Q., Liu, A.-H. & Zhang, Y.-L., 2004. An effective method for raising antisera against beta-defensins: double-copy protein expression of mBin1b in E. coli. *Acta biochimica et biophysica Sinica*, 36(8), pp.571–6.

Yenugu, S. et al., 2003. Antibacterial properties of the sperm-binding proteins and peptides of human epididymis 2 (HE2) family; salt sensitivity, structural dependence and their interaction with outer and cytoplasmic membranes of Escherichia coli. *The Biochemical journal*, 372(Pt 2), pp.473–83.

Yenugu, S. et al., 2004. Antimicrobial actions of the human epididymis 2 (HE2) protein isoforms, HE2alpha, HE2beta1 and HE2beta2. *Reproductive biology and endocrinology*, 2(1), p.61.

You, S.-J. et al., 2010. Multifunctional peptides from egg white lysozyme. *Food Research International*, 43(3), pp.848–855.

Zhang, K. et al., 2005. Molecular Cloning and Characterization of Three Novel Lysozyme-Like Genes , Predominantly Expressed in the Male Reproductive System of Humans , Belonging to the C-Type Lysozyme / Alpha-Lactalbumin Family 1. *Biology of reproduction*, 1071(73), pp.1064–1071.

CHAPTER 3

❖ *Evaluation of functional importance of rat lysozyme-like proteins in male reproduction.*

INTRODUCTION

The main function of the male reproductive system is to produce spermatozoa and maintain them ready for fertilization. Male gametes produced by testes are immature and they undergo maturation in the epididymidis. The maturation event includes structural and physiological changes aided by addition and removal of many proteins from the spermatozoa. Spermatozoa that emerge from the testis are metabolically and translationally inactive. The highly compact DNA structure of the spermatozoa is proposed to be one of the reason for reduced gene expression efficiency of the growing spermatid (Brewer, Corzett, and Balhorn 2002; Chapman and Michael 2003). Reduction in the cytosolic content of the sperm during spermatogenesis is also considered to be another cause. Therefore the spermatozoa produce proteins that are only vital for its survival for which, it depends on mitochondrial ribosomes (Gur & Breitbart 2008). Hence, they depend on the micro environment for performing most of the biological functions, suggesting that the proteins required for their transport and function are gradually supplemented when they pass through the testis and epididymis and the secretions of seminal vesicles and prostate glands. The spermatozoa that are produced by testes does not possess the ability to fertilize ovum. It has to undergo capacitation to acquire the ability, which is believed to begin in male reproductive tract and completes in the female reproductive tract.

‘‘Capacitation’’ is a complex process that involves reorganization of membrane proteins (Zaneveld et al. 1991), metabolism of membrane phospholipids (Zanetti et al. 2010), reduction in membrane cholesterol levels (Osheroff et al. 1999), increased Ca^{2+} influx (DasGupta et al. 1993) and hyperactivation (Cancel et al. 2000). These changes, together with the subsequently induced acrosome reaction (AR) (Lee et al. 1987), are essential for a sperm to bind and penetrate the zona pellucida and thereafter fuse with the oocyte plasma membrane (Naz & Dhandapani 2010).

Acrosome is a cap like structure that is present on the anterior half of the mammalian spermatozoa. It contains hyaluronidase (Lin et al. 1994), acrosin (Yamagata et al. 1998) and other proteins that are required for sperm egg recognition and penetration. Acrosome reaction is an important event that is required for the fusion of sperms with oocyte. During acrosome reaction the cell membrane of the spermatozoa fuses with the outer membrane of the acrosome and the contents of the acrosome flow outwardly through the resulting pores. The acrosome reacted spermatozoa thus releases the digestive enzymes which helps in penetrating the zona pellucida of the oocyte thereby resulting in sperm egg fusion (Zaneveld et al. 1991).

Human LYZL proteins although are reported way back in 2005, their function in mammalian reproduction is not reported except for LYZL3/SLLP1 (Mandal et al. 2003). LYZL3 was found to be expressed in the acrosomal region of the spermatozoa and also in Burkit lymphoma Raji cell line. It is expressed in the lymphocytes in case of malignancies and is therefore identified as a useful marker for hematologic malignancies (Wang et al. 2004). Treatment of oocytes with anti-LYZL3 antibody or recombinant LYZL3 protein resulted in inhibition of sperm binding to oolemma (Mandal et al. 2005). Moreover, the interacting partner of LYZL3 was identified to be SAS1B that is expressed on the oocyte membrane. SAS1B knockout female mice showed reduced fertility (Sachdev et al. 2012). LYZL4 was located in intra-acrosomal region of spermatozoa and also in the principal piece of the sperm tail. Treatment of the sperms with anti-LYZL4 antiserum resulted in reduced oocyte fertilization *in vitro* (Sun et al. 2011). LYZL6 is expressed in testis and epididymis of mouse (Wei et al. 2013). It is also present in the primary spermatocytes, round spermatids, post–acrosomal region and mid piece of the spermatozoa (Wei et al. 2013). The antibacterial activity of LYZL6 also suggests that they may have role in innate immunity in male genital tract. Taken together it is clear that the LYZL proteins are predominantly expressed in male reproductive tract and also on sperm (Zhang et al. 2005), thus hypothesizing that they may

have role in sperm function. Therefore in this part of the work we sought to test the role of LYZL proteins in sperm related function with emphasis on LYZL4 and LYZL6.

MATERIALS AND METHODS

Male Wistar rats aged 90 days were used for this study. They were procured from National Institute of Nutrition, Hyderabad.

Retrieval of spermatozoa from cauda

Adult male Wistar rats were euthanized by cervical dislocation and the cauda was dissected out and placed in a petri plate containing prewarmed capacitation media (M2 media). It was then teased with scalpel to release spermatozoa from the cauda. The resultant spermatozoa were incubated in CO_2 incubator at 37°C for 10 min after which they were counted and resuspended as $5X10^6$ cells/ml. The spermatozoa are then capacitated for 5 h in the presence or absence of antiserum or recombinant proteins.

Treatment of spermatozoa

The possible sperm related functions of LYZL proteins were assessed by two methods, either by treating the spermatozoa with antiserum or recombinant proteins. For antiserum treatment, anti-LYZL4 or anti-LYZL6 serum (1:500) was added to spermatozoa ($5X10^6$ cells/ml). The spermatozoa were then allowed to capacitate in CO_2 incubator at 37°C for 5 h. Acrosome reaction was measured to assess the functional ability of the spermatozoa by treating with the ionophore A23187. For recombinant protein treatment, rat spermatozoa ($5X10^6$ cells/ml) were incubated with recombinant LYZL4 or LYZL6 protein at the concentration of 50 μg/ml. The spermatozoa are then allowed to capacitate in the presence of recombinant protein in CO_2 incubator at 37°C for 5 h, followed by assessment of capacitation and acrosome reaction.

Assessment of capacitation reaction

Capacitation is a complex process and involves a series of steps that can be studied by various techniques. Figure 3.1 describes the methods used for analysing the processes. The ability of the sperm to undergo hyperactivation was measured using computer assisted sperm analysis (CASA). Calcium and cholesterol dynamics were assessed by fluorescence activated cell sorter (FACS) using calcium binding dye Fluo-3-AM and cholesterol binding dye filipin. Tyrosine phosphorylation was assessed by Western blotting and membrane reorganization was assessed using CTC.

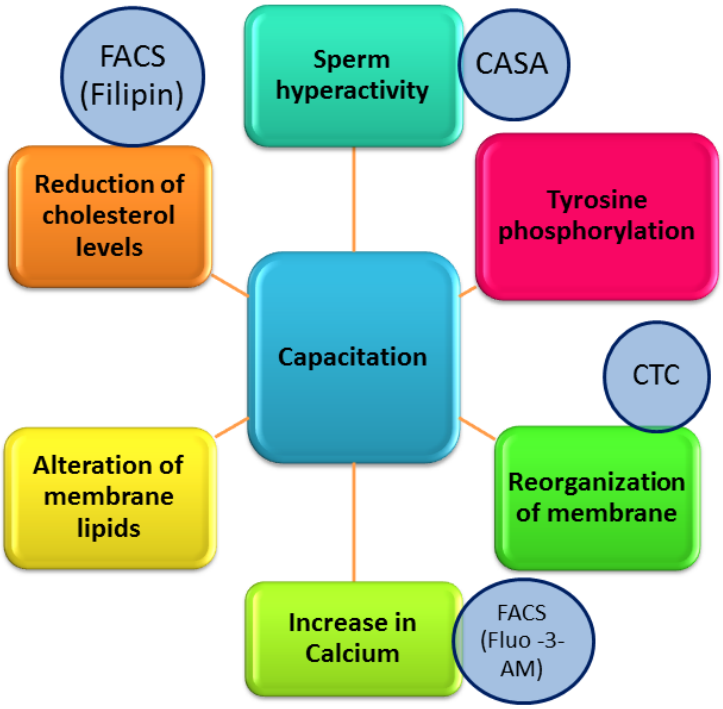

Figure 3.1: *Processes involved in capacitation and the analytical methods used.*

Assessment of capacitation by CTC staining

Assessment of membrane reorganization during capacitation was performed by CTC staining (Ward & Storey 1984). CTC binds to sperm membrane and hence commonly used for assessing the sperm membrane fluidity (Rathi et al. 2001). Spermatozoa obtained from rats

were resuspended in modified Kreb's Ringer bicarbonate buffer (KBR) pH 7.4 at a density of $5x10^6$ cells/ml and treated with recombinant LYZL protein or LYZL antiserum. For CTC staining, a 100 µl sperm suspension was withdrawn at respective time point and mixed with 100 µl CTC stain (0.75mM CTC, 5mM L-cysteine and 150mM NaCl in 20mm Tris buffer pH 7.4) and incubated for 30 sec at room temperature. Thereafter, the sample was fixed with 30 µl of 12.5% glutaraldehyde and a 10µl drop of the fixed spermatozoa suspension was mixed with 5µl of antifade and placed on a glass microscope slide. The droplet was covered with a coverslip. Prepared slides were then stored in the dark until analyses under fluorescence microscope.

Flow cytometry analysis

The flow cytometry analysis was carried out using LSR Fortessa cytometer (BD Biosciences). Fluorescence intensity was measured in atleast 10,000 spermatozoa. They were counted at the rate of 200-300 spermatozoa/sec. The fluorescence intensity and the forward scattering (FSC) was collected in logarithmic mode and the side scattering (SSC) was collected in linear mode. Filter options were used based on the dye to be measured.

Table 9: Details of the dye and the channels used

S. No	Dye	Excitation	Emission	Channel	Mode
1	PSA-FITC	495	515	FITC	Logarithmic
2	Filipin	380	510	Amcyan-A	Logarithmic
3	Fluo 3-AM	506	526	FITC	Logarithmic
4	Propidium iodide	535	616	PE-A	Logarithmic

Assessment of cholesterol efflux by filipin staining

Filipin binds to cholesterol with high affinity and its excitation and emission in the UV range can be exploited to assess the cholesterol distribution in the sperm membrane. Caudal spermatozoa of 90 day old Wistar rat was collected in M2 medium and allowed to liquefy for 10 min in 5% CO_2 at 37°C. The spermatozoa were then diluted to $5X10^6$ cells/ml and treated with recombinant LYZL protein or antiserum to LYZL protein for 5 h. At the end of incubation, spermatozoa were washed twice in PBS followed by incubation with 50 µg/ml filipin for 30 min at room temperature to stain the membrane cholesterol. The spermatozoa were then washed with PBS and propidium iodide (10 µg/ml) was added and incubated for 5 min to differentiate live and dead cells. % population (P1) of the stained cells which losses fluorescence intensity was analysed using FACS (Shadan et al. 2004). Appropriate zero hour, preimmune and buffer controls were maintained.

Microscopic assessment of cholesterol efflux

Spermatozoa stained with filipin were smeared on glass slides and observed under fluorescence microscope with excitation and emission wavelength of 380 nm and 510 nm respectively (Barboni et al. 2011). Decreased fluorescence intensity indicates efflux of cholesterol from the sperm membrane. The spermatozoa are compared with uncapacitated zero hour stained spermatozoa.

Assessment of calcium influx by Fluo-3-AM staining

Fluo-3-AM a calcium binding probe, is a acetoxymethyl ester of Fluo 3. The Fluo-3-AM is permeable to plasma membrane and in the cell the ester part is cleaved by the esterase and the resultant is impermeable to plasma membrane. In the absence of calcium the fluorophore is quenched and in the presence of the calcium the quencher moiety of the probe is engaged in

binding to calcium therefore resulting in fluorescence. Thus, Fluo-3-AM can be used to assess the calcium levels inside the cells. Wistar rats (90 days) were dissected and the caudal spermatozoa were collected in M2 media, and allowed to liquefy at 37°C in CO_2 incubator for 5 min. The spermatozoa were then aliquoted ($5X10^6$ cells/ml) and treated with recombinant LYZL protein or antiserum to LYZL protein for 5 h according to standard protocol. At the end of incubation 10 µM Fluo-3-AM was added to PBS washed spermatozoa and incubated for 20 min. Mean fluorescence intensity (MFI) of spermatozoa was measured in FITC channel of a LSR Fortessa flow cytometer (Zhang et al. 2010). Spermatozoa treated with preimmune sera and without antibody treatment was used as controls. Propidium iodide was used to stain and eliminate dead cells.

Computer assisted sperm analysis (CASA)

Hyperactivation and motility parameters were assessed using CASA, as described earlier (Republic 2008; Vetter et al. 1998). Briefly, spermatozoa diluted in capacitation medium were incubated for 5 h at 37°C. At the end of each hour, 5 µl of spermatozoa were mixed with 30 µl of capacitation medium and observed on a microscopic chamber slide maintained at 37°C. The set up values of the CASA were as follows: frames acquired - 30; frame rate (Hz) - 60; minimum contrast - 100; minimum cell size (pixels) - 7; low average path velocity cut off (µm/sec) - 20; medium average path velocity cut off (µm/sec) - 50; low straight line velocity cut off (µm/sec) - 30; static head intensity limits - 0.14–1.84; static head - size limits - 0.72–8.82; static elongation limits - 0–47; magnification, 1.95 (10x); video frequency (Hz) - 60; bright field - off; slide temperature - 37°C; field selection mode. Based on these kinematic parameters, the non-hyperactivated spermatozoa could be differentiated from the hyperactivated spermatozoa using the SORT facility of the CASA. Spermatozoa with data points ≥15, VCL>300 µm/sec, LIN<40%, ALH>12 µm were sorted as hyperactivated (those exhibiting either circular or helical motility pattern) and spermatozoa with data points ≥15,

VCL<300 µm/sec, LIN>40% and ALH<12 µm were sorted as non-hyperactivated spermatozoa (exhibiting planar motility pattern). The motility parameters such as curvilinear velocity (VCL), linearity (LIN), amplitude of lateral head displacement (ALH) were measured after every hour until 5 h. About 100 spermatozoa were sorted at each time point to assess the hyperactivation.

Microscopic assessment of acrosome status by PSA-FITC staining

Pisum sativum agglutinin (PSA) binds to the glycoprotein present in the sperm membrane and acrosomal matrix. During acrosome reaction there is loss of acrosomal membrane matrix, leading to reduced fluorescence, which can be used to assess acrosome reaction. To determine the role of LYZL proteins in acrosome reaction, caudal spermatozoa were allowed to capacitate in M2 medium in the presence of LYZL recombinant protein or antiserum, after which acrosome reaction was induced by addition of 20 µM ionophore (A23187) for 20 min. Samples were then washed and treated with PSA-FITC (40 µg/ml), which binds to acrosome specific glycoproteins. Spermatozoa were then smeared on microscopic glass slides, air dried and incubated in absolute methanol for 15 min. Methanol-treated smears were incubated with FITC conjugated PSA (50 µg/ml) for 30 min at room temperature. The slides were then washed with distilled water for 15 min to remove excess unbound probe. After drying, smears were examined immediately using a fluorescence microscope (DasGupta, Mills, and Fraser 1993; Mendoza et al. 1992). Spermatozoa incubated with PBS were used as non-capacitated control.

FACS analysis of acrosome reaction by PSA-FITC

Acrosome reaction was induced in spermatozoa ($5X10^6$ cells/ml) using the ionophore A23287 (20 µM). They were then washed with PBS and stained with PSA-FITC (50 µg/ml) to stain the acrosomal region. The intensity of fluorescence was measured using FACS as means of

acrosome reaction. Decrease in fluorescence intensity indicates acrosome reaction. Fluorescence intensity was measured in a flow cytometer using FITC channel (Jaiswal & Eisenbach 1999). The acrosome reacted population (P2) showing less intensity and the acrosome intact spermatozoa (P3) with high fluorescence intensity were gated and analysed.

Raising auto antibodies against LYZL6

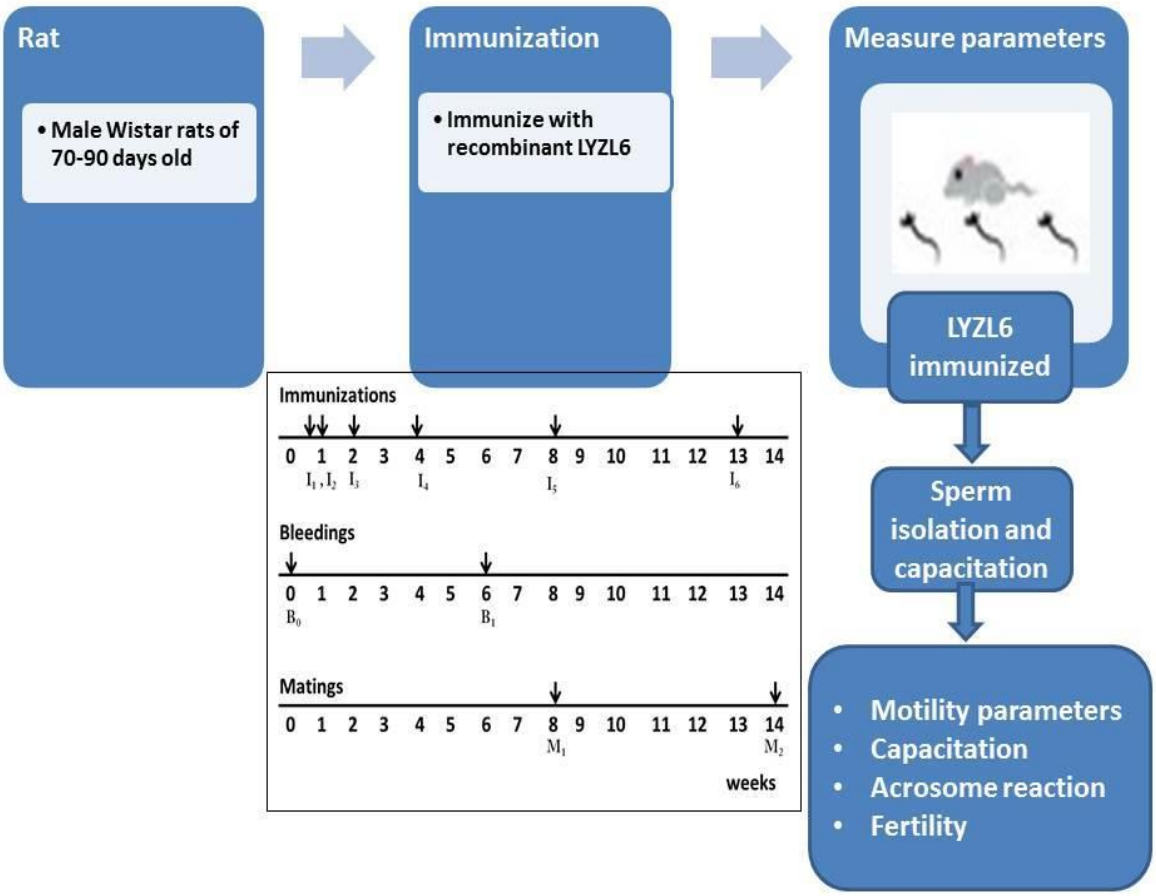

Figure 3.2: *Flow chart for evaluation of* LYZL6 *as immunocontraceptive. Numbers represents week.* I_1, I_2, I_3, I_4, I_5 *and* I_6 *denoted by the arrow shows the time of immunization.* B_0 *and* B_1 *represent blood collection time points.* M_1 *and* M_2 *represents the time period in which animals were kept for mating.*

Male rats aged 90 days were caged in standard day and night conditions and acclimatized. They were immunized with recombinant LYZL6 as per the schedule in figure 3.2. Preimmune serum (B_0) was collected from the tail vein and checked for cross reactivity against recombinant LYZL6 before immunization on day 0. Briefly 100 µg of the protein was mixed with equal volume of Freund's complete adjuvant and administered intradermally (I_1). The second immunization (I_2) was administered on 3rd day after first immunization in the 1st week by injecting 100 µg of recombinant protein mixed with Freund's incomplete adjuvant. Third immunization (I_3) was given in 2nd week and subsequent immunizations were administered as shown in figure 3.2. Antibody titer was checked on 6th week by ELISA or dot blot using serum obtained after first blood collection (B_1) of the immunized animals. After confirmation of the presence of antibody against recombinant LYZL6, immunized animals were caged with adult females on 8th and 14th week to allow mating.

Antibody titre by ELISA

96 well plates were coated with 40 µg/ml of recombinant protein and incubated overnight at 37˚C, followed by incubation at 60˚C for 30 min. The plates were then blocked with 1mg/ml BSA for 2 h and then incubated for 3 h with different dilutions of antiserum against rat LYZL proteins raised in rabbit. They were then washed 4 times with PBS-T (PBS with 0.1% Tween-20), followed by incubation with HRP conjugated anti-rabbit secondary antibody (1:10000). After thorough washing, O-phenylenediamine (OPD) was added to measure the amount of antibody bound to the protein (Wang et al. 2011). The antibody titre is measured in terms of intensity of the colour developed. Higher the O.D, higher is the titer.

To determine the presence of autoantibodies in the testis and epididymis of immunized rats, ELISA was performed with the tissue fluids (Ellerman et al. 1998). The tissue fluids were obtained in 500 µl of PBS followed by centrifugation at 10,000 rpm for 10 min at 4˚C. The

supernatant was quantified for protein concentration and equal quantity of tissue fluid was used for the assay.

Assessment of fertility

Immunized rats that had high antibody titer were subjected to natural mating with females of proven fertility (Ellerman et al. 1998). The animals were caged in the ratio of 1 male to 3 females. The females were checked frequently and the pregnant rats were removed and the number of pups produced was noted. In the immunized rats sperm parameters such as calcium influx, cholesterol efflux, tyrosine phosphorylation, hyperactivation and acrosome reaction were analysed in the spermatozoa obtained from immunized animals.

RESULTS

Assessment of capacitation by chlortetracycline (CTC) staining

CTC staining is widely used to assess the capacitation status of the spermatozoa (Lee et al. 1987). Spermatozoa that underwent capacitation *in vitro* exhibited decreased CTC staining when compared to their uncapacitated counterparts (Figure 3.3). The CTC staining pattern was similar to that of the capacitated control in recombinant LYZL4 or LYZL6 protein treated spermatozoa, implying that addition of protein did not have any effect on sperm capacitation. The staining pattern in LYZL4 or LYZL6 antiserum treated spermatozoa was similar to that in capacitated sperm, indicating that blocking LYZL4 or LYZL6 on sperm surface does not affect membrane reorganization during capacitation. Spermatozoa treated with preimmune serum or buffer control also underwent capacitation (Figure 3.3)

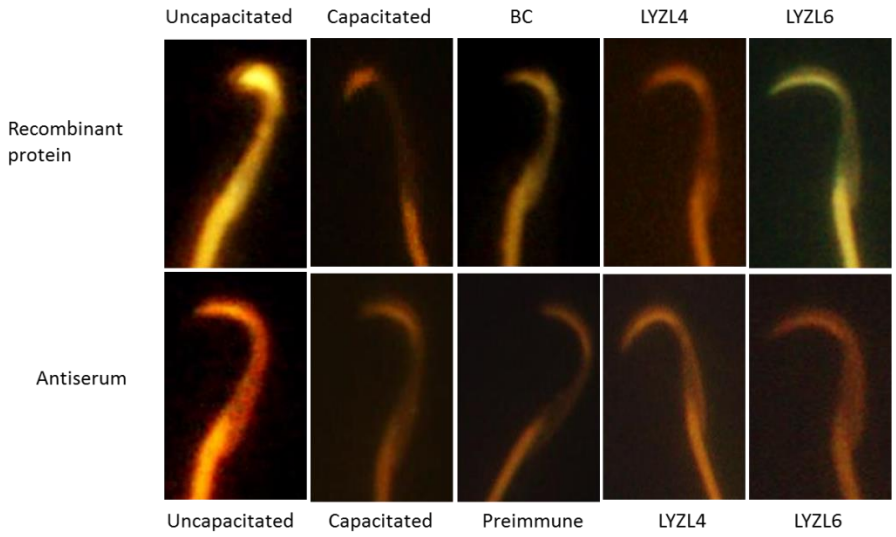

Figure 3.3: *Effect of LYZL proteins on capacitation.* *CTC staining of spermatozoa treated with antiserum or recombinant* LYZL *proteins. BC-buffer control.*

Assessment of capacitation by measuring intracellular Ca^{2+} release

The extent of capacitation was measured in terms of Ca^{2+} release from intracellular stores and is achieved by measuring the fluorescence intensity of calcium binding dye, Fluo-3-AM. Increased fluorescence indicates the occurrence of sperm capacitation. Figure 3.4 shows a typical fluorescence measurement flow cytogram to assess calcium release during sperm capacitation. Spermatozoa suspended in capacitation medium exhibited an increase in Fluo-3-AM fluorescence intensity, indicating the progression of capacitation. The fluorescence peak shifts towards the right in the capacitated spermatozoa due to the binding of Ca^{2+} to Fluo-3-AM. The fluorescence intensity is an indication of extent of Ca^{2+} release. Spermatozoa treated with LYZL4 or LYZL6 recombinant proteins exhibited fluorescence intensity similar to that of capacitated spermatozoa (Figure 3.5A). The buffer control (BC) did not interfere with the measurements. On the other hand, treatment with LYZL4 or LYZL6 antiserum caused a significant decrease in fluorescence intensity when compared to capacitated spermatozoa (Figure 3.5B), suggesting that neutralization of LYZL4 or LYZL6 affects Ca^{2+} release from intracellular stores. Pre-immune serum did not have any effect on Ca^{2+} release.

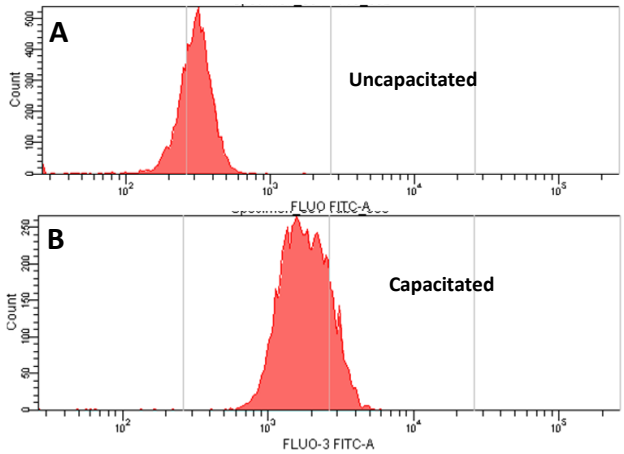

Figure 3.4: *FACS analysis of Fluo-3-AM stained spermatozoa. Representative cytogram of measurement of mean fluorescence intensity (MFI) of uncapacitated (A) and capacitated spermatozoa (B).*

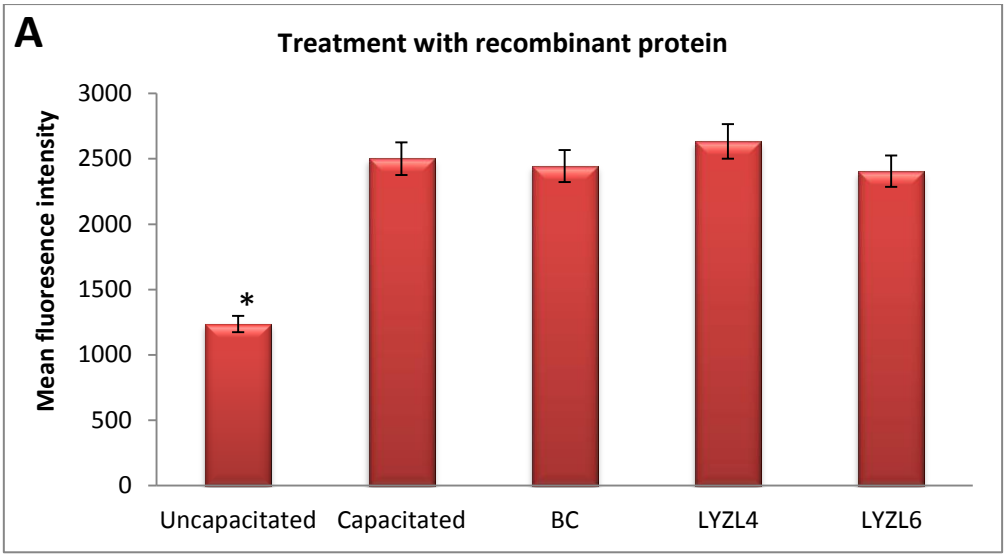

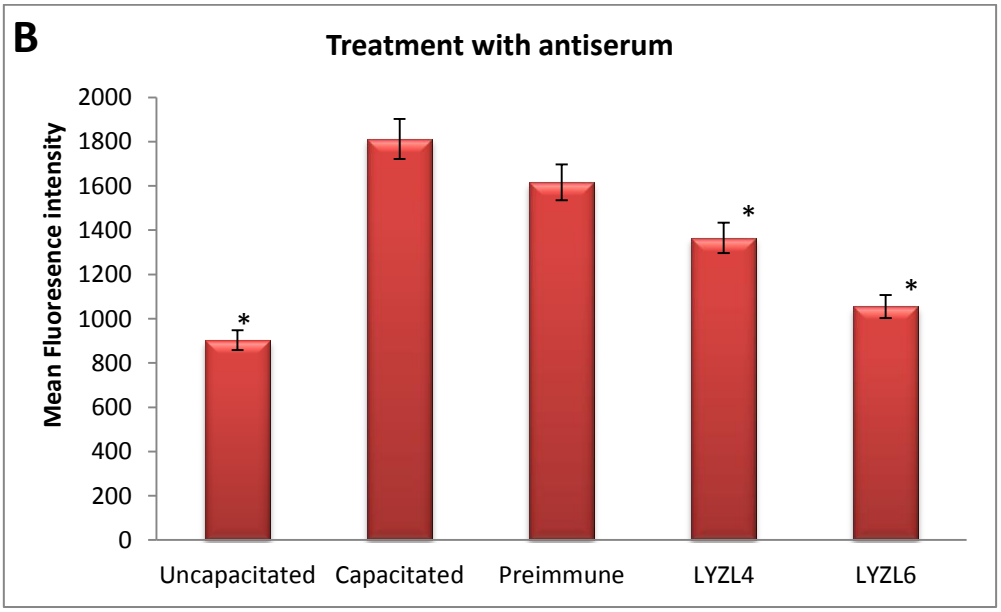

Figure 3.5: *Assessment of capacitation status through calcium influx using Fluo-3-AM. (A)- Mean fluorescence intensity of the spermatozoa incubated with or without recombinant* LYZL4 *or* LYZL6*, BC-buffer control. (B)- Mean fluorescence intensity of the capacitated spermatozoa incubated with or without* LYZL4 *or* LYZL6 *antiserum. Values shown are mean* $\pm$ *SD. * indicates $p<0.05$ compared to capacitated spermatozoa.*

Assessment of capacitation by measuring cholesterol efflux

During capacitation, cholesterol efflux from the sperm surface is a characteristic feature and these dynamics can be monitored by using filipin, a cholesterol binding dye. Uncapacitated spermatozoa exhibited fluorescence uniformly throughout the head region (Figure 3.6A). As cholesterol is lost during capacitation, the fluorescence intensity due to filipin also decreases (Figure 3.6B). In spermatozoa treated with LYZL4 (Figure 3.6D) or LYZL6 (Figure 3.6E) recombinant protein decreased fluorescence was observed similar to that of capacitated spermatozoa. PBS used as buffer control did not affect capacitation (Figure 3.6C). Similarly, spermatozoa treated with LYZL4 or LYZL6 antibody also showed decreased filipin staining indicating the occurrence of capacitation (Figure 3.6I and 3.6J) Pre-immune serum did not affect cholesterol dynamics during capacitation (Figure 3.6H).

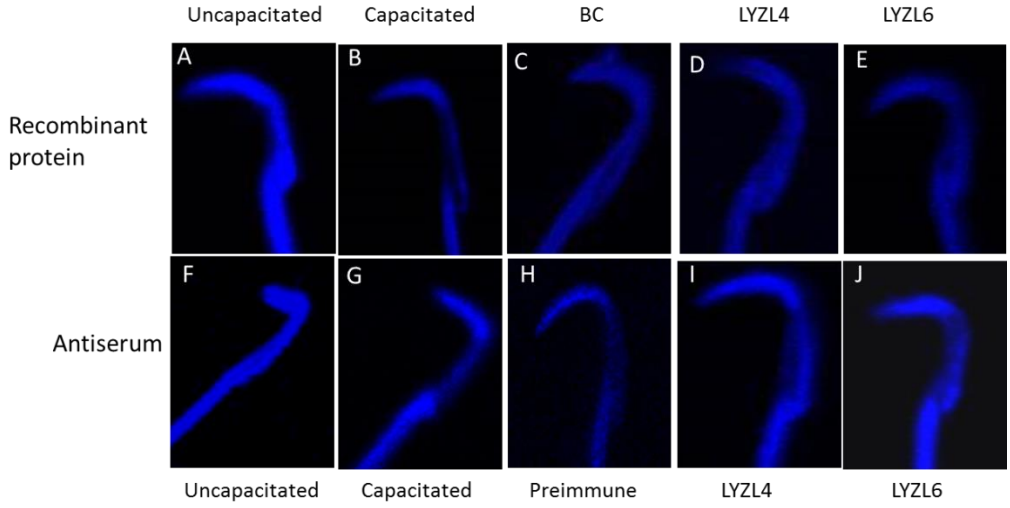

Figure 3.6: *Effect of* LYZL *proteins on cholesterol efflux. Filipin staining of spermatozoa treated with antiserum and recombinant* LYZL *proteins. BC-buffer control.*

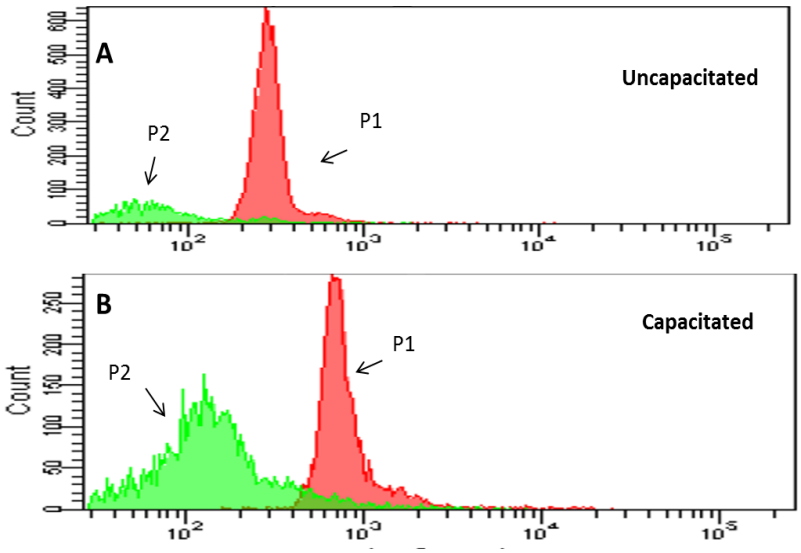

Figure 3.7: *FACS analysis of filipin stained spermatozoa. Representative cytograms of FACS analysis. Measurement of mean fluorescence intensity (MFI) of uncapacitated (A) and capacitated (B) spermatozoa.*

Cholesterol efflux during capacitation was also examined by flow cytometry. Figure 3.7 shows a typical flow cytogram of uncapacitated and capacitated spermatozoa. The population of spermatozoa that did not undergo capacitation (P1) exhibit higher fluorescence intensity, whereas capacitated spermatozoa (P2) exhibit decreased fluorescence intensity due to loss of cholesterol bound filipin. As capacitation progresses, the count of P2 population increases, which is an indicator of the extent of capacitation. The percent of P1 and P2 population was estimated in spermatozoa treated with LYZL proteins or their antiserum.

The P1 population was significantly decreased in spermatozoa subjected to *in vitro* capacitation (Figure 3.8). Spermatozoa pre-treated with LYZL4 or LYZL6 recombinant protein had the P1 population similar to that of capacitated control (Figure 3.8A). Treatment with LYZL4 or LYZL6 antiserum also had a significantly decreased number of P1 population (Figure 3.8B). These results indicate that neither the LYZL proteins not their antiserum could influence the capacitation process *in vitro.*

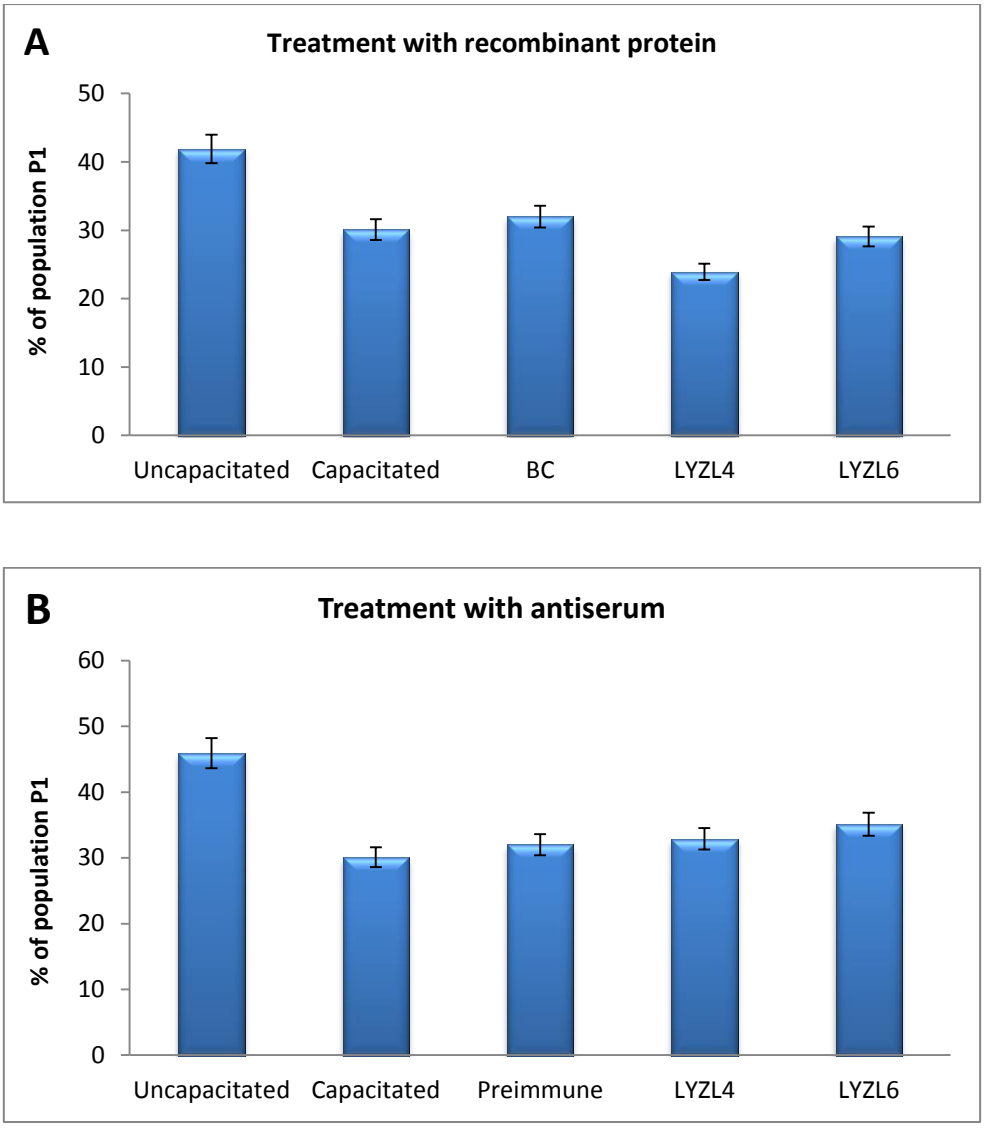

Figure 3.8: *Assessment of capacitation status. (A)- % population of the capacitated spermatozoa after incubation with or without recombinant* LYZL4 *or* LYZL6*. (B)- % population of the capacitated spermatozoa (P1) with or without* LYZL4 *or* LYZL6 *antibody BC- buffer control. Values shown are ± SD.*

Assessment of capacitation by protein tyrosine phosphorylation

Phosphorylation of proteins, specifically at tyrosine residues is a hall mark of capacitation. The extent of phosphorylation during capacitation was detected by Western blotting using phospho tyrosine antibody. As shown in Figure 3.9A, in proteins obtained from uncapacitated spermatozoa tyrosine phosphorylation was lower. Tyrosine phosphorylation seems to be increased in protein obtained from capacitated spermatozoa (Figure 3.9A). In spermatozoa pre-treated with LYZL4 or LYZL6 proteins, tyrosine phosphorylation was similar to that of capacitated spermatozoa (Figure 3.9A). Protein phosphorylation was evident in spermatozoa treated with LYZL4 or LYZL6 antiserum (Figure 3.9B). Pre-immune serum did not affect protein phosphorylation.

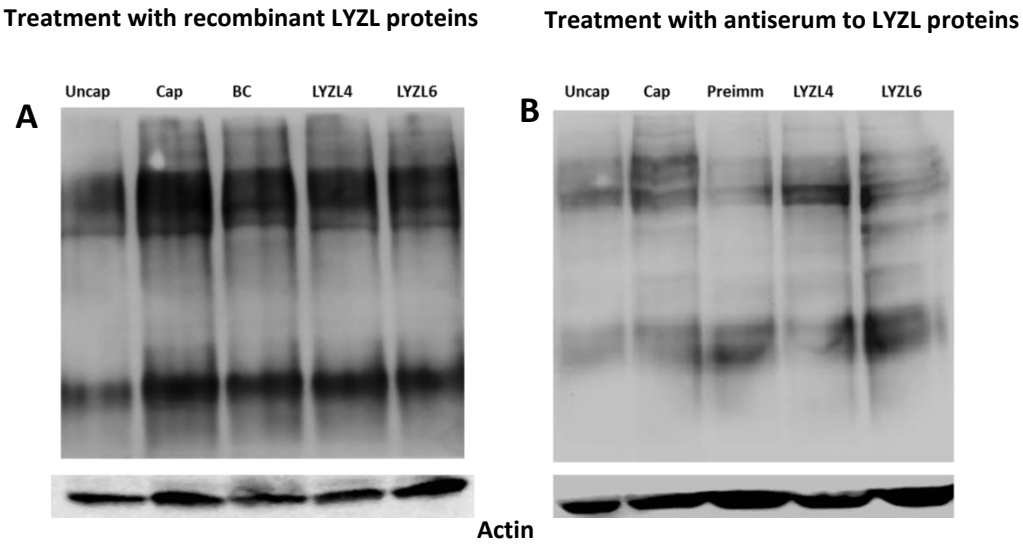

Figure 3.9: *Western blotting for the detection of tyrosine phosphorylation in sperm proteins.Uncap– uncapacitated, Cap- capacitated, BC– buffer control, Preimm- preimmune.*

Role of LYZL proteins in acrosome reaction

In conditions that allow acrosome reaction, a gradual decrease of specific glycoproteins are observed in the acrosomal region. Changes in the levels of these specific glycoproteins can be

detected using FITC tagged PSA lectin. In general, decreased fluorescence is observed in the head region of acrosome as the reaction occurs.

Immunocytochemistry was used to track the fluorescence intensity of PSA-FITC as acrosome reaction occurred. Intense staining was observed in acrosome intact spermatozoa (Figure 3.10A). Appreciable decrease in the FITC fluorescence was observed in acrosome reacted spermatozoa (Figure 3.10B). The buffer control (BC) did not affect the progression of acrosome reaction (Figure 3.10C). PSA-FITC staining was similar to that of acrosome reacted spermatozoa in LYZL4 or LYZL6 proteins pre-treated spermatozoa (Figure 3.10D and E). In spermatozoa pre-treated with LYZL4 antiserum, the PSA-FITC staining was found to be similar to that of acrosome reacted spermatozoa (Figure 3.10H) whereas in case of LYZL6 spermatozoa it was similar to acrosome intact spermatozoa (Figure 3.10I).

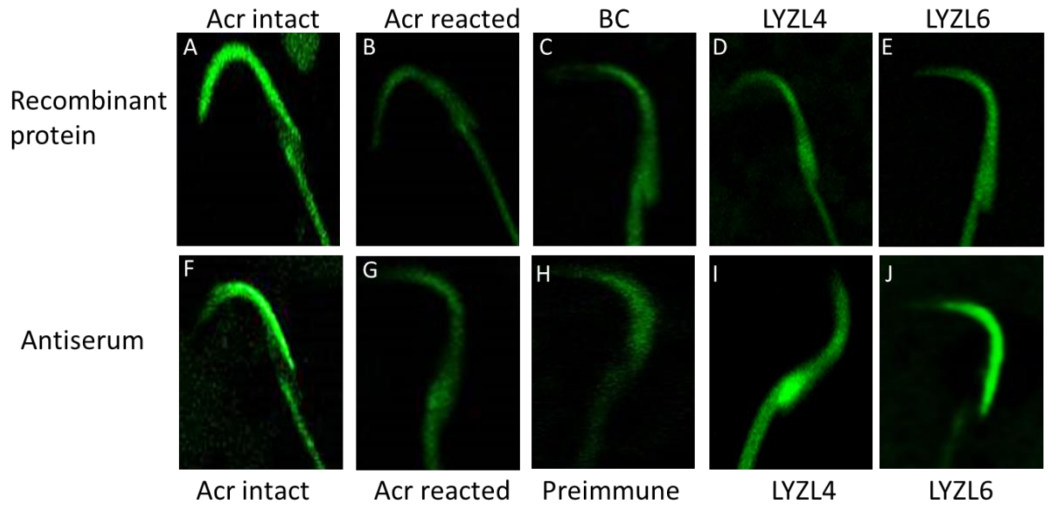

Figure 3.10: *Assessment of acrosome reaction by PSA-FITC staining. (A-E) Microscopic observation of rat spermatozoa treated with or without* LYZL4 *or* LYZL6 *recombinant proteins (A-E) or with* LYZL4 *or* LYZL6 *antiserum (F-J). Acr-acrosome, Preimm-Preimmune, BC-buffer control.*

To quantify the percentage of spermatozoa that have undergone acrosome reaction under different conditions, flow cytometric analyses was carried out. Acrosome intact spermatozoa exhibited higher fluorescence intensity whereas acrosome reacted spermatozoa exhibited lower fluorescence intensity due to loss of PSA-FITC binding proteins (Figure 3.11). Hence, both the populations can be estimated by gating (Figure 3.11A). The percentage of acrosome reacted spermatozoa were significantly higher under the *in vitro* conditions tested (Figure 3.11B). The % of spermatozoa that underwent acrosome reaction after treatment with LYZL4 or LYZL6 protein were similar to that of acrosome reacted control (Figure 3.12A). The number of spermatozoa that underwent acrosome reaction after treatment with LYZL4 or LYZL6 antiserum was decreased when compared to acrosome reacted control (Figure 3.12B).

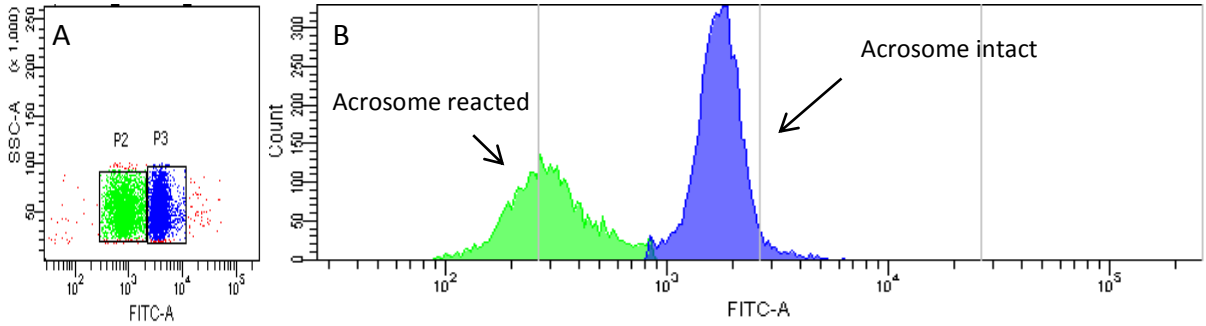

Figure 3.11: *FACS analysis of PSA FITC stained spermatozoa. (A)- Gating of acrosome reacted (P2- with low fluorescence intensity) and acrosome intact (P3- with high fluorescence intensity) spermatozoa. (B,)- Representative cytogram of FACS analysis showing the mean fluorescence intensity (MFI) of acrosome intact and acrosome reacted spermatozoa. Green- acrosome reacted population, blue –acrosome intact population.*

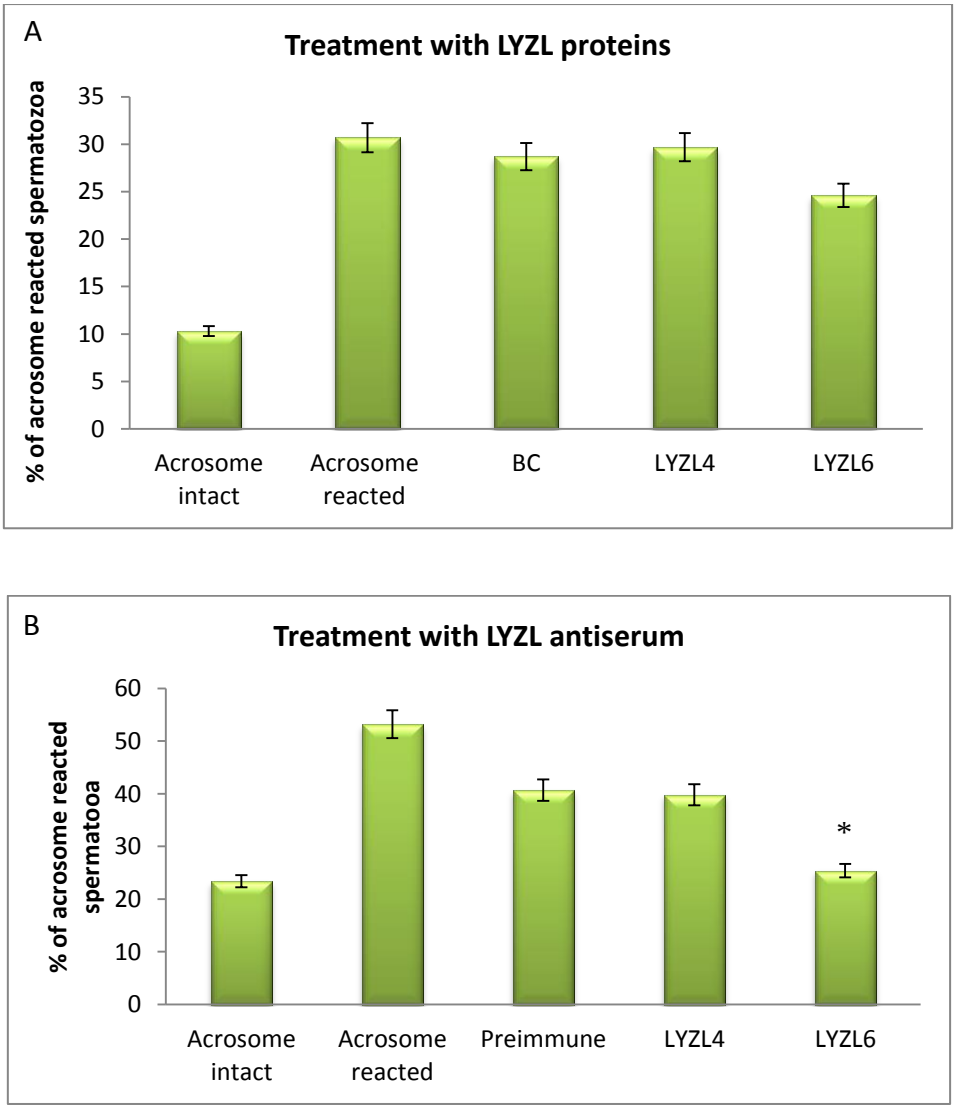

Figure 3.12: *FACS analysis of acrosome reaction. (A) % population of acrosome reacted spermatozoa after incubation with or without* LYZL4 *or* LYZL6 *recombinant proteins. (B)- % population of acrosome reacted spermatozoa after incubation with or without* LYZL4 *or* LYZL6 *antiserum. Values are the mean± SD. * indicates P<0.05 compared to acrosome reacted control.*

Immunocontraceptive potential of LYZL6

The auto antigen model generated by immunizing the rat with recombinant LYZL6 protein was verified by ELISA and the possible function of LYZL6 with regard to male reproduction was assessed.

Enzyme Linked Immunosorbent Assay (ELISA)

Serum was obtained from Wistar rats immunized with recombinant LYZL6 and the antibody titre measured by ELISA. In all the four rats (R1-R4) a dilution dependent antibody titre was detected (Figure 3.13). Preimmune serum did not show any reactivity.

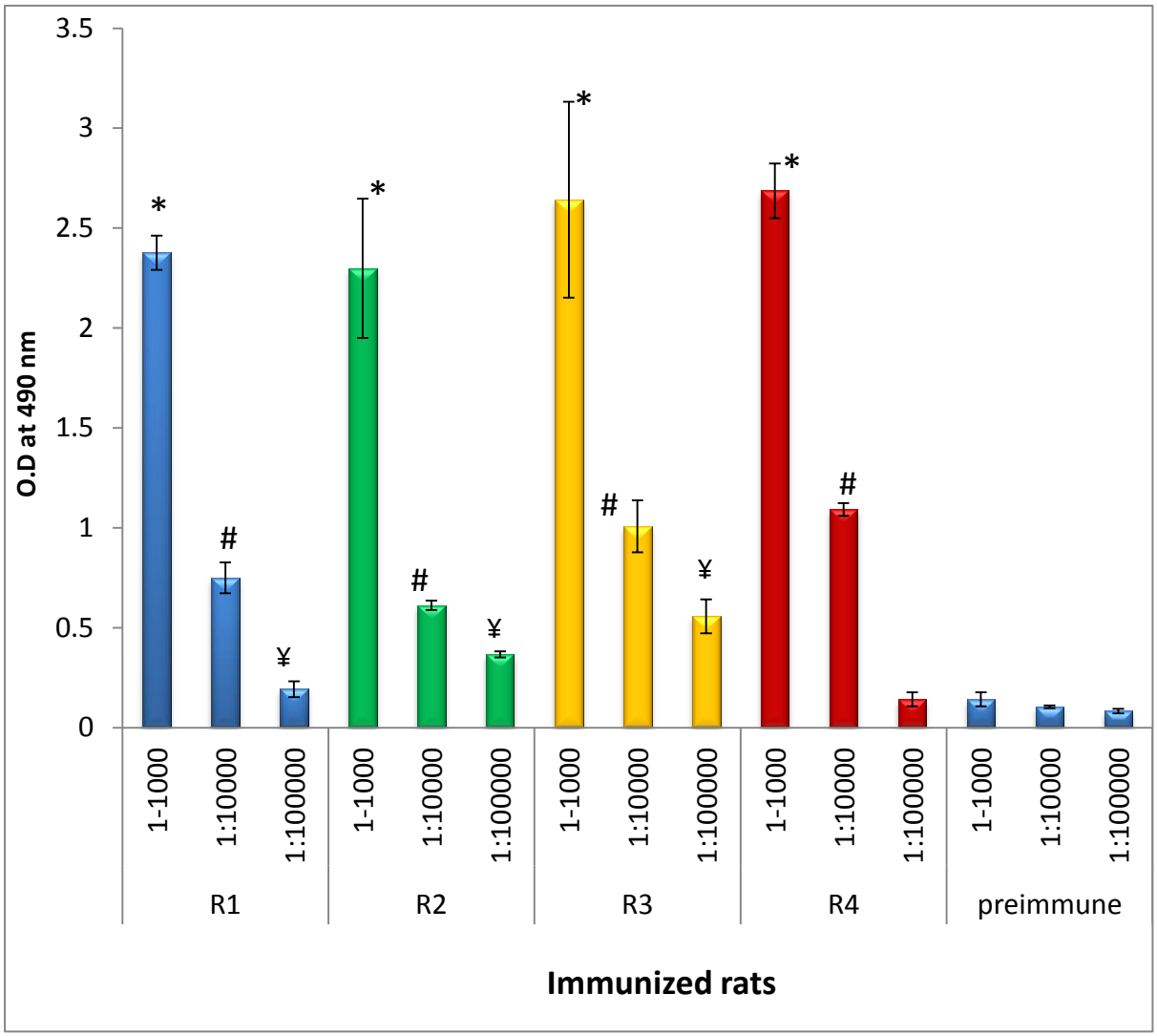

Figure 3.13: *ELISA with serum obtained from* LYZL6 *immunized rats. Graphical representation of serum titres verified by ELISA. Preimmune serum was used as control. R1, R2, R3 and R4 are immunized rats. Values shown are mean ± S.D. *, # and ¥ indicates p <0.05compared to the preimmune serum.*

Reproductive tract tissue fluids were tested for presence of LYZL6 antibody to determine whether the antibodies passed the blood testes barrier. The antibody titre was found to be significantly higher in the fluids obtained from the epididymides and testes of immunized rats when compared to the unimmunized controls (Figure 3.14).

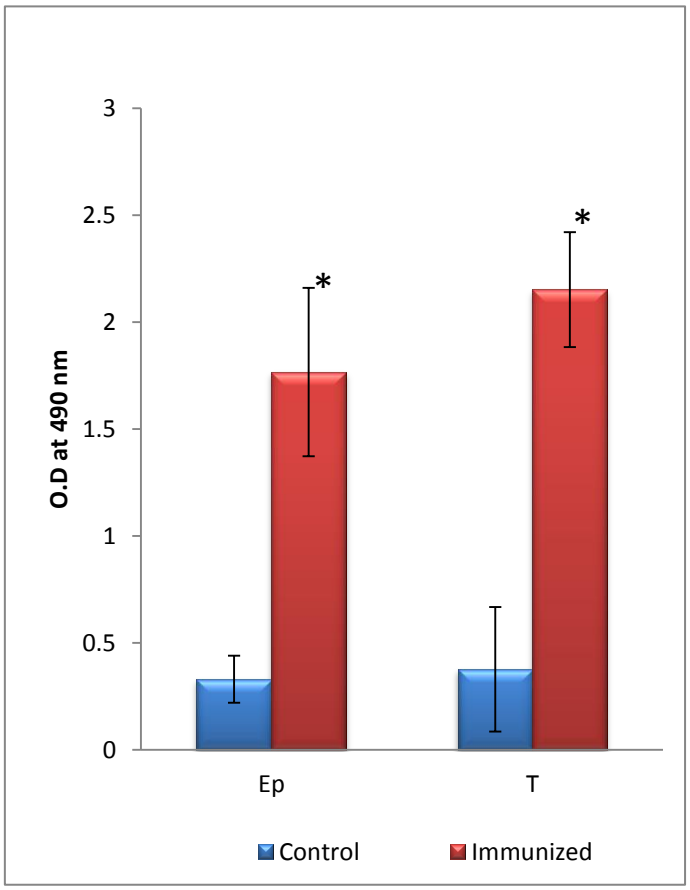

Figure 3.14: ELISA for* LYZL6 *immunized rats. *Antibody titres in the tissue fluids of* LYZL6 *immunized rats. Values shown are mean ± SD. * indicates p <0.05 compared to unimmunized control. Ep-epididymidis, T-Testes.*

Effect of LYZL6 immunization on sperm count

To determine whether the presence of LYZL6 antibodies in the testicular and epididymal fluids may affect germ cell production, the sperm count was analysed. A significant decrease in the sperm count was observed in LYZL6 immunized rats (Figure 3.15).

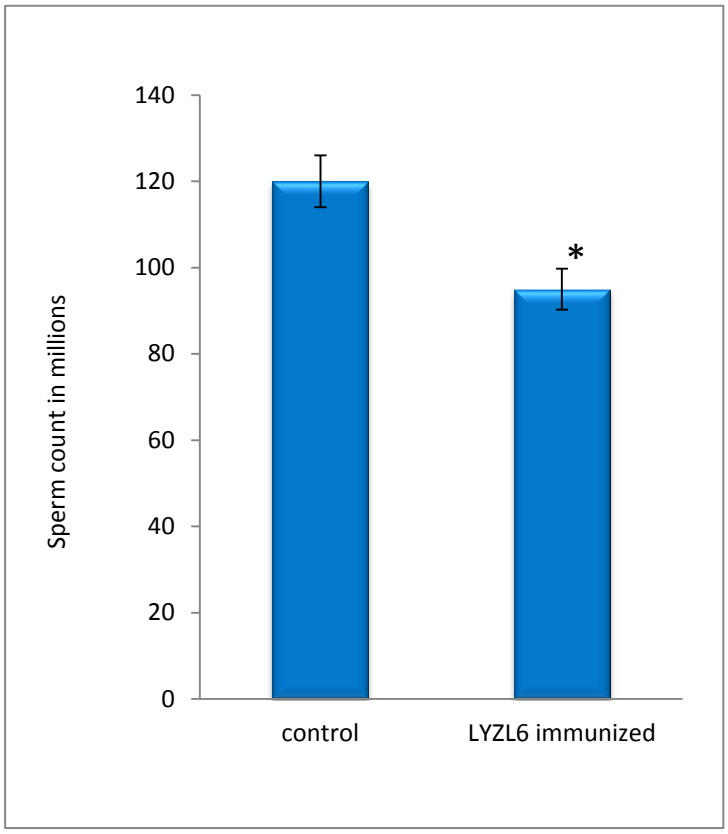

Figure 3.15: Sperm count in* LYZL6 *immunized rats. *Values shown are mean ± SD. * indicates p <0.05 compared to unimmunized control.*

Computer Assisted Sperm Analysis (CASA)

To determine whether the spermatozoa produced by immunized animals have compromised physiological features, CASA was performed. Motility parameters such as path velocity, progressive velocity and track speed were found to be decreased in spermatozoa obtained from immunized rats, when compared to control. These results show that endogenous neutralization of LYZL6 protein results in reduction in motility parameters of spermatozoa.

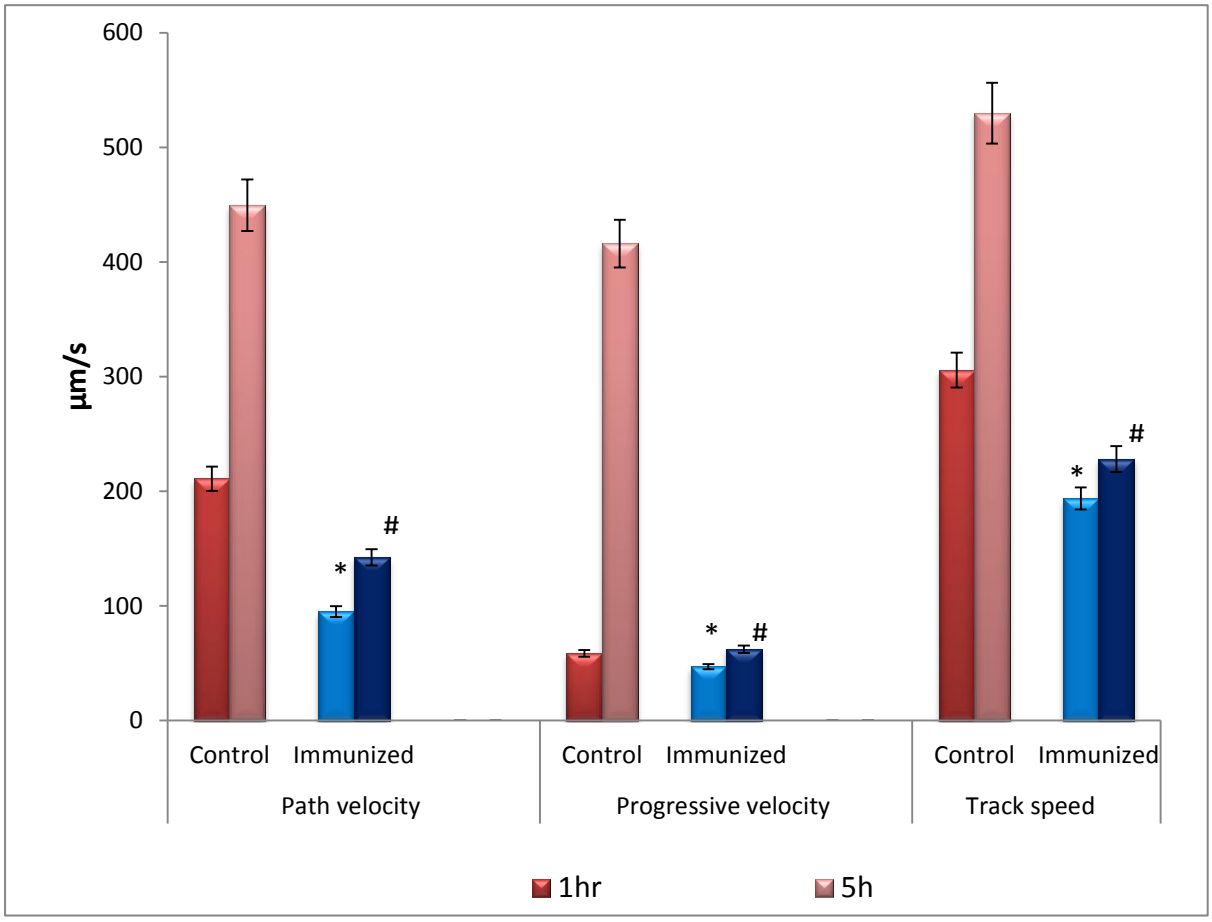

Figure 3.16: Assessment of sperm parameters by CASA. *Spermatozoa were obtained from control and immunized rats and the motility parameters analysed at 1 and 5 h after collection. * and # indicates $p<0.05$ compared to unimmunized control.*

Histopathological evaluation

Cross sections of testes and epididymidis obtained from control and LYZL6 immunized rats were examined under microscope to determine the possible pathomorphological effects. The overall architecture of testis and epididymis were not affected and were similar to the unimmunized control.

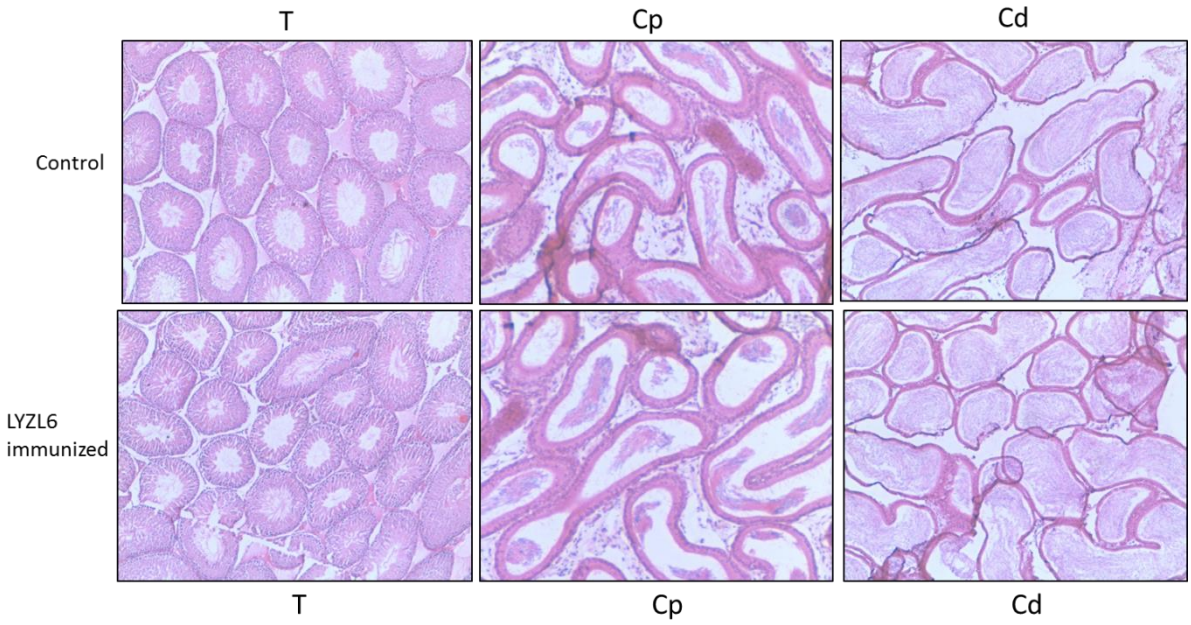

Figure 3.17: Morphological assessment of testes and epididymidis. *Cross sections of testes and epididymidis obtained from* LYZL6 *immunized and control rats were stained with hematoxylin and eosin. Magnification 10X.T-testes, Cp-caput, Cd- cauda.*

Assessment of tyrosine phosphorylation

Tyrosine phosphorylation of the sperm proteins obtained from control and LYZL6 immunized rats under capacitating conditions was analysed. Extensive protein phosphorylation was observed in spermatozoal proteins that were obtained from control rats (Figure 3.18A). Similar phosphorylation pattern was also observed in spermatozoa obtained from LYZL6 immunized rats.

We next determined whether the antiserum obtained from LYZL6 immunized rats can neutralize the LYZL6 protein on control rat spermatozoa and affect sperm function. Tyrosine phosphorylation was evident in spermatozoa pre-treated with antiserum obtained from LYZL6 immunized rats (Figure 3.18B).

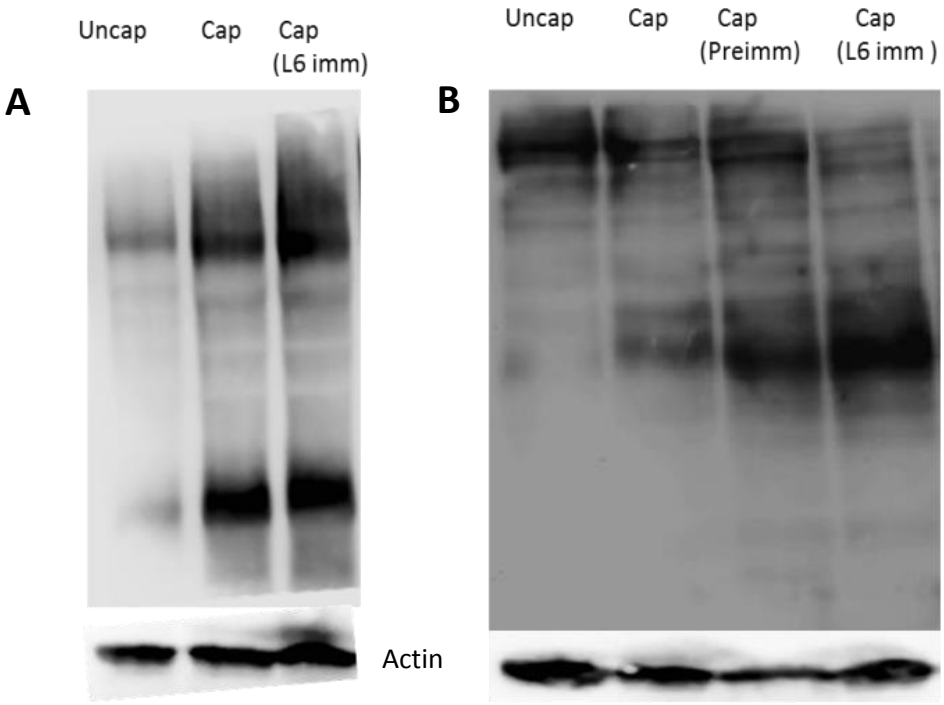

Figure 3.18: Western blotting analysis of* LYZL6 *auto-antigenic rat spermatozoa and* LYZL6 *antiserum (rat) treated spermatozoa.

Effect of LYZL6 immunization of calcium influx

Intracellular calcium level was assessed in LYZL6 immunized animals by using the calcium binding dye Fluo-3-AM. In comparison with unimmunized rat spermatozoa, LYZL6 immunized rat spermatozoa showed decreased calcium influx (decreased mean fluorescence intensity) (Figure 3.19A) reiterating similar results obtained in *in vitro* studies. Analysis of the same using antiserum obtained from LYZL6 immunized rats also confirmed that LYZL6 neutralization resulted in decreased calcium influx (Figure 3.19B).

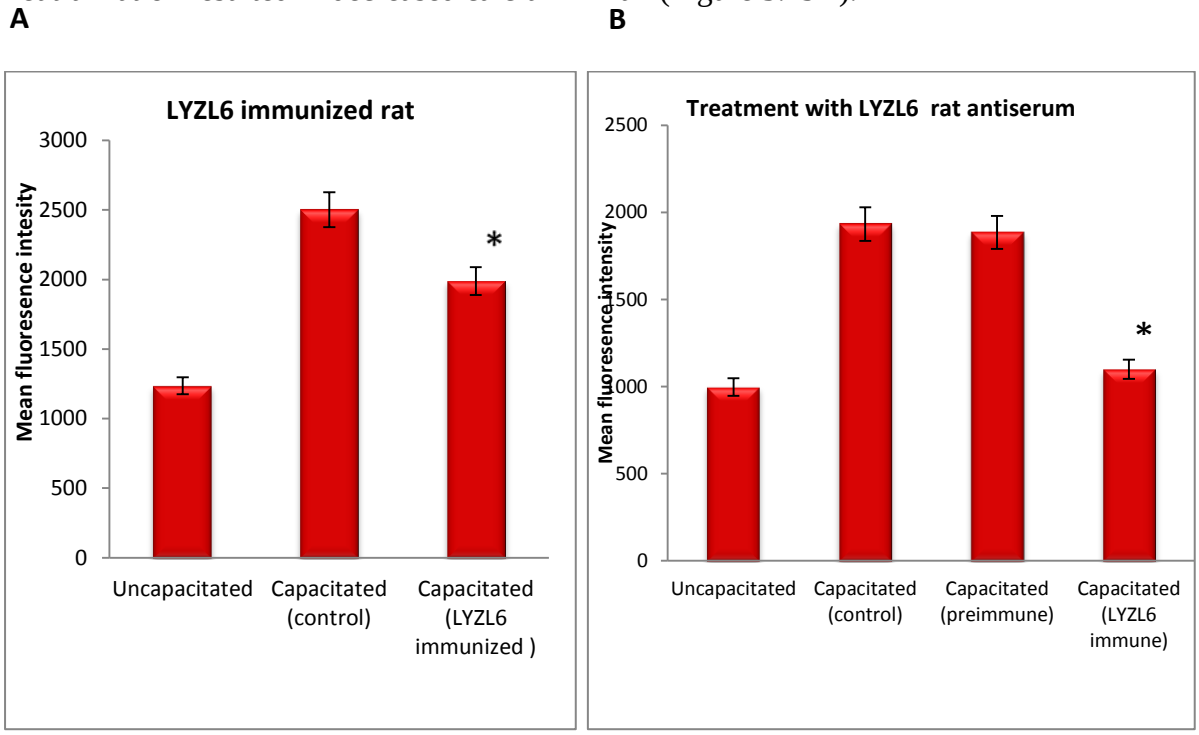

Figure 3.19: *Evaluation of calcium influx in LYZL6 immunized rat. (A) Mean fluorescence intensity of the spermatozoa obtained from unimmunized and LYZL6 immunized rats. (B) Mean fluorescence intensity of the capacitated spermatozoa incubated with or without* LYZL6 rat *antiserum. Values shown are mean* $\pm$ *SD. * indicates* $p<0.05$ *compared to capacitated spermatozoa.*

Effect of LYZL6 immunization on capacitation

Cholesterol efflux of the spermatozoa obtained from LYZL6 immunized rats were analysed to assess the capacitation status using filipin. LYZL6 immunized rat spermatozoa exhibited decreased ability to undergo capacitation (Figure 3.20A). Similar results were obtained on treatment of control spermatozoa with immune sera obtained from LYZL6 immunized rat (Figure 3.20B), suggesting that LYZL6 neutralization may affect capacitation.

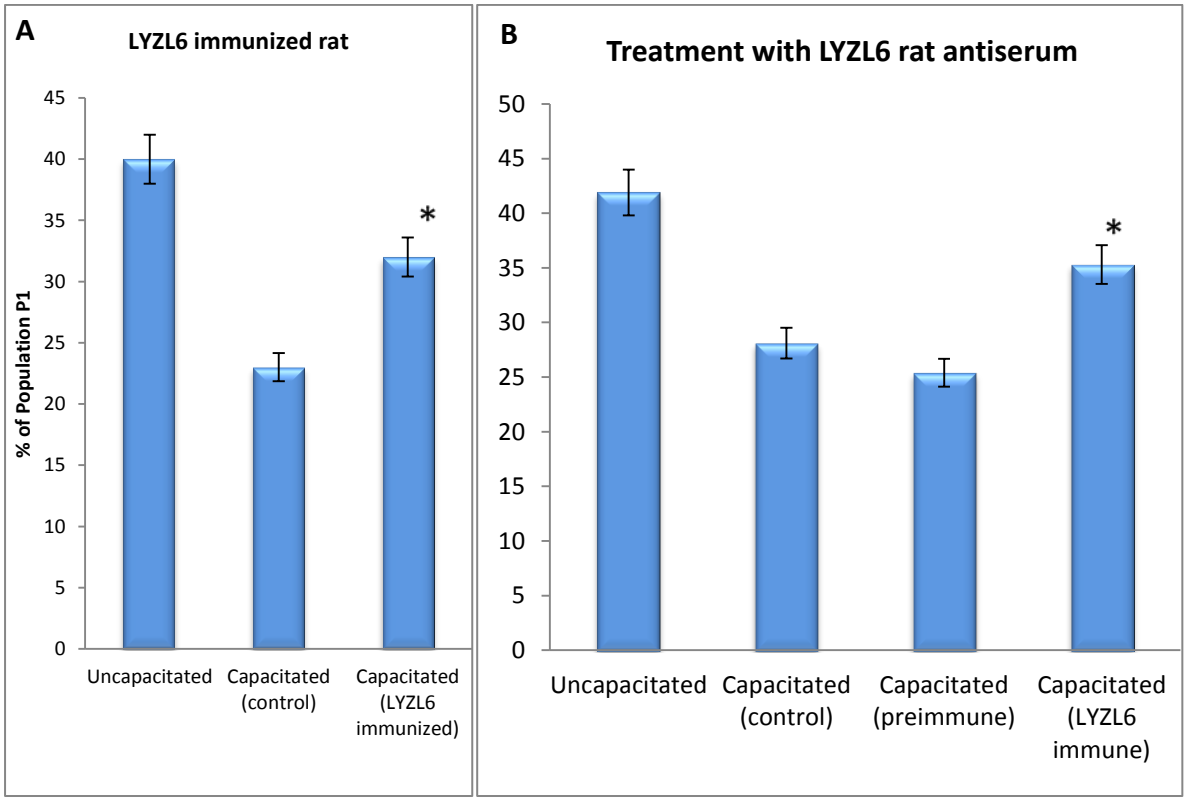

Figure 3.20: Assessment of capacitation status. *(A)- % population of the capacitated spermatozoa (P1) obtained from LYZL6 immunized rats (B)- % population of the capacitated spermatozoa (P1)treated with* LYZL6 *rat antiserum. Values shown are* $\pm$ *SD.* indicates* $p<0.05$ *compared to uncapacitated control.*

Effect of LYZL6 immunization on acrosome reaction

Assessment of acrosome reaction of the spermatozoa obtained from LYZL6 immunized animals was performed by staining the spermatozoa with PSA-FITC and the resultant were analysed by flow cytometry. LYZL6 immunized rat spermatozoa display less ability of undergo acrosome reaction in comparison with unimmunized rat spermatozoa (Figure 3.21A). Control spermatozoa treated with LYZL6 rat antiserum also displayed similar effect suggesting that LYZL6 neutralization is affecting the acrosome reaction (Figure .21B).

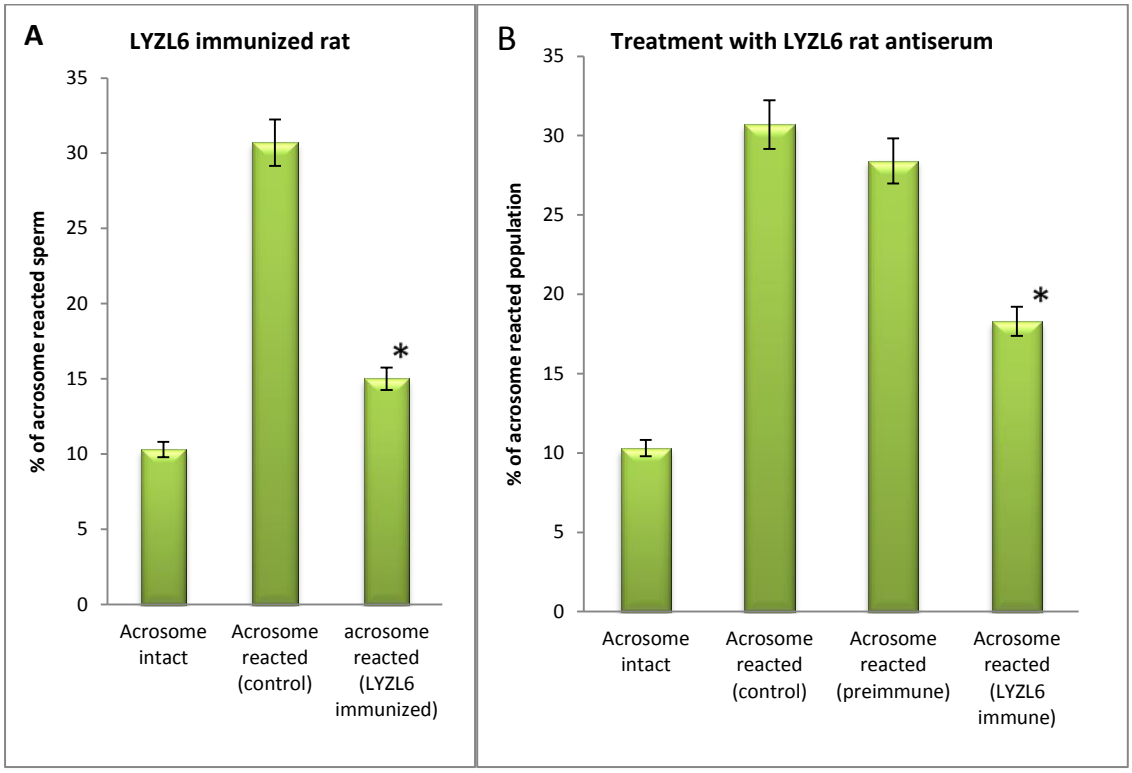

Figure 3.21: FACS analysis of acrosome reaction. *(A) % population of acrosome reacted spermatozoa obtained from* LYZL6 *immunized rat. (B)- % population of acrosome reacted spermatozoa after incubation with* LYZL6 *rat antiserum. Values are the mean+ SD. * indicates P<0.05 compared to acrosome reacted control.*

Fertility studies

Fertility status of the LYZL6 immunized rats were assessed by mating experiments (Table 12). Each immunized rat was mated with three female rats. The average litter size of the control animals was 11, whereas the same was around 3 in LYZL6 rats.

Table 12: Fertility assessment of LYZL6 immunized animals

Immunized male	Females	1st mating No. of pups	Average litter size	2nd mating No. of pups	Average litter size
Control	1	12	11	12	11
	2	10		11	
	3	11		10	
Rat 1	1	10	5.6	7	2.3
	2	7		0	
	3	0		0	
Rat 2	1	7	4.3	6	2
	2	6		0	
	3	0		0	
Rat3	1	0	0	0	0
	2	0		0	
	3	0		0	
Rat 4	1	0	0	0	0
	2	0		0	
	3	0		0	

It is surprising to note that some of the females did not have any litter. The number of animals that did not have pups increased after second mating, the time at which the antibody titer is higher than the previous mating. . Decreased fertility was observed as the antibody titer increased suggesting that with increase in the antibody titre more LYZL6 is neutralized, thus impairing the fertility.

DISCUSSION

Although there are many proteins that are specifically expressed in male reproductive tract, only some of them have an important role in reproductive function. Examples include CRISP1 (Sivashanmugam et al. 1999), ARP (Cohen et al. 2001), Sept4 (Kissel et al. 2005) and Tektin 3 (Roy et al. 2009) etc. Deciphering the functional role of male reproductive tract specific protein is an active area of interest primarily to develop male contraceptives. Hence, novel proteins are being identified and their role in sperm function analysed. In this part of the study we report the functional characterization of rat LYZL proteins with specific reference to male reproduction.

Neutralization of LYZL4 or LYZL6 by adding immune serum inhibited calcium influx, a vital event during capacitation. SPINKL, a serine protease inhibitor Kazal-type-like protein inhibits capacitation in murine spermatozoa (Tseng et al. 2013). SPINKL acts by blocking extracellular calcium ion influx into the spermatozoa, cholesterol efflux from sperm membrane and increase in intracellular cAMP. It is believed that SPINKL may act as an uncapacitation factor, inorder to prevent precocious capacitation and subsequent acrosome reaction. It is possible that LYZL4 or LYZL6 may also have similar function. On the other hand recombinant LYZL proteins did not exhibit any effect on sperm function and these proteins when added externally may not exhibit the same effect than when bond to sperm surface .

Capacitation leads to cholesterol efflux from the sperm membrane and a change in protein to cholesterol ratio, thereby causing increase in membrane fluidity. It is also possibly related to membrane ion transportation and membrane fusion. BSA which is a component of cell culture media and cellular fluid is present in the capacitation medium and it acts as a inducer for cholesterol efflux (Osheroff et al. 1999). Antibodies to FA-1 present in the semen acts as

inhibitor for tyrosine phosphorylation (Menge et al. 1999). Cholesterol efflux from spermatozoal membrane was examined in the spermatozoa treated with antisera against LYZL4 and LYZL6 or the recombinant proteins. We observed that addition of LYZL4 or LYZL6 anti-serum (thus neutralizing LYZL4 or LYZL6 on sperm) did not affect cholesterol efflux. Similarly no difference was observed in cholesterol efflux on addition of recombinant LYZL4 or LYZL6 proteins. This indicates that the LYZL proteins may not be involved in events that lead to cholesterol dynamics during sperm capacitation

Phosphorylation is one of the post-translational regulatory events that occur in many cells inorder to control the signalling cascade. The spermatozoa which emerges from testes is translationally inactive to greater extent and depends on the microenvironment and post translational modifications for its functioning (Kleene 1996). Tyrosine phosphorylation of sperm proteins is an important event that occurs during capacitation (Lewis & Aitken 2001). The effect of neutralizing LYZL4 or LYZL6 by the addition of corresponding antiserum on tyrosine phosphorylation was examined by Western blotting. Pre-incubating spermatozoa with LYZL4 or LYZL6 did not inhibit tyrosine phosphorylation. On the other hand, we did not observe enhanced tyrosine phosphorylation when the spermatozoa were preincubated with recombinant LYZL4 or LYZL6. The role of sperm bound proteins in tyrosine phosphorylation was reported. For example the Sp32, the proacrosin binding protein seems to undergo tyrosine phosphorylation during capacitation (Dubé et al. 2005). Testis specific protein kinase A (PKA) catalytic subunit $C\alpha_2$ is involved in tyrosine phosphorylation of the proteins (Lefièvre et al. 2002); (Nolan et al. 2004). Spermatozoa lacking functional PKAC are unable to undergo tyrosine phosphorylation and thereby capacitation. As most of the tyrosine phosphorylated proteins are present in tail part of the sperm, inhibition of PKA caused loss of hyperactivation which is hallmark of capacitation (Baker et al. 2009). Treatment of spermatozoa with FA-1 monoclonal antibody also resulted in reduced tyrosine

phosphorylation (Naz & Rajesh 2004). Though LYZL4 or LYZL6 are reported to be localised on the sperm surface, they seem to not have a role in the tyrosine phosphorylation during capacitation.

Exocytosis of acrosome to release its vesicular contents (enzymes) to facilitate penetration of sperm into cumulus layer is referred as acrosome reaction. SABP, seminal plasma secretory actin binding protein inhibits acrosome reaction by binding to actin; and its higher level expression in the seminal plasma correlated with infertility (Capková et al. 2007). In this study we analysed the role of LYZL4 and LYZL6 in acrosome reaction by either treating the spermatozoa with LYZL4 or LYZL6 recombinant protein or by incubating with their corresponding antiserum. Though addition of recombinant proteins did not affect acrosome reaction failure of acrosome reactions was observed when incubated with LYZL6 antiserum. This observation clearly demonstrates that the LYZL6 may be limited during sperm maturation

Treatment of spermatozoa with recombinant LYZL4 or LYZL6 did not influence capacitation and acrosome reaction. However, calcium influx during capacitation and acrosome reaction are inhibited when LYZL6 was neutralized by its antiserum. These results suggest that LYZL6 may have a role in both capacitation and acrosome reaction. Further its role seems to be confined only to calcium dynamics during capacitation, which is an indication of the event specific regulation by sperm protein in a multi-step process such as capacitation.

Blood testes barrier is responsible for the immune evasion of spermatozoa which generally do not allow passage of any immunocompetent cells to the systemic circulation. It is reported that accidental exposure of testicular or epididymal or spermatozoal proteins may cause autoimmune reaction resulting in immune infertility. Examples include YWK-II (Zhuang et al. 2006), TSA-1 (Trivedi & Naz 2002) , calpastatin (Liang et al. 1994) and zyxin (Bohring

2003). *In vitro* neutralization of the protein by adding antibody may not mimic the exact neutralization as the *in vivo* conditions are different. Therefore the auto antigen model helps in overcoming the drawback of *in vitro* studies, where antibody against self-protein is raised in the live animal. Presence of antibody against self-protein leads to neutralization of the protein and subsequently its function under *in vivo* conditions. Therefore such strategies can be used to study function of a protein whose distribution is well known. Similar studies were carried out earlier using this strategy. For example eppin an epididymal protein is found to be suitable for immunocontraception (Rand et al. 2011).

Wistar rats that are immunized with recombinant LYZL6, showed the presence of antibody in the serum and epididymal and testicular tissue fluids suggesting the auto-antigenic nature of LYZL6. Immunization study confirms that LYZL6 antibodies have inhibitory effect on calcium influx, cholesterol efflux, acrosome reaction and hypermotility of spermatozoa similar to YLP12, a peptide from ZP protein, which was reported to inhibit capacitation and acrosome reaction (Naz & Packianathan 2000). Anti-mouse sperm monoclonal antibody A-1 showed inhibitory effect against capacitation, acrosome reaction and calcium influx (Kawai et al. 2000).Treatment of sperm with antibodies against sperm agglutination antigen-1 (SAGA1) also showed similar effect where the motility of the sperms are compromised along with inhibition of penetration of zona free hamster (Diekman et al. 1997). However, morphological appearance of the tissues and the sperm did not show any significant abnormality suggesting that the antibodies did not affect the basic architecture related functions of the male reproductive tract organs. These results suggest that LYZL6 neutralization probably has impact on the earlier stages of capacitation. The results of the fertility assessment study performed by mating the immunized rats with control females showed decrease in fertility of the animal as the antibody titer increases in the animal, which may be due to inability of the spermatozoa to undergo capacitation. This suggests that

LYZL6 protein neutralization has far reaching consequences ultimately affecting the fertility of the animal. EPPIN a epididymal protease inhibitor is shown to have similar effects on immunization and it is trialled as immunocontraceptive in macaques (O'rand et al. 2004). Results of the current study were also similar suggesting to hypothesis that LYZL6 can be used as immunocontraceptive. Although in immunized animals, we could observe the compromise in capacitation parameters and acrosome reaction, *in vitro* fertilization studies would give clear picture on the role of LYZL antibodies in fertilization. Studies on restoration of fertile condition on unexposure to antigen would confirm the lasting effect of auto antibodies, which may further emphasize on LYZL6 as immunocontraceptive. In addition, future studies on silencing or knocking out of LYZL6 gene would help in finding out the exact mechanism of action of LYZL6 in fertilization.

REFERENCES

Baker, M.A. et al., 2009. Phosphorylation and consequent stimulation of the tyrosine kinase c-Abl by PKA in mouse spermatozoa; its implications during capacitation. *Developmental biology*, 333(1), pp.57–66.

Barboni, B. et al., 2011. Type-1 cannabinoid receptors reduce membrane fluidity of capacitated boar sperm by impairing their activation by bicarbonate. H. Wang, ed. *PloS one*, 6(8), p.e23038.

Bohring, C.W.K., 2003. Immune infertility: towards a better understanding of sperm (auto)-immunity: The value of proteomic analysis. *Human Reproduction*, 18(5), pp.915–924.

Brewer, L., Corzett, M. & Balhorn, R., 2002. Condensation of DNA by spermatid basic nuclear proteins. *The Journal of biological chemistry*, 277(41), pp.38895–900.

Cancel, A.M. et al., 2000. Objective evaluation of hyperactivated motility in rat spermatozoa using computer-assisted sperm analysis *. *Human Reproduction*, 15(6), pp.1322–1328.

Capková, J., Elzeinová, F. & Novák, P., 2007. Increased expression of secretory actin-binding protein on human spermatozoa is associated with poor semen quality. *Human reproduction (Oxford, England)*, 22(5), pp.1396–404.

Chapman, J.C. & Michael, S.D., 2003. Proposed mechanism for sperm chromatin condensation/decondensation in the male rat. *Reproductive biology and endocrinology*, 1(1), p.20.

Cohen, D.J. et al., 2001. Evidence that human epididymal protein ARP plays a role in gamete fusion through complementary sites on the surface of the human egg. *Biology of reproduction*, 65(4), pp.1000–5.

DasGupta, S., Mills, C.L. & Fraser, L.R., 1993. Ca(2+)-related changes in the capacitation state of human spermatozoa assessed by a chlortetracycline fluorescence assay. *Journal of reproduction and fertility*, 99(1), pp.135–43.

Diekman, A.B. et al., 1997. Biochemical characterization of sperm agglutination antigen-1, a human sperm surface antigen implicated in gamete interactions. *Biology of reproduction*, 57(5), pp.1136–44.

Dubé, C. et al., 2005. The proacrosin binding protein, sp32, is tyrosine phosphorylated during capacitation of pig sperm. *Journal of andrology*, 26(4), pp.519–28.

Ellerman, D.A. et al., 1998. Potential Contraceptive Use of Epididymal Proteins : Immunization of Male Rats with Epididymal Protein DE Inhibits Sperm Fusion Ability. *Biology of Reproduction*, 1036(59), pp.1029–1036.

Gur, Y. & Breitbart, H., 2008. Protein synthesis in sperm: dialog between mitochondria and cytoplasm. *Molecular and cellular endocrinology*, 282(1-2), pp.45–55.

Jaiswal, B.S. & Eisenbach, M., 1999. Detection of partial and complete acrosome reaction in human spermatozoa : which inducers and probes to use ? *Molecular human reproduction*, 5(3), pp.214–219.

Kawai, Y. et al., 2000. Anti-mouse sperm monoclonal antibody, A-1, inhibits sperm capacitation, acrosome reaction and calcium influx into spermatocytes. *Biological & pharmaceutical bulletin*, 23(8), pp.922–5.

Kissel, H. et al., 2005. The Sept4 septin locus is required for sperm terminal differentiation in mice. *Developmental cell*, 8(3), pp.353–64.

Kleene, K.C., 1996. Patterns of translational regulation in the mammalian testis. *Molecular reproduction and development*, 43(2), pp.268–81.

Lee, M.A. et al., 1987. Capacitation and acrosome reactions in human spermatozoa monitored by a chlortetracycline fluorescence assay. *Fertility and sterility*, 48(4), pp.649–58.

Lefièvre, L. et al., 2002. Activation of protein kinase A during human sperm capacitation and acrosome reaction. *Journal of andrology*, 43(5), pp.709–16.

Lewis, B. & Aitken, R.J., 2001. Impact of epididymal maturation on the tyrosine phosphorylation patterns exhibited by rat spermatozoa. *Biology of reproduction*, 64(5), pp.1545–56.

Liang, Z.G. et al., 1994. Human testis cDNAs identified by sera from infertile patients: a molecular biological approach to immunocontraceptive development. *Reproduction, fertility, and development*, 6(3), pp.297–305.

Lin, Y. et al., 1994. A hyaluronidase activity of the sperm plasma membrane protein PH-20 enables sperm to penetrate the cumulus cell layer surrounding the egg. *The Journal of cell biology*, 125(5), pp.1157–63.

Mandal, A. et al., 2005. Mouse SLLP1 , a sperm lysozyme-like protein involved in sperm – egg binding and fertilization. *Developmental biology*, 284(1), pp.126–142.

Mandal, A. et al., 2003. SLLP1, a unique, intra-acrosomal, non-bacteriolytic, c lysozyme-like protein of human spermatozoa. *Biology of reproduction*, 68(5), pp.1525–37.

Mendoza, C. et al., 1992. Distinction between true acrosome reaction and degenerative acrosome loss by a one-step staining method using Pisum sativum agglutinin. *Journal of reproduction and fertility*, 95, pp.755–763.

Menge, A.C. et al., 1999. Fertilization antigen-1 removes antisperm autoantibodies from spermatozoa of infertile men and results in increased rates of acrosome reaction. *Fertility and sterility*, 71(2), pp.256–60.

Naz, R.K. & Dhandapani, L., 2010. Identification of human sperm proteins that interact with human zona pellucida3 (ZP3) using yeast two-hybrid system. *journal of reproductive immunology*, 84(1), pp.24–31.

Naz, R.K. & Packianathan, J.L., 2000. Antibodies to human sperm YLP12 peptide that is involved in egg binding inhibit human sperm capacitation/acrosome reaction. *Archives of andrology*, 45(3), pp.227–32.

Naz, R.K. & Rajesh, P.B., 2004. Role of tyrosine phosphorylation in sperm capacitation / acrosome reaction. *Reproductive biology and endocrinology*, 2(1), p.75.

Nolan, M.A. et al., 2004. Sperm-specific protein kinase A catalytic subunit Calpha2 orchestrates cAMP signaling for male fertility. *Proceedings of the National Academy of Sciences of the United States of America*, 101(37), pp.13483–8.

O'rand, M.G. et al., 2004. Reversible immunocontraception in male monkeys immunized with eppin. *Science*, 306(5699), pp.1189–90.

Osheroff, J.E. et al., 1999. Regulation of human sperm capacitation by a cholesterol efflux-stimulated signal transduction pathway leading to protein kinase A-mediated up-regulation of protein tyrosine phosphorylation. *Molecular human reproduction*, 5(11), pp.1017–26.

Rand, M.G.O. et al., 2011. Functional studies of eppin. *Biochemical Society transactions*, 39(1), pp.1447–1449.

Rathi, R. et al., 2001. Evaluation of In Vitro Capacitation of Stallion Spermatozoa. *Biology of Reproduction*, 65(2), pp.462–470.

Republic, S., 2008. Computer assisted semen analysis of rat spermatozoa after an intraperitoneal administratin of insecticide diazinon. *Zoology and biotechnology*, 41(1), pp.802–806.

Roy, A. et al., 2009. Tektin 3 is required for progressive sperm motility in mice. *Molecular reproduction and development*, 76(5), pp.453–9.

Sachdev, M. et al., 2012. Oocyte speci fi c oolemmal SAS1B involved in sperm binding through intra-acrosomal SLLP1 during fertilization. *Developmental Biology*, 363(1), pp.40–51.

Shadan, S. et al., 2004. Cholesterol Efflux Alters Lipid Raft Stability and Distribution During Capacitation of Boar Spermatozoa 1. *Biology of reproduction*, 71(1), pp.253–265.

Sivashanmugam, P. et al., 1999. Cloning and characterization of an androgen-dependent acidic epididymal glycoprotein/CRISP1-like protein from the monkey. *Journal of andrology*, 20(3), pp.384–93.

Sun, R. et al., 2011. Lyzl4 , a novel mouse sperm-related protein , is involved in fertilization. *Acta biochimica et biophysica sinica*, 3(1), pp.1–8.

Trivedi, R.N. & Naz, R.K., 2002. Testis-specific antigen (TSA-1) is expressed in murine sperm and its antibodies inhibit fertilization. *American journal of reproductive immunology (New York, N.Y. : 1989)*, 47(1), pp.38–45.

Tseng, H.-C. et al., 2013. Mechanisms underlying the inhibition of murine sperm capacitation by the seminal protein, SPINKL. *Journal of cellular biochemistry*, 114(4), pp.888–98.

Vetter, C.M. et al., 1998. Comparison of motility and membrane integrity to assess rat sperm viability. *reproductive toxicology*, 12(2), pp.105–114.

Wang, S. et al., 2011. Phosvitin Plays a Critical Role in the Immunity of Zebrafish Embryos via Acting as a Pattern Recognition Receptor and an. *The journal of biological chemistry*, 286(25), pp.22653–22664.

Wang, Z. et al., 2004. The spermatozoa protein, SLLP1, is a novel cancer-testis antigen in hematologic malignancies. *Clinical cancer research : an official journal of the American Association for Cancer Research*, 10(19), pp.6544–50.

Ward, C.R. & Storey, B.T., 1984. Determination of the time course of capacitation in mouse spermatozoa using a chlortetracycline fluorescence assay. *Developmental biology*, 104(2), pp.287–96.

Wei, J. et al., 2013. Characterisation of Lyzls in mice and antibacterial properties of human LYZL6. *Asian Journal of Andrology*, 14(6), pp.834–830.

Yamagata, K. et al., 1998. Acrosin accelerates the dispersal of sperm acrosomal proteins during acrosome reaction. *The Journal of biological chemistry*, 273(17), pp.10470–4.

Zanetti, S.R. et al., 2010. Biochimie Differential involvement of rat sperm choline glycerophospholipids and sphingomyelin in capacitation and the acrosomal reaction. *Biochimie*, 92(12), pp.1886–1894.

Zaneveld, L.J. et al., 1991. Human sperm capacitation and the acrosome reaction. *Human reproduction (Oxford, England)*, 6(9), pp.1265–74.

Zhang, J. et al., 2010. The effect of anti-eppin antibodies on ionophore A23187-induced calcium influx and acrosome reaction of human spermatozoa. *Human Reproduction*, 25(1), pp.29–36.

Zhang, K. et al., 2005. Molecular Cloning and Characterization of Three Novel Lysozyme-Like Genes , Predominantly Expressed in the Male Reproductive System of Humans , Belonging to the C-Type Lysozyme / Alpha-Lactalbumin Family 1. *Biology of reproduction*, 1071(73), pp.1064–1071.

Zhuang, D. et al., 2006. YWK-II protein/APLP2 in mouse gametes: potential role in fertilization. *Molecular reproduction and development*, 73(1), pp.61–7.

SUMMARY

SUMMARY

Objective 1: Molecular characterization of rat lysozyme like proteins *in silico*

Using *in silico* approaches, we identified six rat *Lyzl* genes namely *Lyzl1*, *Lyzl3*, *Lyzl4*, *Lyzl5*, *Lyzl6* and *Lyzl7*. *Lyzl4* sequence was reported to GenBank. *In silico* studies showed that LYZL proteins are similar to c-type lysozyme. *Lyzl* genes were found to be highly conserved among the vertebrates and are highly homologous to mouse counterparts than with human counterparts. All the LYZL proteins possess the characteristic 4 disulphide bridges similar to that preserved in c-type lysozyme. These proteins are very closely related to each other in sequence similarity, biochemical and structural aspects. LYZL proteins are amphipathic and secretory in nature. Although they are very similar to lysozyme, except for LYZL 1 and 6, the remaining proteins do not conserve the active site amino acids. Molecular modeling studies indicated that LYZL proteins exhibit strikingly similar three dimensional structures among themselves. Docking studies indicated the peptidoglycan binding nature of LYZL proteins. Presence of active site and peptidoglycan binding ability of LYZL1 and 6 suggest that they may be involved in antibacterial mechanism.

Objective 2: Expression profiling and biochemical characterization of rat lysozyme-like proteins

All the rat *Lyzl* mRNA transcripts (*Lyzl1*, *Lyzl3*, *Lyzl4*, *Lyzl5*, *Lyzl6* and *Lyzl7)* are predominantly expressed in testes though some of them are expressed in tissues other than reproductive tract. Their expression is androgen independent. The rat LYZL proteins are localized in the germinal epithelium and on the spermatozoa. Recombinant LYZL1 and 6 possessed muramidase, isopeptidase and antibacterial activities, whereas the remaining

proteins did not, which may be attributed to the absence of active sites. The mechanism of antibacterial action of LYZL1 and LYZL6 involved bacterial membrane damage and leakage of cellular contents. Only LYZL1 and 6 possess peptidoglycan biding ability, whereas LYZL3, LYZL4 and LYZL5 possess hyaluronan binding ability suggesting a possible functional divergence of these proteins. In addition LYZL3, LYZL4 and LYZL7 possessed free radical scavenging property, suggesting that they may act as antioxidants. The secondary structure analysis of the recombinant LYZL proteins indicated the presence of α-helix, β-sheet and random coil with α-helix being the majority.

Objective 3: Functional characterization of rat lysozyme-like proteins

The role of LYZL proteins in sperm function was studied by neutralizing these proteins on sperm surface using specific antibodies. *In vitro* neutralization of LYZL4 did not affect capacitation or acrosome related events. Whereas, neutralization of LYZL6 showed an inhibitory effect on calcium influx during capacitation and acrosome reaction. Treatment of spermatozoa with LYZL4 or 6 recombinant proteins did not influence capacitation or acrosome reaction. The importance of LYZL proteins in germ cell production and maturation *in vivo* was studied using an auto-antigen model generated by injecting recombinant rat LYZL6 into rats. Antibody against LYZL6 was detected in male reproductive tissue fluids confirming the passage of antibody through the blood testes barrier. In the immunized rats, the male reproductive tissue architecture was not affected but, resulted in decreased sperm count. Further, decrease in sperm motility parameters was also observed. LYZL6 immunized animals showed decreased fertility depicting the potential role played by this protein in male reproduction.

Identification of Toll-Like Receptors in the Rat (Rattus norvegicus): Messenger RNA Expression in the Male Reproductive Tract Under Conditions of Androgen Variation

Barnali Biswas[1], Ganapathy Narmadha[1], Mithilesh Choudhary[1], Frank S. French[2], Susan H. Hall[2], Suresh Yenugu[1]

[1]Department of Animal Sciences, University of Hyderabad, Hyderabad, Andhra Pradesh, India;
[2]Laboratories for Reproductive Biology, Department of Pediatrics, University of North Carolina, Chapel Hill, NC, USA

Keywords
Androgens, castration, epididymis, Toll-like receptor

Correspondence
Dr. Suresh Yenugu, Department of Animal Sciences, University of Hyderabad, P.O. Central University, Hyderabad 500046, India.
E-mail: ysnaidu@yahoo.com

Submitted June 4, 2009;
accepted July 9, 2009.

Citation
Biswas B, Narmadha G, Choudhary M, French FS, Hall SH, Yenugu S. Identification of toll-like receptors in the rat (Rattus norvegicus): messenger RNA expression in the male reproductive tract under conditions of androgen variation. Am J Reprod Immunol 2009

doi:10.1111/j.1600-0897.2009.00732.x

Problem
Although the majority of Toll-like receptors (TLRs) are reported in many species, some of them are not yet described in the rat. Further, factors that govern *Tlr* expression in the male reproductive tract have received little attention. We attempt to identify and characterize *Tlr*s in the rat and determine the expression profile under conditions that affect male reproductive tract gene expression.

Method of study
Rat *Tlr5, Tlr10,* and *Tlr11* transcript sequences were submitted to GenBank and *in silico* characterization carried out using bioinformatics tools. RT-PCR analyses using gene specific primers for rat *Tlr1–13* were carried out with RNA isolated from reproductive tract tissues of various experimental groups.

Results
Tlr5, Tlr10, and *Tlr11* identified in this study share features that are characteristic of the known TLRs. Abundant *Tlr* expression was observed in the male reproductive tract of adult and developing rats. Further, *Tlr* expression was also observed in the epididymides of androgen ablated rats.

Conclusion
Tlr5, Tlr10, and *Tlr11* are ubiquitously expressed in the rat. *Tlr*s seem to be expressed during male reproductive tract development and under conditions of androgen ablation, suggesting the preparedness of the male reproductive tract to detect an infection under all conditions of androgen status.

Introduction

The epithelial surfaces of many organs such as the respiratory, reproductive, and digestive systems are exposed to the external environment and are constantly under threat from invading pathogenic microorganisms. Innate immune mechanisms that exist in the body counter these microbial infections. In most organ systems, the presence of complex infection-driven signaling pathways is very well established. The ability of innate systems to recognize and respond to these attacks is largely mediated by a family of type I transmembrane receptors called Toll-like receptors (TLRs).[1,2] They are primarily

© 2009 John Wiley & Sons A/S

expressed on many cell types and have the ability to discriminate and recognize distinct microbial components. Recognition of microbial products by TLRs triggers a variety of signal transduction pathways that differ in nature, magnitude and duration of the inflammatory response.[3] The TLR family consists of 13 members (TLR1–13) that are widely expressed in most of the vertebrate species. Among them TLR1–10 have been identified in humans and the remaining three are confined to rodents.[4] Although the majority of TLRs are reported in many species, TLR5, TLR10, and TLR11 have not been reported in the rat.

Each TLR has been shown to recognize specific components of pathogens. For example, TLR4 recognizes lipopolysaccharide, whereas TLR2 is specific for microbial lipopeptides such as peptidoglycan, lipoteichoic acid, and porins.[5] Recognition of specific cell wall components by TLRs triggers a cascade of events involving a variety of adaptor proteins and protein kinases, finally resulting in the activation of immune response genes.[6,7] Genes that are targeted include those encoding cytokines such as tumor necrosis factor-alpha, interleukin-12p40, interferon-beta, chemokines, adhesion molecules, acute phase proteins, antimicrobial peptides, inducible nitric oxide synthase, and cyclooxygenase 2.[6] Production of proinflammatory cytokines during an inflammatory response is very important for mediating the initial host defense against invading pathogens and opportunistic organisms.[8] They collectively provide immediate protection for hosts and induce the development of adaptive immune responses as well.

Infections of the male reproductive tract can pose a threat to normal reproductive and endocrine functions. Epididymitis, a serious clinical condition characterized by inflammation and obstruction of sperm movement, results from the retrograde extension of micro-organisms from the vas deferens. Infection of the epididymis can lead to the formation of an epididymal abscess. In addition, progression of the infection can lead to involvement of the testicle, causing epididymoorchitis or a testicular abscess.[9,10] The general causative agents of epididymitis are *Escherichia coli, Chlamydia trachomatis*, and *Neisseria. gonorrhea.* Similar to other systems, infection of the male reproductive tract is expected to potentiate immune response via the activation of immune receptors, finally resulting in the induction of many genes including the antimicrobial proteins and peptides.

In the recent past, mechanisms involved in the innate immune responses of the male reproductive tract have become an active area of investigation. For example, the expression of antimicrobial proteins and peptides including defensins has been extensively characterized in the male reproductive tract.[11–13] The expression of lipopolysaccharide-binding protein, an acute phase protein known to play a central role in defense against Gram-Negative bacteria, was demonstrated in the human epididymis.[14] Further, CD14, a 54 kDa glycolipid-anchored membrane glycoprotein, expressed on myeloid cells, which functions as a member of the LPS receptor complex, was demonstrated in the seminal plasma and also on the sperm membranes.[15] A recent study reported the presence of *Tlr1–11* and some of their adaptors in the male reproductive tract of rats.[16] Although, majority of TLRs are reported in the rat, TLR5, TLR10, and TLR11 are not. Further, TLR12 and TLR13 have not been characterized in the male reproductive tract of this species. Hence, *in silico* and *in vivo*, analyses were carried out in this study to identify and characterize *Tlr5*, *Tlr10*, and *Tlr11*. Further, the male reproductive tract specific expression profiles of all previously reported *Tlr*s besides *Tlr12* and *Tlr13* in the rat were also studied. Gene expression in the male reproductive tract is dependent on tissue levels of androgens[17] that are known to change during development. As very little is known about the factors (such as androgens) that may affect *Tlr* expression in the male reproductive tract, attempts were made to characterize the expression profile of all known *Tlr*s under conditions of androgen variation. In this study, we identified and characterized three *Tlr*s, namely, *Tlr5*, *Tlr10*, and *Tlr11* in the rat. Further, we demonstrate that majority of the *Tlr*s analyzed are abundantly expressed in the male reproductive tract of adult and developing rats and also under conditions of androgen ablation.

Materials and methods

Genomics

Using mouse *Tlr5*, *Tlr10*, and *Tlr11* sequence, the rat genome (build RGSC v3.4) was searched using the BLAST program at the NCBI website (http://blast.ncbi.nlm.nih.gov/Blast.cgi), to identify the rat orthologs. Five to six sets of intron spanning primers (Table S1) were designed for each *Tlr* mRNA so that the entire sequence can be amplified in parts. RT-

© 2009 John Wiley & Sons A/S

PCR was performed using rat epididymis mRNA as the template. The specific products were sequenced, aligned and deposited in GenBank. The corresponding exon/intron boundaries were determined by aligning the cDNA with the genomic sequence. The sequences were translated using the tools available at ExPASy proteomics server (http://ca.expasy.org/tools/dna.html). *In silico*, domain analyses were carried out using the InterProScan, a signature recognition search against the integrated resource of protein domains and functional sites (http://www.ebi.ac.uk/Tools/InterProScan). The physical and predicted features of the deduced amino acid sequences were analyzed using tools available at Expasy Proteomics Server (http://ca.expasy.org/).

Table I Gene Specific Primers Used in This Study

Primer name	Sequence	Amplicon size
Tlr1 F	5′-TCT TAC CCT GAA CAA CGT GGA CAC-3′	284
Tlr1 R	5′-AAG CAT GTG GAC CAT GCG TGT TC-3′	
Tlr2 F	5′-CGC TTC CTG AAC TTG TCC AGT ACA G-3′	284
Tlr2 R	5′-GGT TGT CAC CTG CTT CCA GAG TCT C-3′	
Tlr3 F	5′-TGC ACG AAC CTG ACA GAG CTC CAT-3′	357
Tlr3 R	5′-GCT TCT CTG TGA GGT TGA GGT TCA G-3′	
Tlr4 F	5′-GAG ACC AGG AAG CTT GAA TCC CTG C-3′	345
Tlr4 R	5′-TGT CTC CAC AGC CAC CAG ATT CTC-3′	
Tlr5 F	5′-GCC AGA GCC AGA TTG AAG TCT TGA-3′	272
Tlr5 R	5′-GAG AGG CTG GAG TTC ATC TTC ACA-3′	
Tlr6 F	5′-GGT GTG TTC TTG CTC AAT CGG GAC-3′	257
Tlr6 R	5′-CAC CAA GTC CAG AAG AAC ACA GCT C-3′	
Tlr7 F	5′-CTC TCG ATA GCA CAA ACA CCC ATG-3′	263
Tlr7 R	5′-AGA GTC CAC TAA AGC TTC CAG GTC-3′	
Tlr8 F	5′-CCA GAG TCT TCC AAA CTT GGC AAC-3′	277
Tlr8 R	5′-CAA GGC CTT GCC ATA AGC AGT ACA-3′	
Tlr9 F	5′-CAT GCT GGA AGA GCT GAA CCT GAG-3′	300
Tlr9 R	5′-TAT AGG ACA GCA GGA GGT ACT CCA G-3′	
Tlr10 F	5′-GAA CTC TAT CTG GCC CAC CAC AAT-3′	276
Tlr10 R	5′-AAC CTT GGC AAT CCG CGT TAG GCT T-3′	
Tlr11 F	5′-CTC TGA TGT CAC CTT TAC TTG CCA G-3′	272
Tlr11 R	5′-AGA GGT GAT GAA GCC AGG ACC ATT-3′	
Tlr12 F	5′-GCC CAT GTA TCT GAC CAG CTT AGA G-3′	261
Tlr12 R	5′-ACT GAA GTT TGG GGA GCT GCC AGA-3′	
Tlr13 F	5′-GGA TTC AGG TTG TTC CGA GCA ACT-3′	264
Tlr13 R	5′-AGC TGG AGA ACA TGT CAG GAA CCA-3′	
Gapdh F	5′-AGA CAG CCG CAT CTT CTT GT-3′	268
Gapdh R	5′-CTT GCC GTG GGT AGA GTC AT-3′	

Tissue Specimens and RT-PCR

Wistar rat (aged 60–90 days; $n = 3$) tissues were obtained commercially (Zivic Laboratories Inc, Pittsburgh, PA, USA). Prior to shipping on dry ice, tissues were placed in RNA*Later* (Ambion Inc, Austin, TX, USA) solution overnight at 4°C to allow penetration and fixation. Upon arrival, tissues were immediately stored at −70°C. Total RNA was extracted using the TRIzol reagent (Invitrogen, Carlsbad, CA, USA) from the following tissues: caput, corpus, cauda, testis, and seminal vesicle. Total RNA (2 μg) was reverse transcribed using 50 U Stratascript (Stratagene, La Jolla, CA, USA) and 0.5 μg of oligodT (Invitrogen) according to the manufacturer's instructions. A total of 2 μL of the resultant cDNA was amplified by PCR using gene specific primers (Table I) for *Tlrs1–13*. The number of cycles to amplify each cDNA in the linear range was determined by preliminary PCR under the following conditions: 94°C for 1 min followed by 25–35 cycles at 94°C for 30 s, 58°C for 30 s and 72°C for 30 s, and with a final round of extension at 72°C for 10 min. *Tlr*s were amplified using gene specific primers (Table I) for 28–32 cycles and glyceraldehyde phosphate dehydrogenase (*Gapdh*) for 28 cycles. PCR amplified gene products were analyzed by electrophoresis on 2% agarose gels. *Gapdh* expression was used as the internal control. To study the androgen regulation of *Tlr* transcripts, epididymides were obtained from sham operated, castrated and testosterone supplemented Wistar rats ($n = 5$ in each group). Testosterone supplementation was supplied by a 20 mg dihydrotestosterone pellet implanted subcutaneously immediately after castration.[12] All the animals were killed 14 days after castration. All procedures involving animals were performed in accordance with the Guiding Principles in the Care and Use of Animals established by the National Institutes of Health and approved by the Institutional Committee on the use of Animals in Research and Education. For studies on the developmental regulation of *Tlr*s, epididymides from 10- to 60-day-old Wistar rats, one rat for each age, were obtained commercially (Zivic Laboratories Inc).

Results

Tlr5, Tlr10, and *Tlr11* transcripts were discovered on the rat chromosome 13, 14, and 15. The rat *Tlr5*, *Tlr10*, and *Tlr11* cDNA sequences were submitted to GenBank and were assigned the accession numbers FJ750588, FJ755908, and FJ539013 respectively. Expression sequence analysis revealed that *Tlr5* was localized at 13q26 region (Fig. 1a), whereas *Tlr10*

© 2009 John Wiley & Sons A/S

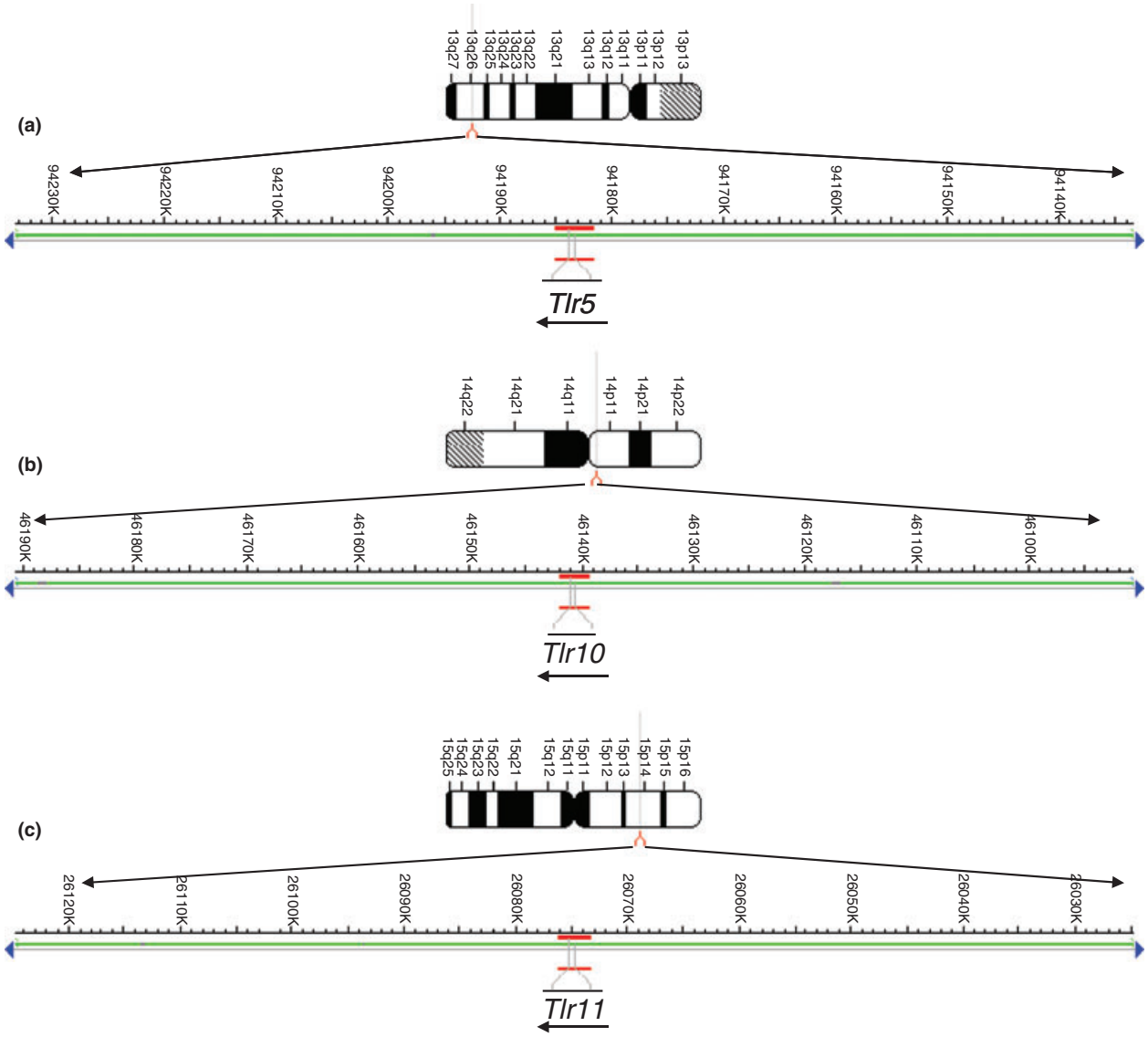

Fig. 1 Rat *Tlr* localization on chromosomes 13, 14, and 15. (a) *Tlr5* on chromosome 13; (b) *Tlr10* on chromosome 14; (c) *Tlr11* on chromosome 15. Arrows indicate direction of transcription. Positions were taken from the MapView (build 3.4) at the National Center for Biotechnology Information (NCBI) website.

was localized at 14p11 (Fig. 1b) and *Tlr11* is present at 15p14 (Fig. 1c). *In silico*, protein translation analyses revealed that single exon encodes the full-length protein. The alignment of rat genomic and protein *Tlr5*, *Tlr10*, and *Tlr11* sequences are shown in Fig. S1 Further analyses reveal that the predicted amino acid sequences of the three TLRs contain the leucine rich repeat (LRR) and Toll/interleukin-1 receptor (TIR) domains, characteristic of the known TLRs (Fig. 2). TLR5 in the rat is predicted to have five LRRs whereas TLR10 and TLR11 contain three LRRs each. Similar to the known TLRs, there is a single TIR domain, a signal peptide and a transmembrane domain in the rat TLR5, TLR10, and TLR11. Further, the cysteine-rich flanking region (CRFR) was found to be present on the C-terminal side of rat TLR5 and TLR10, whereas the same is absent in the rat TLR11 (Fig. 2). The general physical features of the TLRs identified in this study are given in Table II.

© 2009 John Wiley & Sons A/S

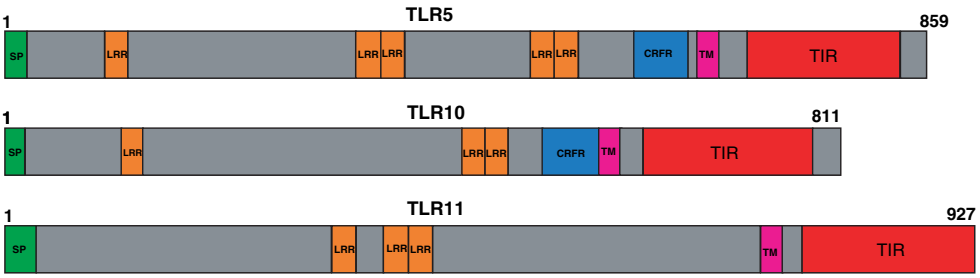

Fig. 2 Rat TLR5, TLR10, and TLR11 predicted domain structure. The predicted amino acid sequences were analyzed using InterProScan sequence search. Numbers indicate the length of the protein. Different domains are indicated in colors – signal peptide (green); LRR (orange); CRFR (blue); transmembrane domain (pink); TIR domain (red).

Table II Predicted General Characteristic Features of Rat TLR5, TLR10, and TLR11

	No. of amino acids	Molecular weight (Da)	Isoelectric point (pI)	Glycosylation sites	Phosphorylation sites			Myristilation sites	Amidation sites
					cAMP	PKC	CK2		
TLR5	859	98053.20	6.79	37, 46, 176, 245, 342, 437, 473, 596, 599, 624, 640	844, 845	48, 310, 379, 412, 571, 626, 701, 752, 806, 854	105, 153, 165, 171, 184, 310, 464, 578, 605, 626, 701	35, 78, 130, 202, 252, 266, 521, 545, 567, 751	842
TLR10	811	93407.93	6.50	33, 189, 330, 395, 427, 575, 778	488, 628	213, 233, 430, 467, 558, 623, 686, 689	51, 99, 115, 125, 178, 269, 290, 324, 32,467, 510, 623, 677, 684	148, 210, 282, 591, 765, 800	–
TLR11	927	105795.29	6.64	25, 46, 73, 117, 342, 362, 380, 396, 402, 506, 620, 699	529	119, 153, 178, 183, 527, 532, 595,625, 631, 639	32, 274, 318, 364, 443, 674, 779, 909	28, 90, 357, 394, 465, 805, 841	–

The male reproductive tract is generally a sterile environment and is not routinely exposed to pathogens as are the respiratory and gastrointestinal tracts. However, an exposure to pathogens would be expected to mount an immediate immune response to prevent any damage to the male reproductive tract and to fertility. To determine whether the male tract constitutively expresses the toll-like receptors of the innate immune machinery, the expression of *Tlr1–13* mRNAs was analyzed. Majority of the *Tlr* mRNA transcripts (*Tlr2, Tlr4, Tlr5, Tlr6, Tlr7, Tlr8, Tlr10,* and *Tlr11*) were found to be abundantly expressed in all tissues of the male reproductive tract (Fig. 3). However, *Tlr1* and *Tlr12* expression was only weakly detected in the male tract. *Tlr3* expression was mostly restricted to the caput with minimal expression in corpus, cauda, and testis (Fig. 3). Similarly *Tlr9* expression was primarily in the seminal vesicle (Fig. 3). To determine whether *Tlr5*, *Tlr10*, and *Tlr11* are ubiquitously expressed, RT-PCR was performed in a variety of tissues obtained from male and female rats. *Tlr5*, *Tlr10*, and *Tlr11* were found to be expressed in the non-reproductive as well as the female reproductive tract tissues in the rat (Fig. 4).

Gene regulation in the male reproductive tract is androgen dependent, which in turn varies with the developmental stage of the animal. To determine whether the innate immune machinery is regulated during the course of development, *Tlr* expression was analyzed in the epididymis, testis, and seminal

© 2009 John Wiley & Sons A/S

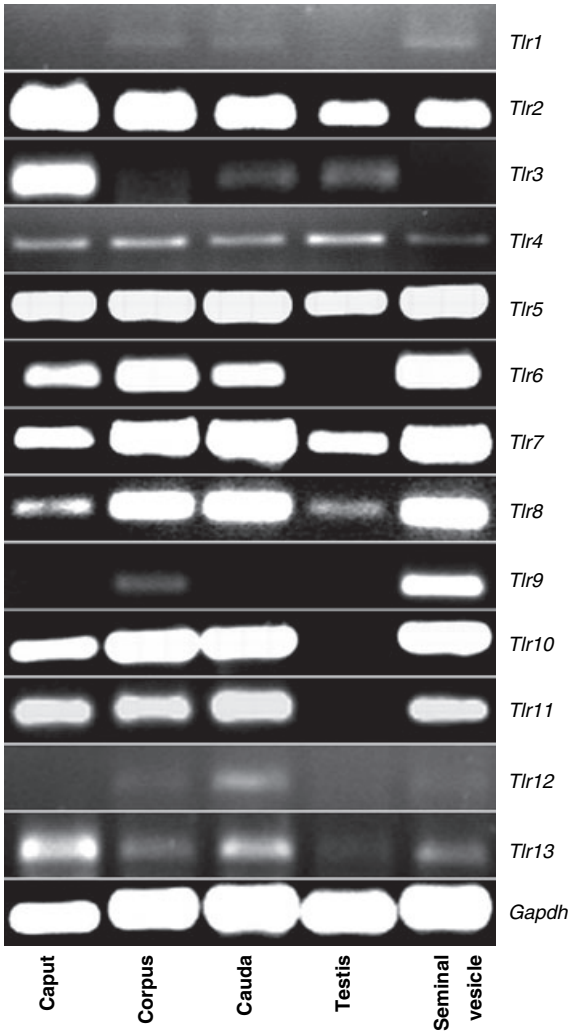

Fig. 3 *Tlr* expression in the rat male reproductive tract. Total RNAs isolated from caput, corpus, cauda, testis, and seminal vesicle were reverse transcribed and PCR amplified. *Gapdh* was used as the internal control.

vesicle of 10- to 60-day-old rats. In the epididymis, as seen in the adult rat, *Tlr1* seems to be not expressed abundantly during the course of the development (Fig. 5). The presence of *Tlr2, 4, 5, 6, 7, 8, 10, 11*, and *12* mRNA was observed at all the stages during development (Fig. 5). The expression of *Tlr3, 9*, and *13* was detected only in the epididymides obtained from 20-, 50-, and 60-day-old rats. An interesting feature is the presence of all the *Tlr* mRNA transcripts in the epididymides of 20- and 50-day-old rats (Fig. 5), suggesting a possible role for TLRs at 20- and 50-day time points during development, besides their role in innate immunity.

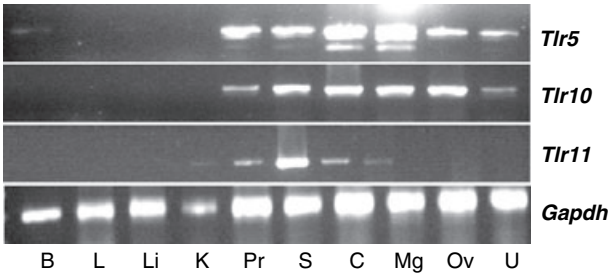

Fig. 4 Tissue distribution of *Tlr5*, *Tlr10*, and *Tlr11* in the rat. RT-PCR analysis was performed using total RNA isolated from Brain, Lung, Liver, Kidney, Prostate, Spleen, Cervix, Mammary gland, Ovary, Uterus. *Gapdh* was used as the internal control.

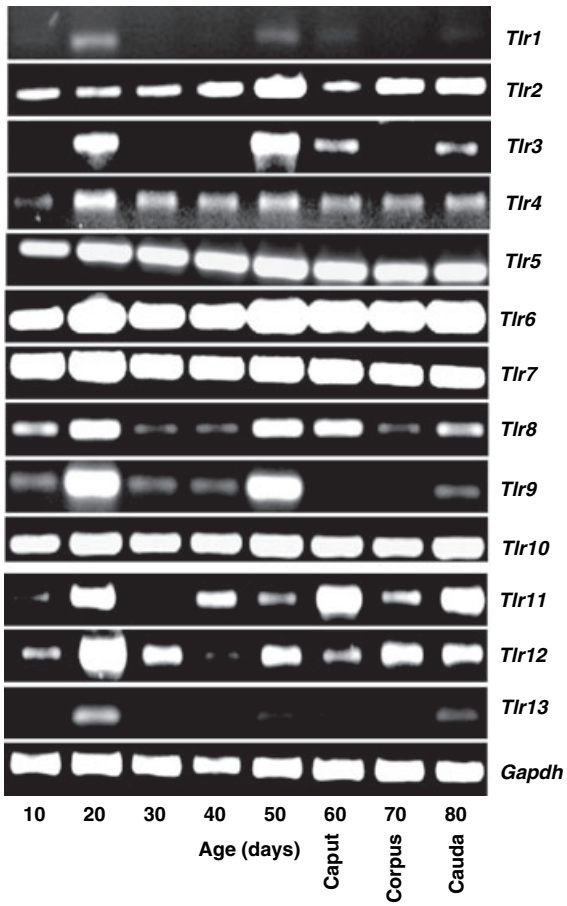

Fig. 5 Developmental regulation of *Tlr1–13* expression in the epididymides of 10- to 60-day rats. RT-PCR for *Tlr1–13* in RNA isolated from epididymides of rats aged 10–60 days.

In the testis, *Tlr5, 7, 8, 10, 11*, and *12* were found to be abundantly present in all the states during development (Fig. 6), whereas *Tlr1, 2, 4, 6, 9*, and *13*

© 2009 John Wiley & Sons A/S

were weakly expressed. *Tlr3*, although weakly expressed in the adult rat testes, was not detected in the testes of developing rats (Fig. 6).

In the seminal vesicle, *Tlr5, 7, 8, 10*, and *11* were found to be abundantly expressed at all the stages of development. However, *Tlr1, 4, 6*, and *9* expression was weak during the course of development (Fig. 7). *Tlr2* and *12* expression was detected in the later part of development, namely, in the seminal vesicles of 30- to 60-day-old rats. 'On the contrary, *Tlr13* mRNA expression was detected up to mid stage of development, i.e. in the seminal vesicles of 10- to 40-day-old rats. *Tlr3* mRNA expression was not detected in the seminal vesicles during the course of development.

To develop our understanding of the relation between androgen levels and immune receptor expression, *Tlr* mRNA levels were analyzed in the epididymides of rats that were either castrated or castrated and supplemented with testosterone (Fig. 8). Interestingly, *Tlr1* and *13* mRNA expression was detected abundantly in the castrated rats, whereas the same was weak in the sham operated and testosterone supplemented groups. Abundant expression of *Tlr2, 5, 6, 7, 8, 9 10, 11*, and *12* and weak expression of *Tlr3* and *Tlr4* was detected in all the three groups suggesting an androgen independent expression (Fig. 8).

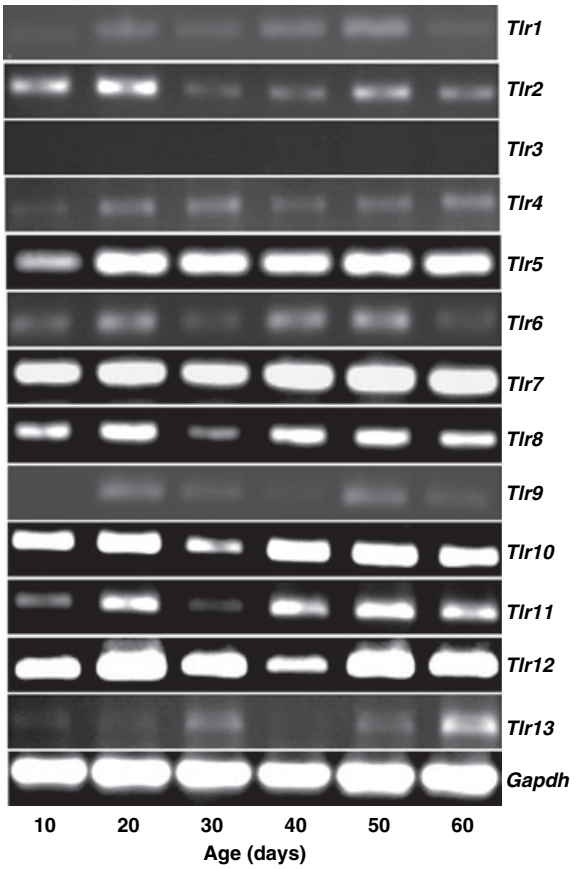

Fig. 6 Age-dependent regulation of *Tlr1–13* in the testes of 10- to 60-day rats. RNA from 10- to 60-day-old rat testes were isolated and reverse transcribed followed by PCR. *Gapdh* expression served as the internal control.

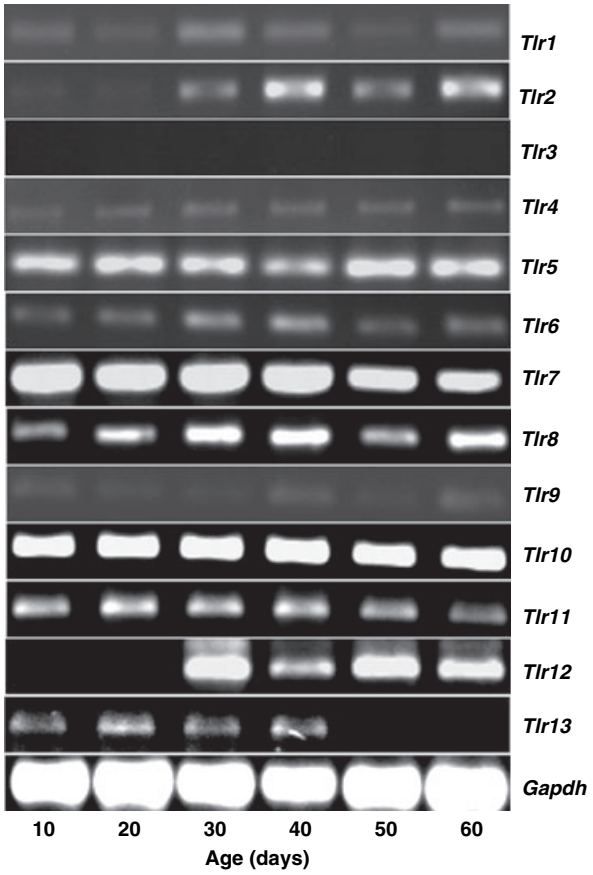

Fig. 7 *Tlr1–13* expression in the seminal vesicle of 10- to 60-day-old rats. RT-PCR analyses were carried out using RNA isolated from the seminal vesicles of rats aged 10–60 days.

Discussion

TLRs, which recognize the molecular patterns of pathogenic organisms, have been well characterized in many species. However, in the rat, not all have been characterized, and in this study we report the identification of rat *Tlr5*, *Tlr10*, and *Tlr11* transcripts.

© 2009 John Wiley & Sons A/S

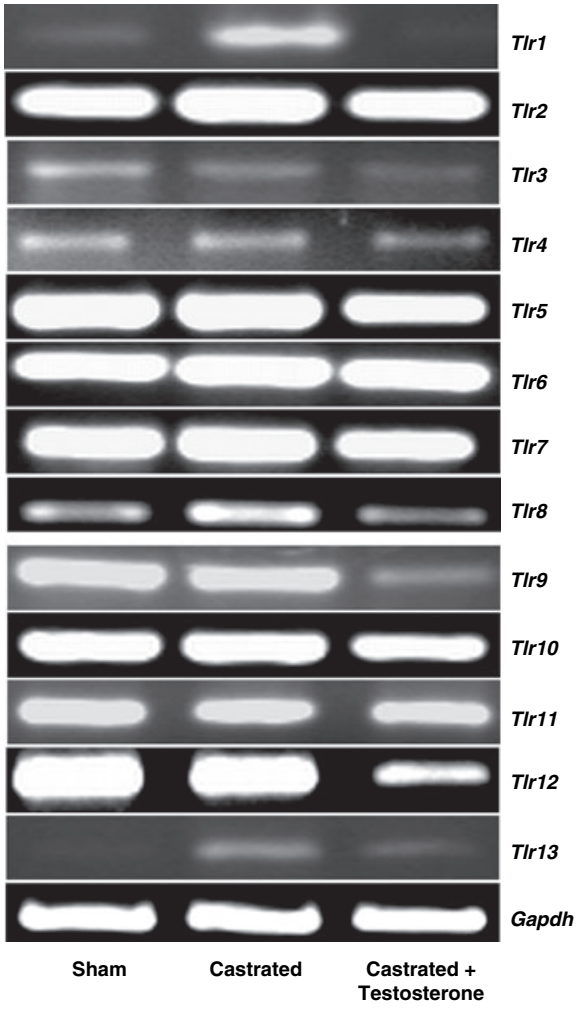

Fig. 8 Effect of androgen ablation on *Tlr1–13* expression in the epididymis. Rats (n = 5 for each group) were sham operated, castrated, or castrated and testosterone replaced immediately after castration. Epididymides were removed 14 days after castration. Gene expression was analyzed using RT-PCR with *Gapdh* as the internal control.

The presence of characteristic LRR and TIR domains in the predicted amino acid sequences of these TLRs suggests that they primarily function to detect pathogens thus sharing the functional features with the known TLRs.

Unlike the respiratory and digestive systems, which are constantly exposed to environmental agents including the pathogens, the male reproductive tract is sterile. Hence, this organ system should be able to initiate a heightened immune response to an infection. Studies on the role and the mechanism of action of innate immune molecules in protecting the male reproductive tract provide a basis for development of new strategies to treat sexually transmitted diseases. Toll-like receptors which form an important component of innate immunity have been implicated in many roles in the male and female reproductive tracts. In the male reproductive tract, TLRs appear to play a role in the control of testicular steroidogenesis and spermatogenesis both in normal and disease conditions.[18] The etiology of prostatitis and prostatic cancer seems to involve TLRs.[18] They have been shown to have a functional role in immune surveillance in the ovary, endometrium,[19,20] uterus,[21] and placenta.[22,23] Further, they are involved in ovarian cancer, pelvic inflammatory disease, intrauterine growth restriction, pre-eclampsia, and preterm birth.[18] A recent study demonstrates the abundance of TLRs in the male reproductive tract of rats.[16] However evidence is lacking in describing the regulation of TLRs in general in the male reproductive tract. Such evidence can provide insights into the role of these innate immune molecules during an infection. This study demonstrates the identification of three *Tlr*s namely *Tlr5*, *Tlr10*, and *Tlr11* in the rat. Further, the expression profile under conditions of androgen variation was also demonstrated, which was not reported in a previous study, wherein the presence of *Tlr*s in the male reproductive tract of rats was analyzed.

In this study, the abundant expression of the majority of TLRs suggests the preparedness of the male reproductive tract to respond to an infection. The presence of other innate molecules such as CD14[15] and MYD88[16] in the male tract along with the TLRs[24] strongly points to the fact that invasion by a pathogen might result in the activation of immune effector pathways that can trigger the production of cytokines and antimicrobial peptides. However, further studies are required to demonstrate the execution of such pathways and the repertoire of factors involved in the male reproductive tract. Abundant *Tlr3* expression was reported in contrast to the weak expression of *Tlr11* in the male reproductive tract.[16] However, by contrast we observed an abundant *Tlr11* and weak *Tlr3* expression. This discrepancy could be because of age and strains of the animals used. Further, male reproductive tract tissues analyzed in this study contain different cell types including the immune cells. It is possible that the expression of *Tlr*s in male reproductive tract tissues could partly be contributed by the immune cells.

© 2009 John Wiley & Sons A/S

Developmental regulation of a wide variety of genes in the male reproductive system has been studied extensively[17] because of the fluctuations of androgens at various stages. For example, rat epididymis tissue androgen decreases from birth until 20 days, but remains at a substantial level of approximately 10 ng/g tissue (35 nM) until approximately 40 days when it begins to increase to adult levels of between 15 and 20 ng/g.[25] Serum testosterone levels in the rat remain low and do not begin to increase to adult levels until 35–40 days.[26] The expression pattern of majority of *Tlr*s in the epididymis did not seem to correlate with the minimal androgen levels from day 20 to day 40 or increased androgen in the adult.[25] suggesting that *Tlr* expression is not androgen dependent during development. However, androgen concentration differs in the testis compared with the epididymis. A steady increase in testosterone levels was reported in the rete testis of 30- to 130-day-old rats.[27,28] In this study, abundant expression of *Tlr*s was detected in the testes of 10- to 60-day-old rats suggesting their constitutive nature of expression, thereby keeping the testes ready for any microbial challenge. Lack of *Tlr3* expression in the testes of developing rats (10–60 days old) is in contrast to its presence in the testes obtained from adult rats (60–90 days old). Conversely, *Tlr10, 11*, and *12* mRNA were detected in the testes developing rats (10–60 days old), whereas their expression was not detected in testes obtained from adult rats (60–90 days old). These discrepancies could be because of the age differences and actual levels of testicular testosterone at the time of tissue collection. Further analyses are required to determine whether *Tlr3, 10, 11*, and *12* expression could be drastically affected within a short window of time. Earlier studies indicate that androgens are important to the development and physiology of the prostate and seminal vesicle.[29,30] In the seminal vesicles of 10- to 60-day-old rats, *Tlr* expression was detected at all ages analyzed similar to the testes. Although testosterone is required for development, further studies are required to determine the role of testosterone on *Tlr* expression during development.

In conclusion, we report the identification of *Tlr5*, *Tlr10*, and *Tlr11* in the rat. The mRNA expression of *Tlr*s is abundant in the male reproductive tract of adult and developing rats. Their expression was also detected in the male reproductive tract of androgen ablated rats.

Acknowledgments

This work was supported by Department of Science and Technology, Government of India, New Delhi, India.

References

1 Kumagai Y, Takeuchi O, Akira S: Pathogen recognition by innate receptors. *J Infect Chemother* 2008; 14:86–92.
2 Kumar H, Kawai T, Akira S: Pathogen recognition in the innate immune response. *Biochem J* 2009; 420:1–16.
3 Dinarello CA: Proinflammatory cytokines. *Chest* 2000; 118:503–508.
4 Roach JC, Glusman G, Rowen L, Kaur A, Purcell MK, Smith KD, Hood LE, Aderem A: The evolution of vertebrate Toll-like receptors. *Proc Natl Acad Sci USA* 2005; 102:9577–9582.
5 Pandey S, Agarwal D: Immunology of toll-like receptors: emerging trends. *Immunol Cell Biol* 2006; 84:333–341.
6 Takeda K, Akira S: Toll-like receptors. *In*. Current Protocol in Immunology, A Ryo (ed.) New Jersey, John Wiley Press, 2007, pp 14.12.1–14.12.13.
7 Randhawa AK, Hawn TR: Toll-like receptors: their roles in bacterial recognition and respiratory infections. *Expert Rev Anti Infect Ther* 2008; 6:479–495.
8 O'Neill LA, Dinarello CA: The IL-1 receptor/toll-like receptor superfamily: crucial receptors for inflammation and host defense. *Immunol Today* 2000; 21:206–209.
9 Schuppe HC, Meinhardt A, Allam JP, Bergmann M, Weidner W, Haidl G: Chronic orchitis: a neglected cause of male infertility? *Andrologia* 2008; 40:84–91.
10 Haidl G, Allam JP, Schuppe HC: Chronic epididymitis: impact on semen parameters and therapeutic options. *Andrologia* 2008; 40:92–96.
11 Yenugu S, Hamil KG, Grossman G, Petrusz P, French FS, Hall SH: Identification, cloning and functional characterization of novel Spag11 isoforms in the Rat. *Reprod Biol Endocrinol* 2006; 4:1–14.
12 Yenugu S, Chintalgattu V, Wingard CJ, Radhakrishnan Y, French FS, Hall SH: Identification, cloning and functional characterization of novel beta-defensins in the rat (Rattus norvegicus). *Reprod Biol Endocrinol* 2006; 4:1–7.
13 Patil AA, Cai Y, Sang Y, Blecha F, Zhang G: Cross-species analysis of the mammalian beta-defensin gene family: presence of syntenic gene clusters and

© 2009 John Wiley & Sons A/S

preferential expression in the male reproductive tract. *Physiol Genomics* 2005; 23:5–17.
14 Malm J, Nordahl EA, Bjartell A, Sorensen OE, Frohm B, Dentener MA, Egesten A: Lipopolysaccharide-binding protein is produced in the epididymis and associated with spermatozoa and prostasomes. *J Reprod Immunol* 2005; 66:33–43.
15 Harris CL, Vigar MA, Rey Nores JE, Horejsi V, Labeta MO, Morgan BP: The lipopolysaccharide co-receptor CD14 is present and functional in seminal plasma and expressed on spermatozoa. *Immunology* 2001; 104:317–323.
16 Palladino MA, Johnson TA, Gupta R, Chapman JL, Ojha P: Members of the Toll-like receptor family of innate immunity pattern-recognition receptors are abundant in the male rat reproductive tract. *Biol Reprod* 2007; 76:958–964.
17 Rodriguez CM, Kirby JL, Hinton BT: Regulation of gene transcription in the epididymis. *Reproduction* 2001; 122:41–48.
18 Girling JE, Hedger MP: Toll-like receptors in the gonads and reproductive tract: emerging roles in reproductive physiology and pathology. *Immunol Cell Biol* 2007; 85:481–489.
19 Davies D, Meade KG, Herath S, Eckersall PD, Gonzalez D, White JO, Conlan RS, O'Farrelly C, Sheldon IM: Toll-like receptor and antimicrobial peptide expression in the bovine endometrium. *Reprod Biol Endocrinol* 2008; 6:53.
20 Allhorn S, Böing C, Koch AA, Kimmig R, Gashaw I: TLR3 and TLR4 expression in healthy and diseased human endometrium. *Reprod Biol Endocrinol* 2008; 6:40.
21 Herath S, Fischer DP, Werling D, Williams EJ, Lilly ST, Dobson H, Bryant CE, Sheldon IM: Expression and function of Toll-like receptor 4 in the endometrial cells of the uterus. *Endocrinology* 2006; 175:562–570.
22 Koga K, Mor G: Expression and function of toll-like receptors at the maternal-fetal interface. *Reprod Sci* 2008; 15:231–242.
23 Koga K, Mor G: Toll-like receptors and pregnancy. *Reprod Sci* 2007; 14:297–299.
24 Palladino MA, Savarese MA, Chapman JL, Dughi MK, Plaska D: Localization of Toll-like receptors on epididymal epithelial cells and spermatozoa. *Am J Reprod Immunol* 2008; 60:541–555.
25 Charest NJ, Petrusz P, Ordronneau P, Joseph DR, Wilson EM, French FS: Developmental expression of an androgen-regulated epididymal protein. *Endocrinology* 1989; 125:942–947.
26 Nayfeh SN, Barefoot SW Jr, Baggett B: Metabolism of progesterone by rat testicular homogenates. II. Changes with age. *Endocrinology* 1966; 78:1041–1048.
27 Harris ME, Bartke A: Concentration of testosterone in testis fluid of the rat. *Endocrinology* 1974; 95:701–706.
28 Harris ME, Bartke A: Androgen levels in the rete testis fluid during sexual development. *Experientia* 1981; 37:426–427.
29 Martikainen P, Harkonen P, Vanhala T, Makela S, Viljanen M, Suominen J: Multihormonal control of synthesis and secretion of prostatein in cultured rat ventral prostate. *Endocrinology* 1987; 121:604–611.
30 Kinghorn EM, Bate AS, Higgins SJ: Growth of rat seminal vesicle epithelial cells in culture: neurotransmitters are required for androgen-regulated synthesis of tissue-specific secretory proteins. *Endocrinology* 1987; 121:1678–1688.

Supporting information

Additional Supporting Information may be found in the online version of this article:

Figure S1. Alignment of rat *Tlr* genomic and protein sequences.

Table S1. Primers Used to Amplify Rat *Tlr5*, *Tlr10*, and *Tlr11*.

Please note: Wiley-Blackwell are not responsible for the content or functionality of any supporting materials supplied by the authors. Any queries (other than missing material) should be directed to the corresponding author for the article.

© 2009 John Wiley & Sons A/S

Research Article

Journal of PeptideScience

Received: 28 December 2009 Revised: 20 March 2010 Accepted: 26 March 2010 Published online in Wiley Interscience: 25 May 2010

(www.interscience.com) DOI 10.1002/psc.1246

The human male reproductive tract antimicrobial peptides of the HE2 family exhibit potent synergy with standard antibiotics

Suresh Yenugu* and Ganapathy Narmadha

Reproductive tract infections pose a serious threat to health and fertility. Due to the emergence of antibiotic resistant pathogens, antimicrobial proteins and peptides of the reproductive tract are extensively characterized in recent years toward developing newer strategies to treat genital tract infections. Pathogen growth inhibition using a combination of naturally occurring male reproductive tract antimicrobial peptides and commonly used antibiotics has not been reported. Checker board analyses were carried out to determine the nature of interaction (synergistic, additive and antagonistic) between HE2α and HE2β2 peptides and the commonly used antibiotics. Using *Escherichia coli* as the target organism, the minimal inhibitory concentration and fractional inhibitory concentration indices were determined. We demonstrate for the first time that the human male reproductive tract antimicrobial peptides HE2α and HE2β2 act synergistically with the commonly used antibiotics to inhibit *E. coli* growth. A combination of HE2α and HE2β2 peptides resulted in an additive effect. Interestingly, the synergistic effects of HE2 peptides were highest with doxycycline and ciprofloxacin, antibiotics generally used to treat epididymitis. Results of this study demonstrate the potential of endogenous HE2 peptides to be pharmacologically important in designing novel strategies to treat reproductive tract infections. Copyright © 2010 European Peptide Society and John Wiley & Sons, Ltd.

Keywords: epididymis; antimicrobial; synergy; fractional inhibitory concentration index

Introduction

Antimicrobial proteins and peptides are widely expressed in both plants and animals. A variety of natural antibiotics belonging to different classes such as defensins, cathelicidins, cecropins and protease inhibitors [1] are found in epithelial tissues of organs that are exposed to the external environment. Among them, well characterized in humans are the defensins, which are broadly classified into three types, viz. alpha, beta and theta defensins depending on their disulfide bonding, tissue distribution and genomic organization. They exhibit broad spectrum antimicrobial activity [2–5], thus forming an important component of the innate immune system. Antimicrobial proteins and peptides including defensins are generally cationic in nature [6] and are believed to exert their bactericidal effect by permeabilizing the bacterial membranes [7], thinning the membrane [8] or by destabilizing the membrane bilayer [9]. In addition to these effects, antimicrobial proteins and peptides kill bacteria by inhibition of macromolecular biosynthesis [10–12] and/or interacting with specific vital components inside the bacteria [13,14].

In the epididymis, a major organ of the male reproductive tract, immature sperm released from the testis develop forward motility and fertilizing ability as a result of a series of sequential maturation steps. A wide variety of proteins including antimicrobial proteins released into the lumen of epididymis bind sperm and are thought to play an important role in epididymal immunity in addition to their role in sperm maturation [15]. Examples of antimicrobial proteins reported in the male reproductive tract include human cationic antimicrobial protein (hCAP18, a cathelicidin) [16], defensins [17–20], the epididymal β-defensin member Bin1b [21], cystatins [22,23], lactoferrin [24] seminalplasmin [25], seminogelin-derived peptides [26] and members of the HE2 family [27]. The HE2 gene located on chromosome 8p23 within the β-defensin gene cluster encodes a series of isoforms containing identical proregions joined to different *C*-terminal peptides [27]. Among them, HE2β1 conserves the characteristic β-defensin-like six-cysteine motif. Furthermore, like the β-defensins, HE2 *C*-terminal peptides are cleaved from their proregions by a furin-like proprotein convertase and these peptides are reported to exist in the epididymal epithelium, luminal fluid and the seminal plasma [28]. We previously identified and characterized an epididymis specific novel defensin, DEFB118, which also conserves the characteristic six-cysteine motif [29]. The antimicrobial activity of HE2α, HE2β1 and HE2β2 proteins and their *C*-terminal peptides against *E. coli* [30] and HE2α against *Neisseria gonorrhea, Staphylococcus aureus* and *Enterococcus faecalis* [31] was previously demonstrated. Their antimicrobial activities are structure dependent, salt tolerant and their mechanism of action involves interacting with and permeabilizing bacterial membranes and inhibition of macromolecular synthesis [30,32–34].

The ability of reproductive tract specific defensins and defensin-like proteins and peptides to display antimicrobial

* *Correspondence to: Suresh Yenugu, Department of Animal Sciences, University of Hyderabad, Hyderabad 500046, Andhra Pradesh, India.*
E-mail: ysnaidu@yahoo.com

Department of Animal Sciences, University of Hyderabad, Hyderabad 500046, Andhra Pradesh, India

Copyright © 2010 European Peptide Society and John Wiley & Sons, Ltd.

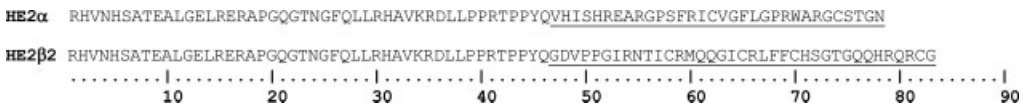

Figure 1. Amino acid sequences of epididymal HE2 proteins. The *C*-terminal amino acid sequences (underlined) of HE2α and β2 were synthesized and used in this study.

activity against *E. coli* and reproductive tract pathogens projects them as potential therapeutic agents to treat sexually transmitted diseases. Current regimens to treat sexually transmitted diseases such as epididymitis involve the administration of antibiotics. For example, when *Chlamydia trachomatis* and *N. gonorrhoeae* are the cause of infection, ceftriaxone and doxycycline are used, whereas when coliform bacterial infections are suspected, ofloxacin or levofloxacin is recommended [35]. Development of resistance by pathogens to conventionally used antibiotics has led to the identification and characterization of a variety of natural and synthetic peptide antibiotics that have the potential to be used to effectively treat infections. However, studies that demonstrate the effectiveness of microbial killing when antibiotics are used in combination with the natural reproductive tract antimicrobial peptides are unknown. In this study, for the first time, we demonstrate the synergistic antibacterial ability of reproductive tract antimicrobial peptides in combination with the commonly used antibiotics to treat genital infections. Results of this study provide vital information for the development of novel strategies to treat sexually transmitted diseases that involve using antibiotics in combination with reproductive tract specific antimicrobial peptides.

Methods

Antibiotics and Peptide Synthesis

Antibiotics used in this study – carbenicillin, amphicillin, ciprofloxacin, kanamycin, chloramphenicol, tetracycline, doxycycline, gentamicin, streptomycin and rifampicin – were obtained commercially (Sigma Aldrich, St Louis, MO). HE2α and HE2β2 *C*-terminal peptides (a kind gift from Dr Susan H. Hall and Dr Frank S. French, Laboratories for Reproductive Biology, University of North Carolina, Chapel Hill, NC) were individually tested in combination with each of the antibiotics. The amino acid sequences of the peptides used are shown in Figure 1. They were synthesized at the Peptide Synthesis Facility, University of North Carolina, Chapel Hill by standard fluoren-9-ylmethoxycarbonyl (f-moc) solid phase procedures using Rainin symphony multiple peptide synthesizer (Rainin Instrument, Woburn, MA). The purified peptides eluted as single peaks upon reverse phase HPLC and were further demonstrated to have the correct molecular weight by MALDI-TOF mass spectrometry.

Fractional Inhibitory Concentration Assay for Synergy

The synergistic antibacterial killing activity of HE2 peptides in combination with antibiotics was carried out by checker board analyses as described earlier [36] using *E. coli* XL-1 blue (Stratagene, La Jolla, CA) as the target organism. Though the incidence of epididymitis is lower with *E. coli* when compared with other reproductive tract pathogens, due to constraints in maintaining and culture of pathogenic organisms, *E. coli* was chosen as the target organism in this study. Initial dose dependent bacterial killing activity of HE2 peptides and antibiotics were analyzed by adding increasing amounts to the microtiter plate wells along with the bacteria to determine the MIC. Control wells were also maintained with no peptide or antibiotic added to the bacteria. Bacterial growth was measured by reading the absorbance at A_{600} 18 h after the addition of the peptide or antibiotic. The MIC is read as the minimal concentration necessary to inhibit growth by at least 90%, when compared to the no peptide or no antibiotic control well. To determine the fractional inhibitory concentrations (FICs), 50 µl of Luria-Bertani medium was added to each well in a 96 well microtiter plate followed by addition of 50 µl of antibiotic to the wells (A1 to A8) in the first row of the microtiter plate and double dilutions added from row 1 to row 7. Then the peptide was added to the wells (1A to 1H) of the first column and double dilutions added from column 1 to column 7. The concentration of each antibacterial agent added ranged between 4X MIC and 1/16X MIC. With these dilutions, row 8 and column 8 serve as antibiotic only treated and peptide only treated controls, respectively. The 64th well (H8) serves as no peptide or no antibiotic control. To each well, 10 µl of bacteria corresponding to 1×10^6 CFU/ml were added and incubated at 37 C for 18 h. The FIC index (FICI) was calculated by the following formula:

$$\text{FICI} = \text{FIC of peptide} + \text{FIC of antibiotic} = (\text{peptide})/(\text{MIC of peptide}) + (\text{antibiotic})/(\text{MIC of antibiotic}) \quad (1)$$

where (peptide) is the concentration of the peptide in the microtiter well that is the lowest inhibitory concentration of the peptide in its column or row and (MIC of peptide) is the MIC of the peptide alone; (antibiotic) and (MIC of antibiotic) are defined in the same way. An FICI of <0.5 indicates synergy, whereas it is considered additive when the index is >0.5 and <1.0. An FICI of >1.0 indicates antagonism. Assays were performed independently three times and the average FICI calculated.

Results

The MICs of the peptides and the antibiotics used in this study were initially determined. The MICs of HE2α and HE2β2 peptides were found to be 17.2 ± 0.6 and 6.4 ± 0.2 µM, respectively (Table 1). The MICs of the different antibiotics used in this study are also given in Table 1.

Our previous studies demonstrated the potent antibacterial killing ability of HE2α and HE2β2 peptides [30–33]. In order to determine whether these two peptides can interact and display enhanced bacterial killing, a checker board analysis was carried out. The average FICI was found to be 0.7 ± 0.1 when HE2α and HE2β2 peptides were used in combination, suggesting an additive nature of interaction (Table 2).

Development of synthetic or natural peptide antibiotics to treat diseases caused by antibiotic resistant pathogens has recently become a major area of investigation. Further, treating antibiotic resistant pathogens with antibiotics in combination with antibacterial peptides is an emerging strategy. To determine whether epididymal antimicrobial peptides can exhibit improved bacterial growth inhibition when used in combination with

 Copyright © 2010 European Peptide Society and John Wiley & Sons, Ltd.

Journal of PeptideScience

Table 1. MIC of the peptides/antibiotics tested

Peptide/antibiotic	MIC (μM)
HE2α	17.2 ± 0.6
HE2β2	6.4 ± 0.2
Ampicillin	14.3 ± 0.8
Chloramphenicol	7.7 ± 0.7
Carbenicillin	12.0 ± 0.3
Ciprofloxacin	1.8 ± 0.3
Doxycycline	10.4 ± 1.1
Gentamicin	1.3 ± 0.2
Kanamycin	0.9 ± 0.1
Rifampicin	6.4 ± 0.7
Streptomycin	0.8 ± 0.1
Tetracycline	1.1 ± 0.1

Table 2. FICI and the nature of interaction between HE2α peptide, HE2β2 peptide and antibiotics

	FICI (nature of interaction)
HE2β2	0.7 ± 0.1 (A)
Ampicillin	0.3 ± 0.06 (S)
Chloramphenicol	0.3 ± 0.04 (S)
Carbenicillin	0.3 ± 0.007 (S)
Ciprofloxacin	0.3 ± 0.04 (S)
Doxycycline	0.2 ± 0.01 (S)
Gentamicin	0.3 ± 0.008 (S)
Kanamycin	0.3 ± 0.001 (S)
Rifampicin	0.3 ± 0.003 (S)
Streptomycin	0.3 ± 0.03 (S)
Tetracycline	0.3 ± 0.02 (S)

(A) indicates additive; (S) indicates synergistic interaction.

Table 3. FICI and the nature of interaction between HE2β2 peptide and antibiotics

	FICI (nature of interaction)
Ampicillin	0.3 ± 0.04 (S)
Chloramphenicol	0.3 ± 0.02 (S)
Carbenicillin	0.2 ± 0.04 (S)
Ciprofloxacin	0.1 ± 0.04 (S)
Doxycycline	0.2 ± 0.007 (S)
Gentamicin	0.2 ± 0.003 (S)
Kanamycin	0.2 ± 0.04 (S)
Rifampicin	0.2 ± 0.002 (S)
Streptomycin	0.1 ± 0.04 (S)
Tetracycline	0.4 ± 0.03 (S)

(A) indicates additive; (S) indicates synergistic interaction.

antibiotics, checkerboard analyses were performed using HE2α or HE2β2 peptide and the commonly used antibiotics against *E. coli*. The nature of the interaction between HE2α peptide and the antibiotics seem to be synergistic as indicated by the average FICI (Table 2). Interestingly, a combination of ciprofloxacin or doxycycline (the most commonly used antibiotics to treat epididymitis) and HE2α peptide exhibited the best growth inhibition, with an FICI of about 0.26 ± 0.01. HE2β2 peptide when used in combination with various antibiotics exhibited synergistic effect (Table 3). Similar to HE2α peptide, its synergistic effect was best when used in combination with ciprofloxacin or doxycycline. The average FICIs of HE2β2 peptide in combination with various antibiotics (ranging from 0.38 to 0.1) seems to be much lower than that observed for HE2α peptide (0.36 to 0.2).

Discussion

Treatment of reproductive tract infections is a global challenge and current regimens involve the use of antibiotics. Prolonged use of antibiotics leads to the development of pathogen resistance, which necessitates the identification of a variety of peptide antibiotics that are promising in treating diseases caused by these antibiotic resistant pathogens. A strategy to circumvent the problem of the emergence of antibiotic resistant bacterial strains is to use new antimicrobial compounds and/or combination therapy. The combination therapy is generally used to increase the *in vivo* activity, to prevent the emergence of drug resistance and to broaden the antimicrobial spectrum. Recently, the increasing incidence of reproductive tract infections and the need to design novel therapeutic approaches to counteract them provided impetus to efforts to identify and characterize novel antimicrobial proteins and peptides of the reproductive tract. Earlier, we demonstrated that HE2 proteins and their *C*-terminal peptides exhibit salt tolerant and structure dependent antimicrobial activities utilizing mechanisms involving permeabilization of both outer and inner bacterial membranes [30] and inhibition of macromolecular synthesis [32]. Further, these peptides have been shown to exhibit antibacterial activity against reproductive pathogens, viz. *N. gonorrhea* and *S. aureus* [31]. There were earlier studies on the combined use of antimicrobial, antifungal and antiviral peptides to inhibit microbial growth in combination with conventionally used antibiotics or drugs [37–39]. However, to our knowledge this is the first report on the nature of interaction and ability of reproductive tract antimicrobial proteins and peptides to kill bacteria in combination with conventionally used antibiotics. Results of this study demonstrate that a combination of the synthetic HE2α and HE2β2 peptides exhibit an additive inhibitory effect on *E. coli* growth. Moreover, HE2α or HE2β2 peptide in combination with an antibiotic acts synergistically to inhibit bacterial growth. These results suggest that HE2α and HE2β2 peptides are potentially valuable for the treatment of reproductive tract infections in combination with antibiotics.

Cationic antimicrobial peptides can cross the outer membrane of Gram-negative bacteria by the self-promoted uptake pathway [40], which involves the high affinity binding of the peptide to surface lipopolysaccharide, resulting in the displacement of divalent cations that stabilize adjacent lipopolysaccharide molecules [41,42] leading to destabilization of the outer membrane. Our previous studies demonstrate that HE2 peptides bring about bacterial killing by membrane permeabilization and inhibition of macromolecular synthesis. It is possible that the synergistic effect observed in this study could be due to enhanced entry of antibiotic into the bacterial cell through the membrane pores created by the peptide. Synergistic action between antimicrobial peptides and antibiotics that involves membrane permeabilization was previously shown for a variety of peptides such as the α helical peptide p18 [38], menstrual hemocidin [43] and defensins [44]. The nature of interaction between the defensins and

 Copyright © 2010 European Peptide Society and John Wiley & Sons, Ltd.

antimicrobial proteins and peptides of the reproductive tract has been demonstrated earlier. For example, cathelicidins or the human CAP18/LL37 can act synergistically with defensins to bring about bacterial killing [45]. Though antimicrobial peptides that cause pores in the membrane are expected to increase the uptake of antibiotics when used in combination, this effect alone was found not to be sufficient to show synergistic effects. For example, synergy was not observed when synthetic peptides that have the ability to permeabilize the membranes of *E. coli* were used in combination with vancomycin or ampicillin [46], suggesting that increased access of intracellular targets to antibiotics due to membrane permeabilization by peptides as well as the secondary effects that the peptides can effect are important for synergy. The synergistic bacterial killing observed when HE2 peptides were used in combination with common antibiotics could be due to their ability to form pores in the membrane facilitating increased entry of antibiotics as well as the secondary effects of these peptides, i.e. inhibition of macromolecular synthesis.

In this study, we observed that a combination of HE2α and β2 peptides exhibited an additive effect. The inability of HE2α and β2 peptides to act synergistically with each other could be due to their similar mechanisms of action on a single target, the bacterial membrane. On the same lines, basing on previous studies it should be mentioned that synergy is not necessarily observed when antimicrobial peptides are used in combination with commonly used antibiotics. Absence of synergism has been attributed to various factors that govern the activity of lytic peptides. For example, no synergy was observed when synthetic antimicrobial peptides were used in combination with antibiotics against *S. aureus* [46]. Similar observation was made when bovine lactoferricin was used in combination with various antibiotics [47]. The absence of synergistic effects in these cases was due to the low MICs of the peptides used and it becomes experimentally difficult to assess synergy. On the same lines, it is also noteworthy to mention that depending on the chemical structures of antibiotics used in combination with polyethylenimine, a polycationic synthetic polymer, the effects were either synergistic or antagonistic or indifferent [48]. PGLa, a synthetic antimicrobial peptide, exhibits synergy with magainin (containing a 23 amino acid hydrophobic tail) but not with certain synthetic peptides that lack this tail [46]. Varying structural features of lytic peptides may allow aggregation or competition between the peptides to bind to the membranes of target organisms, thereby making it difficult to measure the synergistic actions.

In conclusion, we report that the antibacterial peptides of the male reproductive tract exhibit synergistic bacterial killing when used in combination with the conventionally used antibiotics. Results of this study may provide vital information to develop novel strategies to treat reproductive infections.

Acknowledgements

We thank Dr Susan H. Hall and Dr Frank S. French, Laboratories for Reproductive Biology, University of North Carolina, Chapel Hill, USA, for providing the peptides and also for the critical comments during the preparation of the manuscript.

References

1 Ganz T. Antimicrobial polypeptides. *J. Leukoc. Biol.* 2004; **75**: 34–38.
2 Bastian A, Schafer H. Human alpha-defensin 1 (HNP-1) inhibits adenoviral infection in vitro. *Regul. Pept.* 2001; **101**: 157–161.
3 Daher KA, Selsted ME, Lehrer RI. Direct inactivation of viruses by human granulocyte defensins. *J. Virol.* 1986; **60**: 1068–1074.
4 Schibli DJ, Hunter HN, Aseyev V, Starner TD, Wiencek JM, McCray PB Jr, Tack BF, Vogel HJ. The solution structures of the human beta-defensins lead to a better understanding of the potent bactericidal activity of HBD3 against Staphylococcus aureus. *J. Biol. Chem.* 2002; **277**: 8279–8289.
5 Lehrer RI, Ganz T. Defensins of vertebrate animals. *Curr. Opin. Immunol.* 2002; **14**: 96–102.
6 Zasloff M. Antimicrobial peptides of multicellular organisms. *Nature* 2002; **415**: 389–395.
7 Matsuzaki K. Magainins as paradigm for the mode of action of pore forming polypeptides. *Biochim. Biophys. Acta* 1998; **1376**: 391–400.
8 Heller WT, Waring AJ, Lehrer RI, Harroun TA, Weiss TM, Yang L, Huang HW. Membrane thinning effect of the beta-sheet antimicrobial protegrin. *Biochemistry Mosc.* 2000; **39**: 139–145.
9 Gazit E, Boman A, Boman HG, Shai Y. Interaction of the mammalian antibacterial peptide cecropin P1 with phospholipid vesicles. *Biochemistry Mosc.* 1995; **34**: 11 479–11 488.
10 Park CB, Kim HS, Kim SC. Mechanism of action of the antimicrobial peptide buforin II: buforin II kills microorganisms by penetrating the cell membrane and inhibiting cellular functions. *Biochem. Biophys. Res. Commun.* 1998; **244**: 253–257.
11 Subbalakshmi C, Sitaram N. Mechanism of antimicrobial action of indolicidin. *FEMS Microbiol. Lett.* 1998; **160**: 91–96.
12 Boman HG, Agerberth B, Boman A. Mechanisms of action on *Escherichia coli* of cecropin P1 and PR-39, two antibacterial peptides from pig intestine. *Infect. Immun.* 1993; **61**: 2978–2984.
13 Otvos L Jr, O I, Rogers ME, Consolvo PJ, Condie BA, Lovas S, Bulet P, Blaszczyk-Thurin M. Interaction between heat shock proteins and antimicrobial peptides. *Biochemistry Mosc.* 2000; **39**: 14 150–14 159.
14 Lehrer RI, Barton A, Daher KA, Harwig SS, Ganz T, Selsted ME. Interaction of human defensins with *Escherichia coli*. Mechanism of bactericidal activity. *J. Clin. Invest.* 1989; **84**: 553–561.
15 Hall SH, Hamil KG, French FS. Host defense proteins of the male reproductive tract. *J. Androl.* 2002; **23**: 585–597.
16 Malm J, Sorensen O, Persson T, Frohm-Nilsson M, Johansson B, Bjartell A, Lilja H, Stahle-Backdahl M, Borregaard N, Egesten A. The human cationic antimicrobial protein (hCAP-18) is expressed in the epithelium of human epididymis, is present in seminal plasma at high concentrations, and is attached to spermatozoa. *Infect. Immun.* 2000; **68**: 4297–4302.
17 Palladino MA, Mallonga TA, Mishra MS. Messenger RNA (mRNA) expression for the antimicrobial peptides beta-defensin-1 and beta-defensin-2 in the male rat reproductive tract: beta-defensin-1 mRNA in initial segment and caput epididymidis is regulated by androgens and not bacterial lipopolysaccharides. *Biol. Reprod.* 2003; **68**: 509–515.
18 Zaballos A, Villares R, Albar JP, Martinez AC, Marquez G. Identification on mouse chromosome 8 of new beta-defensin genes with regionally specific expression in the male reproductive organ. *J. Biol. Chem.* 2004; **279**: 12 421–12 426.
19 Yamaguchi Y, Nagase T, Makita R, Fukuhara S, Tomita T, Tominaga T, Kurihara H, Ouchi Y. Identification of multiple novel epididymis-specific beta-defensin isoforms in humans and mice. *J. Immunol.* 2002; **169**: 2516–2523.
20 Com E, Bourgeon F, Evrard B, Ganz T, Colleu D, Jegou B, Pineau C. Expression of antimicrobial defensins in the male reproductive tract of rats, mice, and humans. *Biol. Reprod.* 2003; **68**: 95–104.
21 Li P, Chan HC, He B, So SC, Chung YW, Shang Q, Zhang YD, Zhang YL. An antimicrobial peptide gene found in the male reproductive system of rats. *Science* 2001; **291**: 1783–1785.
22 Hamil KG, Liu Q, Sivashanmugam P, Yenugu S, Soundararajan R, Grossman G, Richardson RT, Zhang YL, O'Rand MG, Petrusz P, French FS, Hall SH. Cystatin 11: a new member of the cystatin type 2 family. *Endocrinology* 2002; **143**: 2787–2796.
23 Blankenvoorde MF, van't Hof W, Walgreen-Weterings E, van Steenbergen TJ, Brand HS, Veerman EC, Nieuw Amerongen AV. Cystatin and cystatin-derived peptides have antibacterial activity against the pathogen *Porphyromonas gingivalis*. *Biol. Chem.* 1998; **379**: 1371–1375.
24 Jin YZ, Bannai S, Dacheux F, Dacheux JL, Okamura N. Direct evidence for the secretion of lactoferrin and its binding to sperm in the porcine epididymis. *Mol. Reprod. Dev.* 1997; **47**: 490–496.

 Copyright © 2010 European Peptide Society and John Wiley & Sons, Ltd.

25 Reddy ES, Bhargava PM. Seminalplasmin – an antimicrobial protein from bovine seminal plasma which acts in E. coli by specific inhibition of rRNA synthesis. *Nature* 1979; **279**: 725 – 728.
26 Bourgeon F, Evrard B, Brillard-Bourdet M, Colleu D, Jegou B, Pineau C. Involvement of semenogelin-derived peptides in the antibacterial activity of human seminal plasma. *Biol. Reprod.* 2004; **70**: 768 – 774.
27 Hamil KG, Sivashanmugam P, Richardson RT, Grossman G, Ruben SM, Mohler JL, Petrusz P, O'Rand MG, French FS, Hall SH. HE2beta and HE2gamma, new members of an epididymis-specific family of androgen-regulated proteins in the human. *Endocrinology* 2000; **141**: 1245 – 1253.
28 von Horsten HH, Derr P, Kirchhoff C. Novel antimicrobial peptide of human epididymal duct origin. *Biol. Reprod.* 2002; **67**: 804 – 813.
29 Liu Q, Hamil KG, Sivashanmugam P, Grossman G, Soundararajan R, Rao AJ, Richardson RT, Zhang YL, O'Rand MG, Petrusz P, French FS, Hall SH. Primate epididymis-specific proteins: characterization of ESC42, a novel protein containing a trefoil-like motif in monkey and human. *Endocrinology* 2001; **142**: 4529 – 4539.
30 Yenugu S, Hamil KG, Birse CE, Ruben SM, French FS, Hall SH. Antibacterial properties of the sperm-binding proteins and peptides of human epididymis 2 (HE2) family; salt sensitivity, structural dependence and their interaction with outer and cytoplasmic membranes of *Escherichia coli*. *Biochem. J.* 2003; **372**: 473 – 483.
31 Liao M, Ruddock PS, Rizvi AS, Hall SH, French FS, Dillon JR. Cationic peptide of the male reproductive tract, HE2{alpha}, displays antimicrobial activity against *Neisseria gonorrhoeae*, *Staphylococcus aureus* and *Enterococcus faecalis*. *J. Antimicrob. Chemother.* 2005; **56**: 957 – 961.
32 Yenugu S, Hamil KG, French FS, Hall SH. Antimicrobial actions of the human epididymis 2 (HE2) protein isoforms, HE2alpha, HE2beta1 and HE2beta2. *Reprod. Biol. Endocrinol.* 2004; **2**: 61.
33 Yenugu S, Hamil KG, French FS, Hall SH. Antimicrobial actions of human and macaque sperm associated antigen (SPAG)11 isoforms: influence of the N-terminal peptide. *Mol. Cell. Biochem.* 2006; **284**: 25 – 35.
34 Yenugu S, Hamil KG, Radhakrishnan Y, French FS, Hall SH. The androgen-regulated epididymal sperm-binding protein, human beta-defensin 118 (DEFB118) (formerly ESC42), is an antimicrobial beta-defensin. *Endocrinology* 2004; **145**: 3165 – 3173.
35 Trojian TH, Lishnak TS, Heiman D. Epididymitis and orchitis: an overview. *Am. Fam. Physician* 2009; **79**: 583 – 587.
36 Fidai S, Farmer SW, Hancock RE. Interaction of cationic peptides with bacterial membranes. In *Antibacterial Peptide Protocols*, Vol. 78, Shafer W (ed.). Humana Press: New Jersey, 1997; 187 – 204.
37 Duggineni S, Srivastava G, Kundu B, Kumar M, Chaturvedi AK, Shukla PK. A novel dodecapeptide from a combinatorial synthetic library exhibits potent antifungal activity and synergy with standard antimycotic agents. *Int. J. Antimicrob. Agents* 2007; **29**: 73 – 78.
38 Shin SY, Yang ST, Park EJ, Eom SH, Song WK, Kim Y, Hahm KS, Kim JI. Salt resistance and synergistic effect with vancomycin of alpha-helical antimicrobial peptide P18. *Biochem. Biophys. Res. Commun.* 2002; **290**: 558 – 562.
39 Lawyer C, Pai S, Watabe M, Bakir H, Eagleton L, Watabe K. Effects of synthetic form of tracheal antimicrobial peptide on respiratory pathogens. *J. Antimicrob. Chemother.* 1996; **37**: 599 – 604.
40 Piers KL, Brown MH, Hancock RE. Improvement of outer membrane-permeabilizing and lipopolysaccharide-binding activities of an antimicrobial cationic peptide by C-terminal modification. *Antimicrob. Agents Chemother.* 1994; **38**: 2311 – 2316.
41 Piers KL, Hancock RE. The interaction of a recombinant cecropin/melittin hybrid peptide with the outer membrane of *Pseudomonas aeruginosa*. *Mol. Microbiol.* 1994; **12**: 951 – 958.
42 Hancock RE. Antibacterial peptides and the outer membranes of gram-negative bacilli. *J. Med. Microbiol.* 1997; **46**: 1 – 3.
43 Mak P, Siwek M, Pohl J, Dubin A. Menstrual hemocidin HbB115-146 is an acidophilic antibacterial peptide potentiating the activity of human defensins, cathelicidin and lysozyme. *Am. J. Reprod. Immunol.* 2007; **57**: 81 – 91.
44 Singh PK, Tack BF, McCray PB Jr, Welsh MJ. Synergistic and additive killing by antimicrobial factors found in human airway surface liquid. *Am. J. Physiol. Lung Cell Mol. Physiol.* 2000; **279**: L799 – L805.
45 Nagaoka I, Hirota S, Yomogida S, Ohwada A, Hirata M. Synergistic actions of antibacterial neutrophil defensins and cathelicidins. *Inflamm. Res.* 2000; **49**: 73 – 79.
46 Ulvatne H, Karoliussen S, Stiberg T, Rekdal O, Svendsen JS. Short antibacterial peptides and erythromycin act synergically against *Escherichia coli*. *J. Antimicrob. Chemother.* 2001; **48**: 203 – 208.
47 Vorland LH, Osbakk SA, Perstolen T, Ulvatne H, Rekdal O, Svendsen JS, Gutteberg TJ. Interference of the antimicrobial peptide lactoferricin B with the action of various antibiotics against *Escherichia coli* and *Staphylococcus aureus*. *Scand. J. Infect. Dis.* 1999; **31**: 173 – 177.
48 Khalil H, Chen T, Riffon R, Wang R, Wang Z. Synergy between polyethylenimine and different families of antibiotics against a resistant clinical isolate of *Pseudomonas aeruginosa*. *Antimicrob. Agents Chemother.* 2008; **52**: 1635 – 1641.

 Copyright © 2010 European Peptide Society and John Wiley & Sons, Ltd.

OPEN ACCESS Freely available online

PLoS one

Characterization of a Novel Lysozyme-Like 4 Gene in the Rat

Ganapathy Narmadha, Katakam Muneswararao¤, Angireddy Rajesh, Suresh Yenugu*

Department of Animal Sciences, University of Hyderabad, Hyderabad, India

Abstract

Lysozyme-like proteins (LYZLs) belong to the class of c-type lysozymes and are not well characterized in many species including the rat. In this study, using *in silico* and molecular biology techniques, we report the identification, cloning and characterization of rat *Lyzl4* gene and also determine the expression pattern of *Lyzl1*, *Lyzl3* and *Lyzl6*. The rat *Lyzl* genes were found to be distributed on three chromosomes and all of them retained the characteristic eight cysteine signature of c-type lysozyme. Homology modeling of rat LYZL4 indicated that its structure is similar to that of the mouse SLLP1. In the male reproductive tract of rat, Lyzl gene expression was confined to the testis. *Lyzl1* and *Lyzl4* were found to be expressed in tissues beyond the male reproductive tract, whereas *Lyzl3* and *Lyzl6* were not. *Lyzl* expression in the developing (10–60 day old) rats was androgen dependent in the testis. Immunodetection using antibodies against rat LYZL4 revealed the presence of LYZL4 protein in the germinal layer of the testes and on the sperm tail. Recombinant LYZL4 did not exhibit antibacterial, muramidase and isopeptidase activities characteristic to c-type lysozyme. To the best of our knowledge, for the first time we report the characterization of *Lyzl* genes in the rat. Results of our study indicate that rat LYZL proteins may have an important role in male reproductive tract function.

Citation: Narmadha G, Muneswararao K, Rajesh A, Yenugu S (2011) Characterization of a Novel Lysozyme-Like 4 Gene in the Rat. PLoS ONE 6(11): e27659. doi:10.1371/journal.pone.0027659

Editor: Avadhesha Surolia, National Institute of Immunology, India

Received September 15, 2011; **Accepted** October 21, 2011; **Published** November 15, 2011

Copyright: © 2011 Narmadha et al. This is an open-access article distributed under the terms of the Creative Commons Attribution License, which permits unrestricted use, distribution, and reproduction in any medium, provided the original author and source are credited.

Funding: The authors have no support or funding to report.

Competing Interests: The authors have declared that no competing interests exist.

* E-mail: ysnaidu@yahoo.com

¤ Current address: Laboratory for the conservation of endangered species (LaCONES), Center for Cellular and Molecular Biology, Uppal, Hyderabad, India

Introduction

In the 1930s Alexander Flemming discovered lysozyme (EC 3.2.17), a remarkable bactericidal agent [1]. Basing on their physical and functional properties, a wide variety of lysozymes have been identified. They are mainly classified into six families, namely, g-type (goose type), c-type (chicken-type), invertebrate type (I-type), phage, bacterial and plant [2]. Among them, the c-type are widely distributed across the species [3,4,5,6] and in various organ systems including the male reproductive tract. C-type lysozymes are N-acetylglucosamine binding proteins and are of two types, namely, the non-calcium binding c-lysozymes and the calcium-binding c-lysozymes [7]. The enzymatic action of c-type lysozyme involves the hydrolysis of beta-1,4 glycosidic bonds between C-1 of N-acetylmuramic acid and C-4 of N-acetylglucosamine in the peptidoglycan of bacterial cell walls. Its ability to act on bacterial membranes confers the bactericidal activity and thereby has a role in innate immunity [3].

The male reproductive tract is a dynamic organ system involved in both endocrine and reproductive functions. Spermatozoa that emerge from the testis are immature, non-motile and lack fertilizing ability. Their passage through the epididymis allows interaction with a wide variety of epididymal secreted proteins resulting in acquisition of motility and fertilizing ability. Proteins secreted into the epididymal lumen [8] include defensins [9,10], lipocalins [11], cathelicidins [12], members of the sperm associated antigen 11 family [13], protease inhibitors [14,15,16] and enzymes including the c-type lysozyme [17,18].

In humans, besides the c-lysozyme, lysozyme like genes were identified [19] and some of them (*LYZL2*, *LYZL/SLLP1*, *LYZL4* and *LYZL6*) are found to be expressed in the male reproductive tract [17,18]. Spermatozoa incubated with antibodies to human SLLP1 failed to fertilize eggs, thereby demonstrating a role in male reproductive function [18]. Similarly, incubation of spermatozoa with the mouse LYZL4 antibodies resulted in loss of fertilizing ability [20]. However, the role of other three mouse c-lysozymes in the reproductive tract is not yet clear. Unlike the human and mouse counter parts, the rat *Lyzl* genes are not characterized. In the rat genome available at GenBank, of the four c-type lysozymes (*Lyzl1*, *Lyzl3*, *Lyzl4* and *Lyzl6*), *Lyzl4* sequence is predicted, whereas the other three were annotated using the whole genome shot gun analyses. Except for their gene identification, the functional role is not reported till now.

In this study, we report the identification and characterization of the rat *Lyzl4*. Further, the expression profile of the *Lyzl* transcripts (*Lyzl1, Lyzl3, Lyzl4 and Lyzl6*) was analyzed and their androgen dependence determined. Their possible contribution to the male reproductive tract immunity was analyzed.

Results

In silico analyses

Using gene specific primers, rat *Lyzl4* mRNA transcript was amplified and sequenced. It is located on chromosome 8, whereas *Lyzl1*, *Lyzl3* and *Lyzl6* are present on chromosome 10 and 17 (Figure 1). The *Lyzl4* sequence was submitted to GenBank and was

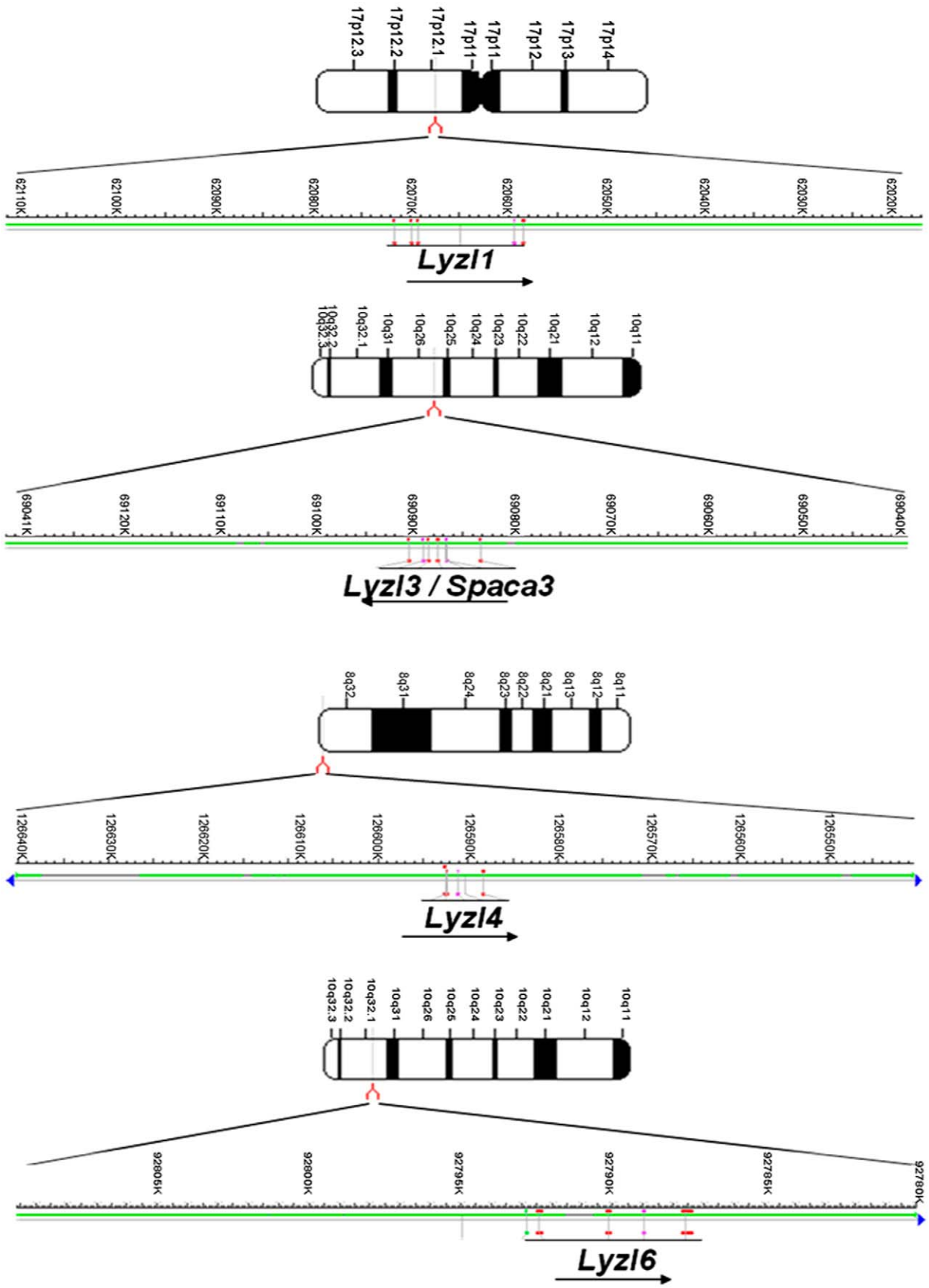

Figure 1. Rat *Lyzl* gene localization. Arrows indicate direction of transcription. Positions were taken from the Mapview (RGSC v3.4) at the National Center for Biotechnology Information (NCBI) website.
doi:10.1371/journal.pone.0027659.g001

assigned the accession number HM125534. *In silico* protein translation analyses revealed that LYZL4 is encoded by four exons (Figure 2), which is in agreement with the predicted *Lyzl4* sequence available at GenBank. It is thought to be secretory because of the presence of a signal peptide. The predicted physical characteristics of the rat LYZL proteins are given in Table 1. An important feature is that all the rat LYZL proteins retained the characteristic eight cysteine signature of c-type lysozymes (Figure 3A). In LYZL4 one of the essential amino acids (aspartate) of c-type lysozyme active site is replaced by glycine (Figure 3A). Similarly, in LYZL3, aspartate is replaced by aspargine, suggesting that LYZL3 and LYZL4 may not exhibit lysozyme activity. However, the essential amino acids of the active site are conserved in LYZL1 and LYZL6 (Figure 3A). Loss of aspartate in the lysozyme active site was also observed in the human and mouse LYZL4 (Figure 3B). Sequence analyses reveal that the rat LYZL proteins are highly homologous to their mouse and human counterparts (Table 1). Similarly, based on the ClustalW2 score, the homology among the rat LYZL proteins was also found to be high (Table 2). Rat LYZL4 displays a high degree of homology with mouse SLLP1 (Figure 3C). Homology modeling using mouse SLLP1 as the template was carried out to determine the three dimensional structure of rat LYZL4 (Figure 4A and 4B). LYZL4 seems to be structurally similar to the mouse SLLP1 except at few residues as shown in the superimposed image (Figure 4C). There are 7 helices and 4 disulphide bridges that are conserved between

Lyzl4

```
1     cctcttttctg tttttcattc cctctcctcc tatctctccc ttccacactc ttcctgacca
61    ctccccccgcc ccgatcccct cgcccccagt gcctctcttt tccctgggaa gtccaatgtc
121   tctgtgacct tggaaggagc cgcctgagac tctctgttca gctggcaccc acagccctga
                            M  Q  L  Y   L  V  L   L  L  I   S  Y  L  L   (14)
181   gccgccagag cctggagaag ATGCAGCTGT ACCTGGTGCT TCTCCTCATC AGCTACTTGC
        T  P  I   G  A  S   I  L  G  R   C  V  V   A  K  K   L  Y  D  G   (34)
241   TGACTCCGAT TGGTGCCTCC ATTTTGGGGC GCTGCGTGGT GGCTAAGAAA CTCTATGACG
            G  L  N   Y  F  E   G  Y  S  L   E  N  W                       (47)
301   GGGGCTTAAA TTATTTTGAG GGCTACAGCC TTGAAAACTg taagtaggac cctttcaggc
361   cctctctcct caccgcccca tgccatccca tccccctacc accagcgtct tctcacccca
                              V  C  L   A  Y  F  E   S  K  F   N  P  S   (60)
421   cacactgttc cacctcttag gGGTGTGCCT GGCTTATTTT GAGAGCAAGT TCAACCCCTC
        A  V  Y   E  N  S  R   D  G  S   T  G  F   G  L  F  Q   I  R  D   (80)
481   GGCTGTCTAT GAGAACTCAC GAGATGGCTC CACCGGCTTC GGCCTCTTTC AGATCCGCGA
        N  E  W   C  D  H  G   K  N  L  C  S  V   S  C  T  A              (97)
541   CAATGAATGG TGTGACCATG GCAAGAACCT CTGCAGTGTG TCCTGCACGG gtgggtccct
601   ttcgctccag tccctcgggg ggggggcggg ggaggagcct gcagaacctg catgtttgga
661   ggagacaggg agagggaacc ggctgtgtct gaagctcatc cctgagaggt ggagtgctag
//
1561  taaagagagc atttcccgct accctgattg atgaggagtg tccagggttt tcagcctctg
1621  tgaaggcagg cagtgggacg ggagttatgg cgtggagaga taagtttgct gtcctcggat
                                          L  L   N  P  N   L  K  D    (105)
1681  tccacagcat caacctactc cacttccttc ctagCTTTAC TGAATCCCAA CTTAAAGGAT
      T  I  E  C   A  K  K   I  V  K   G  K  Q  G   M  G  A   W         (123)
1741  ACAATCGAGT GTGCCAAGAA AATCGTGAAA GGAAAACAAG GGATGGGAGC ATGGtgagtg
1801  ggtgtgtgca gctcaccctg gaggttagag ggatgggagc atggtgagtg ggtgtctgca
1861  gctcaccctg gaggttaggg ggtgggagca tggtaggtgg gtgtctgcag ctcaccctgg
//
4261  tgagcgctaa gaacttcaaa agcctgaggt ccacactgga gagacgcaga tgtcccaggg
4321  ccagccaggc aggcatgggc aagcatgacc ctggggaccc caagctctga ctacaaggaa
                                          P  V   W  S  R   N  C  Q    (131)
4381  ctggtgctca tcactctctg gccttccctc cgcaggCCCG TCTGGTCCAG GAACTGCCAG
      L  S  D  I   L  D  R   W  L  D   G  C  E  L   *                  (145)
4441  CTGTCGGACA TTCTGGATCG GTGGCTGGAT GGCTGTGAGC TGTAGGCGCC TGTGTGGTCC
4501  TGCCTCACTT GCCGGCCGTG TCTTGGGACT GAGGGCGCTT TTCTGTTTGC TGCTTCAATC
4561  CATCCGGTTA TCTCACCACT GATTGCTCCA GATGGAAAGG GACAACAGTC CTCACTTCAT
4621  CCGGGGGtac aaggtgcaga ataaaccagc tagttactca acctgggcct gaagtctctg
4681  cctattatat tatcgccagt tattatatcg ccagcggaat ggccata
```

Figure 2. Rat chromosomal sequence aligned with *Lyzl4* mRNA and predicted amino acid sequence. Exons are in upper case letters and introns in lower case. Amino acids are indicated in single letters. Numbers in parentheses indicate amino acids of the protein. The gene sequence was extracted from GenBank NW_047803.1. The rat *Lyzl4* cDNA sequence was submitted to Genbank and was assigned the accession number HM125534. Predicted signal peptide cleavage site is indicated in bold italics. Posttranslational modification sites are indicated: single underlined – phosphorylation.

doi:10.1371/journal.pone.0027659.g002

Table 1. General characteristic features of rat lysozyme-like proteins.

	LYZL1	LYZL3	LYZL4	LYZL6
Amino acids	148	163	145	148
Molecular weight	16589.9	18303.7	16304.8	17027.6
Signal peptide	1-19	1-35	1-19	1-19
pI	8.38	6.4	5.79	5.74
Active site	Conserved (Glu-54 & Asp 71)	NIL	NIL	Conserved (Glu-54 & Asp 71)
Localization	Secretory	Secretory	Secretory	Secretory
Homology with human counterpart	86%	89%	86%	84%
Homology with mouse counterpart	95%	95%	97%	93%
Amino acids involved in disulfide bonds	25 & 145, 49 & 133, 83 & 98, 94 & 112	41 & 161, 65 & 149, 99 &114, 110 & 128	25 & 143, 49 & 130, 84 & 95, 91 & 109	25 & 145, 49 & 133, 83 & 98, 94 & 112
Myristylation sites	NIL	NIL	NIL	NIL
O-glycosylation sites	NIL	NIL	NIL	NIL
Phosphorylation sites	19, 55, 135, 138, 59, 102, 53, 57, 32, 39 72		70, 133, 63	88,81,86

doi:10.1371/journal.pone.0027659.t001

the mouse SLLP1 and rat LYZL4. The beta sheets present between residues 43–60 in mouse counterpart are absent in the rat LYZL4. A change in secondary structure pattern was also observed near residue 23 wherein a helix is formed in case of mouse SLLP1 and not in rat LYZL4. According to Ramachandran plot, 90.8% of the residues lie in the most favored regions and 9.2% in the additionally allowed regions (Figure 4D). There are no disallowed regions predicted. The generated model seems to be reliable with the good Ramachandran plot values with a G-factor of -0.12 (Figure 4D). The RMSD value was 0.405 which was within the agreeable limit. The similarity in structural and tissue localization of rat LYZL4 and mouse SLLP1 suggests that they may exhibit similar function.

Lyzl gene expression in the rat

Using RT-PCR analyses, the expression pattern of rat *Lyzl* genes was determined in the male reproductive tract. All the *Lyzl* genes analyzed in this study were found to be expressed specifically in the testes (Figure 5). To determine if the expression pattern of *Lyzl* mRNA transcripts is male reproductive tract specific, RT-PCR was performed in a variety of tissues obtained from male and female rats. *Lyzl1* was found to be expressed in the heart, lung and spleen, whereas *Lyzl4* was found to be expressed in the brain, lung, ovary and uterus (Figure 6). *Lyzl3* and *Lyzl6* expression was not found in these tissues suggesting that their expression is highly male reproductive tract specific (Figure 6).

Androgen dependent expression

Gene expression in the male reproductive tract is under the influence of androgens [21,22]. To elucidate the influence of androgen variation, PCR analyses for *Lyzl*s were carried out using total RNA isolated from the epididymides and testes of 10–60 day old rats. Though the expression of *Lyzl* transcripts is absent in the epididymis obtained from the adult rats (Figure 5), it is possible that they may be expressed in the younger rats during postnatal development. In the epididymis, none of the *Lyzl*s analyzed in this study were expressed at all the ages during development (Figure 7A). In the testes, *Lyzl1*, 3 and 6 were expressed starting from day 30 during postnatal development, whereas *Lyzl4* was expressed in all the age groups (Figure 7B).

Immunolocalization

Since *Lyzl4* was the only one predicted among the *Lyzl*s analyzed in this study and that its expression was found to be present during all stages of postnatal development, we further studied its expression pattern at the protein level in the testis using polyclonal antibodies raised against LYZL4. It was found to be expressed in the germinal epithelium and concentrated on the developing spermatozoa (Figure 8). Using immunofluorescence, we observed that LYZL4 is expressed only in the tail region of the sperm obtained from adult rat (Figure 9), suggesting that LYZL4 may contribute to the motility of the spermatozoa.

Muramidase, isopeptidase and antimicrobial activities

LYZL4 being a c-type lysozyme is expected to exhibit the hydrolytic activity of glycosyl bonds. Hence, its muramidase and isopeptidase activities were analyzed. At the concentrations tested (1 and 5 μM) no activity was displayed by LYZL4 (Figure 10A and 10B). The positive control, lysozyme, displayed potent muramidase and isopeptidase activities. The antimicrobial activity of lysozyme is well known. To determine whether recombinant rat LYZL4 protein exhibits antimicrobial activity, its ability to kill *E. coli* was tested using colony forming unit (CFU) assay. LYZL4 (10–100 μg/ml) did not display any antibacterial activity at all the concentrations tested (Figure 10C). The negative control, LCN6, an epididymal lipocalin, did not show any detectable antibacterial activity when incubated for 2 h at concentrations up to 100 μg/ml (data not shown).

Discussion

C-type lysozyme is expressed in most species and because of its ability to act on microbial membranes, it is thought to play an important role in innate immune defense. In the recent years, lysozyme-like proteins were identified and characterized in the human and mouse [17,18,20]; their expression being reported in

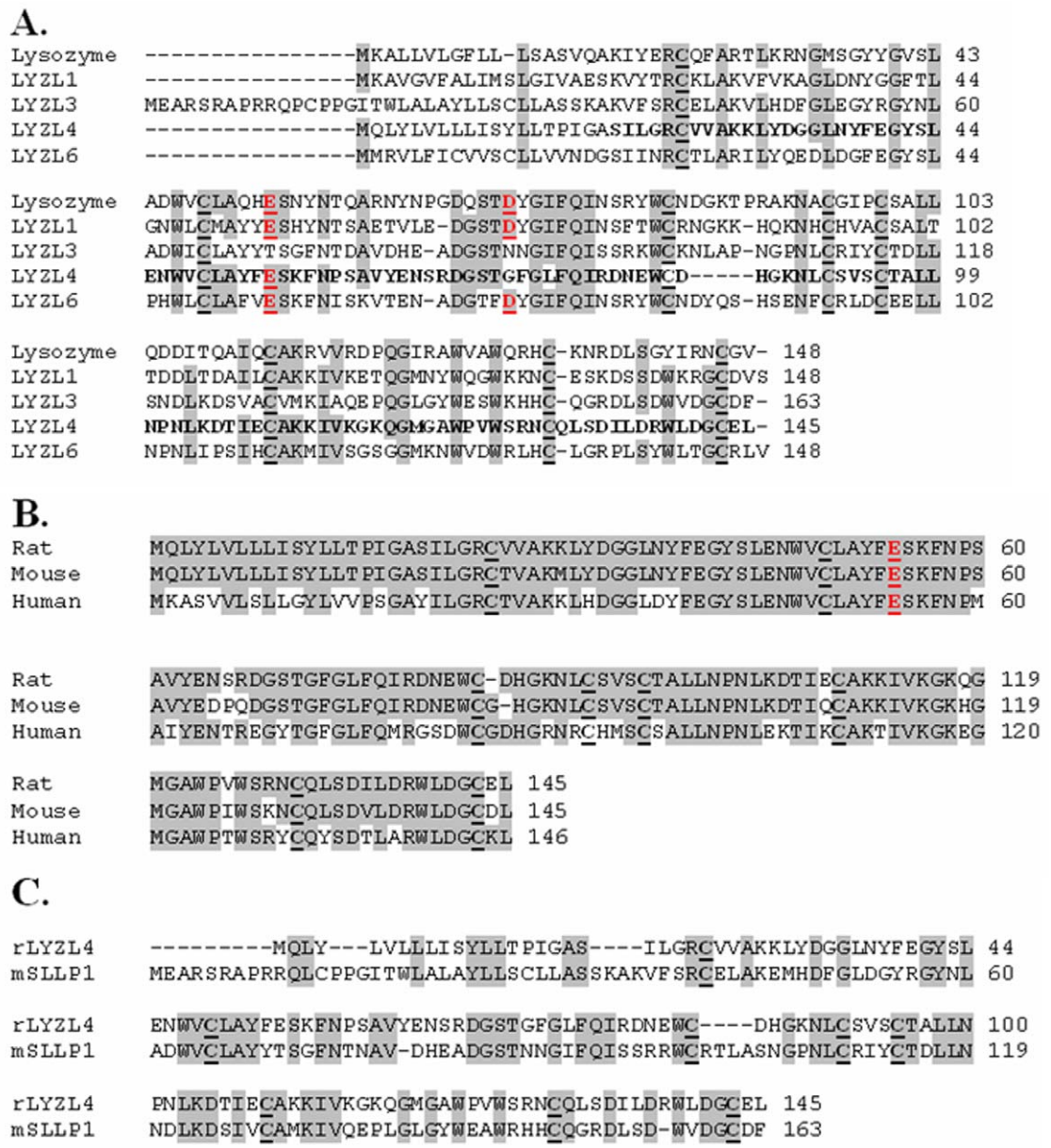

Figure 3. Multiple sequence alignment of LYZL proteins. A) Rat LYZL proteins. **B**) Alignment of rat, mouse and human LYZL4 protein sequences. The conserved amino acid residues are shaded. Amino acids in the active site responsible for the enzyme activity are shown in red. The eight cysteines of the c-type lysozyme signature are indicated in bold and underlined. The LYZL4 sequence shown in bold was expressed as a recombinant protein. C) Alignment of rat LYZL4 and mouse SLLP1.
doi:10.1371/journal.pone.0027659.g003

the male reproductive tract. The mRNA and protein expression pattern of human and mouse LYZLs varied within the male reproductive tract, suggesting that they may play different roles in these two species [17,18,20]. However, the expression pattern of lysozyme-like genes and proteins are not characterized in the rat. In this study, we analyzed their mRNA and LYZL4 protein expression to determine whether rat lysozyme-like gene function is similar to that of human and mouse.

In our rat genome mining, we identified four *Lyzl* genes distributed on chromosomes 8 (*Lyzl4*), 10 (*Lyzl3* and 6) and 17 (*Lyzl1*). Basing on the accession number, *Lyzl4* was found to be predicted. However, we did not find any literature that describes the identification and characterization of rat *Lyzl1*, 3 and 6, though they are shown as reported in GenBank. Hence, we submitted only the sequence of *Lyzl4* to Genbank. *In silico* analyses revealed that *Lyzl4* present on chromosome 8 is encoded by 4 exons, which is in agreement with the gene structure available at GenBank. Its homology with its human and mouse counter parts suggests that LYZL4 is highly conserved. The four rat *Lyzl* genes are distributed on three chromosomes. Such distribution of *Lyzl* genes on three chromosomes was also observed in human and mouse, indicating a possible organizational conservation. Homology between the rat LYZL proteins suggests that they might have originated from a common progenitor and may share a common physiological function. The presence of eight cysteine signature in the rat LYZLs supports the classification of these to the c-type lysozyme family.

Table 2. Homology (ClustalW2 score) between rat LYZL proteins.

	Rat-Lysozyme	LYZL1	LYZL3	LYZL4	LYZL6
Rat Lysozyme		41	38	36	37
LYZL1			41	42	37
LYZL3				43	37
LYZL4					46
LYZL6					

doi:10.1371/journal.pone.0027659.t002

Homology modeling reveals a close structural similarity of rat LYZL*4* with mouse SLLP1. Such structural similarity suggests conservation of c-type lysozyme like proteins between the species.

To the best of our knowledge, we report for the first time the expression pattern of *Lyzl* mRNA transcripts in the rat. Testis specific expression of *Lyzl6* and *Lyzl3* observed in this study implies a potential role for these genes in testicular function. Though *Lyzl1*, *3* and *4* were expressed in other tissues, their expression was confined to the testis in the male reproductive tract. Such specific mRNA expression was previously reported for other *Lyzl* genes. *Lyzl4* expression in the mouse was found to be testis specific [20]. Similarly, the human *SLLP1* was found to be expressed specifically in the testis [18], whereas the other three human c-type lysozyme like genes identified were expressed in the testis/epididymides [17]. Reproductive tract specific expression was also demonstrated for other genes such as *Spag11e* [23], *DEFB118* [24] and members of the HE2 family [13]. Contrary to the expression pattern of *Lyzl* transcripts of human, the expression of rat *Lyzl* genes in non-reproductive and female reproductive tissues suggests that they may have functions beyond male reproductive tract physiology. Similarly, the expression of *Lyzl2* and *3* mRNA transcripts in the mouse was also found to be present in other tissues beyond the reproductive tract. Results of this study and others reported earlier indicate that variability in tissue specific mRNA expression could contribute to the varied functional role of *Lyzl* genes in different species.

Developmental regulation of a wide variety of genes due to the fluctuations of androgens at various stages in the male reproductive system has been studied extensively [25]. Androgen levels in the rat epididymis decline from birth until 20 days but remain at a substantial level of approximately 10 ng/g tissue (35 nM) until approximately 40 days when the levels begin to increase to that of the adult, between 15–20 ng/g [26]. Serum testosterone levels in

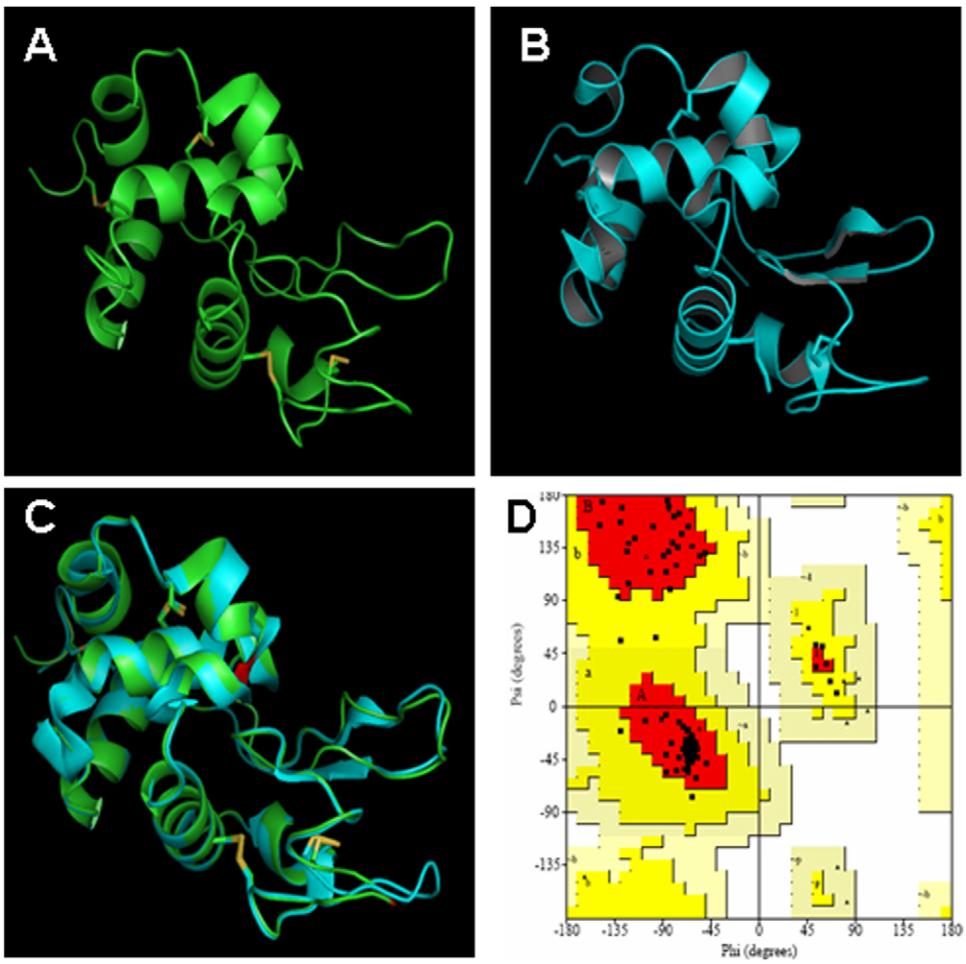

Figure 4. Homology modeling of rat LYZL4. A) Cartoon model of rat LYZL4. Disulfide bonds are indicated in yellow. **B**) Mouse SLLP1 protein model used as template. **C**) Rat LYL4 and mouse SLLP1 cartoon superimposition. **D**) Ramachandran plot for the rat LYZL4.
doi:10.1371/journal.pone.0027659.g004

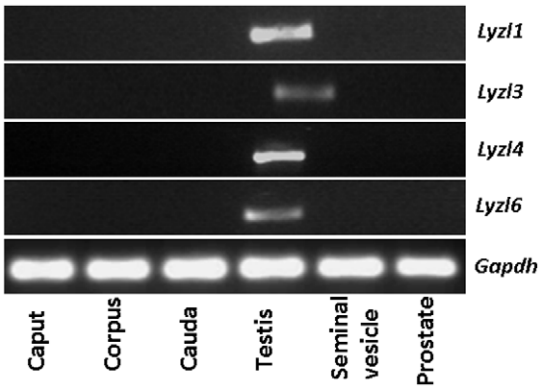

Figure 5. *Lyzl* expression in the rat male reproductive tract. Total RNA isolated from caput, corpus, cauda, testis, seminal vesicle and prostate were reverse transcribed and PCR amplified.
doi:10.1371/journal.pone.0027659.g005

the young rat remain low and do not begin to increase to adult levels until 35–40 days of age [27]. Absence of *Lyzl* transcripts in the epididymides obtained from 20–60 day old rats, suggests that their expression pattern is not androgen dependent in this organ system. Testicular androgen variation during development in the rat was reported to be significantly different from the epididymis. A steady increase in testosterone levels occurs in the rete testis of 30-130 day old rats [28,29]. In this study, the presence of *Lyzl1*, *3* and *6* mRNA transcripts was observed in the testes starting from 30 day post natal development, whereas *Lyzl4* was expressed in all the age groups, though minimally during 10-30 days. The expression pattern of *Lyzl* transcripts analysed in this study seem to correlate with the minimal androgen levels from day 20 to day 40 and increased androgen in the adult [26], suggesting that *Lyzl* expression may be androgen dependent during development in the testis. Androgen dependent expression of *Lyzl4* during development was reported in the mouse [20]. Further studies are required to determine the molecular mechanisms that operate in controlling the expression of *Lyzl* transcripts during development.

To demonstrate whether *Lyzl4* mRNA expression correlates with the protein expression, immunohistochemistry was performed on testicular sections. LYZL4 protein expression in the testes was observed in the germinal epithelium and on the maturing spermatozoa. It is possible that LYZL4 secreted into the lumen could bind to the sperm and aid in their development. Region specific gene expression of a wide variety of testicular and epididymal proteins on the sperm are reported [21]. The presence of LYZL4 specifically on the sperm tail suggests that it is involved in contributing to sperm motility. However, it is intriguing to note that though it is not expressed in the epididymis it is localized on the sperm tail. It is possible that LYZL4 is added on to the surface in the testis and this protein may continue to be present in the tail region in the epididymis.

The catalytic mechanism of c-type lysozymes involves the interaction of Glu-35 and Asp-52 of the active site with beta-1,4 glycosidic bond of the substrate. In this study, rat LYZL4 did not exhibit any muramidase and isopeptidase activity at the concentrations tested. This could be due to the replacement of aspartate by glycine in the catalytic site. Such loss of activity due to "changed" amino acids was reported for human SLLP1 and mouse LYZL4 [18,20] Epididymal proteins secreted into the lumen play a key role in sperm maturation. Besides this, some of them are known to exhibit potent antimicrobial activity, thereby forming important components of male reproductive tract innate immunity. Lysozyme, because of its ability to cleave the glycosydic bond of peptidoglycan, displays potent antimicrobial activity. In this study, we demonstrate that LYZL4 did not display any antibacterial activity against *E. coli*. The human c-type lysozyme like SLLP1, was non-bacteriolytic similar to the lack of antibacterial activity of rat LYZL4 observed in this study. The inability of rat LYZL4 to exhibit bacterial killing could be due to the modification in its active site.

In conclusion, for the first time, we report the identification of rat Lyzl4 and the expression pattern of Lyzl1, 3 and 6. In the male reproductive tract, their expression was confined to the testes. Lyzl expression seems to be androgen dependent in the testes. Immunolocalisation revealed that Lyzl4 mRNA is translated and the protein is localized on the germinal epithelium and on the sperm tail. LYZL4 did not exhibit antibacterial, muramidase and isopeptidase activities. Results of our study indicate that LYZL4 may play a crucial role in the testis and may also contribute to the motility of the sperm. Further studies are required to demonstrate the molecular mechanisms by which LYZL4 may contribute to these functions.

Materials and Methods

In silico analyses

Gene and protein notation used in this study was based on HUGO nomenclature. Gene symbols are italicised, with only the first letter in uppercase and the remaining letters in lowercase (*Lyzl*). Protein designations are the same as the gene symbol, but are not italicised, all uppercase letters (LYZL). The rat *Lyzl4* predicted sequence and *Lyzl1*, *Lyzl3* and *Lyzl6* sequences were obtained from the rat genome (build RGSC v3.4) at the NCBI website (http://www.ncbi.nlm.nih.gov/). Gene specific

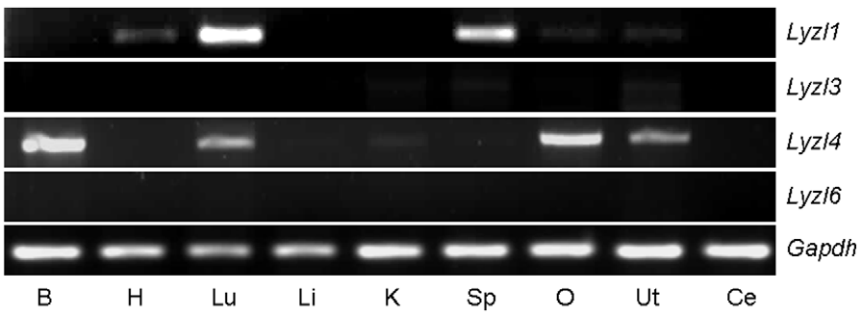

Figure 6. Tissue distribution of *Lyzl1, 3, 4* and *Lyzl6* in the rat. RT-PCR analysis was performed using total RNA isolated from **B**rain, **H**eart, **L**ung, **L**iver, **K**idney, **Sp**leen, **O**vary, **Ut**erus and **C**ervix.
doi:10.1371/journal.pone.0027659.g006

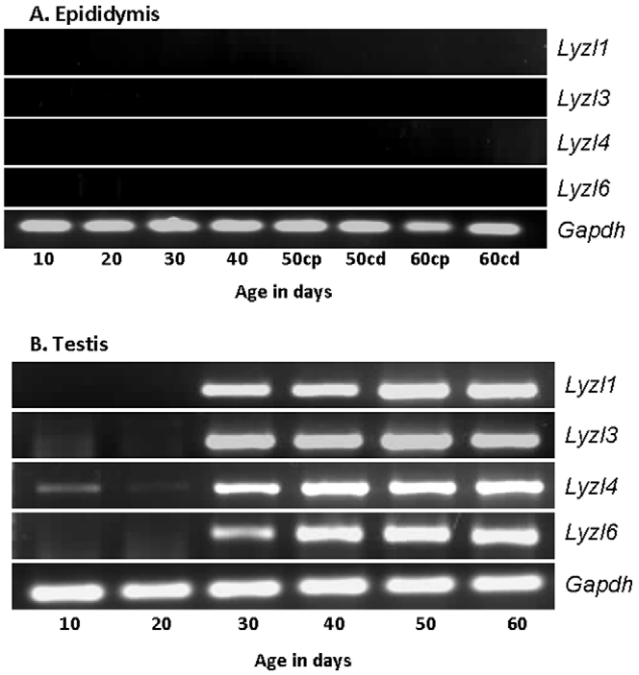

Figure 7. Developmental expression pattern of *Lyzl* transcripts in the epididymides and testes of rats. RT-PCR for *Lyzl1, 3, 4* and *Lyzl6* was performed using RNA isolated from the epididymides and testes of 10–60 day old rats.
doi:10.1371/journal.pone.0027659.g007

primers were designed for each *Lyzl* mRNA (Table 3). RT-PCR was performed using rat testis mRNA as the template. The *Lyzl4* PCR amplicons were sequenced, aligned and deposited in GenBank. The corresponding exon/intron boundaries were determined by aligning the cDNA with the genomic sequence. The sequences were translated and the predicted physical features of the deduced amino acid sequences were analyzed using tools available at ExPASy proteomics server (http://ca.expasy.org/).

The rat lysozyme like 4 (LYZL4) protein structure was predicted by homology modeling using MODELLER9v5. Basing on the BLAST search against PDB, the mouse sperm c-type lysozyme like protein 1 (SLLP1; PDB code 2GOI) was chosen as template because of its sequence similarity. The reliability of modeled structure was validated by Ramachandran plot analyses using PROCHECK and the correlation in structure between the

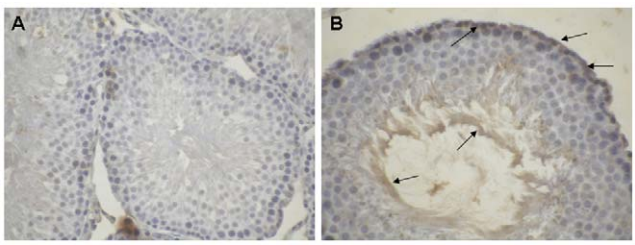

Figure 8. Immunolocalization of rat LYZL4 in the rat testis. Serial sections of the rat testis were incubated with antigen preadsorbed (A) and LYZL4 polyclonal antibody (B). Magnification – 40X.
doi:10.1371/journal.pone.0027659.g008

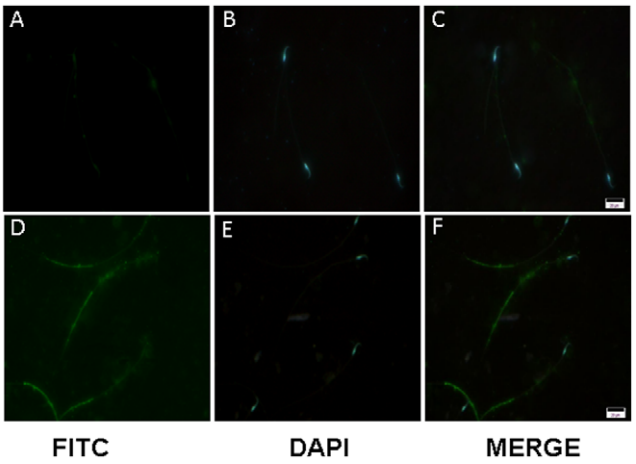

Figure 9. Immunofluorescence detection of LYZL4 on the rat sperm. A–C, Immunofluorescent staining using antibody preincubated with antigen. **D–F**, Immunofluorescent staining with LYZL4 antibody alone.
doi:10.1371/journal.pone.0027659.g009

template and model was verified by analyzing the RMSD values using PyMOL.

Tissue specimens and RT-PCR

Wistar rats (aged 60–90 days; n = 3) were obtained from National Institute of Nutrition, Hyderabad, India. Tissues collected were placed in RNA*Later* (Ambion Inc, Austin, TX, USA) solution overnight at 4°C to allow penetration and fixation and stored at -70°C. Total RNA was extracted using the TRIzol reagent (Invitrogen, Carlsbad, CA, USA) from the following tissues: the three regions of the epididymis (caput, corpus and cauda), testis, prostate, seminal vesicle, brain, liver, lung, kidney, heart, spleen, cervix, ovary and uterus. Total RNA (2 µg) was reverse transcribed using 200 U SuperSciptIII (Invitrogen, Carlsbad, CA, USA) and 0.5 µg of oligodT (Invitrogen, Carlsbad, CA, USA) according to the manufacturer's instructions. 2 µl of the resultant cDNA was amplified by PCR using gene specific primers (Table 1) for *Lyzl1*, *Lyzl3*, *Lyzl4*, *Lyzl6* and *Gapdh*. PCR was performed under the following conditions: 94°C for 2 min followed by 25–35 cycles at 94°C for 30 sec, 56°C for 30 sec and 72°C for 30 sec, and with a final round of extension at 72°C for 10 min. PCR amplicons were analyzed by electrophoresis on 2% agarose gels. For studies on the developmental regulation of *Lyzl* genes, epididymides and testes were collected from 10–60 day old Wistar rats (n = 3) purchased from the National Institute of Nutrition, Hyderabad, India.

Recombinant protein production

Recombinant LYZL4 protein was prepared as described earlier [30]. Briefly, the open reading frame that corresponds to the rat LYZL4 full length without the signal peptide (amino acid sequence shown in bold in Figure 3) was cloned into pQE30 expression vector (Qiagen, Valencia, CA, USA). *E. coli* (BL-21) was transformed with pQE30 vector containing rat *Lyzl4* cDNA according to the supplier's instructions. Fusion protein expression was induced with 1 mM isopropyl-1-thio-β-D-galactoside for 3 h at 37°C. 1% glucose was maintained in the medium to avoid baseline expression of the protein prior to induction. Bacterial lysate incubated with nickel-nitrilotriacetic acid-agarose (Qiagen) for 1 h to allow binding of His-tagged recombinant protein to the resin, was then transferred to a

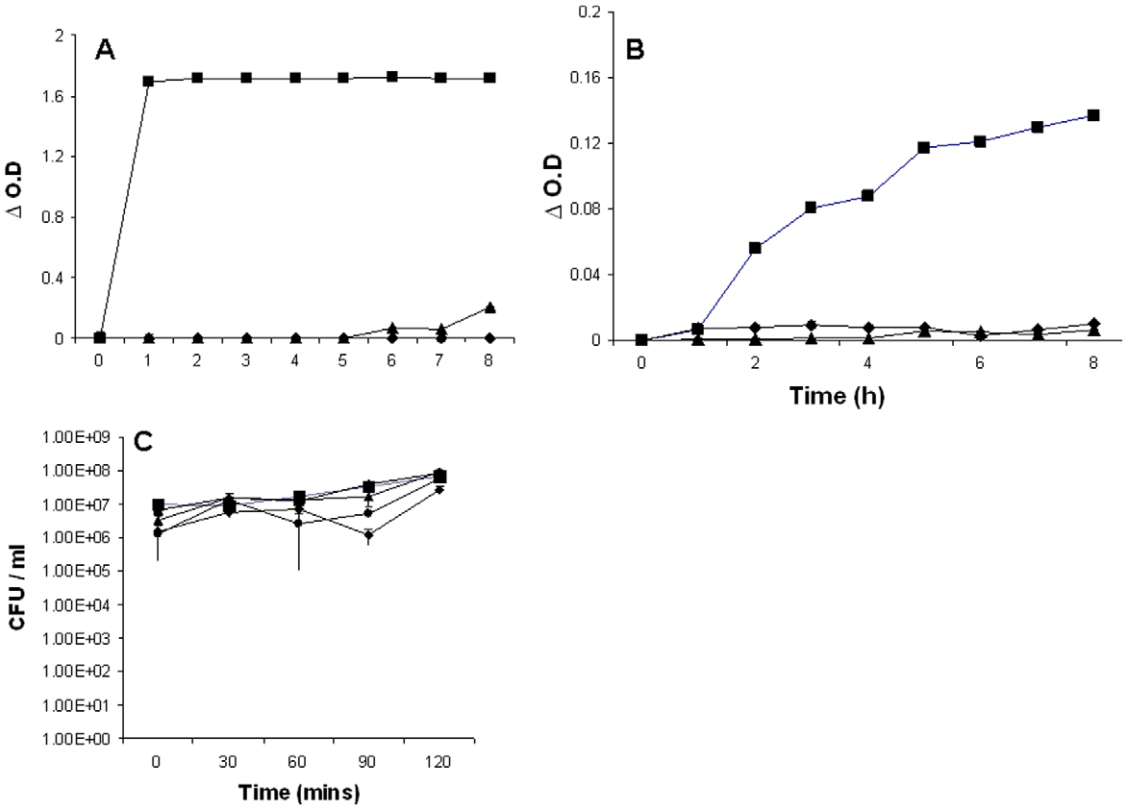

Figure 10. Muramidase, isopeptidase and antibacterial activities of rat LYZL4. A, B) 1 (▲) and 5 (♦) μM rat recombinant LYZL4 protein was incubated at 37°C and the formation of product due to muramidase and isopeptidase activities was measured spectrophotometrically at 450 and 405 nm respectively. 1.71 μM (25 μg/ml) lysozyme (■) was used as a positive control. **C**) Mid-log phase *E. coli* were incubated with 0 (■), 10 (▼), 25 (▲), 50 (•) and 100 (♦) μg/ml rat recombinant LYZL4 protein for 0–120 min. Values shown are Mean ± S.D.
doi:10.1371/journal.pone.0027659.g010

column, washed and eluted according to the manufacturer's recommendations. The His-tagged recombinant LYZL4 protein contained the following additional amino acid residues at the N-terminus (MRGSHHHHHHGS) due to the construction of the vector. Fractions were analyzed on 15% gradient polyacrylamide Tris-Tricine gels and stained with Coomassie blue G250. Further, the identity of the protein was confirmed by Western blotting using anti-His-tag antibody. Fractions containing purified protein were pooled and dialyzed against phosphate buffered saline (pH 7.4) to remove urea.

Table 3. Gene specific primers used in this study.

Gene	Direction	Sequence
Lyzl1	Forward	5′-TGTCGG TGT CTT CGC CCT AAT T-3′
	Reverse	5′-GAC GAG TCT TTG CTC TCA CAG T-3′
Lyzl3	Forward	5′-TCC AGC AAG GCC AAG GTC TTC A-3′
	Reverse	5′-TAG AAG TCA CAG CCA TCC ACC CA-3′
Lyzl4	Forward 1	5′-ATG TGG GCA CTG TTG ACA CCA -3′
	Reverse 1	5′-CTA CAC CAT TGA TCC TGC TCC A-3′
	Forward 2	5′-GTG GTG ATT GAG GAT TCC TTC AG-3′
	Reverse 2	5′-ATG GAG GCA CCA ATC GGA GTC A-3′
	Forward 3	5′-ATG CAG CTG TAC CTG GTG CTT CT-3′
	Reverse 3	5′-GCT GGTTTATTCTGCACCTTGTAC C-3′
Lyzl6	Forward	5′-TAT CTG TGT GGT GAG CTG CCT TCT-3′
	Reverse	5′-TGC ACA GTG GAT GGA TGGAAT GAG -3′

doi:10.1371/journal.pone.0027659.t003

Antibody production and immunodetection

Antibodies to detect rat LYZL4 were raised in our laboratory. Briefly, rabbits were immunized with recombinant LYZL4 protein mixed with complete adjuvant followed by booster doses 4 and 6 weeks after initial immunization. Antiserum was collected 2 weeks after the second booster dose. For immunohistochemical staining, testes were fixed in Bouin's fluid and embedded in paraffin. Five micron thick sections were taken and treated with xylene and graded alcohol (70-100%). The sections were then treated with 1% Triton-X 100 to facilitate permeabilisation followed by treatment with 3% H_2O_2. LYZL4 was detected by incubating the sections using polyclonal antibodies (1:250 dilution) raised in rabbit followed by biotin conjugated secondary antibody (1:500 dilution) against rabbit IgG raised in goat. Immunostaining was detected using a Vectastain Elite ABC kit (avidin- biotin-complex horse radish peroxidase) (Vector Laboratories Inc., Burlingame, USA). Diaminobenzidine, the chromogen, produced a brown reaction product. Sections were counter-stained with hematoxylin. For the control staining, antibodies were preincubated with antigen (LYZL4 recombinant protein). Immunofluorescence on the sperm was detected by using anti-rabbit secondary antibodies tagged with FITC. Photographs were taken using a color digital imaging system attached to a Leica Photomicroscope. Surgical procedures

were conducted using the guidelines for the care and use of laboratory animals and this study was specifically approved by the Institutional Animal Ethics Committee of University of Hyderabad (LS/IAEC/YS/11/07).

Antibacterial assay

Colony forming units (CFU) assay was employed to test the antibacterial activity as described previously [30]. Briefly, overnight cultures of *E. coli* XL-1 Blue (Stratagene, La Jolla, CA, USA) were allowed to grow to mid-log phase (A_{600} = 0.4 – 0.5) and diluted with 10 mM sodium phosphate buffer (pH 7.4). Approximately 2×10^6 CFU/ml of bacteria were incubated at 37°C with 10–100 µg/ml of the LYZL4 recombinant protein and aliquots of the assay mixture were taken at 30, 60, 90 and 120 min after the start of incubation. After incubation, the assay mixtures were serially diluted with 10 mM sodium phosphate buffer (pH 7.4) and 100 µl of each was spread on a Luria–Bertani agar plate and incubated at 37°C overnight to allow full colony development. The resulting colonies were hand counted and plotted as log CFU/ml. As a negative control, the epididymal lipocalin, LCN6 (recombinant protein expressed and purified using the same procedure followed for LYZL4) was used in the assays. Values shown are Mean ± S.D. Statistical analyses were performed using Sigma plot software.

Muramidase (lysozyme) assay

The muramidase activity of recombinant rat LYZL4 was determined using a standard protocol described earlier [6]. Briefly, rat LYZL4 (1 µM and 5 µM) was incubated with 2 ml of *M. lysodeikticus* (Sigma Aldrich, USA) cells in 50 mM KH_2PO_4-NaOH buffer, pH 7.0 and the decrease in turbidity was monitored at 450 nm in a spectrophotometer.

Isopeptidase assay

The isopeptidase activity of recombinant rat LYZL4 was measured according to the method described earlier [6], wherein, the substrate, L-γ-glutamine-p-nitroanilide (L- γ -Glu-pNA) is cleaved to produce p-nitroanilide (pNA), which can be detected at 405 nm. Rat LYZL4 (1 µM and 5 µM) was added to the reaction mixture containing 1.75 mM substrate in 0.05 M MOPS buffer. The formation of pNA was monitored spectrophotometrically at 405 nm.

Acknowledgments

We thank the facilities extended by UGC-SAP, UGC-CAS, DBT-CREBB and FIST programs at University of Hyderabad.

Author Contributions

Conceived and designed the experiments: GN. Performed the experiments: GN KM AR. Analyzed the data: GN KM AR SY. Contributed reagents/materials/analysis tools: SY. Wrote the paper: SY GN.

References

1. Fleming A (1922) On a remarkable bacteriolytic element found in tissues and secretions. Proc R Soc Lond B Biol Sci 93: 306–317.
2. Jolles P (1996) Lysozymes—Model Enzymes in Biochemistry and Biology. Boston: Birkhäuser Verlag.
3. Jolles P, Jolles J (1984) What's new in lysozyme research? Always a model system, today as yesterday. Mol Cell Biochem 63: 165–189.
4. Ito Y, Yoshikawa A, Hotani T, Fukuda S, Sugimura K, et al. (1999) Amino acid sequences of lysozymes newly purified from invertebrates imply wide distribution of a novel class in the lysozyme family. European Journal of Biochemistry 259: 456–461.
5. Joskova R, Silerova M, Prochazkova P, Bilej M (2009) Identification and cloning of an invertebrate-type lysozyme from Eisenia andrei. Developmental and Comparative Immunology 33: 932–938.
6. Takeshita K, Hashimoto Y, Ueda T, Imoto T (2003) A small chimerically bifunctional monomeric protein: Tapes japonica lysozyme. Cellular and Molecular Life Sciences 60: 1944–1951.
7. Dautigny A, Prager EM, Pham-Dinh D, Jolles J, Pakdel F, et al. (1991) cDNA and amino acid sequences of rainbow trout (Oncorhynchus mykiss) lysozymes and their implications for the evolution of lysozyme and lactalbumin. Journal of Molecular Evolution 32: 187–198.
8. Hall SH, Hamil KG, French FS (2002) Host defense proteins of the male reproductive tract. J Androl 23: 585–597.
9. Yenugu S, Hamil KG, Radhakrishnan Y, French FS, Hall SH (2004) The androgen-regulated epididymal sperm-binding protein, human beta-defensin 118 (DEFB118) (formerly ESC42), is an antimicrobial beta-defensin. Endocrinology 145: 3165–3173.
10. Yenugu S, Chintalgattu V, Wingard CJ, Radhakrishnan Y, French FS, et al. (2006) Identification, cloning and functional characterization of novel beta-defensins in the rat (Rattus norvegicus). Reprod Biol Endocrinol 4: 1–7.
11. Hamil KG, Liu Q, Sivashanmugam P, Anbalagan M, Yenugu S, et al. (2003) LCN6, a novel human epididymal lipocalin. Reprod Biol Endocrinol 1: 112.
12. Travis SM, Anderson NN, Forsyth WR, Espiritu C, Conway BD, et al. (2000) Bactericidal activity of mammalian cathelicidin-derived peptides. Infect Immun 68: 2748–2755.
13. Hamil KG, Sivashanmugam P, Richardson RT, Grossman G, Ruben SM, et al. (2000) HE2beta and HE2gamma, new members of an epididymis-specific family of androgen-regulated proteins in the human. Endocrinology 141: 1245–1253.
14. Hamil KG, Liu Q, Sivashanmugam P, Yenugu S, Soundararajan R, et al. (2002) Cystatin 11: a new member of the cystatin type 2 family. Endocrinology 143: 2787–2796.
15. Blankenvoorde MF, van't Hof W, Walgreen-Weterings E, van Steenbergen TJ, Brand HS, et al. (1998) Cystatin and cystatin-derived peptides have antibacterial activity against the pathogen *Porphyromonas gingivalis*. Biol Chem 379: 1371–1375.
16. Hiemstra PS, Maassen RJ, Stolk J, Heinzel-Wieland R, Steffens GJ, et al. (1996) Antibacterial activity of antileukoprotease. Infect Immun 64: 4520–4524.
17. Zhang K, Gao R, Zhang H, Cai X, Shen C, et al. (2005) Molecular cloning and characterization of three novel lysozyme-like genes, predominantly expressed in the male reproductive system of humans, belonging to the c-type lysozyme/alpha-lactalbumin family. Biology of Reproduction 73: 1064–1071.
18. Mandal A, Klotz KL, Shetty J, Jayes FL, Wolkowicz MJ, et al. (2003) SLLP1, a unique, intra-acrosomal, non-bacteriolytic, c lysozyme-like protein of human spermatozoa. Biology of Reproduction 68: 1525–1537.
19. Irwin DM, Biegel JM, Stewart CB (2011) Evolution of the mammalian lysozyme gene family. BMC Evol Biol 11: 166.
20. Sun R, Shen R, Li J, Xu G, Chi J, et al. (2011) Lyzl4, a novel mouse sperm-related protein, is involved in fertilization. Acta Biochim Biophys Sin (Shanghai) 43: 346–353.
21. Cornwall GA, Hann SR (1995) Specialized gene expression in the epididymis. Journal of Andrology 16: 379–383.
22. Hinton BT, Lan ZJ, Rudolph DB, Labus JC, Lye RJ (1998) Testicular regulation of epididymal gene expression. J Reprod Fertil Suppl 53: 47–57.
23. Zhou CX, Zhang YL, Xiao L, Zheng M, Leung KM, et al. (2004) An epididymis-specific beta-defensin is important for the initiation of sperm maturation. Nat Cell Biol 6: 458–464.
24. Liu Q, Hamil KG, Sivashanmugam P, Grossman G, Soundararajan R, et al. (2001) Primate epididymis-specific proteins: characterization of ESC42, a novel protein containing a trefoil-like motif in monkey and human. Endocrinology. 142: 4529-4539. Endocrinology 142: 4529–4539.
25. Rodriguez CM, Kirby JL, Hinton BT (2001) Regulation of gene transcription in the epididymis. Reproduction 122: 41–48.
26. Charest NJ, Petrusz P, Ordronneau P, Joseph DR, Wilson EM, et al. (1989) Developmental expression of an androgen-regulated epididymal protein. Endocrinology 125: 942–947.
27. Nayfeh SN, Barefoot SW Jr., Baggett B (1966) Metabolism of progesterone by rat testicular homogenates. II. Changes with age. Endocrinology 78: 1041–1048.
28. Harris ME, Bartke A (1974) Concentration of testosterone in testis fluid of the rat. Endocrinology 95: 701–706.
29. Harris ME, Bartke A (1981) Androgen levels in the rete testis fluid during sexual development. Experientia 37: 426–427.
30. Yenugu S, Hamil KG, Birse CE, Ruben SM, French FS, et al. (2003) Antibacterial properties of the sperm-binding proteins and peptides of human epididymis 2 (HE2) family; salt sensitivity, structural dependence and their interaction with outer and cytoplasmic membranes of *Escherichia coli*. Biochem J 372: 473–483.